Ring-Opening Polymerization of Cyclic Hemiacetal Esters for the Preparation of Hydrolytically and Thermally Degradable Polymers

A Dissertation
SUBMITTED TO THE FACULTY OF
UNIVERSITY OF MINNESOTA
BY

Angelika Susanne Elisabeth Neitzel

IN PARTIAL FULFILLMENT OF THE REQUIREMENTS
FOR THE DEGREE OF
DOCTOR OF PHILOSOPHY

Marc A. Hillmyer, Advisor

February, 2018

Acknowledgements

I have many people to thank for their support during my time as a doctoral student as well as to acknowledge those who have been instrumental in my personal development prior to these past 5 years. First and foremost, I would like to thank my advisor, Marc Hillmyer, for teaching me not only how to be a good scientist but also the value of emotional intelligence in working with others. The environment in Marc's group has been exceptional, featuring a perfect balance between high expectations, constructive criticism, and passion for science. I always felt in charge of my PhD and the direction it took, a luxury that someone who enjoys working independently appreciates highly. I was allowed to struggle through problems on my own and thereby felt that my accomplishments were truly my own. That is not to say that Marc did not work hard to support each one of us in our individual journeys, be it financially or by making himself accessible as much as possible to his students. Above all, I admire Marc's undying optimism, level of organization, and professionalism, traits that I hope to continually develop more for myself. I am also immensely grateful that Marc believed in me and always found positive things to say to keep me going when I was overtaken by cynicism. Working in Marc's group would have certainly been different if we were not located at the University of Minnesota, an institution I have come to love dearly. The polymer community with all of its diverse members has been a true inspiration for aspiring scientists and I feel grateful that I serendipitously wound up in the state of Minnesota. I would like to acknowledge Professor Gary Gray, my first instructor for organic chemistry who introduced me to the powerful field of organic synthesis. Professor Gray facilitated my entry into the honors organic lab taught by Professor Tom Hoye, an experience that was a deciding factor in my career. Tom impressed

me with his level of passionate, childlike and thereby pure enthusiasm for science, and his incredible eloquence. I will never forget the many times we sat down together and discussed scientific problems while time flew by unnoticed. I would also like to thank Prof. Tim Lodge who let me work beside him two years in a row as a graduate teaching assistant. I very much appreciated Tim's authenticity and his concise yet often humorous teaching style. I would like to thank Prof. Frank Bates for taking the time to entertain philosophical discussions with me that have had a great impact on me. I also want to thank Frank for propagating his passion for polymer science which made his lectures a pleasure to attend. Prof. Dan Frisbie deserves special mention as if it wasn't for his help I would have never entered into the materials science program. Beyond the faculty at Minnesota I need to thank staff members and my lab mates who shaped the day by day of graduate school. Laura Seifert, Jennifer Henderson, Julie Prince, and Teresa Bredahl were of great help throughout these five years and I sincerely thank them for making the administrative and logistical aspects of graduate school as simple to deal with as they did. Letitia Yao and Ben Geisbauer helped me many times with lab-related questions and always made me laugh. When I started in Marc's group, Justin Kennemur was one of the first to make me feel welcome in the group and to share his passion for polymer science with me. Mark Martello, Debbie Schneiderman, and James Gallagher were my office mates early on and I enjoyed our banter and their mentorship as I was learning the ropes. Maria Miranda was of incredible help when I first studied polymerization kinetics. Matt Petersen helped my transition from organic synthesis to polymer chemistry and I was very fortunate that we worked together productively to co-author my first paper in the group. I certainly benefitted greatly from working next to Paula Delgado, Myungeun Seo, and Justin Kennemur early on in the lab

and our discussions about the projects we were engaged in at the time. I want to thank Stacey Saba, Lindsay Johnson, and Jake Brutman, who entered into the group the same year I did and who helped me in their own ways at different points in our shared journey. Thomas Vidil and Sebla Onbulak brought sunshine and happiness into my life and I will always look back fondly to all the great memories we made over the past two years. Leo Oquendo has been both a reliable friend and lab mate and I will remember him always for his dark humor, his admirable work ethic, and passion for science. Michael Maher has been an invaluable friend for the short period of time that we have known each other and I will miss our coffee hours. I want to thank Phil Dirlam, Madalyn Radlauer, Yanzhao Wang, Sam Dalsin, Alex Todd, David Goldfeld, Eric Silver, Luke Kassekert, Leonel Barreda, Annabelle Watts, Adrian Amador, and all the group members I inevitably forgot to list here for making the group a great place to work. Finally, I would like to thank Guilhem DeHoe for stimulating scientific and philosophical discussions, for making me laugh when I was frustrated, and for being supportive of me over the past years, both inside and outside of the lab. I feel truly blessed for having met so many wonderful people in the Hillmyer group and am confident that I will stay good friends with many of my lab mates over the years to come. Finally, I would like to thank my family for supporting me in this journey as well as both university and non-university affiliated friends: Stephanie Lenz, Ina Brandenburg, Zoe Sommers-Haas, Michael Loeper, Giota Kyriakou, Akash Arora, Sadie Johnson, Brittany Forkus, Abe Coleman, Olu Ogunyankin, César Chaidez, Filippo Caschera, and Luke Styles. Science doesn’t happen in a vacuum and it’s due to all the great people I met and their influences on my life that I have been able to finish this chapter of my life.

Für Lydia, Christian und Susanne

Abstract

Polymers that are biodegradable in natural environments are desirable components of next generation sustainable materials. To date, polylactide is the most successful industrially compostable polyester available at only a small premium relative to polystyrene. Biodegradation of polyesters under industrial composting conditions proceeds *via* hydrolysis, followed by mineralization of polylactide oligomers to carbon dioxide, water, and humus. Hydrolysis of polylactide precedes mineralization and thereby presents the rate-limiting step in this process. The work in this thesis is motivated by the need to further tailor hydrolytic degradation profiles of sustainable polymers to allow for their degradation in a variety of natural environments. In this work we demonstrate the synthesis of novel cyclic hemiacetal ester monomers that are transformed to hydrolytically and thermally degradable polyhemiacetal esters. A thorough discussion of the polymerization mechanism under Lewis- and Brønsted acid catalysis was attained in this process to aid the scientific community in using these molecules most efficiently.

TABLE OF CONTENTS

List of Figures

List of Tables

List of Schemes

List of Appendix Schemes

Chapter 1 .

Introduction

1.1 Background

1.1.1 Sustainable plastics

Plastic materials have contributed heavily to the increasing standard of living for people all around the globe. From commodity materials, such as packaging, to specialty plastics, such as intricately designed drug delivery vehicles, it is difficult to envision our lives without this exceptionally versatile class of materials. Since plastics introduction to society as commodity materials, scientists and engineers have continually optimized them in an effort to improve function while reducing cost. However, over the last decades, concerns regarding both origin and end of life of plastics have prompted scientist to return to the drawing board and challenged the community to push for the development of sustainable, yet affordable alternatives. The term sustainable implies that materials are renewably sourced and offer end of life options such as biodegradation, chemical recycling, and degradation under otherwise specified conditions, and repurposing by reprocessing. These two pillars of sustainability are further explored in the following paragraphs to put the work presented in this thesis into context.

As the variety of commercial plastics is simply overwhelming, polyethylene, the globally most widely sold polymer to date, will serve as a representative example. Polyethylene is produced from ethylene, a hydrocarbon building block commonly obtained from petroleum via steam cracking on the order of 150 million tons per year. Ethylene is used to produce polyethylenes of different architectures, most notably high density (HDPE) and low density polyethylene (LDPE), which are assigned the recycling categories 2 and 4 respectively. Products based on HDPE include the rigid storage containers for milk,

shampoo, and juices, meanwhile the more elastic LDPE serves as cling wrap and the plastic bags used at grocery stores.

Petroleum is a fossil fuel that has formed in the earth's crust over millions of years at high temperatures and pressures. Since the 1850s when the first oil refinery became operational in the US, field production of crude oil has increased from 1,000 to roughly 8 million barrels per day.[1] How much oil has been consumed in total and how much oil is left are two controversial questions. Regardless, it can be readily understood that oil is removed from the earth's crust at a much faster rate than it is formed, which defines a non-renewable resource. Finally, it is to be expected that, with diminishing oil reserves, the price of petroleum will rise until eventually the materials that we now take for granted as cheap and disposable will no longer be affordable to the average consumer, which will especially hurt the developing nations.

Biomass is an abundant resource and, unlike petroleum, it is renewed on timescales more compatible with the pace at which humans consume plastic materials. A push for obtaining chemical monomers from plant matter has motivated the development of methodology in modern catalysis and metabolic engineering to produce both known chemical monomers as well as novel monomers for the synthesis of next generation polymers. For example, styrene, which is commonly obtained from petroleum, has been synthesized from naturally occurring carboxylic acids by decarbonylation[2,3] and produced by glucose fermentation in *Escherichia coli*.[4] On the other hand, organometallic and synthetic organic chemists are working to establish efficient routes to obtain monomers that polymer chemists developing degradable polymers have identified as monomers of interest, including lactones, cyclic carbonates, and epoxides amongst others.

Amenability to degradation comprises the other requirement that must be met by sustainable alternatives to contemporary plastics. With ever-increasing plastics consumption, aggregation of plastics in our environment and oceans is an unintended yet very serious consequence that has been thoroughly described elsewhere.[5] Due to the relative chemical inertness of the hydrocarbon polymers that dominate the market, these substances can last indefinitely in the environment, exhibiting primarily mechanical degradation with exposure to natural forces. Especially low-weight plastic packaging is rarely recycled and difficulties in its collection and retention have led to losses of 80-100 billion USD annually.[6] Therefore, materials that one would deem safe, practical, and economical should be degradable or recyclable via processes that generate innocuous products, are completed within reasonable time frames, and are not highly energy intensive.

One way to address end-of-life concerns in conventional plastics is by replacing some of them with structurally distinct polymers that feature chemical functional groups amenable to biodegradation, ideally matching the other desirable properties of the hydrocarbon polymer role model. It is important to keep in mind that the descriptor biodegradable holds very little meaning when the conditions and time frames under which the material biodegrades are not explicitly stated. In this work the focus will be on plastics that are certified as industrially compostable where the conditions and time frame for biodegradation are outlined by the American Society for Testing and Materials (ASTM) standard D 6400.[7,8]

1.1.2 Motivation

The most successful class of hydrolytically degradable polymers are the polyesters, specifically polylactide-based products are becoming increasingly commercially relevant

as industrially-compostable alternatives to consumer plastics. The bacterially produced polyhydroxyalkanoates comprise another class of polyesters that have garnered significant attention in the development of biodegradable and biocompatible plastics used in disposable consumer products as well as for biomedical applications.[9] Ester bonds are hydrolytically degradable under either acidic or basic conditions, although in the academic setting preference is usually given to the latter as it is not governed by the equilibrium considerations of acid-catalyzed processes.[10] Enzymatic or other hydrolysis of polyesters produces polyester oligomers and hydroxyacid units, which can be further broken down by soil microbes to carbon dioxide, water, and humus in a process called mineralization (Figure 1.1).[11-13]

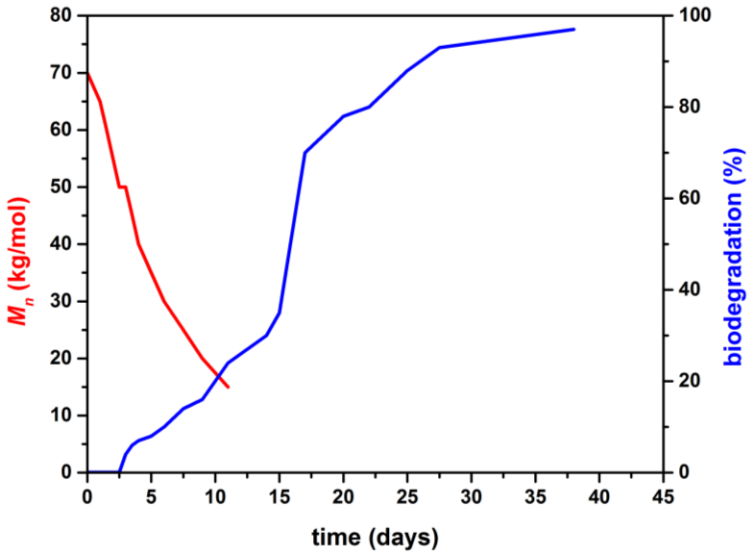

Figure 1.1. Hydrolysis and mineralization of polylactide in an industrial composting facility adapted from NatureWorks.[14]

The polymer characteristics that are relevant to degradation include the chemical structure and molar mass of the polymer, its crystallinity,[15] and polymer sequence.[16] Industrial composting facilities employ elevated temperatures of 40 – 63 °C, regularly aerate their soil, and monitor air flow and humidity in order to facilitate microbial

biodegradation of plastics in the timeframe prescribed by the ASTM standard. The work in this thesis is motivated by the need to further fine-tune the hydrolysis kinetics of biodegradable polymers, such that in applications like in, briefly used packaging, biodegradation of the plastic may occur in places such as marine environments in an acceptable time frame.

1.2 Hemiacetal Esters in Synthetic Organic and Polymer Chemistry

1.2.1 The hemiacetal ester bond

Unlike its thoroughly studied relative, the acetal, the hemiacetal ester (HAE) has not received nearly as much attention in the literature. Claisen first reported the synthesis of 1-ethoxyethyl acetate, a linear hemiacetal ester derived from the reaction of acetic acid with 1,1-diethoxyethane, in 1898 **(**Scheme 1.1).[17] He noted the facile decomposition of this compound to ethanol, acetaldehyde, and acetic acid when subjected to hydrolysis with cold or boiling water but did not investigate the hemiacetal esters further. It wasn't until two decades later that the synthesis of a series of hemiacetal esters, via reaction of metal carboxylates with chlorodimethylether, was reported.[18] In this study, the authors found that increasing the alkyl chain length of the hemiacetal esters correlated with an increase in their hydrolytic and thermal stabilities.

Scheme 1.1. Early reports of hemiacetal ester synthesis

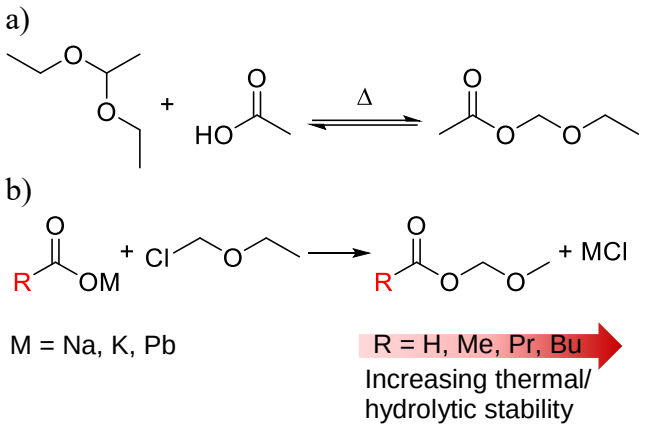

In the 1950's it was first recognized that pyrolysis of HAEs yields enol ethers and thus they were used as precursors to a number of, at the time unprecedented, enol ethers (Scheme 1.2.a).[19,20] The hydrolysis and thermal degradation of HAEs was systematically studied in the 1980's, showing the comparatively higher reactivity of hemiacetal esters under hydrolysis and pyrolysis conditions when compared to acetals and acylals.[21] Furthermore, it was found that, under anhydrous conditions, acetals could be transformed to aldehydes *via* a hemiacetal trifluoroacetic acid (TFA) ester intermediate (Scheme 1.2.b).[22] This presented an important complement to the literature, outlining the deprotection of acetals to aldehydes while avoiding hydrolysis of other reactive functional groups in the substrates. The intermediate hemiacetal TFA ester was identified by the characteristic diastereotopic protons in the ^{1}H NMR spectrum and it was later discovered that hemiacetal trifluoroacetic acid esters dissociate to form a low concentration of oxonium ion (Scheme 1.2.b). This made them of interest as electrophilic substrates in organic synthesis[23] but also led to their use as latent initiators in the cationic polymerization of vinyl ethers and sulfides.

Scheme 1.2. Various transformations of hemiacetal esters (HAEs)

a) Pyrolysis of HAEs to enol ethers

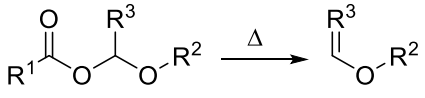

b) Hemiacetal TFA ester dissociation

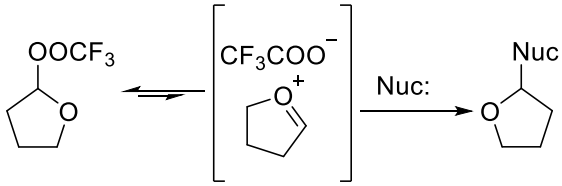

c) Acetal deprotection with anhydrous TFA

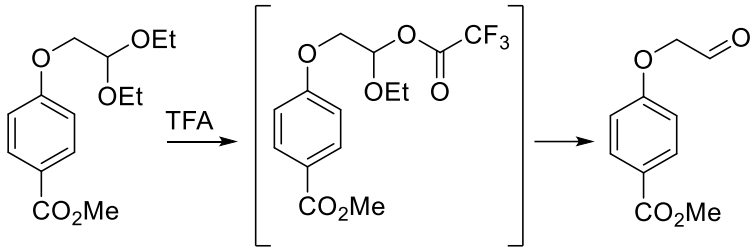

1.2.2 Hemiacetal esters as latent initiators in cationic polymerization

During the investigation into the mechanism of acylated olefin formation during treatment of electron-rich vinyl ethers or sulfides with trifluoroacetic anhydride, Endo and coworkers observed the formation of polymeric products (Scheme 1.3).[24] Upon further study they proposed the dissociation of an intermediate hemiacetal trifluoroacetic acid ester to the oxonium/trifluoroacetate ion pair, of which the oxonium ion served as a cationic initiator for vinyl ether/sulfide polymerization. This interesting observation inspired several research groups to utilize linear hemiacetal esters, such as the one formed from reaction of isobutyl vinyl ether with acetic acid or trifluoroacetic acid, as initiators in the living cationic polymerization of vinyl ethers.[25-29]

Scheme 1.3. Operative mechanisms in the synthesis of acylated enol and thioethers from vinyl ethers and sulfides

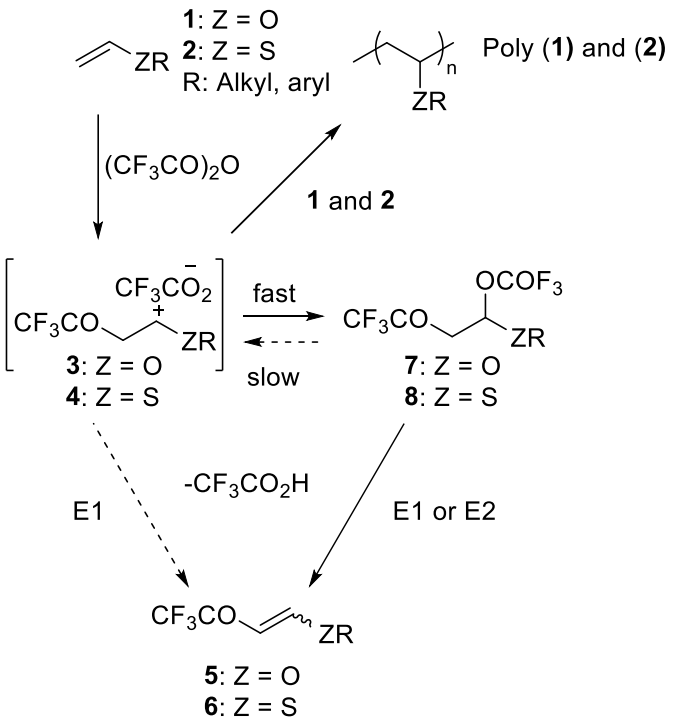

This methodology was further extended when Sawamoto and coworkers investigated a cyclic hemiacetal ester, 7-methoxyoxepan-2-one (MOPO), as an initiator in the cationic ring-expansion polymerization (REP) of vinyl ethers (Scheme 1.4).[30] Using tin tetrabromide ($SnBr_4$) as the Lewis acid catalyst, the researchers were able to evade counteranion exchange of the MOPO carboxylate for the exogenous anion (in this case bromide generated from $SnBr_4$) and suppress formation of an enol ether at the propagating chain-end, both of which would lead to the formation of linear rather than cyclic poly(isobutyl vinyl ether). The cyclic polymers obtained exhibited broad dispersities ($Đ$), albeit molar mass increased over time as expected for a living polymerization. It was hypothesized that the broad molar mass distributions were due to dynamic ring-fusion events, which the authors ultimately successfully constricted via post-polymerization

dilution of the still active system.[31] More results in the cationic REP of vinyl ethers have been recently disclosed in a minireview elsewhere.[32]

Scheme 1.4. Ring-opening expansion polymerization of vinyl ethers

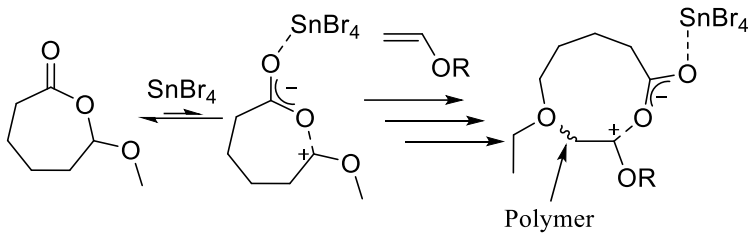

1.2.3 Polyaddition of dicarboxylic acids to divinyl ethers

While some focused on utilizing the hemiacetal ester bond as an initiator in cationic polymerizations of vinyl ethers, some also took interest in producing polyhemiacetal esters and probing their thermal properties. The first report on polyhemiacetal ester synthesis described the systematic tuning of thermal degradation temperatures of polyhemiacetal esters as a function of the spacer length separating hemiacetal ester bonds in the backbone of the polymer (Scheme 1.5).[33] The polyhemiacetal esters were synthesized *via* polyaddition of dicarboxylic acids to divinyl ethers in good to high yields with molar masses up to 14 kg/mol and $Đ$ = 1.5-3. Reports following the articles by Endo, Sawamoto, Ouchi, and Higashimura took advantage of hemiacetal ester bonds primarily as thermally- or hydrolytically-degradable components of polymer networks and polymer side chains.[34-36]

Scheme 1.5. Synthesis of polyhemiacetal esters with variable thermal degradation temperatures

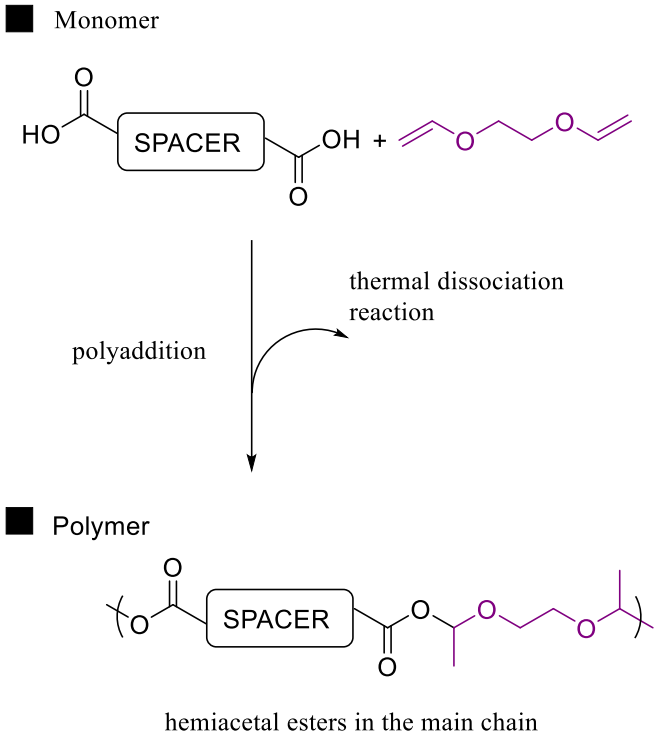

1.3 Ring-opening Polymerization of Cyclic Hemiacetal Esters

1.3.1 Ring-opening polymerization of cyclic hemiacetal esters

In 2010, polyhemiacetal ester synthesis received revived attention when Miller and coworkers postulated[37] and later probed[38] the ring-opening copolymerization of the cyclic hemiacetal ester 1,3-dioxolan-4-one (DOX) with (–)-lactide and tin(II) 2-ethylhexanoate in an effort to produce marine-degradable poly((–)-lactide). Lactones ring-open polymerize in the presence of Lewis acids, such as tin(II) 2-ethylhexanoate, via a coordination-insertion mechanism where a metal catalyst (M) reacts with an initiator, such as an alcohol (ROH), to form a metal alkoxide (MOR) *in situ*.[39] Upon coordination of the metal alkoxide to the lactone carbonyl, the catalyst complex inserts the alkoxide into the carbon-oxygen bond. After collapse of the newly formed metal alkoxide bond, the carbonyl reforms, ring-

opening the lactone to the propagating metal alkoxide (Scheme 1.6.a). If we apply the same logic to cyclic hemiacetal ester polymerization, one can envision metal alkoxide insertion into the carbonyl by a similar mechanism, and ring-opening the monomer to the propagating hemiacetal anion/metal cation pair (Scheme 1.6.b).

Scheme 1.6. Coordination-insertion mechanism in the ROP of lactones with Lewis acids (a) and its translation to the ROP of cyclic HAEs (b)

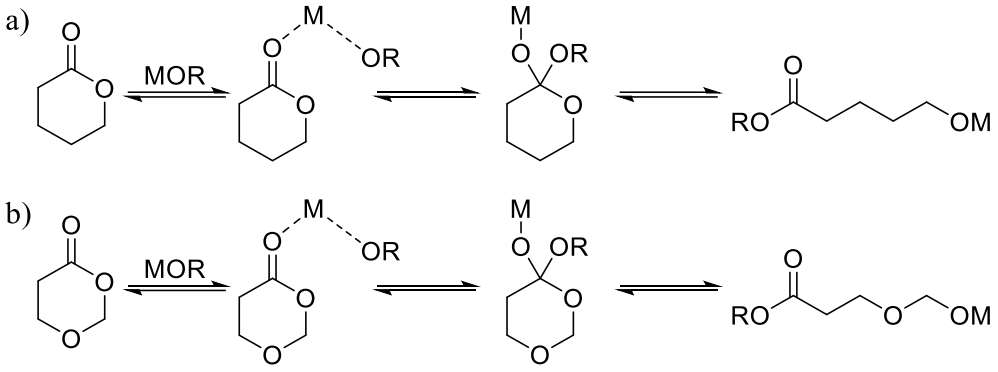

When a DOX/(–)-lactide mixture was subjected to classic lactone ROP conditions (in toluene at 120 °C with tin(II) 2-ethylhexanoate and benzyl alcohol), a polymer, which exhibited additional signals by proton nuclear magnetic resonance (^{1}H NMR) spectroscopy to those expected for poly((–)-lactide), was obtained. From collective characterization data the authors concluded that some DOX had been incorporated into the copolymer, especially since the putative copolymers exhibited enhanced degradation kinetics in marine-water.

Scheme 1.7. Copolymer predicted from ROP of 1,3-dioxolan-4-one with (–)-lactide

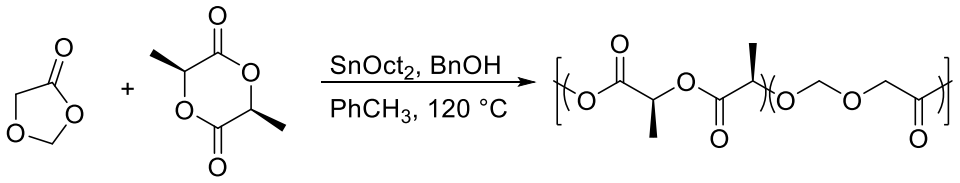

However, careful review of the ^{13}C NMR data presented in the supporting information to the manuscript raised some concerns as no signals beyond those of PLA

were observed. Furthermore, the differential scanning calorimetry data (DSC) for the DOX homopolymer was in good agreement with polyglycolide, a well-known polyester that would result from extrusion of formaldehyde during the polymerization of the DOX monomer. In Chapter 2 we discuss the concurrent expulsion of aldehyde as a pathway from cyclic hemiacetal esters to polyesters and in Chapter 3 we show in the supporting information that reproduction of the copolymerization of DOX and (–)-lactide under the conditions employed by Martin et. al results in the production of poly(lactide-*co*-glycolic acid) *via* extrusion of formaldehyde.

1.3.2 Cyclic hemiacetal esters as precursors to polyesters

The concurrent expulsion of aldehyde during cyclic HAE ring-opening polymerization was optimized by Shaver and coworkers, who synthesized several substituted 1,3-dioxolan-4-ones and screened a variety of metal-alkoxide catalysts to achieve controlled ROP of their monomers to polyesters *via* elimination of aldehyde or ketone (Scheme 1.8.a).[40] Many of the substituted 1,3-dioxolan-4-ones could be synthesized *via* condensation of inexpensive hydroxyacids with aldehydes or ketones in good to high yields. Starting with enantiopure hydroxyacids enabled control over stereochemistry in the polyester as no racemization of the stereocenter was observed under the polymerization conditions During the catalyst screening process the authors repeated the experimental conditions reported previously for DOX ROP with tin (II) 2-ethylhexanoate and found that formaldehyde was predominantly lost in this process, affording polyglycolide in the homopolymerization of DOX and (–)-lactide /glycolic acid copolymers in the copolymerization of DOX/(–)-lactide. Most importantly, the Shaver lab demonstrated that the avenue to polyesters *via* cyclic HAE ROP is interesting in its own right and can present

an economical path to polymers like isotactic poly(mandelic acid), a thermoplastic with properties similar to those of polystyrene. We are confident that others will recognize the value of employing cyclic HAEs as masked esters in the entropically-driven ROP to otherwise difficult-to-access polyesters.

Scheme 1.8. Efficient production of polyesters and polyester copolymers *via* entropically-driven ROP of cyclic HAEs

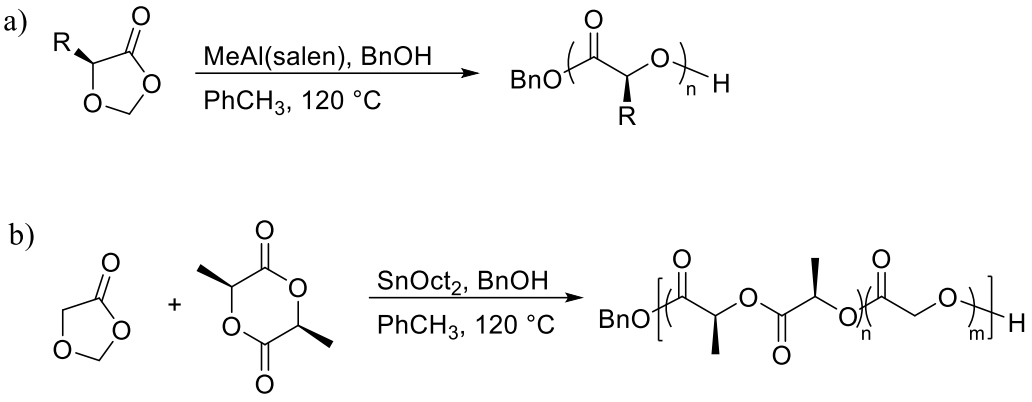

1.4 Conclusion and Outlook

The hemiacetal ester is an interesting functional group of high reactivity to thermal and hydrolytic stimuli. When incorporated strategically into molecules and macromolecules, responsive points are put in place that can trigger degradation in a tunable manner. In order to modulate polymer properties, controlled polymerization protocols must be further developed to span a wider selection of available monomers, giving preference to those deemed renewable and economical. Cyclic hemiacetal esters are amenable to controlled ring-opening polymerization and several can be produced from inexpensive and renewable starting materials. There remains much to be learnt about these monomers and we are confident more questions will be answered in time.

References

1) U.S. Field Production of Crude Oil (Thousand Barrels per Day) https://www.eia.gov/dnav/pet/hist/LeafHandler.ashx?n=PET&s=MCRFPUS2&f=A (accessed Aug 31, 2017).

2) Miranda, M. O.; Pieterangelo, A.; Hillmyer, M. A.; Tolman, W. B. *Green Chem.* **2012**, *14*, 490−494

3) John, A.; Hogan, L. T.; Hillmyer M. A; Tolman W. B. *Chem. Commun.* **2015**, *51*, 2731−2733.

4) McKenna, R.; Nielsen, D. R. *Metab. Eng.* **2011**, *13*, 544−554

5) Andrady, A. L. *Marine Poll. Bull.* **2011**, *62*, 1596−1605.

6) World Economic Forum, Ellen Mac Arthur Foundation and McKinsey and Company, The New Plastics Economy Rethinking the Future of Plastics; 2016; [report] http://www.ellenmacarthurfoundation.org/publications.

7) Wynkoop, M. (2017). *COMMERCIAL COMPOSTING, "GREEN-WASHING" AND ECO LABELS*. [ebook] World Centric. Available at: http://worldcentric.org/images/newsletter/Compostable%20vs%20%20Biodegradable.pdf [Accessed 28 Aug. 2017].

8) ASTM Standard D6400, 2012, "Standard Specification for Labeling of Plastics Designed to be Aerobically Compostable in Municipal or Industrial Facilities," ASTM International, West Conshohocken, PA, 2012, DOI: 10.1520/D6400-12, www.astm.org.

9) Reddy, C. S. K.; Ghai, R.; Kalia, R. V. C. *Bioresour Technol.* **2003**, *87*, 137–146.

10) Wade, L. G. *Organic chemistry*, 6th ed.; Pearson Prentice Hall: Upper Saddle River, NJ, 2006.

11) Li, S.; Vert, M. In *Degradable Polymers*; Springer Netherlands, 2002; pp 71–131.

12) Andrady, A. L. *J. Macromol. Sci. Polym. Rev.* **1994**, 34, 25–76.

13) Tokiwa, Y.; Calabia, B. P.; Ugwu, C. U.; Aiba, S. *Int. J. Mol. Sci.* **2009**, *10*, 3722–3742.

14) Graph adapted from http://www.natureworksllc.com/The-Ingeo-Journey/End-of-Life-Options/Composting, Accessed 05/26/2015.

15) Qian, H.; Wohl, A. R.; Crow, J. T.; Macosko, C. W.; Hoye, T. R. *Macromolecules* **2011**, *44*, 7132−7140.

16) Washington, M. A.; Swiner, D. J.; Bell, K. R.; Fedorchak, M. V.; Little, S. R.; Meyer, T. Y. *Biomaterials* **2017**, *117*, 66–76.

17) Claisen, L. *Ber. Dtsch. Chem. Ges*. **1898**, *31*: 1010–1019.

18) Clark, F. E.; Cox, S. F.; Mack, E. *J. Am. Chem. Soc.* **1917,** *39*, 712–716.

19) Erickson, J.; Woskow, M. *J. Org. Chem*. **1958**, *23*, 670−672.

20) Keith, D. D.; Tortora, J. A.; Yang, R. *J. Org. Chem*. **1978**, *43*, 3711−3713.

21) Gallucci, R. R.; Going, R. C. *J. Org. Chem.* **1982**, *47*, 3521−3524.

22) Li, W.; Li, J.; Wu, Y.; Fuller, N.; Markus, M. A. *J. Org. Chem.* **2010**, *75*, 1077-1086.

23) Bihovsky, R.; Kumar, M. U.; Ding, S. Goyal, A. *J. Org. Chem*. **1989**, *54*, 4291−4293.

24) Moriguchi, T.; Endo, T. *J. Org. Chem*. **1995**, *60*, 3523−3528.

25) Aoshima, S.; Higashimura, T. *Macromolecules* **1989**, *22*, 1009−1013.

26) Kamigaito, M.; Sawamoto, M.; Higashimura, T. *Macromolecules* **1991**, *24*, 3988−3992.

27) Shohi, H.; Sawamoto, M.; Higashimura, T. *Macromolecules* **1992**, *25*, 58−63.

28) Moriguchi, T.; Endo, T.; Takata, T.; Nakane, Y. *Macromolecules* **1995**, *28*, 4334–4339.

29) Hashimoto, T.; Iwata, T.; Minami, A.; Kodaira, T. *J. Polym. Sci., Part A: Polym. Chem.* **1998**, *36*, 3173−3185.

30) Kammiyada, H.; Konishi, A.; Ouchi, M.; Sawamoto, M. *ACS Macro Lett*. **2013**, *2*, 531−534.

31) Kammiyada, H.; Ouchi, M.; Sawamoto, M. *Polym. Chem.* **2016**, *7*, 6911−6917.

32) Ouchi, M.; Kammiyada, H.; Sawamoto, M. *Polym. Chem.* **2017**, *8*, 4970−4977.

33) Otsuka, H.; Endo, T. *Macromolecules* **1999**, *32*, 9059−9061.

34) Vidil, T.; Tournilhac, F.; Musso, S.; Robisson, A.; Leibler, L. *Prog. Polym. Sci.* **2016**, *62*, 126–179

35) Komatsu, H.; Hino, T.; Endo, T. *J. Polym. Sci. A Polym. Chem.* **2006**, *44*, 3966−3977.

36) Komatsu, H.; Ochiai, B.; Endo, T. *J. Polym. Sci. A Polym. Chem.* **2008**, *46*, 1427−1439.

37) Miller, S. A. Polyesteracetals. U.S. Patent 2009/066417, December 2, **2009**.

38) Martin, R. T.; Camargo, L. P.; Miller, S. A. *Green Chem.* **2014**, *16*, 1768−1773.

39) Löfgren, A.; Albertsson, A.-C.; Dubois, P.; Jérôme, C. *J Macromol. Sci. Polymer Rev*. **1995**, *35*, 379−418.

40) Cairns, S. A.; Schultheiss, A.; Shaver, M. P. *Polym. Chem.* **2017**, *8*, 2990−2996.

Chapter 2 :

Divergent Mechanistic Avenues to an Aliphatic Polyesteracetal or Polyester from a Single Cyclic Esteracetal*

The work in this chapter was carried out in collaboration with Dr. Matthew Petersen and Prof. Efrosini Kokkoli in the department of chemical engineering and materials science at the University of Minnesota.

* Reproduced in part with permission from Neitzel, A. E.; Petersen, M. A.; Kokkoli, E.; Hillmyer, M. A. Divergent Mechanistic Avenues to an Aliphatic Polyesteracetal or Polyester from a Single Cyclic Esteracetal. *ACS Macro Lett*. **2014**, *3*, 1156-1160.

2.1 Introduction

The development of polymers with pH responsiveness is important for needs in biomedicine, sensing, electronic materials, textile, and filtration applications.[1-8] Macromolecules can be strategically designed to respond to changes in pH through conformational changes triggered by reversible protonation or by irreversible chain degradation.[9] Simple polyesters are a well-understood example of the latter class but hydrolyze rather slowly at physiologically relevant pH ranges (4.5−7.4).[10,11] Polymers that degrade rapidly present tremendous opportunities for drug delivery[12-17] as well as for the development of new materials that break down in natural environments.[18-19]

Acetal or ketal functional groups are excellent candidates for facilitating degradation due to their acid-sensitive nature, and their incorporation in the main chain or as pendant groups of a nondegradable backbone has been reported.[20-23] Routes to polymers containing this functionality in their backbone include cationic,[24,25] step growth,[26-32] or metathesis polymerizations.[33,34] According to a 2010 patent disclosure, an alternating ester/acetal copolymer, poly(1,3-dioxolan-4-one), was accessed from the ring-opening polymerization (ROP) of a five-membered ring precursor. Furthermore, a statistical copolymer of 1,3-dioxolan-4-one (DOX) and lactide was reported. While the patent provided little in the way of characterization data for poly(1,3-dioxolan-4-one),[35] a more recent publication details the synthesis of a variety of copolymers of DOX and lactide and reports up to 36% DOX incorporation. A computational study of the ring strain in DOX suggests that DOX is slightly less strained than γ-butyrolactone, and the authors' reason that the unfavorable thermodynamics of polymerization can be offset by copolymerization with lactide. Finally, the degradation studies in distilled and oceanic water of a copolymer

containing 4% DOX and 96% lactide displayed a 2% reduction in mass over the course of 40−50 days.[36]

Enticed by the marriage of the ester and acetal functionalities in a degradable polymer backbone, we set out to synthesize and study the ring-opening polymerization (ROP) of 2-methyl-1,3- dioxane-4-one (MDO). This six-membered monomer can be prepared by a simple Baeyer−Villiger oxidation of the commercial precursor 2-methyltetrahydrofuran-3-one (see section 2.4 for experimental details). Alternatively MDO can be accessed from condensation of 3-hydroxypropionic acid with acetaldehyde,[37,38] both of which can be derived from biomass.[39] We found that diethylzinc ($ZnEt_2$), a catalyst commonly used in the ROP of lactones,[40-42] readily polymerizes neat MDO (~10 M) in the presence of benzyl alcohol as the initiator. At high loadings of catalyst ($[ZnEt_2]_0$ = 30−100 mM) the reaction proceeds to essentially complete conversion within several hours. We discovered that catalyst concentration played an important role in the outcome of the polymerization. In fact, two repeating unit structures could be obtained from this one monomer solely by varying the catalyst concentration (Scheme 2.1).

Scheme 2.1. Tunable ROP of MDO to Two Distinct Structures.

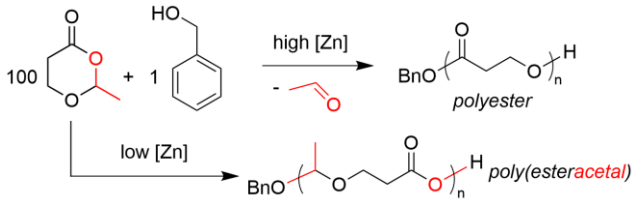

2.2 Results and Discussion

At high loadings of $[ZnEt_2]_0$ over a range of $[MDO]_0$/ $[BnOH]_0$ ratios we generated polymers with molar masses from 7.9 to 43 kg mol^{-1} (representative polymerization: $[ZnEt_2]_0$ = 100 mM, $[MDO]_0$ = 10.1 M (neat), $[BnOH]_0$ = 100 mM, t_{polym} = 8 h, 23 °C).

The polymer products were isolated as white solids by precipitation and exhibited narrow molar mass distributions ($Đ \leq 1.23$) as determined by size exclusion chromatography (SEC). However, the ^{1}H and ^{13}C nuclear magnetic resonance (NMR) spectra of these polymers at full conversion showed almost no (< 1%) incorporation of the acetal methyl and methine moieties present in MDO. Instead, the major resonances were in excellent agreement with poly(3-hydroxypropionic acid) (PHPA),[43] consistent with loss of acetaldehyde (as confirmed by ^{1}H NMR spectroscopy using diluted MDO, Figure 2.17) under these conditions (Figure 2.1A and Scheme 2.1). This was further supported by melting transition temperatures (T_m) for the PHPA samples ranging from 59 to 77 °C and glass transition temperatures (T_g) ranging from −34 to −28 °C (Figure 2.10), as well as a clear repeat unit of m/z = 72.02 by mass spectrometry (Figure 2.9) consistent with the expected value.[41]

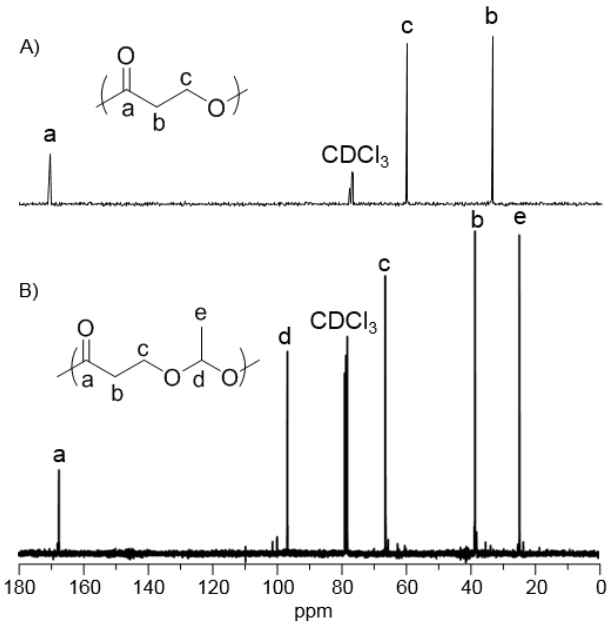

Figure 2.1. Representative ^{13}C NMR spectra and structural assignments of two distinct polymers synthesized by diethylzinc-catalyzed bulk polymerization of MDO. At higher catalyst concentrations (A, 30-100 mM) PHPA was formed, while at lower catalyst concentrations (B, 0.4–14 mM) PMDO was formed. Spectra are of samples HPA594 ($[ZnEt_2]_0$ = 31 mM, $[MDO]_0$ = 9.9 M, $[BnOH]_0$ = 15 mM, t_{polym} = 8 h, 23 °C, M_n = 43 kg/mol) and MDO66 ($[ZnEt_2]_0$ = 2 mM, $[MDO]_0$ = 10.1 M, $[BnOH]_0$ = 84 mM, t_{polym} = 72 h, M_n = 8 kg/mol).

Interestingly, at low $[ZnEt_2]_0$ loadings, the polymerization of MDO led to a retention of acetal structural units in the polymer backbone as expected in the ROP of cyclic esters. At $[ZnEt_2]_0$ = 0.4−14 mM a clear viscous material was isolated from the polymerization of MDO. At these low catalyst loadings, the MDO polymerization was slower and reached a limiting conversion of approximately 60% (see below). The splitting pattern of the diastereotopic methylene protons (ddd at δ = 3.85 ppm in $CDCl_3$, see Figure 2.11) and the distinctive resonances in the ^{13}C NMR spectra when compared with PHPA (Figure 2.1B) were consistent with complete retention of the acetal functional group in the polyesteracetal PMDO (Scheme 2.1). Furthermore, the clearly defined ^{13}C resonances and the absence of resonances for polyacetaldehyde[44] suggest perfectly alternating ester and acetal units. The absence of a singlet at 5.1 ppm in the PMDO ^{1}H NMR spectrum, which

is expected for methylene protons of a benzoyl ester end group, indicated an initiation process that did not proceed via attack of the initiator at the ester functionality. Instead, two doublets and a quartet were observed between 4.5 and 5 ppm, which is in good agreement with a benzyl acetal end group. From this we suggest that at low zinc concentrations benzyl alcohol initiates polymerization via attack at the acetal functionality, generating a propagating zinc carboxylate.

Using low concentrations of zinc, PMDO samples with molar masses ranging from 7.6 to 30 kg mol^{-1} were synthesized by varying $[MDO]_0/[BnOH]_0$ as described above for PHPA (representative polymerization: $[ZnEt_2]_0$ = 2 mM, $[MDO]_0$ = 10.1 M, $[BnOH]_0$ = 84 mM, t_{polym} = 72 h, 23 °C). SEC data for PMDO indicated that molar mass distributions ($Đ$ ≈ 1.6, see below) were broader than those observed for PHPA prepared from MDO at high zinc concentration. The PMDO samples exhibited low T_g values (−32 to −25 °C) but no melting transitions (Figure 2.14). ESI-MS showed a clear MDO repeat unit at m/z = 116.05 (Figure 2.13).

Bulk polymerization of MDO at high catalyst loadings was tracked by ^{1}H NMR analysis of aliquots from the reaction (see Figure 2.15). The linear relationship between the natural logarithm of the monomer concentration versus time over the course of two half-lives suggests a reaction rate that is first order in monomer (Figure 2.16). At these diethylzinc loadings, the polymerization of MDO to PHPA proceeds to >99% conversion with the concurrent elimination of acetaldehyde. This thermodynamic driving force is analogous to CO_2 expulsion observed during polymerization of *N*-carboxyanhydrides and cyclic carbonates.[45-47] Similarly, the expulsion of acetone has been observed during the 4-dimethylaminopyridine-catalyzed copolymerization of an epoxide with Meldrum's acid.[48]

Apparent molar masses and dispersities as a function of monomer conversion were tracked for both polymerizations by SEC. The linear correlation shown in Figure 2.2 is consistent with a controlled chain-growth mechanism for both PMDO and PHPA. The larger dispersity values in the case of PMDO are likely due to the relatively unfavorable polymerization thermodynamics; significant depolymerization even at low monomer conversion can lead to broader molar mass distributions.[49-53]

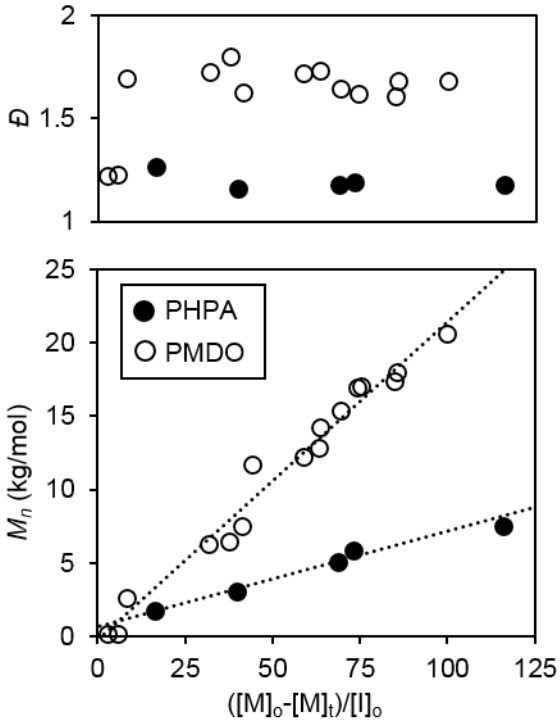

Figure 2.2. Number average molar mass M_n (closed symbols) and dispersity $Đ$ (open symbols) as determined by SEC calibrated with polystyrene standards. At high catalyst concentrations (●, $[ZnEt_2]_0$ = 87 mM) PHPA was formed. At low catalyst concentrations (▲, $[ZnEt_2]_0$ = 1.0 mM), PMDO was formed but monomer was not completely consumed $[M]_{max}/[M]_0 \approx 0.6$. For PHPA, $[MDO]_0$ = 9.3 M and $[BnOH]_0$ = 46 mM. For PMDO, $[MDO]_0$ = 10.1 M and $[BnOH]_0$ = 49 mM.

When monitoring MDO bulk polymerization at low catalyst loadings we determined that this reaction proceeds over several days and achieves ~60% limiting conversion to PMDO at room temperature (Figure 2.15), and the rate of conversion to PMDO also appears to be first order in monomer (Figure 2.16). Using experimentally

established densities the equilibrium monomer concentration for MDO under low catalyst concentration conditions was determined to be $[M]_{eq}$ = 4.53 M (23 °C). Values for $[M]_{eq}$ were then determined from 23 to 60 °C and used to compute the thermodynamic parameters for the ROP of MDO to PMDO. The ceiling temperature for the neat monomer was calculated to be 81 °C (ΔH_p^0 = −11.6 kJ/mol and ΔS_p^0 = −52 J/(mol K), see Figure 2.18), consistent with related six-membered lactones.[54,55]

To determine the order of both polymerizations in [Zn] we measured the initial polymerization rates over several high- and low-catalyst concentration ranges and created double logarithmic plots of k_{app} versus $[ZnEt_2]_0$ (Figure 2.3, also see Figures 2.19−2.21). These were broadly consistent with a first-order rate dependence on catalyst concentration under conditions where the acetal functionality is retained ($-d[MDO]/dt \propto [ZnEt_2]^{0.9\pm0.1}$) and a second-order rate dependence at loadings where acetaldehyde is eliminated ($-d[MDO]/dt \propto [ZnEt_2]^{1.9\pm0.2}$). Deviation from integer orders of reaction may be due to impurities or more complex aggregation phenomena, but this was not further investigated.[56-58]

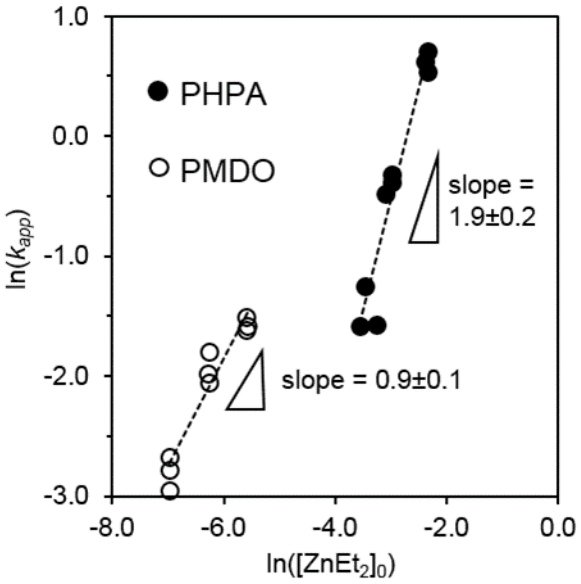

Figure 2.3. Kinetic plots used to determine the order of polymerization in $[ZnEt_2]_0$. Rate constants (k_{app}) were determined at various concentrations of $[ZnEt_2]_0$. The slope of $\ln(k_{app})$ versus $\ln([ZnEt_2]_0)$ was used to establish the order of the reaction in $[ZnEt_2]_0$. At low catalyst loadings (▲, $[ZnEt_2]_0$ = 0.93 to 3.7 mM, R^2 = 0.92) the acetal group was maintained, and the slope of the plot indicated that $-d[MDO]/dt \propto [ZnEt_2]^{0.9\pm0.1.}$ At higher catalyst loadings (●, $[ZnEt_2]_0$ = 28 to 96 mM, R^2 = 0.93), the acetal group was eliminated, and the plot slope indicated that $-d[MDO]/dt \propto [ZnEt_2]^{1.9\pm0.2}$. In all cases polymerizations were conducted using $[MDO]_0$ = 10.1 M and $[BnOH]_0$ = 99 ± 7 mM at 23 °C.

We speculate that aggregation of zinc propagating centers coordinated through alkoxide oxygens[59] facilitates acetal elimination at higher relative catalyst concentrations, leading to PHPA. We envisioned that this proceeds through a six-membered transition state formed after coordination and ring opening of MDO, which then collapses to yield a 3-HPA repeat unit with concomitant release of acetaldehyde (Scheme 2.2).

Scheme 2.2. Proposed 6-Membered Transition State for Acetaldehyde Elimination.

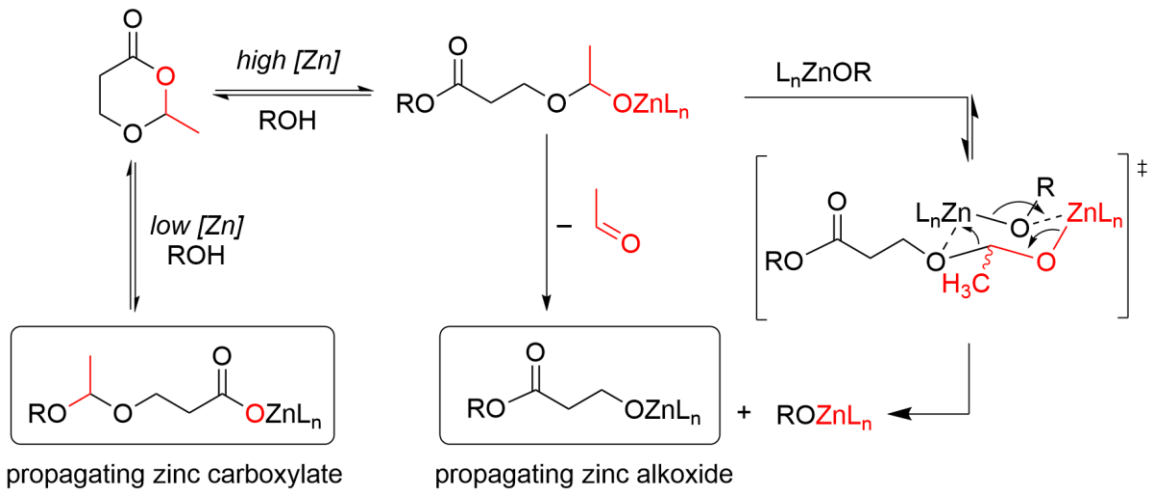

To assess if incorporation of the acetal moiety enhanced polymer susceptibility to degradation under acidic conditions, samples of PHPA and PMDO were subjected to degradation at pH 7.4, 6.4, 5.4, and 4.4 (Figure 2.4). PHPA did not degrade appreciably at any pH, consistent with other aliphatic polyesters over this short time scale.[8,60-62] In contrast, PMDO exhibited significant degradation at all pH levels, especially at low pH (4.4), where apparent molar mass decreased 6-fold over 240 h. This degradation rate is consistent with other systems incorporating acetal linkages as pendent groups[27] and parallels the enhanced degradation observed for lactide-1,3-dioxolane-4- one copolymers.[36] The rate of degradation we observed was, as expected, slower than for polymers incorporating more hydrolytically sensitive ketals.[29,30]

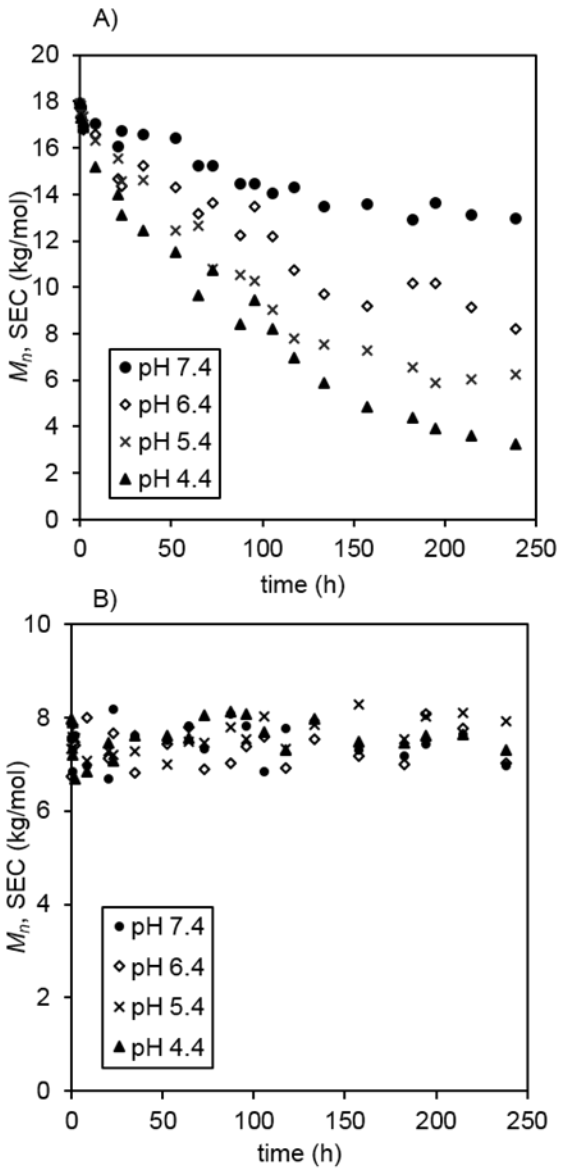

Figure 2.4. Degradation of A) PMDO and B) PHPA as a function of pH. Samples were subjected to degradation at room temperature in a 100 mM phosphate-citrate buffer, periodically lyophilized, and analyzed by SEC to determine changes in molar mass.

2.3 Conclusion

In summary, we have demonstrated the synthesis and characterization of the acid-labile polyesteracetal PMDO and the biodegradable polyester PHPA from a single monomer, MDO. Using diethylzinc as the catalyst, controlled polymerizations were achieved at both high and low catalyst concentrations. At high catalyst concentrations, the

polymerization was driven toward the formation of PHPA due to the expulsion of acetaldehyde. This is notable as it achieves high conversions to PHPA with narrow molar mass distributions over practical time periods. Comparable molar mass distributions have only been achieved by the lanthanide-catalyzed solution polymerizations of β-propiolactone.[63] Macrocyclic,[43] condensation,[64] microbial,[65,66] and other ring-opening[67,68] syntheses generally give broader distributions than we observe in the case of MDO to PHPA. At low catalyst concentrations, acetal elimination could be entirely suppressed to deliver the acid-labile polymer PMDO. The formation of distinct products was rationalized by the first-order versus second-order dependency of the rate laws on initial diethylzinc concentration for PMDO and PHPA, respectively. A mechanistic hypothesis in good agreement with both the kinetics and ^{1}H NMR data was put forth for both PMDO and PHPA formation. Further investigation into the mechanism of ROP of cyclic esteracetals is currently underway in our laboratories. Findings described herein not only are intriguing in the context of homopolymer synthesis but also open up attractive avenues toward block- and random copolymer synthesis from a single monomer.

2.4 Supporting Information

Materials and Analysis

All chemicals were obtained from Sigma-Aldrich (Milwaukee, WI) and used as received unless otherwise noted. ^{1}H, ^{13}C, and COSY NMR spectra were obtained at room temperature on a Varian spectrometer in $CDCl_3$ at 300 MHz and 500 MHz for ^{1}H and COSY NMR spectra and 75 MHz for ^{13}C NMR spectra. Reported chemical shifts were referenced to $CHCl_3$ at 7.26 ppm for ^{1}H NMR spectra and 77.23 ppm for ^{13}C NMR spectra.

Integrations of ^{1}H NMR data for calculations of molar mass are referenced to the methylene protons of BnOH at 5.10 ppm for PHPA and to the aryl protons at 7.3 ppm for PMDO. Elemental Analysis of MDO was performed by Atlantic Microlab (Norcross, GA). DSC was carried out using a TA Instruments Q2000 at a scanning rate of 5 °C/min. DSC data analysis was performed using TA Instruments TRIOS software using the second heating curve. ESI-MS data were acquired using a Bruker BioTOF instrument using samples dissolved at approximately 0.05 mg/mL in 9:1 MeOH:CH_2Cl_2 and data were analyzed using Bruker DataAnalysis software with masses calibrated to poly(propylene glycol) standards. PMDO samples were analyzed by SEC using an Agilent 1260 series chromatograph (THF, 35 °C, 1 mL/min) with three Styragel columns and equipped with an Optilab T-rEX RI detector. SEC for PHPA samples was performed using a Hewlett-Packard series 1100 liquid chromatography system ($CHCl_3$, 35 °C, 1 mL/min), equipped with a Hewlett-Packard 1047A RI detector and three PLgel 5 μm MIXED-C columns. Significant peak broadening occurred during SEC for PMDO in $CHCl_3$ and for PHPA in THF, even at high dilutions. As a result, SEC of PMDO used THF and SEC of PHPA used $CHCl_3$. In both cases, apparent molar masses were reported versus polystyrene standards (Polymer Laboratories).

Synthesis of 2-methyl-1,3-dioxan-4-one (MDO)

MDO was prepared by Baeyer-Villiger oxidation of racemic 2-methyltetrahydrofuran-3-one (Sigma FG ≥ 97%) using *m*CPBA as the oxidant.[40,43,69-71] Reactions were performed with a 1.2 molar excess of 77 % active oxygen content *m*CPBA to 2-methyltetrahydrofuran-3-one at approximately 10 w/v % in CH_2Cl_2. The *m*CPBA was dissolved in methylene chloride, dried over $MgSO_4$, and filtered. The filtrate was cooled

to 0 °C in an ice bath and 2-methyltetrahydrofuran-3-one was added dropwise under stirring. The solution was brought to room temperature and stirred for an additional 2.5 h. Upon full conversion, the precipitated *meta*-chlorobenzoic acid byproduct was removed by repeated filtration at –78 °C, and solvent volume was reduced after each filtration step until no further precipitate was observed. CH_2Cl_2 was then evaporated to give a ca. 10 w/v % solution, which was transferred to a separatory funnel and washed with saturated sodium bicarbonate until no further carbon dioxide emission was evident. The water layer was extracted 3 times and the combined organic layers were dried with brine and magnesium sulfate, filtered, and the solvent removed in vacuo to yield a crude oil, which was dried over calcium hydride and distilled (44 °C at 400 mTorr) to give racemic MDO as a clear oil in up to 75 % yield. The monomer was stored over 3 Å molecular sieves in the glove box at –23 °C. ^{1}H NMR ($CDCl_3$): δ 5.43 (q, 1 H, J = 5.5 Hz, -O-CH(CH3)-O-), 4.22 (ddd, J = 11, 8.5, 2.5 Hz, 1 H, -C(O)-CH2-CH2-O-), 3.94 (ddd, J = 11.5,10.5, 5.5 Hz, 1 H, -C(O)-CH2-CH2-O-), 2.81 (ddd, J = 18, 11, 8.5 Hz, 1 H, -C(O)- CH2-CH2-O-), 2.61 (ddd, J = 18, 6, 2.5 Hz, 1 H, -C(O)-CH2-CH2-O-), 1.52 (d, J = 5.5 Hz, 3 H, - O-CH(CH3)-O-). ^{13}C NMR ($CDCl_3$): δ 167.35, 101.08, 63.23, 29.84, 21.02. Elemental Analysis: Calculated: C: 51.72%, H: 6.94%. Experimental: C: 51.92%, H: 7.07%. T_m = 10.8 °C by DSC.

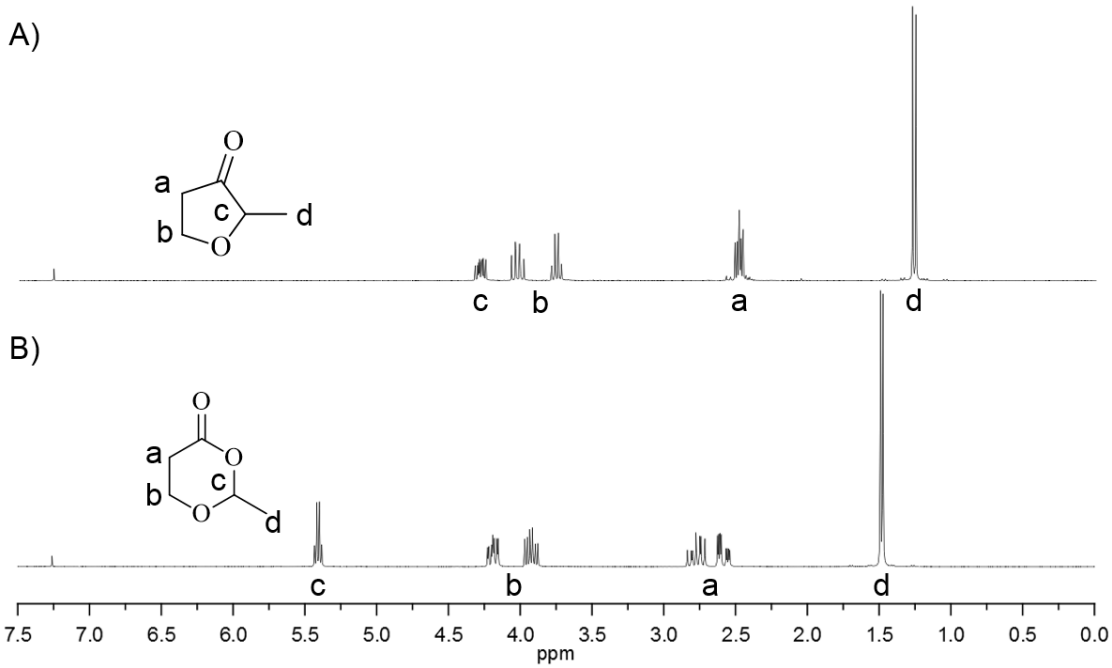

Figure 2.5. [1]H NMR spectra and proton assignments for A) 2-methyltetrahydrofuran-3-one precursor and B) 2-methyl-1,3-dioxan-4-one (MDO) after Baeyer-Villiger oxidation and purification.

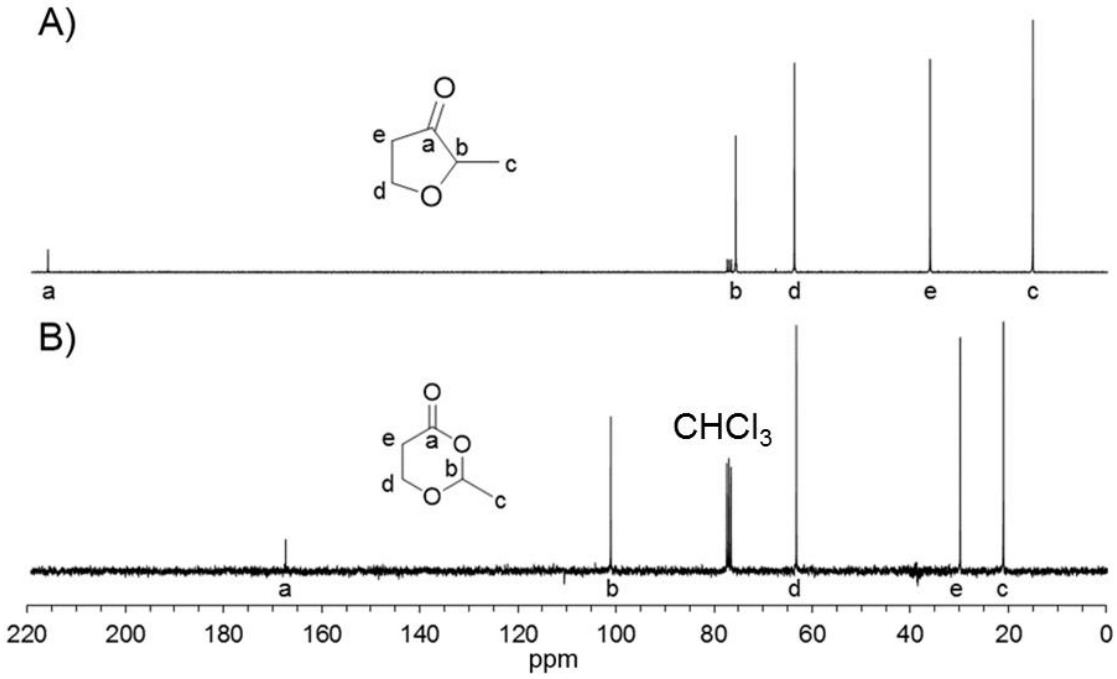

Figure 2.6. ^{13}C NMR spectra and structural assignments for A) 2-methyltetrahydrofuran-3-one starting material and B) MDO monomer after purification from Baeyer-Villiger oxidation of the furanone precursor.

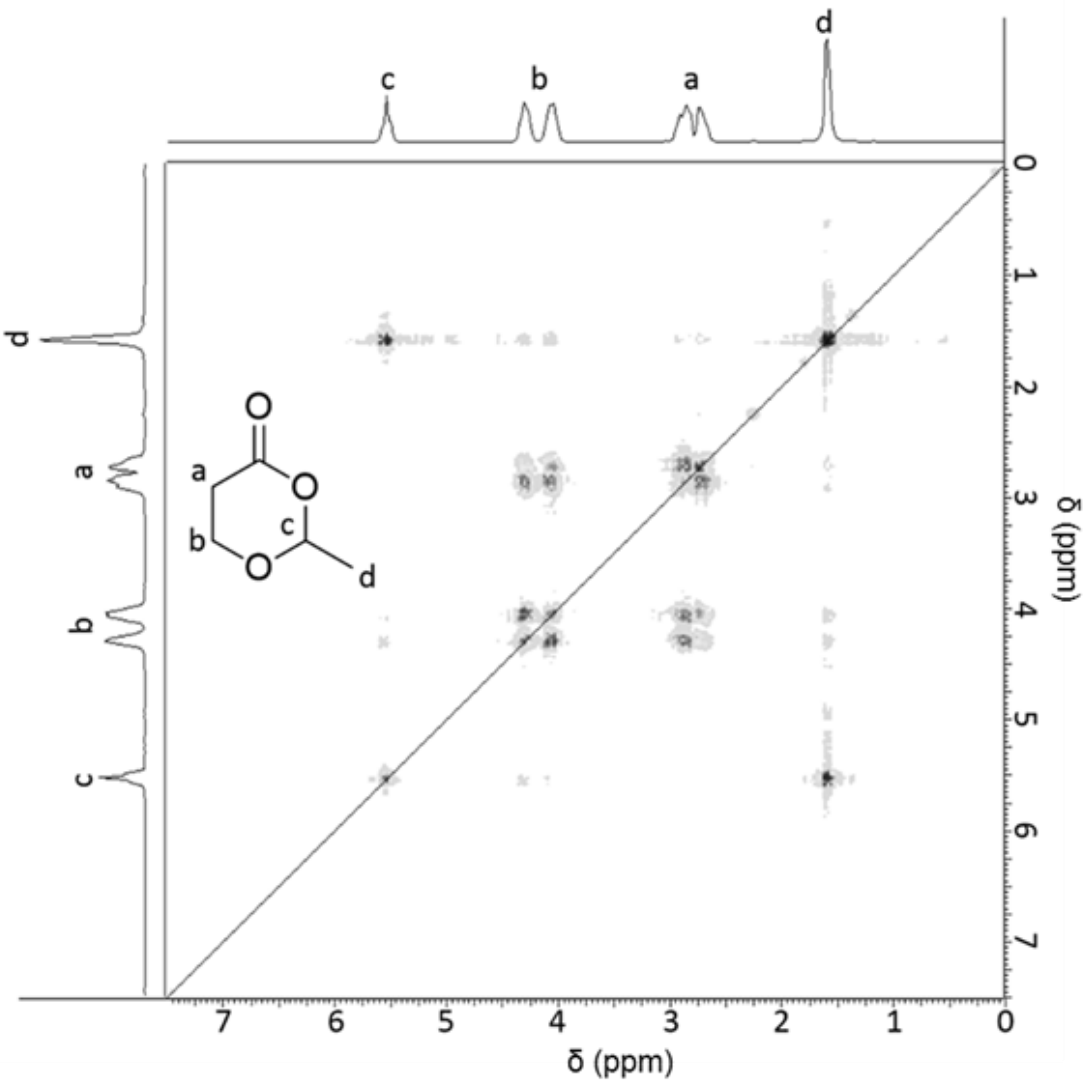

Figure 2.7. COSY spectrum of MDO with corresponding assignments.

Synthesis of PHPA and PMDO

Polymerizations using diethyl zinc catalyst for ROP of MDO were set up in a dry box using flame-dried glassware with a Teflon stir bar and were sealed prior to removal from the box. For a typical polymerization, racemic MDO monomer (generally 1.5 g) was added to a pressure vessel. An appropriate amount of benzyl alcohol initiator was added to target the desired molar mass, using an ultimate conversion of 55% for PMDO and 80% for PHPA for calculations. Diethyl zinc catalyst (1.0 M in hexanes), typically using circa $[Et_2Zn]_0$:$[BnOH]_0$ = 0.02:1 for high-acetal PMDO and $[C]_0$:$[I]_0$ = 2:1 for low-acetal PHPA, was then added to the reaction mixture via micro syringe. The reaction vessels were sealed, removed from the glove box and allowed to stir at the desired temperature. Aliquots removed for analysis by SEC and ^{1}H NMR spectroscopy were obtained in the glove box. To quench the catalyst, reaction vessels were opened to air, and the reaction mixture was dissolved in CH_2Cl_2. Polymers were then precipitated by drop wise addition of the dissolved reaction mixture into 9:1 hexanes: THF, and dried under vacuum. For a representative sample of PHPA: ^{1}H NMR ($CDCl_3$): δ 7.31 (m, 0.028 H, *Ph*-CH_2-O-), 5.10 (s, 0.012 H, Ph-C*H*$_2$-O-), 4.35 (t, *J* = 3.6 Hz, 2 H, –C(O)-C*H*$_2$-CH_2-O-), 2.65 (t, *J* = 3.6 Hz, 2 H, –C(O)-CH_2-C*H*$_2$-O-). ^{13}C NMR ($CDCl_3$): δ 170.45, 60.25, 33.76. For a representative sample of PMDO: ^{1}H NMR ($CDCl_3$): δ 7.31 (m, 0.075 H, *Ph*-CH_2-O-), 5.92 (q, 1 H, *J* = 5 Hz, -O-C*H*(CH_3)-O-), 4.85 (q, 0.014 H, *J* = 5.5 Hz, Ph-CH_2-O-C(CH_3)*H*-O-), 4.65 (d, 0.014 H, *J* = 11.5 Hz, Ph-C*H*$_2$-O-), 4.52 ppm (d, 0.014 H, *J* = 11.5 Hz, Ph-C*H*$_2$-O-), 3.93 (ddd, *J* = 16.5, 10.5, 5 Hz, 1 H, -C(O)-CH_2-C*H*$_2$-O-), 3.8 (ddd, *J* = 16, 11, 5 Hz, 1 H, -C(O)-CH_2-C*H*$_2$-O-), 2.57 (dd, J_1 = J_2 = 6 Hz, 2 H, -C(O)-C*H*$_2$-CH_2-O-), 1.33 (d, *J* = 5.4 Hz, 3 H, -O-CH(C*H*$_3$)-O-). ^{13}C NMR ($CDCl_3$): δ 171.04, 96.59, 64.50, 32.23, 20.84.

Table 2.1. Several polymers were synthesized by bulk polymerization of 2-methyl-1,3-dioxan-4-one (MDO) monomer using diethyl zinc catalyst and benzyl alcohol initiator. At high catalyst loadings, nearly all acetal groups were eliminated as acetaldehyde, resulting in PHPA. The targeted number average degree of polymerization for each polymer is indicated by the number in the sample name.

Sample	M_n, NMR (kg/mol)	M_n, SEC (kg/mol)	$Đ$	Repeat (ESI-MS)	% acetal (NMR)	T_g (°C)	T_m (°C)
HPA110	8	8*	1.14*	72.02	<1	-34	59
HPA131	9.5	9*	1.22*	72.02	<1	-31	73
HPA594	43	35*	1.23*	72.02	<1	-28	77

*Using $CHCl_3$ SEC calibrated with polystyrene standards.

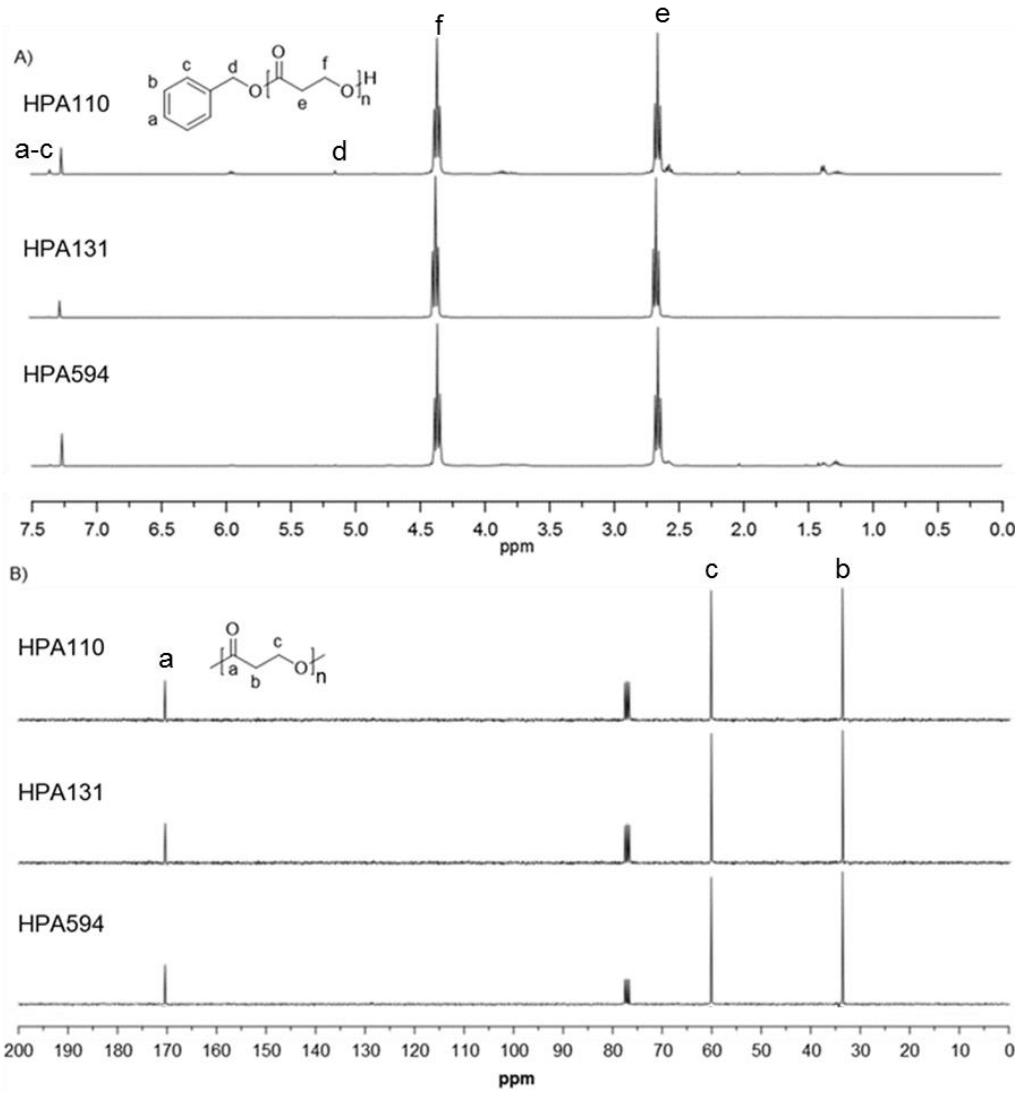

Figure 2.8. NMR spectra and structural assignments for several molar masses of PHPA synthesized by bulk polymerization of MDO using diethyl zinc catalyst and benzyl alcohol initiator with peak assignments for A) ^{1}H and B) ^{13}C spectra.

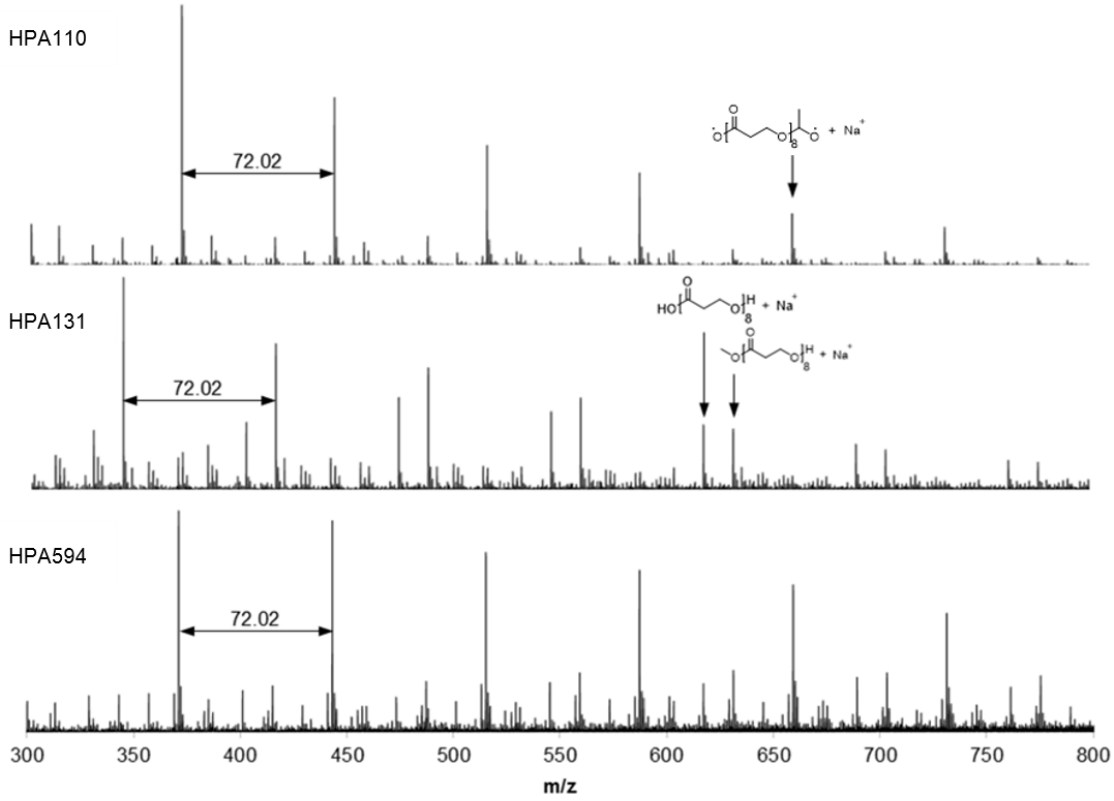

Figure 2.9. Electrospray ionization (ESI-MS) mass spectra of PHPA for several molar masses using 9:1 MeOH:CH_2Cl_2, where the numbers in sample names indicate the number-average degree of polymerization. The repeat unit of m/z = 72.02 found in all polymers is consistent with a molecule lacking acetal functionality, resulting in a 3-HPA repeat unit. High molar mass peaks were not observed, potentially as a result of polymer fragmentation during ionization. Exact m/z values for all polymers were consistent with retention of a single acetal, possibly as an "uneliminated" end group. For HPA131 and HPA594, a peak consistent with a methanol adduct could also be observed.

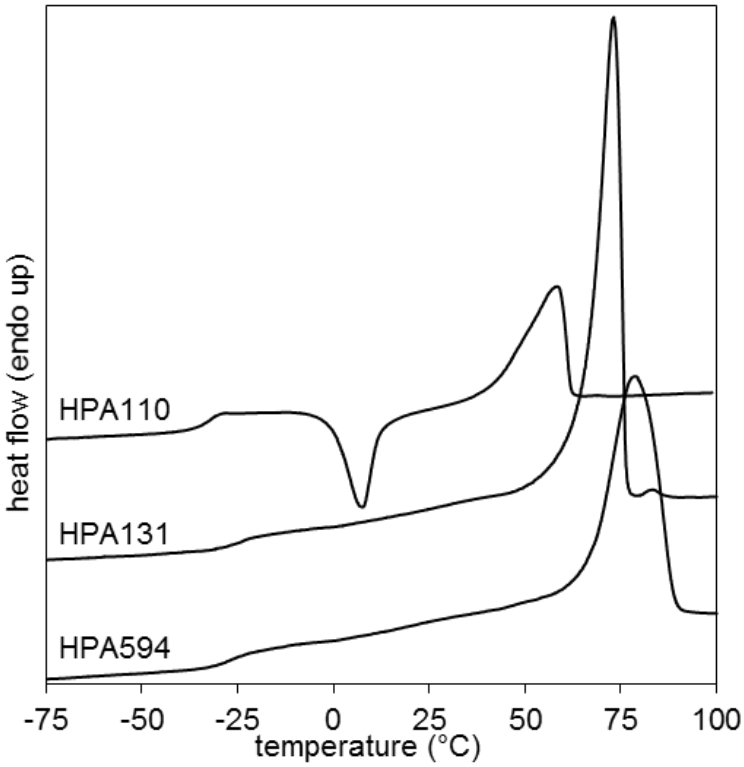

Figure 2.10. DSC thermograms for PHPA samples, with the numbers in sample names indicating the number-average degree of polymerization. Clear melting transitions (T_m) were apparent for these polymers, ranging from 58 °C to 79 °C, indicating crystallinity. The glass transition temperature (T_g) was quite low, ranging from -27 °C to -33 °C. Traces have been shifted vertically to aid visual comparison but relative peak heights and slopes have not been adjusted.

Table 2.2. Several polymers were synthesized by bulk polymerization of MDO. At low catalyst loadings, the acetal group was retained, resulting in PMDO. The targeted number average degree of polymerization for each polymer is indicated by the number in the sample name.

Sample	M_n, NMR (kg/mol)	M_n, SEC (kg/mol)	$Đ$	Repeat (ESI-MS)	% acetal (NMR)	T_g (°C)	T_m (°C)
MDO66	7.6	8*	1.62*	116.05	>98	-32	-
MDO77	9	11*	1.62*	116.05	>98	-25	-
MDO259	30	34*	1.61*	116.05	>98	-31	-

*Using THF SEC calibrated with polystyrene standards

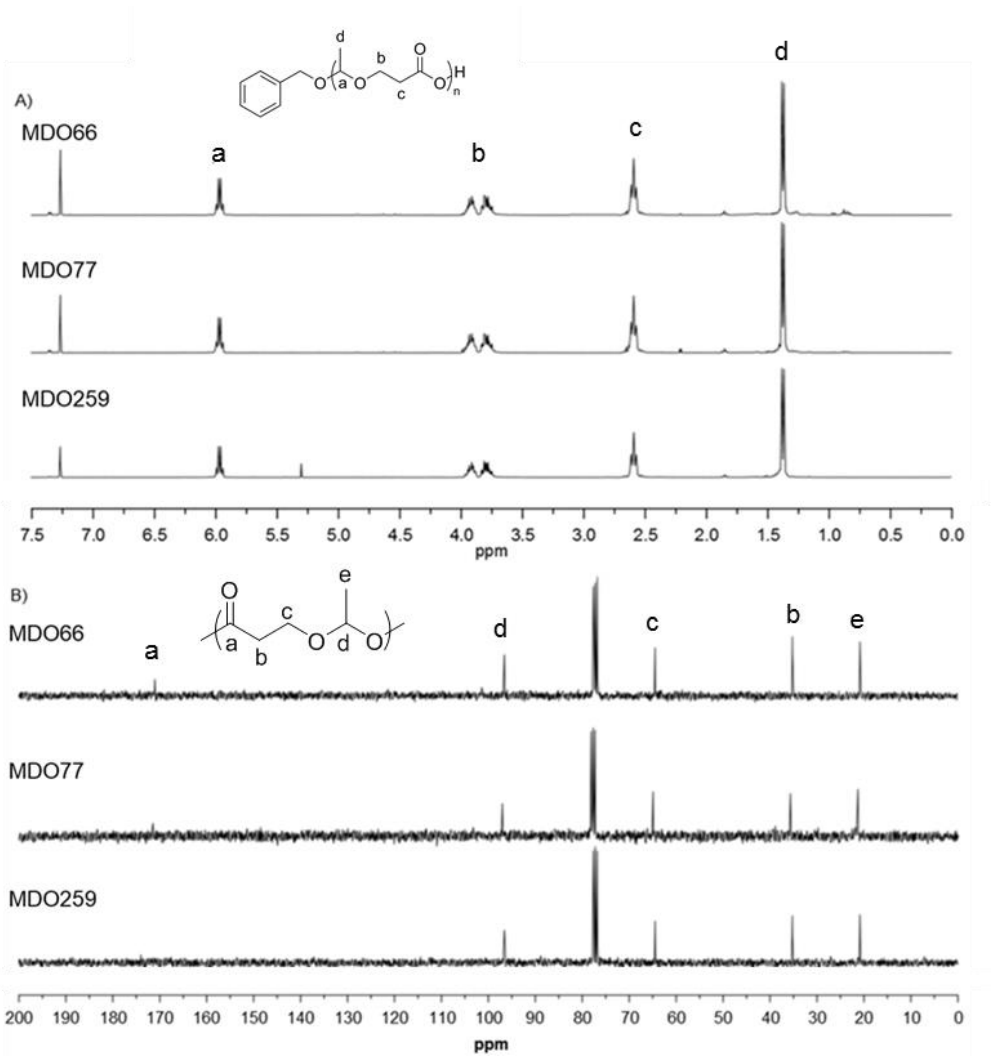

Figure 2.11. NMR spectra and structural assignments for several molar masses of PMDO synthesized by bulk polymerization of MDO using diethyl zinc catalyst and benzyl alcohol initiator with peak assignments for A) ^{1}H and B) ^{13}C spectra. The number in sample names refers to the number-average degree of polymerization.

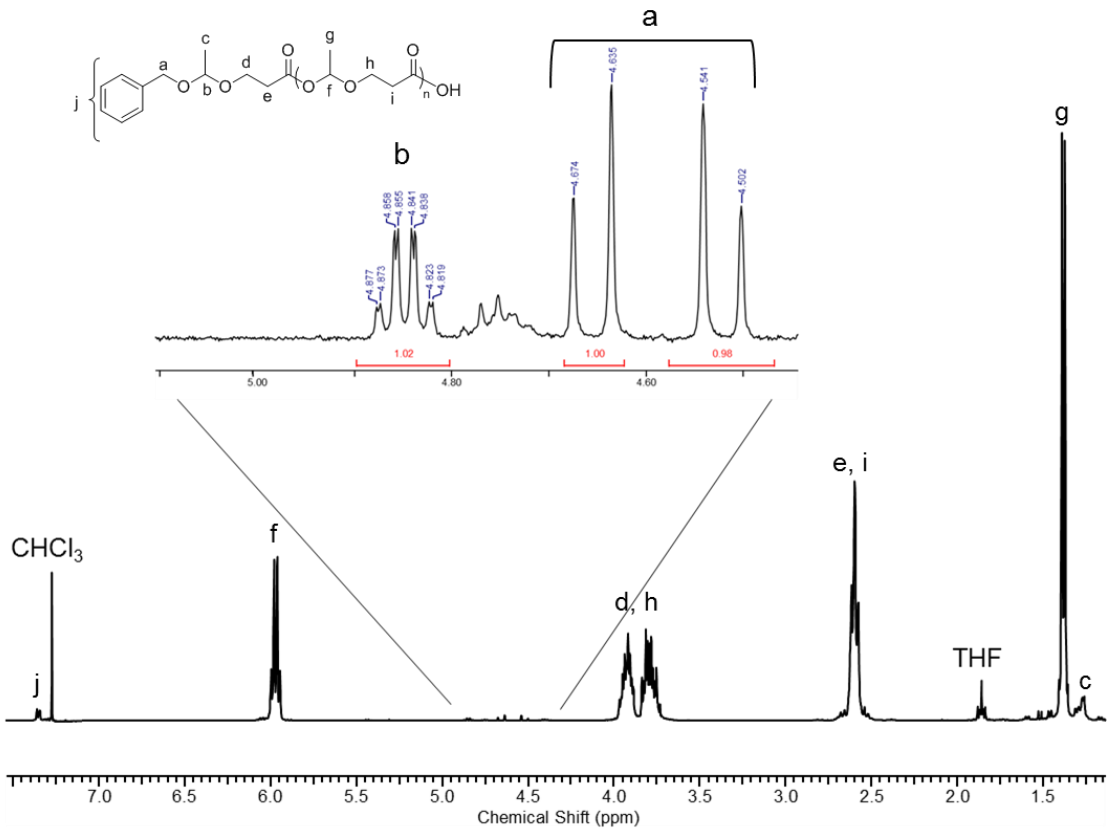

Figure 2.12. ^{1}H NMR spectrum of precipitated PMDO. The region corresponding to the end group methylene and methine protons have been magnified. The apparent splitting of the quartet at 4.85 ppm can be attributed to the different possible stereoisomers. Furthermore, identical signals appearing in very close proximity but at relative low intensity to the polymer backbone peaks can also be attributed to different possible stereoisomers arising from the acetal sterocenter along the backbone.

Evidence for a Propagating Zinc Carboxylate Species in the Formation of PMDO

To test the possibility of a propagating zinc carboxylate species two experiments were carried out.

1. In the glove box 500 mg of MDO was weighed into a scintillation vial equipped with a stir bar. Then 1 μL of 1 M diethylzinc was added directly into the monomer via microsyringe, followed by a spatula tip (~1 mg) of benzoic acid. The solution was capped and allowed to stir in the glove box for 16 hours. The viscous liquid was dissolved in methylene chloride and precipitated into 9:1 hexanes/THF and dried. A sample was removed for ^{1}H NMR analysis which verified the formation of PMDO and the presence of a benzoic ester endgroup.
2. To study the initiation step in PMDO synthesis, 1 equivalent of MDO (250 mg) was combined with 1 equivalent of benzyl alcohol (0.23 mL) at low zinc concentration (1.7 mM) in a scinitillation vial in the glove box. The solution was stirred for 16 hours and then an aliquot was removed to study the species present. Analysis of the corresponding ^{1}H NMR spectrum revealed the presence of multiple species, including residual monomer and benzyl alcohol. The mixture was separated via flash column chromatography (60:1 silica/sample, gradient elution from 7:3 hexanes/EtOAc to 4.5:5.5 hex:EtOAc) to isolate the major species, which were then identified as 3-(1-(benzyloxy)ethoxy)propanoic acid and benzyl 3-hydroxypropanoate. Referencing back to the crude mixture the ratio of 3-(1-(benzyloxy)ethoxy)propanoic acid to benzyl 3-hydroxypropanoate was 1.2. For 3-(1-(benzyloxy)ethoxy)propanoic acid: ^{1}H NMR ($CDCl_3$): δ 7.35 (m, 5 H, *Ph*-CH_2-O-), 4.85 (q, J = 5.5 Hz, 1 H, Ph-CH_2-O-C(CH_3)*H*-O-), 4.65 (d, J = 12

Hz, 1 H, Ph-C(H)*H*-O-), 4.55 (d, *J* = 12 Hz, 1 H, Ph-C(*H*)H-O-), 3.90 (dt, *J* = 10, 6 Hz, 1 H, Ph-CH_2-O-C(H)CH_3-O-C(H)*H*-), 3.78 (dt, *J* = 10, 6 Hz, 1 H, Ph-CH_2-O-C(H)CH_3-O-C(*H*)H-), 2.63 (t, *J* = 6 Hz, 2 H, Ph-CH_2-O-C(H)CH_3-O-C(H)H-CH_2-), 1.37 (d, *J* = 5.5 Hz, 3 H, Ph-CH_2-O-C(H)CH_3-O-). For benzyl 3-hydroxypropanoate: ^{1}H NMR ($CDCl_3$): δ 7.35 (m, 5 H, *Ph*-CH_2-O-), 5.16 (s, 2 H, Ph-CH_2-O-), 3.88 (t, *J* = 6 Hz, 2 H, Ph-CH_2-O-C(O)-CH_2-CH_2-OH), 3.5 (bs, 1 H, Ph-CH_2-O-C(O)-CH_2-CH_2-O*H*), 2.62 (t, *J* = 6 Hz, 2 H, Ph-CH_2-O-C(O)-CH_2-).

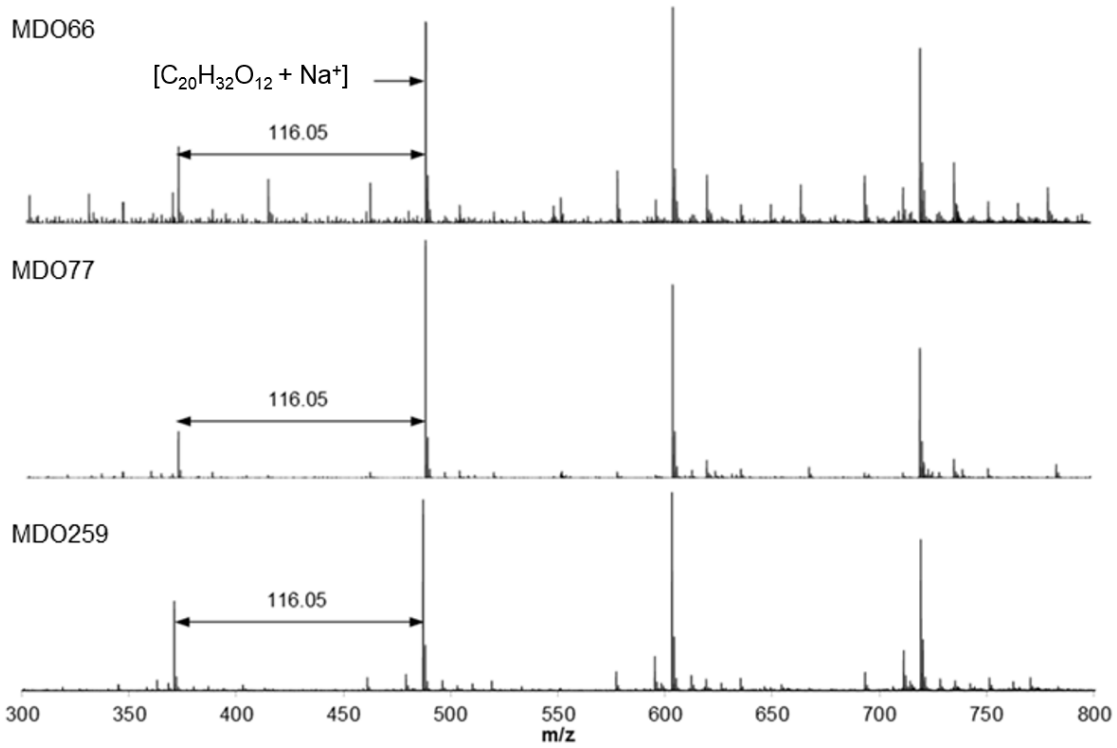

Figure 2.13. ESI-MS in 9:1 MeOH: CH_2Cl_2 for several molar masses of PMDO, with numbers in the sample names indicating the number-average degree of polymerization. As with PHPA samples, high molar mass ions were not observed, but the repeat unit is consistent with retention of the acetal functionality.

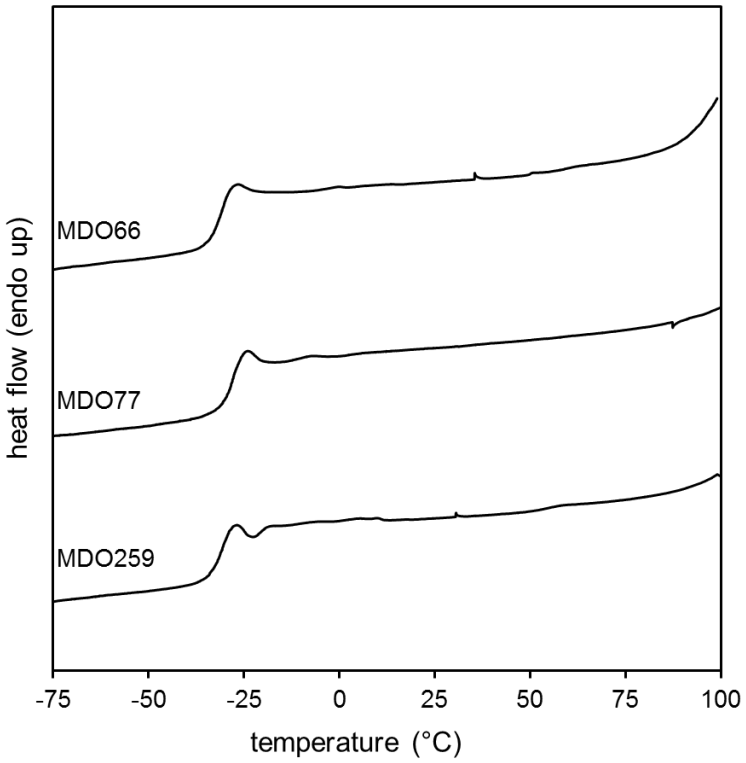

Figure 2.14. DSC thermograms for PMDO samples, with the numbers in sample names indicating the number-average degree of polymerization. Unlike PHPA, no significant crystallinity was observed in PMDO samples, as evidenced by the lack of a melting endotherm. The endotherm in MDO66 at high temperature was attributed to decomposition. The glass transition temperature (T_g) for PMDO, like that of PHPA polymers, was quite low, ranging from –26 °C to –32 °C. Traces have been shifted vertically to aid visual comparison.

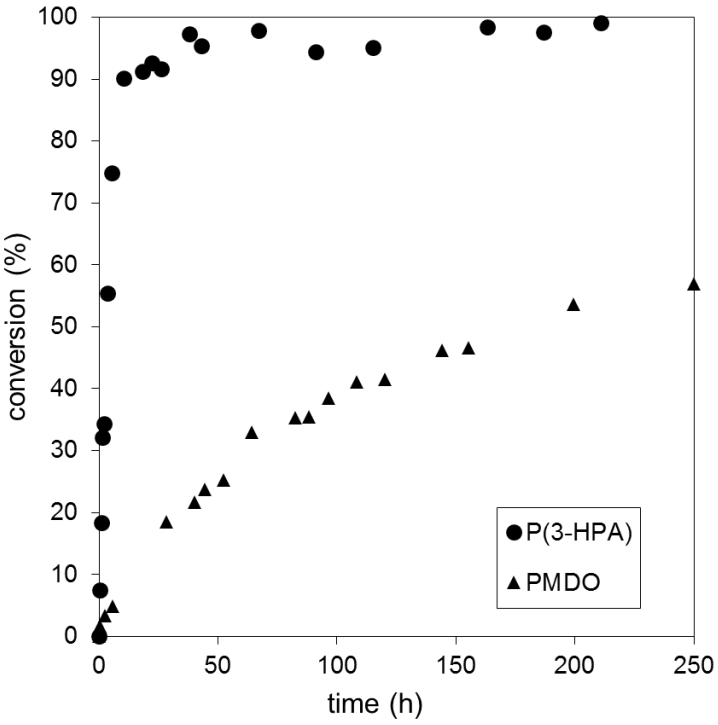

Figure 2.15. Bulk polymerization of MDO to PMDO and PHPA respectively as determined by ^{1}H NMR spectroscopy of quenched aliquots. For polymerization of MDO to PHPA, $[MDO]_o$ = 9.3 M, $[ZnEt_2]_o$ = 87 mM, and $[BnOH]_o$ = 46 mM. For polymerization of MDO to PMDO, $[MDO]_o$ = 10 M, $[ZnEt_2]_o$ = 1 mM), and $[BnOH]_o$ = 50 mM. The lower $[MDO]_0$ value in the polymerization to PHPA results from the added volume of hexanes originating from the 1 M solution of diethylzinc in hexanes.

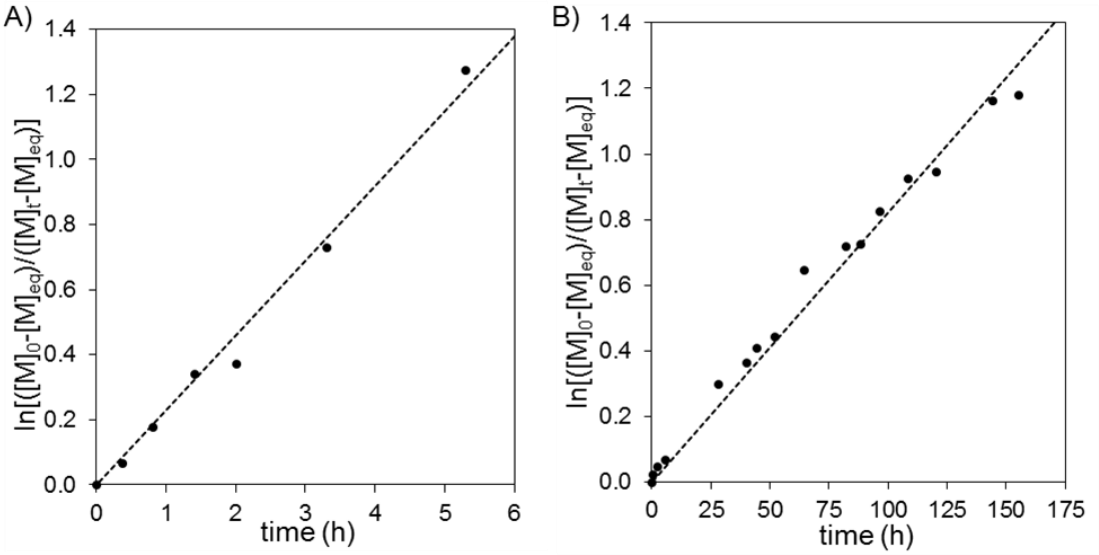

Figure 2.16. Bulk polymerizations of MDO shown in Figure 2 were tracked by ^{1}H NMR to determine pseudo-first order rate constants at 23 °C under both high-catalyst conditions leading to PHPA (A, $[ZnEt_2]_0$ = 87 mM), and low-catalyst conditions leading to PMDO (B, $[ZnEt_2]_0$ = 1 mM). Using $[M]_{eq}$ = 0 M for the high-catalyst polymerization, it was determined that k_{app} = 0.24 h^{-1}. Using $[M]_{eq}$ = 4.53 M for the low-catalyst polymerization, it was determined that k_{app} =0.0079 h^{-1}. For polymerization to PHPA, $[MDO]_0$ = 9.3 M and $[BnOH]_0$ = 46 mM. For polymerization to PMDO, $[MDO]_0$ = 10 M and $[BnOH]_0$ = 50 mM.

In Situ Monitoring of Acetaldehyde Elimination

To monitor byproduct formation, a polymerization was performed as a 1 M solution in dry CD_2Cl_2. The solvent (750 μL) was added to a flame-dried round-bottom flask containing a Teflon-coated stir bar. MDO was then added (to [MDO] = 1 M) followed by benzyl alcohol (to [BnOH] = 10 mM). After stirring for 10 min, diethylzinc was added (1 M in hexanes, to $[ZnEt_2]$ = 20 mM). This solution was allowed to mix for 5 minutes, then loaded into a dry NMR tube and sealed in the glove box. Over the next several hours, ^1H NMR spectra of the reaction were periodically collected and used to monitor polymerization and byproducts.

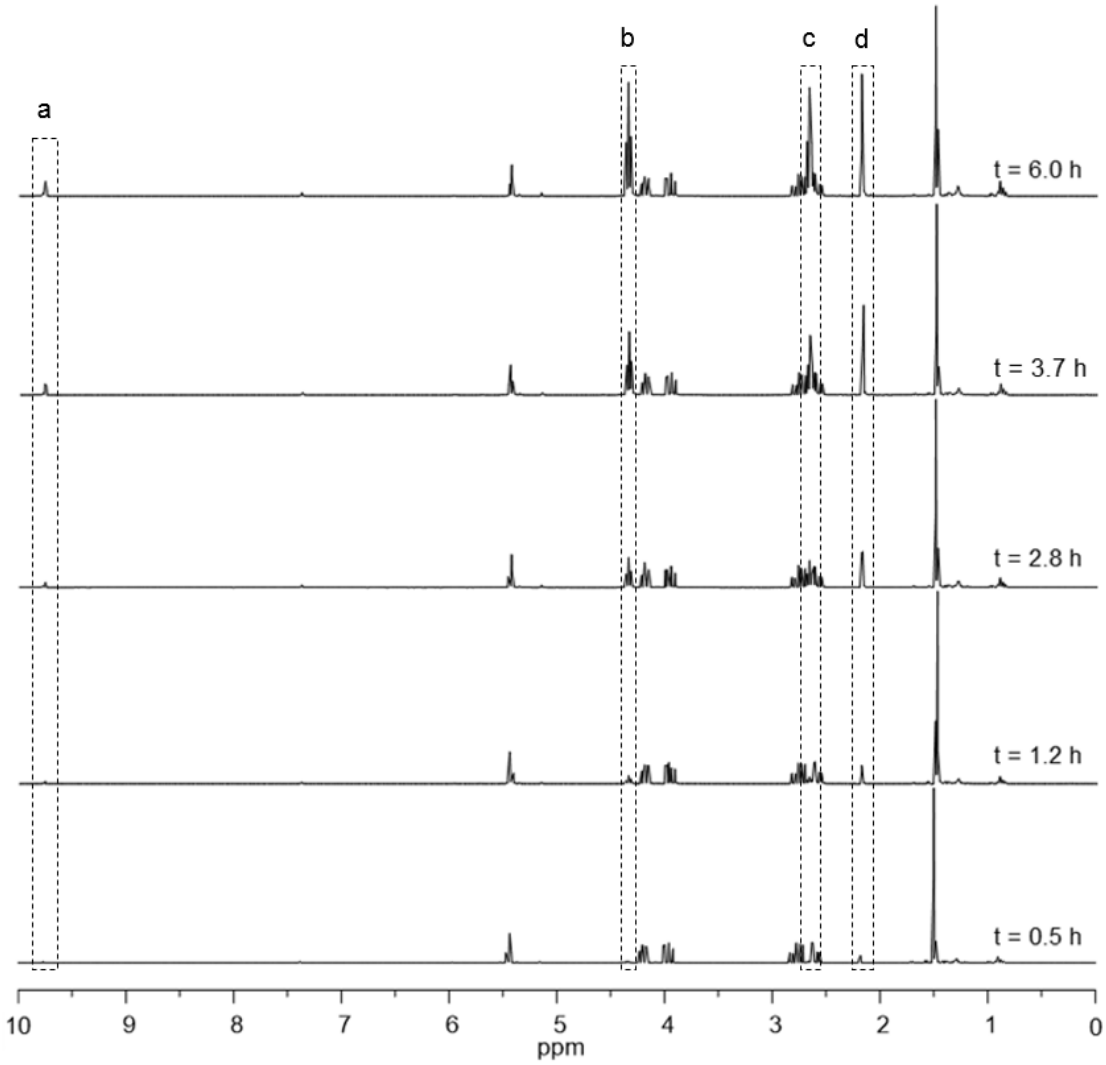

Figure 2.17. To investigate the loss of the MDO acetal functionality, the polymerization of MDO to PHPA was performed in CD_2Cl_2 to allow *in situ* tracking of byproducts using ^1H NMR spectroscopy. As the polymerization proceeded, the increase in resonances from PHPA methylene protons at 4.35 (b) and 2.65 ppm (c) was accompanied by a commensurate increase in resonances at δ = 9.77 (a) and 2.18 (d) ppm consistent with acetaldehyde. Polymerizations were conducted using $[MDO]_o$ = 1 M, $[BnOH]_o$ = 10 mM, and $[ZnEt_2]_o$ = 20 mM at room temperature.

Control Experiment with Butyraldehyde

To probe whether aetaldehyde was reversibly eliminated during the formation of PMDO, a control polymerization was carried out in the presence of butyraldehyde. In the glove box 500 mg MDO, 4.4 μL BnOH, ca. 50 mg butyraldehyde, and 0.8 μL Et_2Zn were added to a scintillation vial equipped with a stir bar. The reaction mixture was sealed and allowed to stir at room temperature over 4 days. The vial was then removed from the glove box, opened to air, and a small aliqout diluted with 0.65 mL $CDCl_3$ for ^1H NMR analysis. The spectrum showed formation of PMDO, as well as sequences of HPA, and resonances corresponding to butyraldehyde. However, no resonances consistent with incorporation of the foreign aldehyde into the polymer was observed. It was thus concluded that acetaldehyde was not eliminated and reincorporated during polymerization to PMDO.

Density Measurements

The density of MDO was measured by determining the mass of known volumes of the monomer dispensed by a calibrated micropipette. Nine separate measurements were taken to determine ρ_{MDO} = 1.183 ± 0.018 g/mL. To measure the density of PMDO, a volumetric flask with a fritted glass cap was filled with cyclohexane, a poor solvent for PMDO. The flask was capped, any bubbles excluded, excess cyclohexane allowed to evaporate until mass measurements stabilized for 30 s, and then the mass of cyclohexane and flask was recorded. A known mass of PMDO was then added to the flask and the vessel was again capped, which displaced a volume of cyclohexane. This cyclohexane was wiped off and the solvent residue was allowed to evaporate until the mass had again stabilized for 30 s. The mass of the flask, the remaining cyclohexane and the added polymer was then

measured. The volume of the excluded cyclohexane and the density of the polymer were calculated using ρ_{CHX}= 0.7781 g/mL and the known mass of the added polymer. This measurement was carried out four times (n=4) to determine that the density of PMDO at room temperature was 1.421 ± 0.072 g/mL. For calculations involving the density of PHPA, the room temperature density of the polymer was taken to be 1.38 g/mL based on literature values.[72]

Thermodynamic Characterization

To explore the source of the limited conversion observed for PMDO, a series of experiments were conducted to measure equilibrium monomer conversions of identical reaction mixtures at a variety of temperatures. In a sample reaction, 1 g (8.62 mmol) of MDO was combined with 8.9 μL of (89 μmol) benzyl alcohol in the glove box and allowed to mix thoroughly for approximately 10 minutes. 1.7 μL of $ZnEt_2$ (1 M in hexanes, 1.7 μmol) was then added and allowed to mix for an additional 10 minutes. The reaction was then split into four separate reaction vessels, each of which was sealed. These were brought to temperatures ranging from 23 °C to 60 °C and stirred for at least 14 days. The vessels were opened to air, the reaction mixture dissolved in $CDCl_3$, and the fraction of remaining monomer determined using ^{1}H NMR spectroscopy. From these experiments, $[M]_{eq}$ values for a given temperature were calculated using ρ_{MDO} = 1.183 g/mL and ρ_{PMDO} = 1.421 g/mL. Values of $[M]_{eq}$ for each temperature were measured in at least three separate experiments. Integrations used to determine monomer conversion in ^{1}H NMR spectra (methylene protons from MDO at δ = 4.22 ppm and PMDO at δ = 3.76 ppm as well as methyl protons from MDO at 1.52 ppm, and PMDO at 1.33 ppm) did not change appreciably over several

days, suggesting depolymerization was not a significant factor after opening to air and dilution. Equation [1] was then used to determine the thermodynamic parameters ΔH_p and ΔS_p from equilibrium monomer concentration measurements (Figure S12), where $[M]_s$ was taken to be 1 M.

$$R \ln\left(\frac{[M]_{eq}}{[M]_s}\right) = \Delta H_p \left(\frac{1}{T}\right) - \Delta S_p \qquad [1]$$

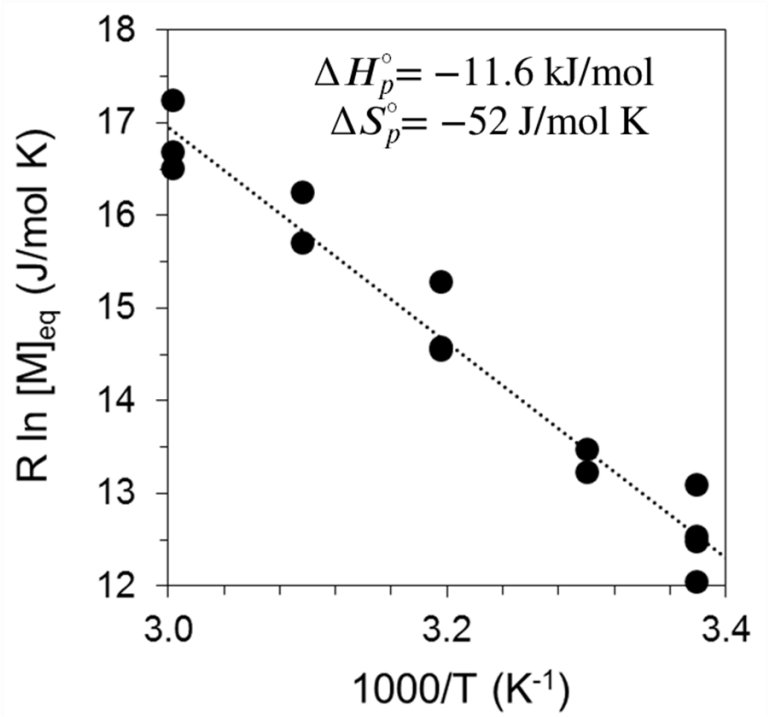

Figure 2.18. Thermodynamics of the ring-opening polymerization of MDO to PMDO. Parallel polymerizations were performed in the bulk using [BnOH]o = 220 mM and [ZnEt2]o = 4 mM from 23 to 60 °C, with polymerizations allowed to proceed for at least two weeks to ensure that equilibrium had been reached before quenching at the reaction temperature. Final monomer conversions were used to calculate values of $[M]_{eq}$ at each temperature using ρ_{MDO} = 1.183 g/mL and ρ_{PMDO} = 1.421 g/mL. Using these data it was possible to calculate ΔH_p = -11.6 kJ/mol and ΔS_p = -51.8 J/mol K.

As a control experiment to determine if the value of $[M]_{eq}$ would shift reversibly with temperature, a polymerization was set up as described for the above equilibrium experiments but not initially split into separate reaction vessels. This reaction was allowed to react at 40 °C for 7 days. An aliquot taken from the reaction at this point showed that 43% of MDO had been converted to PMDO over 7 days ([M] = 6.3 M). In a glove box, the viscous liquid was split into two vessels which were each sealed and allowed to react for an additional 14 days, one at room temperature and one at 60 °C. The vessels were then opened, the reaction mixture dissolved in $CDCl_3$, and conversion measured by ^1H NMR spectroscopy, from which values of [M] were determined. The conversion of the room temperature reaction reached 58% ([M] = 4.7 M) while the polymerization at 60 °C reached 33% ([M] = 7.2 M). These values were consistent with $[M]_{eq}$ values measured in samples heated directly to these temperatures and indicated that equilibrium monomer concentration could be reversibly shifted by a change in temperature.

Catalyst Activity

To verify that the diethyl zinc catalyst was not deactivated after extended time periods, a bulk polymerization was set up using 1 g of MDO under conditions yielding PMDO ($[ZnEt_2]_0$ = 2 mM, $[BnOH]_0$ = 100 mM). The reaction was sealed and allowed to proceed for 21 days at room temperature. An aliquot of the viscous liquid was taken and found to have reached 58 % conversion (by ^1H NMR spectroscopy, degree of polymerization 58, and apparent molar mass 4.5 kg/mol by SEC). The liquid was then split into two separate reaction vessels and monomer (approximately 0.5 g) added to one portion. Both were sealed and allowed to react for an additional 5 days at room temperature

before opening to air. The sample with no additional monomer maintained the same conversion of MDO at 21 days and had an apparent molar mass of 4.6 kg/mol by SEC. The sample with additional monomer had an increased degree of polymerization (74 by ^{1}H NMR spectroscopy) and its apparent molar mass by SEC had increased to 11.0 kg/mol. This increase suggests that the catalyst remains active even after weeks in the reaction medium.

Initial Rates Studies

To study the rate of formation of PHPA as a function of catalyst reactions were set up on a scale of 250 mg MDO with a monomer to initiator ratio of 100. A stock solution of monomer and initiator was prepared to run multiple reactions in parallel. Into separate scintillation vials the appropriate amount of a 1 M solution of diethylzinc was dispensed and the hexanes were allowed to evaporate under the inert atmosphere. The mass loss was monitored using a scale in the glove box. To the pure diethylzinc solution was then added the stock solution of MDO and BnOH and aliquots were removed every so often for analysis by ^{1}H NMR spectroscopy.

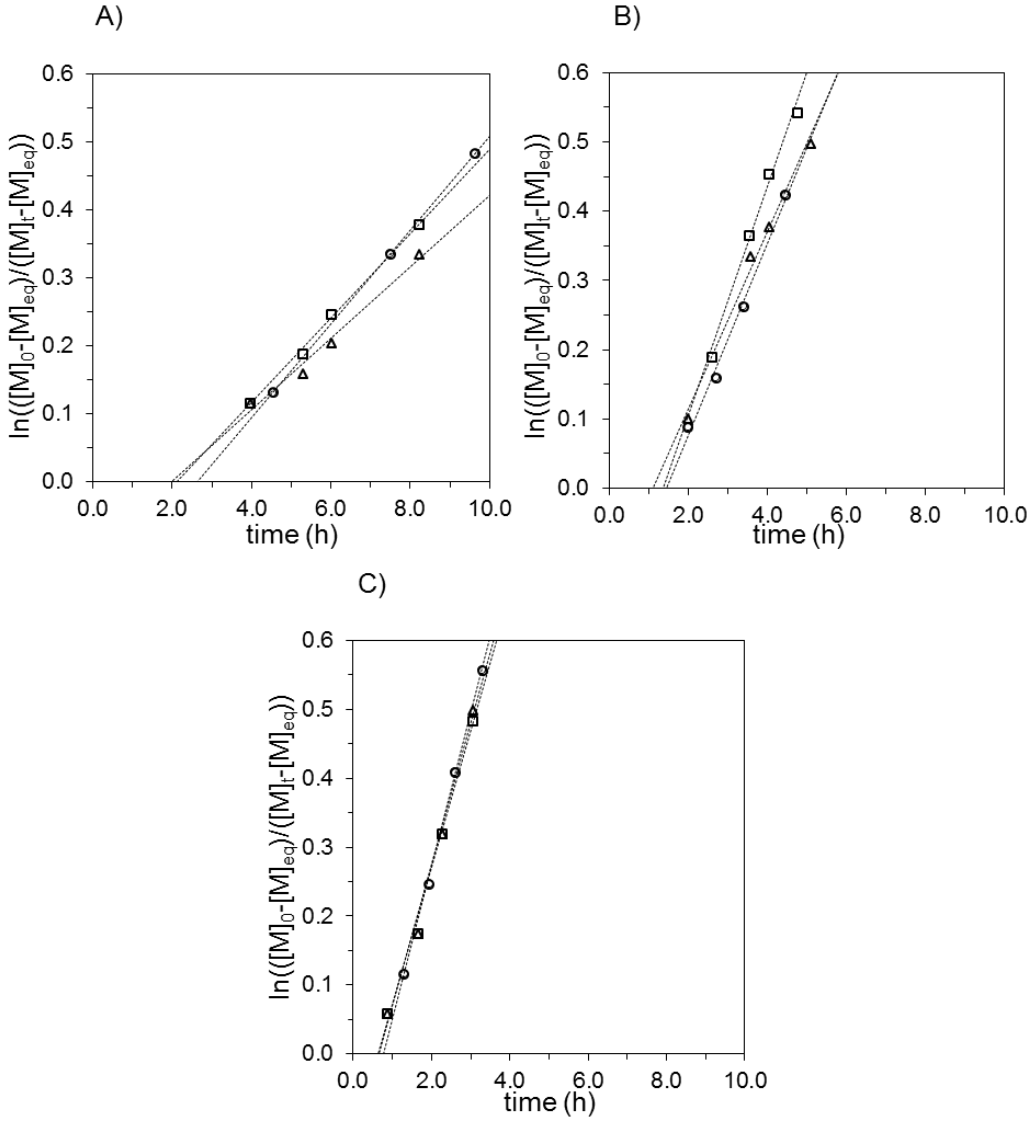

Figure 2.19. Plots of kinetic data used to extract values of k_{app} at several values of $[ZnEt_2]_0$ with sufficiently low catalyst loadings to generate PMDO. Conditions: A) $[MDO]_0$ = 10.1 M, $[ZnEt_2]_0$ = 0.9 mM, $[BnOH]_0$ = 103 mM; B) $[MDO]_0$ = 10.1 M, $[ZnEt_2]_0$ = 1.9 mM, $[BnOH]_0$ = 103 mM; C) $[MDO]_0$ = 10.1 M, $[ZnEt_2]_0$ = 3.7 mM, $[BnOH]_0$ = 102 mM. All experiments were conducted under a nitrogen atmosphere and conversion was tracked by ^{1}H NMR spectroscopy. The catalyst, received as a 1 M solution in hexanes, was added directly into a mixture of monomer and initiator. Aliquots were periodically removed from the glove box, immediately diluted with 0.65 mL $CDCl_3$, and analyzed by ^{1}H NMR. Dotted lines are linear fits to the data, the slopes of which used to determine k_{app} for each experiment shown in Figure 3 using $[M]_{eq}$ = 4.53 M. Observed induction times may be rationalized by a slower rate of initiation of zinc benzyl alkoxide with MDO when compared to the rate of propagation of zinc alkoxide with monomer.

To study the rate of formation of PHPA as a function of catalyst reactions were set up on a scale of 500 mg MDO with a monomer to initator ratio of 100. A stock solution of monomer and initiator was prepared to run multiple reactions in paralell. The stock solution was split into different vials to which the appropriate amount of diethylzinc (1 M in hexanes) was added via microsyringe (directly into the monomer/initiator solution). Aliquots were removed every so often for analysis by ^{1}H NMR.

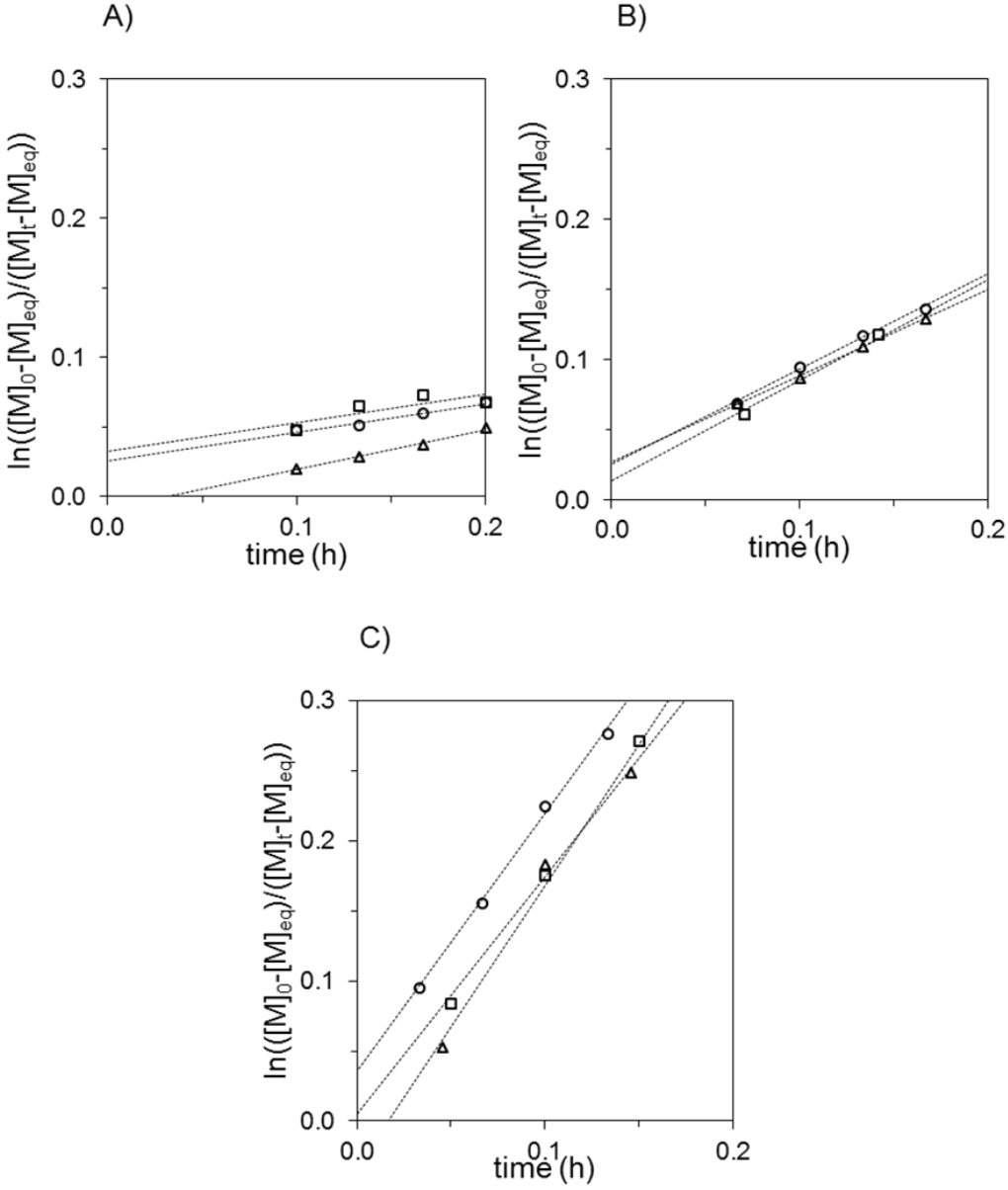

Figure 2.20. Plots of kinetic data used to extract values of k_{app} at several values of $[ZnEt_2]_0$ with sufficiently high catalyst loadings to generate PHPA. A) $[MDO]_0$ = 10.1 M, $[Et_2Zn]_0$ = 33 ± 6 mM, $[BnOH]_0$ = 97 ± 20 mM. B) $[MDO]_0$ = 101. M, $[ZnEt_2]_0$ = 48 ± 3 mM, $[BnOH]_0$ = 99 ± 6 mM; C) $[MDO]_0$ = 10.1 M, $[ZnEt_2]_0$ = 95 ± 2 mM, $[BnOH]_0$ = 97 ± 2 mM. All experiments were conducted under a nitrogen atmosphere and conversion was tracked by ^{1}H NMR. The catalyst, received as a 1 M solution in hexanes, was added to tared vials and the solvent was evaporated, which was asserted by the mass loss. Aliquots were periodically removed from the glove box, immediately diluted with 0.65 mL $CDCl_3$, and analyzed by ^{1}H NMR. Dotted lines are linear fits to the data, the slopes of which were used to determine k_{app} for each experiment shown in Figure 3 using $[M]_{eq} = 0$.

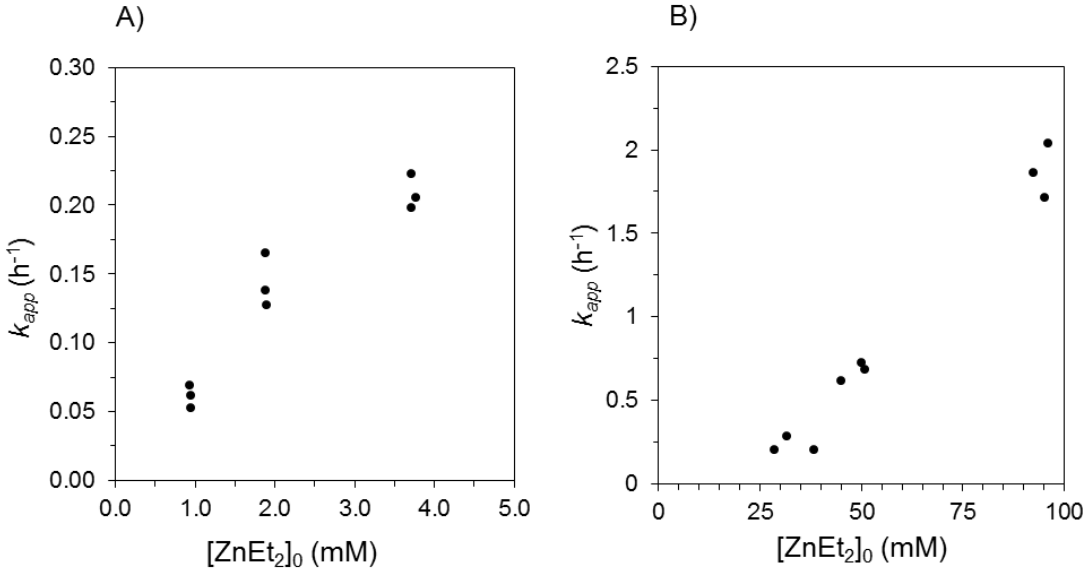

Figure 2.21. Kinetic plots of dependence of polymerization rate of MDO on $[ZnEt_2]_0$. Rate constants (k_{app}) were determined at various concentrations of $[ZnEt_2]_0$ from Figures S15 and S16 and plotted vs $[ZnEt_2]_0$. A) Formation of PMDO at low catalyst loadings, $[ZnEt_2]_0$ = 0.9 to 3.7 mM B) Formation of PHPA at high catalyst loadings, $[ZnEt_2]_0$ = 28 to 96 mM.

An important discovery made during the initial rate studies was that it was crucial to use the same batch of monomer throughout. Although the ^{1}H NMR and ^{13}C NMR of the monomer appeared very clean, liquid chromatography coupled to mass spectrometry (LC-MS) analysis revealed the presence of a low concentration of MDO oligomers, containing a 3-hydroxypropionate and a carboxylic acid end group. We were not able to quantify the exact amount of oligomers present in each monomer sample due to the variation in ionization efficiency between molecules. However, comparative analysis of different monomer batches revealed that the composition varied between monomer samples. We reasoned that based on the state of purity of the monomer by ^{1}H NMR the concentration of oligomeric material must be very low. Refrigeration of the monomer at –20 °C in the glove box prevented ongoing oligomerization/polymerization. However, during the initial rate

studies results varied slightly between monomer batches due to the variation in concentration of catalytic carboxylic acid.

Degradation

To track polymer degradation, samples of PHPA (M_n, SEC = 17.9 kg/mol) and PMDO (M_n, SEC = 8.1 kg/mol) were added to a series of 1 dram vials as thin films. Phosphate-citrate buffer (100 mM) at pH 7.4, 6.4, 5.4, or 4.4 was then added to each vial along with a Teflon-coated stir bar. The vials were then capped at stirred at room temperature. Periodically, a vial of each polymer and each pH was removed from stirring, the time noted, frozen, and lyophilized. The lyophilized polymer was then dissolved in solvent ($CHCl_3$ for PHPA or THF for PMDO), filtered through a 0.2 μm PTFE membrane, and analyzed by SEC to determine its apparent molar mass. This value was then plotted as a single point in the M_n versus time plot shown in Figure 4 for PMDO and PHPA.

References

1) Huck, W. T. S. *Mater. Today* **2008**, *11*, 24−32.

2) Liu, F.; Urban, M. W. *Prog. Polym. Sci.* **2010**, *35*, 3−23.

3) Hu, J.; Liu, S. *Macromolecules* **2010**, *43*, 8315−8330.

4) Hoffman, A. S. *Adv. Drug Delivery Rev.* **2013**, *65*, 10−16.

5) Meng, H.; Jinlian, H. *J. Intell. Mater. Syst. Struct.* **2010**, *21*, 859−885.

6) Roy, D.; Cambre, J. N.; Sumerlin, B. S. *Prog. Polym. Sci.* **2010**, *35*, 278−301.

7) Esser-Kahn, A. P.; Odom, S. A.; Sottos, N. R.; White, S. R.; Moore, J. S. *Macromolecules* **2011**, *44*, 5539−5553.

8) Petersen, M. A.; Hillmyer, M. A.; Kokkoli, E. *Bioconjug. Chem.* **2013**, *24*, 533−543.

9) Binauld, S.; Stenzel, M. H. *Chem. Commun.* **2013**, *49*, 2082−2102.

10) Petersen, M. A.; Yin, L.; Kokkoli, E.; Hillmyer, M. A. *Polym. Chem.* **2010**, *1*, 1281−1290.

11) Panyam, J.; Labhasetwar, V. *Adv. Drug Delivery Rev.* **2012**, *64, Supple*, 61−71.

12) Doane, T. L.; Clemens, B. *Chem. Soc. Rev.* **2012**, *41*, 2885−2911.

13) Faraji, A. H.; Wipf, P. *Biorg. Med. Chem.* **2009**, *17*, 2950−2962.

14) Pangburn, T. O.; Petersen, M. A.; Waybrant, B.; Adil, M. M.; Kokkoli, E. *J. Biomech. Eng.* **2009**, *131*, 074005−074005-20.

15) Levine, R. M.; Scott, C. M.; Kokkoli, E. *Soft Matter* **2013**, *9*, 985−1004.

16) Geisow, M. J.; Evans, W. H. *Exp. Cell Res.* **1984**, *150*, 36−46.

17) Tannock, I. F.; Rotin, D. *Cancer Res.* **1989**, *49*, 4373.

18) Ali Shah, A.; Hasan, F.; Hameed, A.; Ahmed, S. *Biotechnol. Adv.* **2008**, *26*, 246−265.

19) Miller, S. A. *ACS Macro Lett.* **2013**, *2*, 550−554.

20) Murthy, N.; Thng, Y. X.; Schuck, S.; Xu, M. C.; Fréchet, J. M. J. *J. Am. Chem. Soc.* **2002**, *124*, 12398−12399.

21) Zhang, L.; Bernard, J.; Davis, T. P.; Barner-Kowollik, C.; Stenzel, M. H. *Macromol. Rapid Commun.* **2008**, *29*, 123−129.

22) Lee, S. J.; Min, K. H.; Lee, H. J.; Koo, A. N.; Rim, H. P.; Jeon, B. J.; Jeong, S. Y.; Heo, J. S.; Lee, S. C. *Biomacromolecules* **2011**, *12*, 1224−1233.

23) Gillies, E. R.; Fréchet, J. M. J. *Chem. Commun.* **2003**, 1640−1641.

24) Penczek, S. *J. Polym. Sci., Part A Polym. Chem.* **2000**, *38*, 1919−1933.

25) Szymanski, R.; Kubisa, P.; Penczek, S. *Macromolecules* **1983**, *16*, 1000−1008.

26) Heller, J.; Penhale, D. W. H.; Helwing, R. F. *J. Polym. Sci. Polym. Lett. Ed.* **1980**, *18*, 293−297.

27) Tomlinson, R.; Klee, M.; Garett, S.; Heller, J.; Duncan, R.; Brocchini, S. *Macromolecules* **2002**, *35*, 473−480.

28) Schacht, E.; Toncheva, V.; Vandertaelen, K.; Heller, J. *J. Control. Release* **2006**, *116*, 219−225.

29) Jain, R.; Standley, S. M.; Fréchet, J. M. J. *Macromolecules* **2007**, *40*, 452−457.

30) Heffernan, M. J.; Murthy, N. *Bioconjug. Chem.* **2005**, *16*, 1340−1342.

31) Paramonov, S. E.; Bachelder, E. M.; Beaudette, T. T.; Standley, S. M.; Lee, C. C.; Dashe, J.; Fréchet, J. M. J. *Bioconjug. Chem.* **2008**, *19*, 911−919.

32) Heller, J.; Barr, J.; Ng, S. Y.; Abdellauoi, K. S.; Gurny, R. *Adv. Drug Delivery Rev.* **2002**, *54*, 1015−1039.

33) Khaja, S. D.; Lee, S.; Murthy, N. *Biomacromolecules* **2007**, *8*, 1391−1395.

34) Wolfe, P. S.; Wagener, K. B. *Macromol. Rapid Commun.* **1998**, *19*, 305−308.

35) Miller, S. A. Polyesteracetals. U.S. Patent 2009/066417, December 2, 2009.

36) Martin, R.T.; Camargo, L.P.; Miller, S.A. *Green Chemistry* **2014**, *16*, 1768−1773.

37) Yamashita, M.; Nishida, H. Process for Preparation of 1,3-Dioxane-4-one Compounds by Cyclization. JP 09194450 A 19970729, March 31, 1997.

38) Juge, S.; Genet, J.-P.; Mallart, S. Preparation of 1,3-dioxan-4-one Derivatives as Intermediates for Beta-Hydroxy-Alpha-Amino Acids. FR 2 632 642-A1, June 14, 1988.

39) Werpy, T.; Petersen, G.; Aden, A.; Bozell, J.; Holladay, J.; White, J.; Manheim, A.; Elliot, D.; Lasure, L.; Jones, S.; Gerber, M.; Ibsen, K.; Lumberg, L.; Kelley, S. *Top Value Added Chemicals from Biomass Volume I—Results of Screening for Potential Candidates from Sugars and Synthesis Gas*, Pacific Northwest National Laboratory and the National Renewable Energy Laboratory, 2004.

40) Lowe, J. R.; Martello, M. T.; Tolman, W. B.; Hillmyer, M. A. *Polym. Chem.* **2011**, *2*, 702−708.

41) Tsuruta, T.; Matsuura, K.; Inoue, S. *Die Makromol. Chemie* **1964**, *75*, 211−214.

42) Le Hellaye, M.; Fortin, N.; Guilloteau, J.; Soum, A.; Lecommandoux, S.; Guillaume, S. M. *Biomacromolecules* **2008**, *9*, 1924−1933.

43) Zhang, D.; Hillmyer, M. A.; Tolman, W. B. *Macromolecules* **2004**, *37*, 8198−8200.

44) Goodman, M.; Brandup, J. *J. Polym. Sci., Part A Gen. Pap.* **1965**, *3*, 327−340.

45) Kricheldorf, H. R. *Angew. Chem. Int. Ed.* **2006**, *45*, 5752−5784.

46) Deming, T. J. *J. Polym. Sci., Part A Polym. Chem.* **2000**, *38*, 3011−3018.

47) Nava, H. Methods of Preparing Polyesters from Cyclic Organic Carbonates in the Presence of Alkali Metal-Containing Catalysts. U.S. Patent 5,714,568, February 3, 1998.

48) Ramis, X.; Salla, J. M.; Manteco, A.; Gonza, L. *J. Appl. Polym. Sci.* **2009**, *111*, 1805−1811.

49) Deming, T. J. *J. Polym. Sci., Part A Polym. Chem.* **2000**, *38*, 3011−3018.

50) Greer, S. C. *Annu. Rev. Phys. Chem.* **2002**, *53*, 173−200.

51) Das, S. S.; Andrews, A. P.; Greer, S. C. *J. Chem. Phys.* **1995**, *102*, 2951−2959.

52) Zhuang, J.; Das, S. S.; Nowakowski, M. D.; Greer, S. C. *Physica A* **1997**, *244*, 522−535.

53) Poland, D. *J. Chem. Phys.* **1999**, *111*, 8214−8224.

54) Save, M.; Schappacher, M.; Soum, A. *Macromol. Chem. Phys.* **2002**, *203*, 889−899.

55) Martello, M. T.; Burns, A.; Hillmyer, M. A. *ACS Macro Lett.* **2012**, *1*, 131−135.

56) Williams, C. K.; Breyfogle, L. E.; Choi, S. K.; Nam, W.; Hillmyer, M. A.; Tolman, W. B. *J. Am. Chem. Soc.* **2003**, *125*, 11350−11359.

57) Chamberlain, B. M.; Cheng, M.; Moore, D. R.; Ovitt, T. M.; Lobkovsky, E. B.; Coates, G. W. *J. Am. Chem. Soc.* **2001**, *123*, 3229−3238.

58) Chisholm, M. H.; Gallucci, J.; Phomphrai, K. *Inorg. Chem.* **2002**, *41*, 2785−2794.

59) Turova, N.; Turevskaya, E.; Kessler, V. G.; Yanovskaya, M. I. *The Chemistry of Metal Alkoxides*; Kluwer Academic Publishers, 2002.

60) Wanamaker, C. L.; Tolman, W. B.; Hillmyer, M. A. *Biomacromolecules* **2009**, *10*, 443−448.

61) Li, S.; Garreau, H.; Vert, M. *J. Mater. Sci. Mater. Med.* **1990**, *1*, 123−130.

62) Stridsberg, K.; Albertsson, A. C. *Polymer* **2000**, *41*, 7321−7330.

63) Yamashita, M.; Takemoto, Y.; Ihara, E.; Yasuda, H. *Macromolecules* **1996**, *29*, 1798−1806.

64) Nanba, T.; Ito, H.; Kobayashi, H.; Hayashi, T. Preparation of poly(hydroxyalkanoates) with low cost and good safety. JP 06329774 A 19941129, November 29, 1994.

65) Andreeβen, B.; Steinbüchel, A. *Appl. Environ. Microbiol.* **2010**, *76*, 4919−4925

66) Doi, Y. *Macromol. Symp.* **1995**, *98*, 585−599.

67) Gresham, T. L.; Jansen, J. E.; Shaver, F. W. *J. Am. Chem. Soc.* **1948**, *70*, 998−999.

68) Ouhadi, T.; Heuschen, J. M. *J. Macromol. Sci. Part A - Chem.* **1975**, *9*, 1183−1193.

69) Vangeyte, P.; Jérôme, R. *J. Poly. Sci. Part A: Polym. Chem.* **2004**, *42*, 1132–1142.

70) Zupancich, J. A.; Bates, F. S.; Hillmyer, M. A. *Macromolecules* **2006**, *39*, 4286–4288.

71) Lowe, J. R.; Tolman, W. B.; Hillmyer, M. A. *Biomacromolecules* **2009**, *10*, 2003–2008.

72) Cao, A.; Kasuya, K.; Abe, H.; Doi, Y.; Inoue, Y. *Polymer***1998**, *39*, 4801–4816.

Chapter 3 :

Organocatalytic Cationic Ring-Opening Polymerization of a Cyclic Hemiacetal Ester*

* Reproduced in part with permission from Neitzel, A. E.; Haversang, T. J.; Hillmyer, M. A. Organocatalytic Cationic Ring-Opening Polymerization of a Cyclic Hemiacetal Ester. *Ind. Eng. Chem. Res.* **2016**, *55*, 11747−11755.

3.1 Introduction

The United Nations recently predicted that the world population would increase to 11 billion people by 2100.[1] This population increase will undoubtedly be accompanied by a rise in demand for high-quality, affordable, and sustainable materials. Synthetic polymers constitute the building blocks for the plastic products abundant in today's society. Specifically, hydrocarbon polymers, such as polyethylene (PE), polypropylene (PP), and polystyrene (PS) comprise a large fraction of commercial plastics.[2] However, microorganisms capable of enzymatically degrading the typically heteroatom-rich macromolecules found in nature generally do not assimilate such hydrocarbon polymers.[3] The inability of traditional polymers to biodegrade represents an urgent environmental concern that has prompted synthetic polymer chemists to explore routes to biodegradable polymer structures. Polylactide (PLA) is a renewable polyester that can be produced at only a small premium, relative to PS, facilitating its use in various applications. While PLA is industrially compostable, it does not degrade easily under the anaerobic conditions typical of landfills. Furthermore, the infrastructure required to collect, transport, and industrially compost aliphatic polyesters is still in its infancy, and consumers are often not aware of the proper disposal procedures. Many aliphatic polyesters, including PLA, biodegrade via a two-step process. First, polymer backbone bonds must be enzymatically or otherwise hydrolyzed to produce oligomers, which are subsequently broken down further to return water, carbon dioxide, and humus.[4] Generally, the polyester degradation rate is impacted by the structure of the polymer backbone, including the electrophilicity of the carbonyl atoms and the presence or absence of bulky substituents. In addition, the hydrophobicity of the material and its crystallinity also influence the degradation rate.[5]

Hemiacetal esters are known to be more hydrolytically and thermally labile than their acetal and ester counterparts.[6,7] The hydrolytic and thermal lability of polyhemiacetal esters makes them attractive candidates as components of biodegradable plastics, as well as for processes that require the selective etching of one component (e.g., nanolithography).[8] In 2014, Martin et al. explored the synthesis of the cyclic hemiacetal ester monomer 1,3-dioxolan-4-one (DOX).[9] The authors attempted the controlled batch copolymerization of the cyclic hemiacetal ester with L-lactide with the goal of producing marine-degradable poly(L-lactide-co-DOX) statistical copolymers. Upon careful review of the data presented in this work, we concluded that compelling evidence for the incorporation of acetal units into the macromolecules was absent. Based on attempts to reproduce one of the copolymerizations, we provide evidence that suggests that these previously reported polymers were actually statistical copolymers of glycolic acid (GA) and lactide (LA), rather than the targeted poly(hemiacetal esters) (see Figures 3.27−3.29 in the Supporting Information). PGA-co-PLA copolymers, which would result from the loss of formaldehyde during the copolymerization, are interesting in their own right and should exhibit enhanced degradation, compared to the PLLA homopolymer.[10]

We note that, in order to produce polyhemiacetal esters, rather than polyesters from cyclic monomers, it is important to find polymerization conditions that are mild and selective to avoid the elimination of aldehydes. Near the same time as the publication by Martin et al., we described the anionic ring-opening polymerization (ROP) of the cyclic hemiacetal ester 2-methyl- 1,3-dioxan-4-one (MDO) (Scheme 3.1).[11] In the presence of benzyl alcohol (BnOH) initiator and catalytic diethylzinc (Et_2Zn), we found that this monomer can be polymerized by ring-opening either at the acetal or at the ester

functionality to produce poly(2-methyl-1,3-dioxan-4-one) (PMDO) or the aliphatic polyester poly(3-hydroxypropionic acid) (PHPA), respectively. Interestingly, the elimination of acetaldehyde—and, thus, the formation of PHPA—was favored at higher catalyst concentrations. However, at low catalyst loadings ($[MDO]_0/ [Et_2Zn]_0 \geq 700$), the monomer ring-opened at the acetal to produce a benzyl acetal end group and a propagating zinc carboxylate. Under these conditions, acetaldehyde was not lost, and carboxylic-acid-terminated PMDO was formed. Unfortunately, this process was somewhat inefficient, requiring over 24 h to reach equilibrium at the low catalyst loading employed to suppress concurrent acetaldehyde elimination.

Scheme 3.1. Previously employed anionic ring-opening polymerization of MDO

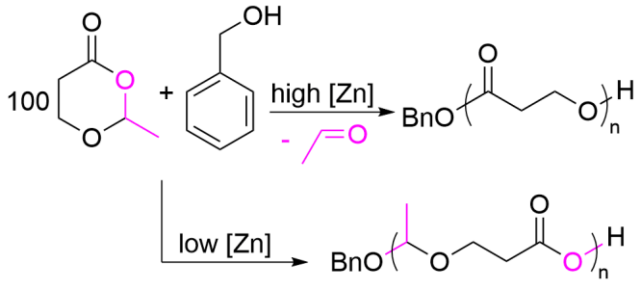

Because of these practical limitations, we sought to identify more active catalysts for the polymerization of MDO and to develop conditions that would suppress acetaldehyde elimination observed in the anionic ROP of MDO. We reasoned that the ROP of MDO might be promoted under cationic polymerization conditions. The cationic ring-opening polymerization (CROP) of heterocycles is known to proceed via two distinct mechanisms: an activated monomer (AM) and active chain-end (ACE) mechanism.[12] The activated monomer mechanism relies on an exogenous nucleophile to act as the initiating species. With this pathway, molar mass control is achieved by adjusting the initial monomer:initiator ratio. Conversely, with an ACE mechanism, each propagating chain is

initiated by a molecule of monomer. Although there are examples of CROP via the ACE mechanism that demonstrate molar mass control as a function of the monomer to cationic initiator ratio (i.e., the Brønsted acid employed), it is more often the case that side reactions result in a loss of molar mass control.[13]

To our knowledge, the mechanism and kinetics of the CROP of cyclic hemiacetal esters has not been previously demonstrated, although it has been recently shown that a 7-membered cyclic hemiacetal ester acts as an effective initiator in the ring-expansion living cationic polymerization of isobutyl vinyl ether.[14] In this work, we report the CROP of the cyclic hemiacetal ester MDO using a variety of organic acid catalysts. We show that polymerization of MDO can proceed via both AM and ACE pathways, with the dominant mechanism determined by the initial concentration of exogenous initiator.

3.2 Results and Discussion

We first investigated diphenylphosphoric acid (DPP),[15] an inexpensive organocatalyst that has been previously employed in the cationic ring-opening polymerization of lactones and cyclic carbonates.[16,17] We observed rapid polymerization of neat MDO to PMDO upon treatment with DPP in the presence of benzyl alcohol at room temperature. We initially aimed for low molar mass PMDO to facilitate end-group analysis by ^{1}H NMR spectroscopy. We targeted 5 kg/mol PMDO, accounting for an equilibrium monomer concentration of $[M]_{eq}$ = 4.53 M, i.e., ~60% conversion starting with neat MDO. An initial polymerization of neat MDO ($[MDO]_0 \approx 10.1$ M, $[MDO]_0/[DPP]_0 = 1000$, and $[MDO]_0/[BnOH]_0 = 80$) became noticeably viscous over 1 h. Analysis of the resultant PMDO by size-exclusion chromatography multiangle laser light-scattering (SEC-MALLS) using tetrahydrofuran (THF) as the mobile phase indicated that the number-average molar

mass (M_n) of the purified PMDO was 8.2 kg/mol with a dispersity ($Đ$) of 1.25. Structural analysis by ^{1}H NMR spectroscopy verified the production of PMDO with the incorporation of BnOH into the polymer backbone as a benzyl acetal end group (Scheme 3.2).

Scheme 3.2. The activated monomer (AM) and active chain-end (ACE) mechanisms adapted to the CROP of MDO

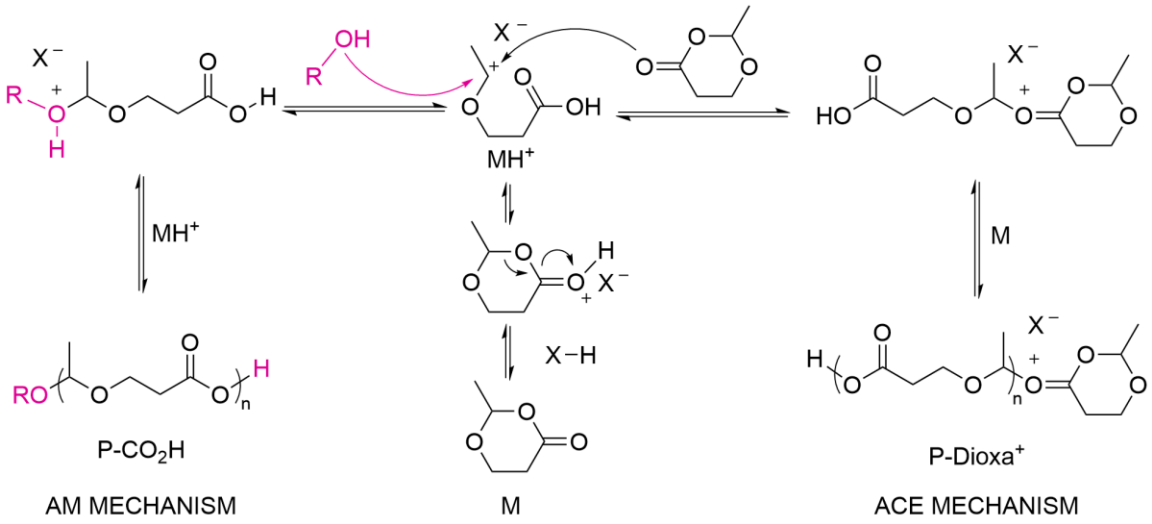

Encouraged by the superior activity of DPP over diethylzinc as the catalyst for MDO polymerization, we set out to synthesize polymers of different molar masses by varying $[BnOH]_0$. However, at higher theoretical molar masses ($M_{n,theo}$), the observed molar masses of the resultant PMDO samples were consistently lower than the theoretical values (see Table 3.4 in the Supporting Information). As noted previously, with an activated monomer mechanism, one would anticipate good molar mass control over a wide range of $[BnOH]_0$. Therefore, we reasoned that there are two likely causes for this discrepancy: either the cationic polymerization of MDO proceeds via an AM mechanism and adventitious initiators present in the monomer initiate surplus chains, or backbiting reactions diminish the average molar mass of PMDO. The latter is expected to be more prominent in the ACE mechanism as the propagating chain-end is a charged species of

comparatively higher reactivity and lower selectivity than the propagating species in the AM mechanism.

Although both ^{1}H and ^{13}C NMR spectral data suggested that the MDO monomer was highly pure, without apparent adventitious initiators, we sought to further rule out the former possibility by carrying out a chain-extension experiment. Neat MDO was polymerized to 50% conversion ($[MDO]_0/[BnOH]_0$ = 81, $[MDO]_0/[DPP]_0$ = 1000), and the reaction mixture was analyzed by THF SEC-MALLS. The addition of fresh MDO from the same batch led to an increase in the molar mass from M_n = 8.5 kg/mol to M_n = 10.6 kg/mol with $Đ$ = 1.25 both before and after chain extension. A new population of low-molar-mass PMDO molecules was not observed upon chain extension, indicating that no new chains were initiated by nucleophilic contaminants or other pro-initiators in the second monomer aliquot (see Figure 3.5 in the Supporting Information).

Convinced by this experiment that MDO was quite pure, we developed the following mechanistic hypothesis: in the polymerization of MDO without exogenous initiator, polymerization occurs via an ACE mechanism, where a monomer molecule (M) initiates by ring-opening a protonated monomer molecule (MH+) to afford a dioxacarbenium ion (P-Dioxa+) as the propagating species. On the other hand, when an added alcohol initiator is present, the polymerization occurs via the AM mechanism. In this case, the ring-opening of MH+ by an exogenous nucleophile, such as an alcohol (ROH), affords a carboxylic acid propagating chain end (P-CO_2H). We suspected that, at lower target molar masses (where the relative concentration of initiator is high), the AM mechanism would dominate; meanwhile, at higher target molar masses (where the relative

concentration of initiator is low), competition between AM and ACE mechanisms would lead to loss over molar mass control.

We proceeded to study PMDO polymerization under conditions thought to favor the AM mechanism ($[MDO]_0/[DPP]_0 = 2140$ and $[MDO]_0/[BnOH]_0 = 85$) and monitored the molar mass evolution during the early stages of the polymerization by SEC. We observed a linear increase in molar mass with conversion in this low-molar-mass regime (see Figure 3.1, as well as Table 3.5 in the Supporting Information). However, a positive, nonzero intercept was observed. This may be explained by some contribution of the ACE mechanism under these conditions, which would invalidate the assumption that all chainends are derived from BnOH initiation only. SEC traces of low-molar-mass polymers exhibited a fairly broad signal ($Đ \approx 2$), including a low-molar-mass tail consistent with cyclic oligomers of PMDO.

(a)

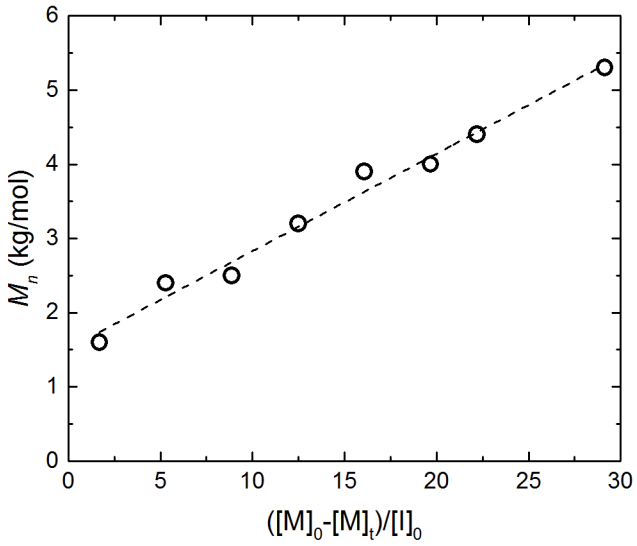

(b)

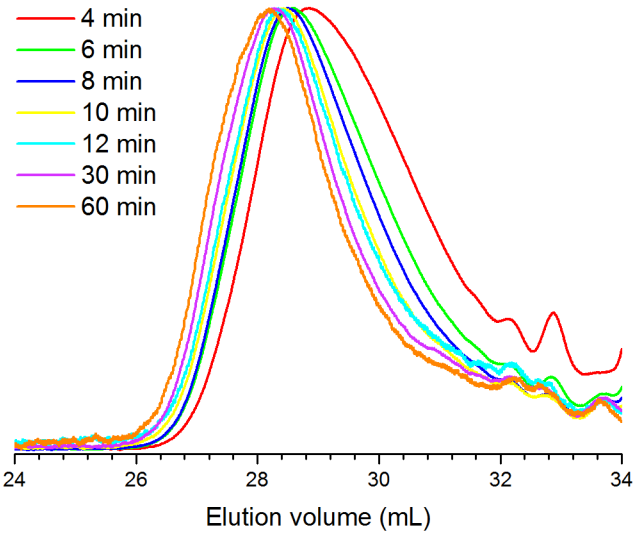

Figure 3.1. (a) PMDO molar mass as a function of conversion monitored using THF SEC and conventional calibration analysis relative to PS standards. (b) Stacked SEC traces of the quenched polymerization aliquots from (a) at indicated times. The polymerization was carried out in neat MDO ($[MDO]_0$ = 10.1 M) with $[MDO]_0/[DPP]_0$ = 2,142 and $[MDO]_0/[BnOH]_0$ = 85. Each aliquot was quenched with 1 mL THF containing 1 μL NEt_3 prior to analysis.

Despite the marginal control of molar mass resulting from competition of ACE and AM mechanisms at low initiator concentrations, we were able to synthesize several different end-functionalized, low-molar-mass PMDO samples ($M_n \approx 5$ kg/ mol,

$[MDO]_0/[ROH]_0$ = 80) by initiating with a variety of functionalized alcohol initiators (Table 3.1). We anticipate that low-molar-mass PMDO equipped with a functional handle can be employed as a macroinitiator or further derivatized as desired. In all cases, we were able to verify the end-group structures by ^{1}H NMR spectroscopy (see Figures 3.6−3.15 in the Supporting Information). We also observed a quartet at 4.73 ppm, together with other signals very similar to those of linear PMDO (Figures 3.6−3.15, especially pronounced in Figure 3.14). These resonances became much more prominent when the polymerization was carried out at higher dilutions, suggesting that unimolecular ring formation, which affords cyclic PMDO, eventually dominates over bimolecular propagation as $[MDO]_0$ approaches $[M]_{eq}$.[18] Interestingly, entry 5 produced a 4:1 mixture of linear to cyclic PMDO resonances, as corroborated by ^{1}H NMR spectroscopy (Figure 3.14).

Table 3.1. CROP of MDO with various functionalized alcohol initiators and DPP as the catalyst

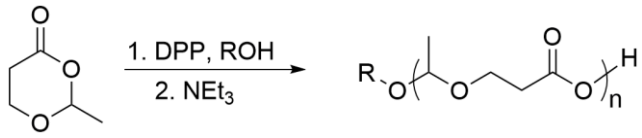

Entry	ROH	Conversion[a] (%)	Yield[b] (%)	$M_{n,theo}$[c] (kg/mol)	M_n[d] (kg/mol)	$Đ$[d]
1	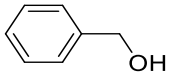	50	75	4.6	4.1	2.1
2	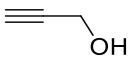	50	88	4.6	5.0	2.0
3	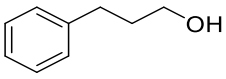	55	82	5.1	4.8	2.1
4	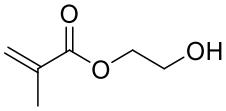	56	84	5.2	4.7	2.2
5[e]	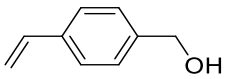	57	96	5.3	4.3	2.5

[a]Determined from ^{1}H NMR integrations. [b]Calculated taking into account conversion. [c]Theoretical value calculated from (% conversion)([MDO]$_0$/[ROH]$_0$)M_0. [d]Determined from THF SEC relative to PS standards. [e]This reaction produced some macrocyclics in addition to linear PMDO as evidenced by ^{1}H NMR analysis (Figure 3.14). All reactions were run in bulk ([MDO]$_0$ = 10.1 M) at room temperature with [MDO]$_0$/[ROH]$_0$ = 80 and [MDO]$_0$/[DPP]$_0$ = 1,000. Reactions were quenched using equimolar amounts of NEt_3 to DPP. Polymers were purified by precipitation into cold 9/1 hexanes/THF, and dried under reduced pressure for 21 hours.

It is worth noting that, while the thermal instability of PMDO may be advantageous for applications where a labile component is desired (e.g., lithography), it makes the purification and processing of PDMO challenging. All precipitated polymers in Table 3.1

were dried under reduced pressure at room temperature, as we observed decomposition of PMDO under reduced pressure at 50 °C (Figure 3.21 in the Supporting Information). To increase the thermal stability of PMDO, we successfully esterified the carboxylic acid terminus by treating the precipitated polymer with a dimethylformamide (DMF) solution of 1,8- diazabicyclo[5.4.0]undec-7-ene (DBU) and methyl iodide. ^{1}H NMR spectroscopic data of the reprecipitated PMDO was consistent with a methyl ester end group on the polymer and the relative integrations of the new methyl signal to the benzyl acetal group indicated that PMDO was quantitatively end-capped (Figure 3.22 in the Supporting Information). Thermogravimetric analysis (TGA) of end-capped PMDO exhibited a 25 °C increase in thermal stability, when compared with PMDO prior to endcapping (Figure 3.2). This observed increase may be explained by the absence of an acidic moiety capable of catalyzing degradation of the polymer backbone and/or the thermally driven depolymerization from the chain end.

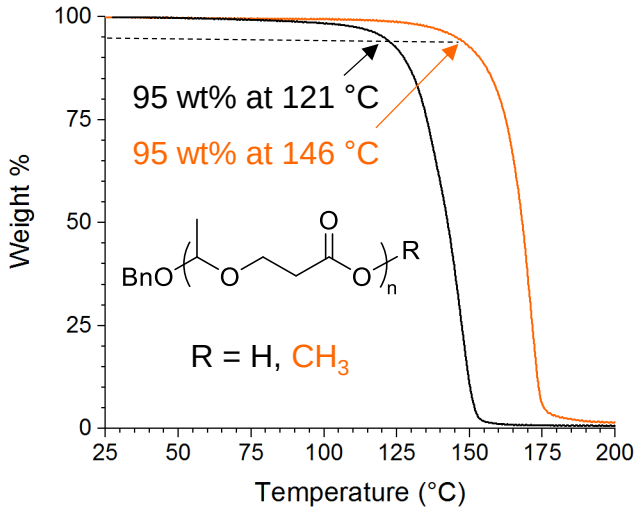

Figure 3.2. Thermogravimetric analysis of 8 kg/mol PMDO that has been end-capped contrasted with PMDO prior to end-capping. The thermal degradation experiment was carried out under nitrogen atmosphere with a heating ramp of 10 °C/min.

We also probed polymerization of MDO via an ACE mechanism by treating neat MDO with DPP in the absence of exogenous initiator. We observed an increase in the viscosity of the reaction mixture within only a couple of minutes, and both ^{1}H NMR and SEC data confirmed the formation of high-molar-mass PMDO. ^{1}H NMR spectroscopic end group analysis of purified polymers prepared without alcohol initiator revealed the appearance of a doublet of doublets at ~6.4 ppm, consistent with a vinyl ether end group (Figure 3.23 in the Supporting Information). This presumably resulted from α-hydride elimination from an intermediate oxonium ion formed in the ACE pathway.

Isolated reports of CROP of selected cyclic acetals and ethers suggest that it is possible to control polymer molar mass by the monomer:acid ratio, $[M]_0/[XH]_0$, where XH is a generic Brønsted acid.[19] However, within the range of catalyst loadings we studied, there was no clear relationship between molar mass and concentration of $[DPP]_0$ (Table 3.2). We therefore concluded that DPP did promote CROP of MDO by an ACE mechanism that was not well-controlled. Regardless, the ACE mechanism consistently gave access to

higher-molar-mass PMDO (>30 kg/ mol) than was achievable with added alcohol initiator or with our previously established conditions for the zinc-alkoxide-promoted ROP of MDO.

Table 3.2. Molar mass as a function of $[MDO]_0/[DPP]_0$ for PMDO prepared by an ACE mechanism

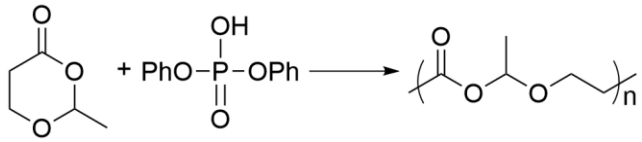

Entry	$\frac{[MDO]_0}{[DPP]_0}$	Time (min)	Conversion[a] (%)	Yield[b] (%)	M_n[c] (kg/mol)	$Đ$[c]
1	1,000	374	46	55	45	1.2
2	2,000	260	41	82	42	1.2
3	3,000	346	35	76	33	1.5
4	4,000	1080	33	79	35	1.4

[a]Determined from relative ^{1}H NMR integrations of MDO and PMDO resonances respectively. [b]Yield takes into account the reported conversion. [c]Determined from THF SEC-MALLS. All polymers were dissolved in 1 mL $CDCl_3$ containing 1 μL NEt_3, precipitated into cold 9/1 hexanes/THF, and dried under reduced pressure.

In an effort to identify an acid catalyst that would facilitate the controlled CROP of MDO via an ACE mechanism, we investigated a wide variety of acids and alkylating agents that have been successfully employed in the controlled CROP of cyclic acetals.[19] However, these catalysts caused immediate decomposition of the monomer, even at low temperature (−20 °C) and under more dilute conditions (Table 3.5 in the Supporting Information). We reasoned that these strong acid catalysts were quite aggressive and therefore pursued an organic acid with a pK_a more similar to DPP (pK_a = 3.88 in dry DMSO).[15] In addition, we sought a triflate counterion with low nucleophilicity to improve control over the polymerization.[20] Pyridinium triflate (PyHTfO) is a commercially available salt that meets both of the aforementioned constraints. However, in the bulk polymerization of MDO,

similar results were observed with PyHTfO as with DPP; high-molar-mass polymers could be accessed, but there was no clear relationship between $[MDO]_0$/ $[PyHTfO]_0$ (Table 3.6 in the Supporting Information). Furthermore, some of the pyridine appeared to be incorporated as a pyridinium chain end, presumably via attack by pyridine onto the propagating dioxacarbenium ion (Figure 3.24 in the Supporting Information). A bulky tetrakis[3,5-bis- (trifluoromethyl)phenyl]borate diphenylphosphoric acid (DPP [BArF]4−) catalyst was also employed but proved to not yield much improvement over the use of DPP. Similarly, dry hydrochloric acid in diethyl ether (1 M) led to the successful polymerization of MDO and produced results akin to those achieved with DPP.

Molar mass analysis by THF SEC-MALLS of the polymerization by the ACE mechanism indicated that molar mass was actually highest at low conversions and decreased with increasing MDO conversion (see Table 3.3, as well as Tables 3.7 and 3.8 in the Supporting Information), eventually plateauing around $M_n \approx 30$ kg/mol. This seemed to suggest that, without an exogenous initiator, initiation from activated MDO is slower than propagation of the chain, which is consistent with the prediction that MDO is a poor nucleophile. In fact, we observed molar masses of $M_n \gtrsim 100$ kg/mol after only 2 min when conversion was still <5% (as determined by no-D ^{1}H NMR kinetics experiments under the same conditions;[21] (see Figure 3.25(a) in the Supporting Information). Analysis of entry 10 in Table 3.3 via matrix-assisted laser desorption/ionization time-of-flight (MALDI-TOF) mass spectrometry corroborated the formation of low-molar-mass (≤2 kg/mol) cyclic PMDO in the polymerization of MDO via an ACE mechanism (Figure 3.26 in the Supporting Information).

Table 3.3. Molar mass evolution with time of the DPP-catalyzed MDO CROP via ACE mechanism

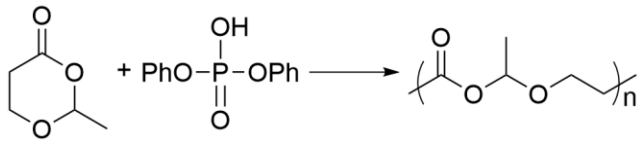

Entry	Time (min)	M_n[a] (kg/mol)	$Đ$[a]
1	2	120	2.1
2	4	56	1.3
3	6	51	1.3
4	8	45	1.4
5	10	46	1.3
6	12	49	1.3
7	30	40	1.3
8	60	36	1.3
9	90	34	1.2
10[b]	120	32	1.2

[a]Determined from THF SEC-MALLS. [b]This aliquot was analyzed by MALDI-TOF (Figure 3.26). The polymerization was conducted in neat MDO ($[MDO]_0$ = 10.2 M, $[MDO]_0/[DPP]_0$ = 1,068). DPP solution (0.12 M in DCM) was transferred to a scintillation vial and solvent was removed under reduced pressure. MDO was then added to the dry DPP. All aliquots were quenched with 1 mL THF containing 1 μL NEt_3.

Kinetics of MDO CROP via AM and ACE Pathways Catalyzed by DPP.

We also monitored the CROP of neat MDO with and without benzyl alcohol initiator using no-D ^1H NMR experiments.[21] In the CROP of MDO, we observed conversions close to 60% (the established equilibrium conversion) with added alcohol initiator but without an exogenous initiator present the polymerization generally did not exceeded 50% conversion, especially when $[DPP]_0$ was low (see Figures 3.25(a) and 3.25(b)). This can possibly be explained by side reactions that irreversibly quench the charged species in solution or by some catalyst deactivation in the ACE mechanism. For a

polymerization with $[MDO]_0$ = 9.7 M, $[MDO]_0$/ $[BnOH]_0$ = 50, and $[MDO]_0/[DPP]_0$ = 2770, the consumption of benzyl alcohol initiator is complete by ^{1}H NMR spectroscopy after 15 min (see Figure 3.3a). The resonance for the chemically equivalent methylene protons of benzyl alcohol at 4.7 ppm (Figure 3.3a, time = 0 min) decreased in intensity as two doublets and a quartet (Figure 3.3a, protons a, a′and proton b), indicative of a benzyl acetal end group, emerged. A low-intensity signal corresponding to methylene protons of a benzyl ester was also observed (Figure 3.3a, protons c), suggesting that a fraction of the alcohol is consumed via competitive initiation at the ester functionality of MDO. However, benzyl ester end groups were not observed in purified PMDO, indicating that the alcohol, produced by initiation at the ester and subsequent acetaldehyde extrusion from the hemiacetal, did not propagate. Plotting alcohol consumption with conversion in semilogarithmic coordinates afforded a straight line, consistent with a first-order dependence of the rate of initiation (R_i) on $[BnOH]_0$ (Figure 3.3b).

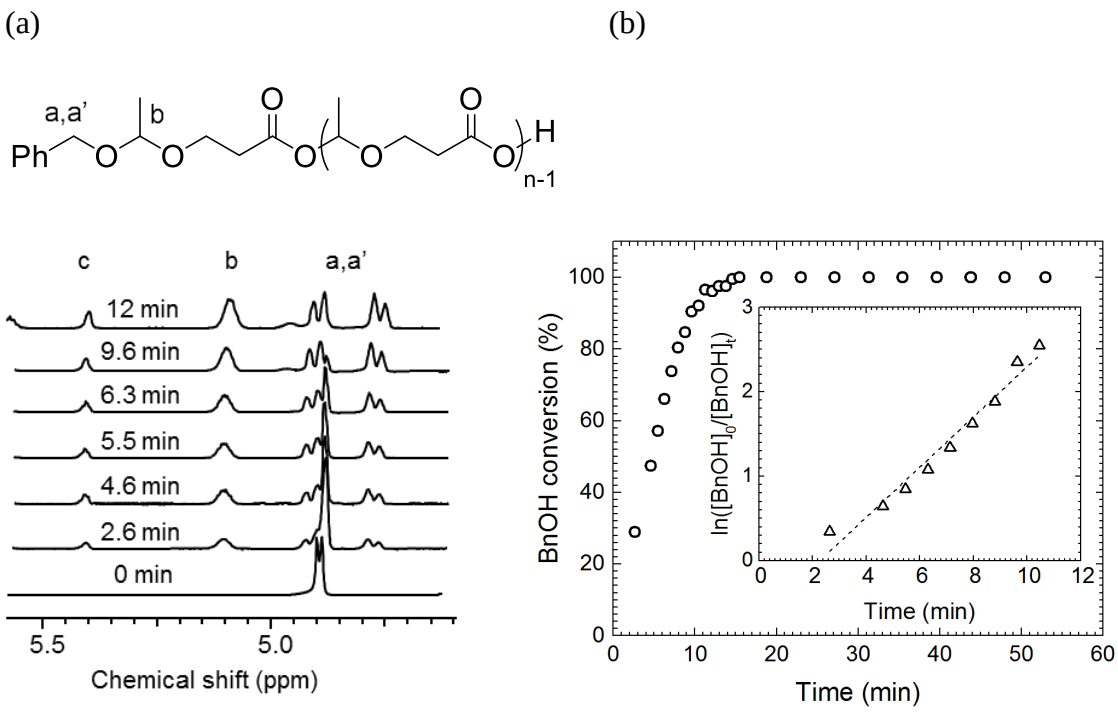

Figure 3.3. Initiation kinetics for the cationic ring-opening polymerization of MDO in the presence of BnOH and DPP with $[MDO]_0$ = 9.7 M, $[BnOH]_0$ = 0.2 M, and $[DPP]_0$ = 3.8 mM. (a) ^{1}H NMR overlay of no-D spectra showing the disappearance of the benzyl alcohol methylene protons at δ = 4.9 ppm (in MDO) and growing in of a benzyl acetal end group at δ = 4.78 (d, 1H, PhC*H*$_2$OCHCH$_3$O), 4.88 (d, 1H, PhC*H*$_2$OCHCH$_3$O), and 5.11 (q, 1H, PhCH$_2$OC*H*CH$_3$O). A minor signal at 5.4 ppm (protons c) corresponding to benzyl ester methylene protons is also observed. This results from alcohol ring-opening at the ester functionality of MDO followed by acetaldehyde extrusion. (b) Benzyl alcohol conversion (○) as a function of time. The inset semilogarithmic anamorphosis of the data (Δ) suggests that the rate of initiation has a first order dependence on $[BnOH]_0$ (k_{app} = 0.30 ± 0.02 min^{-1}, R^2 = 0.96).

With a benzyl alcohol initiator, MDO conversion increases linearly with time over the first 20 min until 30% conversion is reached. Above 30% conversion, the rate of propagation R_p decreases drastically, such that it takes an additional 140 min to approach 50% conversion (data denoted by open circles (○), Figure 3.4a). In comparison, the rate of polymerization is significantly slower without an exogenous alcohol initiator (denoted by open triangles (Δ), Figure 3.4a). Semilogarithmic anamorphoses of the MDO conversion data presented in Figure 3.4a afforded concave down, rather than linear, slopes (Figure

3.4b). This effect was more pronounced in the case of MDO CROP with BnOH (data denoted by solid circles (●), Figure 3.4b).

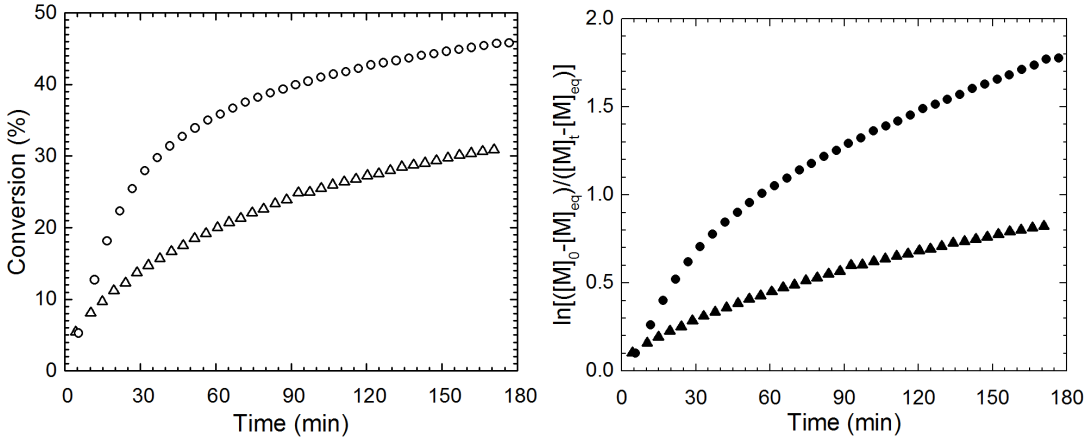

Figure 3.4. (a) Conversion of MDO to PMDO as a function of time for $[MDO]_0$ = 9.9 M and $[DPP]_0$ = 3.8 mM (Δ) and for $[MDO]_0$ = 9.8 M, $[DPP]_0$ = 3.8 mM, and $[BnOH]_0$ = 0.13 M (○). (b) The data from (a) in semilogarithmic coordinates without BnOH (▲) and with BnOH (●).

Neat MDO polymerization employing variable $[DPP]_0$ with no $[BnOH]_0$ (Figure 3.25(a)) and constant $[BnOH]_0$ (Figure 3.25(b)) was also studied by no-D ^{1}H NMR spectroscopy[21]). In both cases, the initial rates of polymerization were observed to increase with an increase in $[DPP]_0$. The rate of polymerization at low $[DPP]_0$ leveled off at lower conversions, leading to lower overall conversions. The decrease in overall conversion was more pronounced in the case of MDO polymerization without an alcohol initiator and at low $[DPP]_0$, suggesting that the acidic protons in solution are eventually quenched during CROP via an ACE mechanism.

Penczek, Kubisa, and co-workers have thoroughly studied the kinetics of CROP via AM and ACE mechanisms for several heterocycles including cyclic acetals and lactones.[22] The authors have concluded that it is rarely possible to avoid backbiting and end-to-end cyclization reactions in the ACE mechanism. This can be rationalized by the presence of a

reactive dioxacarbenium ion at the propagating chain end, which can react with the electron-rich oxygen atoms of the polymer backbone to yield macrocycles (Scheme 3.3). As the concentration of monomer decreases, such unimolecular backbiting reactions become increasingly competitive with bimolecular propagation events. On the other hand, in the AM mechanism, the propagating species is neutral and, therefore, less prone to unimolecular side reactions. In the case of MDO CROP, we also observed competition between AM and ACE mechanisms.

In the AM mechanism, acidic protons are distributed between monomer and alcohol molecules during initiation. This can be expressed by the following chemical pre-equilibrium:

$$[MH^+] + [ROH] \quad \overset{K_{eq}}{\rightleftharpoons} \quad [M] + [ROH_2^+] \tag{1}$$

where K_{eq} is the equilibrium constant associated with this proton transfer. Initiation occurs via attack of an alcohol molecule (ROH) on a protonated MDO molecule (MH^+). The rate of initiation in the activated monomer mechanism ($R_{i,AM}$) can be written as

$$R_{i,AM} = k_{i,AM}\,[MH^+][ROH] \tag{2}$$

Similarly, the rate of propagation in the AM mechanism ($R_{p,AM}$) of MDO CROP can be written as

$$R_{p,AM} = k_{p,AM}[MH^+][P\text{-}CO_2H] \tag{3}$$

where [P-CO_2H] denotes the concentration of propagating polymer chains. It is important to note that, unlike in the AM mechanism of cyclic ethers, acetals, and lactones, the propagating species in MDO CROP via AM mechanism is a carboxylic acid, rather than an alcohol.

In the ACE mechanism, a molecule of unprotonated MDO (M) acts as the initiator and ring-opens MH+ to yield a propagating dioxacarbenium ion. The $R_{i,ACE}$ can then be expressed as

$$R_{i,ACE} = k_{i,ACE}\,[MH^+][M] \quad (4)$$

Similarly, $R_{p,ACE}$ is a function of the concentration of propagating dioxacarbenium ion (P-dioxa$^+$) and unprotonated MDO:

$$R_{p,ACE} = k_{p,ACE}\,[\text{P-dioxa}^+][M] \quad (5)$$

It can be seen from eqs 4 and 5 that $R_{i,ACE}$ and $R_{p,ACE}$ are functions of [M], which sets it apart from the AM mechanism, where $R_{i,AM}$ and $R_{p,AM}$ are functions of the protonated monomer only.

Without the addition of an alcohol initiator (and assuming a negligible concentration of adventitious initiators), the polymerization of MDO is expected to proceed exclusively via an ACE mechanism. In Figure 3.4b, deviation from linearity in the semilogarithmic plot of MDO consumption with conversion is apparent in polymerizations under both AM and ACE conditions. The polymerization rate thereby appears to neither have a first-order nor zero-order dependence on MDO monomer concentration. In CROP, deviations from a rate with singular dependence on monomer concentration have been rationalized by differences in the relative basicities of monomer and polymer.[23] If the monomer has a higher pK_a than the polymer, there is a higher probability that the acidic protons are located on the monomer than the polymer chain. In the opposite scenario, the acidic protons have a higher probability to be localized on the polymer chain, causing a decline in R_p with time.

Therefore, the decrease in $R_{p,ACE}$ is consistent with PMDO being more basic than MDO. When an alcohol initiator is added to the polymerization, an even more pronounced decrease in $R_{p,AM}$ was observed after the initial 20 min of reaction (●, Figure 3.4a). From Figure 3.4b, it can be deduced that this decrease is not solely due to the lower monomer concentration. Furthermore, this deviation cannot be purely a result of the difference in relative monomer and polymer basicity, because this value is not expected to change upon the addition of a small amount of alcohol initiator. We believe that the decrease in $R_{p,AM}$ is a manifestation of the superposition of MDO consumption via the competing AM and ACE mechanisms. The plot in Figure 3.4b can be deconstructed into two linear regimes: an initial regime, where the AM mechanism dominates, and a second regime, where the ACE mechanism and associated side reactions become competitive as the concentration of protonated monomer and the concentration of protonated polymer decrease and increase, respectively.

Based on our findings, we suggest that MDO CROP with DPP and an alcohol initiator proceeds via concurrent AM and ACE mechanisms, with the contribution of each being a function of $[M]/[MH^+]$. The AM mechanism will be favored if $[MH^+]$ is kept as high as possible and [M] as low as possible throughout the polymerization. This approach has been successfully employed in the controlled synthesis of polyethers from epoxides.[24] Unfortunately, monomer-starved conditions are not amenable to MDO CROP, because of the high $[M]_{eq}$ associated with the ring-opening of MDO to PMDO, which effectively prohibits the polymerization of MDO at low [M].

From the collective data acquired for MDO CROP, we were able to identify the major operative mechanistic pathways illustrated in Scheme 3.3. MDO CROP without the

addition of alcohol proceeds via an ACE mechanism, where unprotonated MDO (M) initiates a chain via attack on protonated MDO (MH^+). Referring to the evolution of molar mass with time data, we infer that $R_{i,ACE} \ll R_{p,ACE}$, resulting in the production of high-molar-mass PMDO at low conversions. The following incremental decrease in molar mass with time can be rationalized by reversible backbiting reactions, affording cyclic PMDO (k_{bb} = rate constant associated with backbiting). Cyclic PMDO can be ring-opened and further decrease molar mass by additional backbiting processes or undergo deprotonation of the oxonium ion ($P\text{-}Ox^+$) to generate a terminal vinyl ether (k_{dp} = rate constant associated with deprotonation). The addition of ROH to the system opens up an additional avenue for MDO CROP via the AM mechanism. Although initiation and propagation by an AM mechanism can be favored in principle, suppression of the ACE mechanism contribution in MDO CROP is expected to diminish conversion, because it requires monomer concentrations well below $[M]_{eq}$. Hence, PMDO of different architectures and with different end groups is produced even in the presence of an alcohol initiator, where the contribution of the ACE mechanism becomes more pronounced as [M] approaches $[M]_{eq}$.

Scheme 3.3. Mechanistic pathways for the formation of PMDO with observed end groups and architectures under CROP conditions

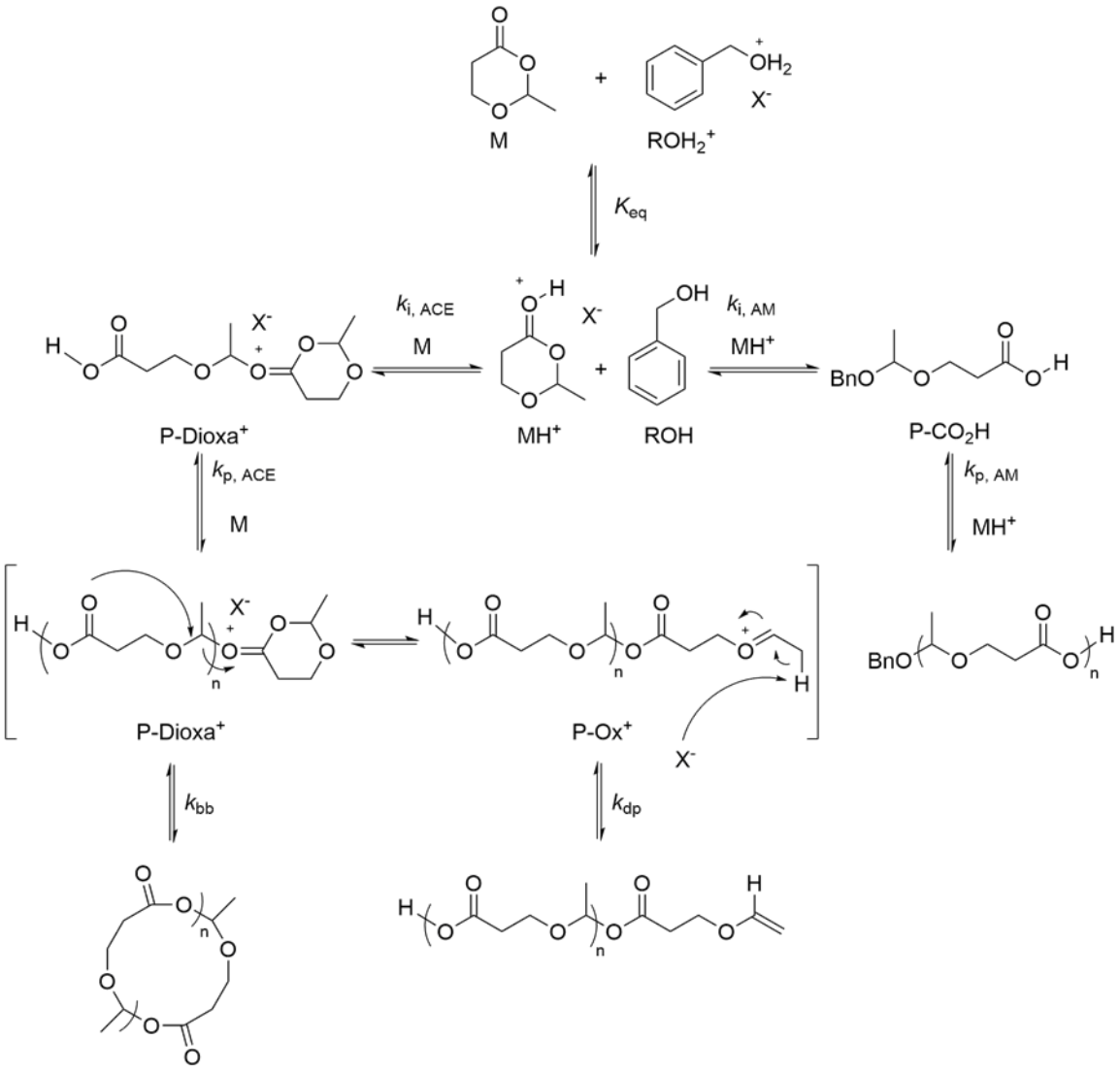

3.3 Conclusion

We have studied the cationic ring-opening polymerization of the cyclic hemiacetal ester MDO via activated monomer and active chain-end mechanisms to yield hydrolytically and thermally labile PMDO. We were able to produce end-functionalized PMDO of molar masses in good agreement with theoretical values using high initial concentrations of various simple alcohol initiators and the mild organocatalyst DPP. The

aforementioned results notwithstanding, we also synthesized high-molar-mass PMDO without added initiator via an ACE route. Both with and without an exogenous initiator, the rates of polymerization were faster than in our previously studied polymerization of MDO under anionic conditions. Furthermore, polymerization of MDO under cationic conditions effectively suppressed the formation of poly(3-hydroxypropionic acid). We believe that our observations will benefit those undertaking polyhemiacetal ester synthesis in the future and that our findings will provide useful guidelines for the handling and polymerization of this class of monomers.

3.4 Supporting Information

Materials and Analysis

All chemicals were obtained from Sigma-Aldrich (Milwaukee, WI) and used as received unless otherwise noted. Methylene chloride (DCM) was purified with an M. Braun solvent purification system and degassed before it was brought into the glove box. The cyclic hemiacetal ester, 2-methyl-1,3-dioxan-4-one (MDO), was synthesized from the commercial 2- methyltetrahydrofuran-3-one as reported previously.[11] However, we would like to point out that DCM often contains trace hydrochloric acid. It is therefore advisable to remove trace acid from the solvent before utilizing it in the synthesis of this monomer. Diphenylphosphoric acid (DPP) was ground into a fine powder and dried under high vacuum (50 mTorr) overnight. Catalyst stock solution was prepared using a volumetric flask and dry DPP and DCM in the glove box. Capillaries containing deuterated benzene (C_6D_6) were prepared from pipettes by flame-sealing one end, adding 100 µL C_6D_6, and sealing the other end shut with a blow torch. Benzyl, propargyl, and 3- phenyl-1-propanol

were purified by simple distillation over calcium hydride (CaH_2) prior to use. (4-vinylphenyl)methanol was generously donated by Tong Wang.

Characterization.

^1H and ^{13}C nuclear magnetic resonance (NMR) spectra were obtained on either a 400 or 500 MHz Bruker Avance III HD. Chemical shifts were referenced to tetramethylsilane (TMS) at 0.00 ppm for ^1H and ^{13}C NMR spectra taken in $CDCl_3$ containing 10 % w/v TMS. All spectra taken in other deuterated solvents were referenced to the respective residual protonated solvent signal. For all NMR kinetics experiments the relaxation delay was set to at least 10 seconds. Thermal gravimetric analysis was performed on a TA Instruments Q500 TGA under the conditions specified. Differential scanning calorimetry (DSC) was carried out using a TA Instruments Q2000 at a scanning rate of 5 °C/min. DSC data analysis was performed using TA Instruments TRIOS software using the second heating curve. Polymer samples were injected into an Agilent 1260 S3 series chromatograph (THF, 25 °C, 1 mL/min) with three Styragel columns. Molar mass analysis was carried out using size exclusion chromatography with multi-angle laser light-scattering (SEC-MALLS) to determine absolute weight average molar mass (M_w) with a dn/dc = 0.044 mL/g and conventional calibration analysis relative to polystyrene standards using THF SEC equipped with an Optilab T-rEX RI detector. Matrix-assisted laser desorption/ionization time-of-flight (MALDI-ToF) analysis was carried out on an Applied Biosystems-Sciex 5800 MALDI-TOF/TOF mass spectrometer.

Representative Procedure for the Bulk Polymerization of MDO in Presence of DPP and Benzyl Alcohol.

The bulk polymerizations of MDO in the presence of diphenylphosphoric acid catalyst and benzyl alcohol were carried out in a nitrogen atmosphere glovebox using oven dried glassware and a Teflon stir bar. For a standard polymerization, diphenylphosphoric acid was weighed in a polystyrene weigh boat (typically 3 milligrams), and then transferred into a tared 20 mL scintillation vial. Once the catalyst was added, benzyl alcohol was added into the scintillation vial volumetrically, using a microsyringe. The vial was tared again, and the MDO monomer was added to the vial by mass (typically 1.4 grams). The scintillation vial was then capped and left to stir at room temperature inside of the glove box. During the reaction, aliquots for ^{1}H NMR spectroscopy and THF SEC analysis were removed from the reaction vessel using glass pipettes, and placed into 1 mL glass vials containing a quenching solution (CH_2Cl_2 or $CDCl_3$ or THF with NEt_3), which were then capped and removed from the glove box. After 40 minutes the scintillation vial was removed from the glovebox and the reaction was quenched in a fume hood. Once the quenching solution was added, the reaction mixture was capped, and left to stir in the fume hood for ten minutes. After ten minutes, the reaction mixture was drawn up into a glass pipette and added dropwise into 150 mL solution containing 135 mL of hexanes and 15 mL of THF to precipitate the polymer. The precipitate wasthen dissolved into 0.7 mL of CH_2Cl_2, and precipitated two more times, each time into clean solutions of 9:1 hexanes to THF. After three precipitations, the remaining precipitant was quantitatively transferred into a clean, tared scintillation vial, and then dried overnight under high vacuum (50-100 mTorr).

Representative Procedure for End Capping PMDO.

PMDO was synthesized using the standard polymerization technique as described and precipitated three times, and dried prior to end capping. Before end capping, the unmodified PMDO was characterized by ^{1}H NMR spectroscopy, THF SEC-MALLS, and TGA. The number of carboxylic chain ends was calculated using the mass of PMDO and the number average molar mass of the PMDO sample, as determined by THF SEC-MALLS. For a typical end capping reaction, PMDO (typically 200 milligrams) was dissolved in 0.5 mL of N, N dimethylformamide (DMF) in a 20 mL scintillation vial containing a Teflon stir bar.[25] Once dissolved in DMF, 1 equivalent of DBU and 1.2 equivalents of methyl iodide were added into the reaction vessel volumetrically, via micro syringes. The reaction mixture was then capped and left to stir in a fume hood for 90 minutes. After 90 minutes, 20 mL of dichloromethane was added to the scintillation vial. The reaction mixture was then added to a 125 mL separatory funnel and washed once with an equal volume of aqueous solution of 10% sodium thiosulfate to remove any excess iodine. The organic layer was then dried over magnesium sulfate and then gravity filtered into a tared 20 mL scintillation vial. The bulk of the solvent was removed by rotary evaporation, and the vial was then left under high vacuum overnight. The dried, end-capped PMDO was then analyzed by ^{1}H NMR, SEC-MALLS, TGA, and DSC.

Representative Procedure for no-D ^{1}H NMR Kinetics Experiments (where $[MDO]_0$ = 10.1- 10.2 M).

A stock solution of DPP was prepared in the glove box using dry DPP and either DCM or THF as the solvent. DPP was weighed into a 10 mL volumetric flask, dissolved, and diluted to the 10 mL mark with solvent. The desired volume of DPP stock solution was

transferred into a dry NMR tube using a microsyringe and the tube sealed with a septum. Solvent was removed under high vacuum. The tube was then returned to the glove box where a glass capillary containing ca. 100 µL C_6D_6 was added into it. At this point, alcohol initiator was added to the dry DPP in the NMR tube, if applicable. The NMR tube was then resealed with a septum and parafilm. A C_6D_6 capillary and neat MDO (0.545 g, 0.46 mL) were placed into a separate NMR tube, which was sealed with a septum and parafilm. The neat NMR tube was used to lock (on C_6D_6) and shim (on the methyl peak of neat MDO) on the spectrometer. The NMR tube containing only DPP (and alcohol, if applicable) was weighed. Once good shims were obtained with the neat MDO sample, MDO was injected into the tube containing DPP (and alcohol) and a timer was started. The reaction was inserted into the spectrometer and briefly shimmed again. NMR spectra were then obtained periodically. After the experiment finished, the mass of the NMR tube with the added MDO was determined to calculate mass of MDO. From this the ratios of $[MDO]_0/[DPP]_0$ and $[MDO]_0/[BnOH]_0$ were calculated as well as overall yields in the case of isolated samples.

Representative Procedure for no-D ^{1}H NMR Kinetics Experiments (where $[MDO]_0$ < 10.1- 10.2 M).

In a glove box, MDO was weighed into a dry NMR tube containing a C_6D_6 capillary. Alcohol was added at this point via microsyringe (if applicable). Solvent was added using a glass syringe (in the case of solution polymerization of MDO). The NMR tube was sealed with a septum and parafilm and placed in a NMR spectrometer. The C_6D_6 signal was used to lock and the methyl resonance of the monomer to shim. Once satisfactory shims were obtained the tube was recovered from the instrument and a stock solution of DPP was injected via microsyringe (timer was started at this time) and the tube

inverted to assure complete mixing. The tube was then re-inserted into the spectrometer. The sample was briefly shimmed and spectra were collected periodically.

Tables 3.4-3.9

Note: When we analyzed polymerization mixtures after quenching with a small amount of triethylamine (NEt_3) in either tetrahydrofuran (THF) or deuterated chloroform ($CDCl_3$), the apparent conversions were much higher than when following the reaction by no-D ^{1}H NMR (cf. Figures S19 (a) and (b)). When we treated MDO with NEt_3 and other hindered bases we observed degradation of the monomer into acetaldehyde and several other unidentified compounds, as well as a small amount of PMDO. Hence conversion data was artificially inflated upon MDO decomposition in the quenched aliquots (thus the conversions reported for quenched aliquots in the following table are not accurate and instead it is better to refer to the neat no-D ^{1}H NMR kinetics). Without quenching however we observed degradation of the polymer with time, especially in solution.

Table 3.4. Polymerizations of MDO with DPP and variable $[BnOH]_0$

Entry	$M_{n,theo}$[a] (kg/mol)	Conversion[b] (%)	M_n[c] (kg/mol)	M_w[c] (kg/mol)	$Đ$[c]	M_n[d] (kg/mol)	M_w[d] (kg/mol)	$Đ$[d]
1	60	54	18	20	1.2	2.7	5.9	2.2
2	80	60	14	21	1.3	11	18	1.7
3	160	60	27	37	1.4	16	25	1.6

[a]Theoretical value calculated from (% conversion)($[MDO]_0/[ROH]_0$)M_0.[b]Determined from ^{1}H NMR integrations [c]Determined from THF SEC-MALLS with a dn/dc of 0.042. [d]Determined from THF SEC using conventional calibration analysis relative to polystyrene standards.All reactions were run in ($[MDO]_0$ = 10.19 M) at room temperature and under inert atmosphere and all reactions were quenched with equimolar amounts of NEt_3 to DPP. Entry 1 reaction was done on a 40.1 mmol scale of MDO with $[MDO]_0/[ROH]_0$ = 850 and $[MDO]_0/[DPP]_0$ = 4000. Entries 2 and 3 were both done on a 12.07 mmol of MDO and $[MDO]_0/[DPP]_0$ = 1000.

Table 3.5. Molar mass evolution with time for MDO CROP with DPP and BnOH

Entry	Time (min)	Conversion[a] (%)	Conversion[b] (%)	M_n[c] (kg/mol)	M_w[c] (kg/mol)	$Đ$[c]
1	2	7	2	1.6	3.8	2.3
2	4	18	6.2	2.4	4.4	1.9
3	6	30	10.5	2.5	5.6	2.2
4	8	38	14.7	3.2	6.1	1.9
5	10	N.A.[d]	18.9	3.9	7	1.8
6	12	N.A.[d]	23.1	4	7.1	1.8
7	30	N.A.[d]	26.1	4.4	7.9	1.8
8	60	N.A.[d]	34.3	5.3	8.8	1.7

[a]Determined from relative ^{1}H NMR integrations of MDO and PMDO resonances respectively of the quenched aliquots at the indicated times. [b]Calculated from neat MDO ^{1}H NMR kinetics experiments with $[MDO]_0/[DPP]_0$ = 2,000 and $[MDO]_0/[BnOH]_0$ = 85. [c]Determined from THF SEC using conventional calibration analysis relative to polystyrene standards. [d]Residual monomer had visibly degraded due to treatment with NEt_3 and hence the apparent conversion was higher than predicted for $[M]_{eq}$ = 4.53 M. The polymerization was conducted in neat MDO ($[MDO]_0$ = 10.19 M, $[MDO]_0/[DPP]_0$ = 2,142, $[MDO]_0/[BnOH]_0$ = 85, and $M_{n,theo}$ = 6 kg/mol). DPP solution (0.12 M in DCM) was transferred to a scintillation vial containing a stir bar and solvent was removed under high vacuum. MDO was then added to the dry DPP in a glove box. All aliquots were quenched with 1 mL THF containing 1 μL NEt_3.

Table 3.6. Cationic initiators probed for MDO CROP via an ACE mechanism

Entry	Initiator	$[MDO]_0/[I]_0$	Time (h)	Product
1[a]	Et_3OPF_6	245	20	decomposition
2[a]	CF_3SO_3H	211	4	decomposition
3[a]	CF_3SO_3Me	200	4	decomposition
4[a]	$(CF_3SO_2)_2O$	200	4	decomposition
5[b]	$BF_3 \cdot Et_2O$	1,000	0.25	decomposition
6[b]	$Sc(OTf)_3$	1,000	0.25	decomposition

[a]Reactions carried out in DCM (2.15M) and at - 20 °C. [b]Reactions carried out in the bulk at rt.

Table 3.7. CROP of MDO via and ACE mechanism with variable $[PyHTfO]_0$

Entry	$[MDO]_0 : [PyHTfO]_0$	Time (h)	Conversion[a] (%)	Yield[b] (%)	M_n[c] (kg/mol)	M_w[c] (kg/mol)	$Đ$[c]
1	2,000	18.5	36	37	64	78	1.2
2	817	18.25	43	43	82	98	1.2
3	500	5	n.d.	42	82	99	1.2
4	315	1	25	44	69	88	1.3
5[d]	98	1	54	30	---	---	---
6[e]	208	2	54	30	20	25	1.3

[a]Determined by ^{1}H NMR. [b]Reaction mixtures were only precipitated once, hence yields may exceed conversion. [c]Determined by THF SEC-MALLS. [d]Quenched with sodium phenoxide, $[MDO]_0$/[NaOPh] = 95. [e]Run with $[MDO]_0[BnOH]_0$ = 200. Polymerizations were run by first weighing solid PyHTfO into a 20 mL scintillation vial, then neat MDO was added. All mixtures were precipitated once into 9:1 hexanes:THF, dried under high vacuum, and analyzed by ^{1}H NMR and THF SEC-MALLS. Entry 5, quenched with sodium phenoxide, showed significant decomposition by ^{1}H NMR upon precipitation and was therefore not further analyzed by THF SEC-MALLS.

Table 3.8. Molar mass evolution with time for MDO CROP with DPP and no exogenous initiator

Entry	Time (min)	Conversion[a] (%)	M_n[b] (kg/mol)	M_w[b] (kg/mol)	D[b]	M_n[c] (kg/mol)	M_w[c] (kg/mol)	D[c]
1	2	18	95	130	1.3	35	53	1.5
2	4	20	70	85	1.2	31	57	1.9
3	6	34	101	130	1.2	31	59	1.9
4	8	31	43	60	1.4	27	52	1.9
5	10	37	N.A.	N.A.	N.A.	N.A.	N.A.	N.A.
6	12	40	37	50	1.4	24	47	2.0
7	30	46	30	39	1.3	19	36	1.9
8	60	54	27	35	1.3	17	33	1.9
9	90	59	24	33	1.4	16	32	2.0
10	120	57	24	33	1.4	17	32	1.9

[a]Determined from relative ^{1}H NMR integrations of MDO and PMDO resonances respectively of the quenched aliquots at the indicated times. [b]Determined from THF SEC-MALLS. Determined from THF SEC using conventional calibration analysis relative to polystyrene standards. The polymerization was conducted in neat MDO ($[MDO]_0$ = 10.19 M, $[MDO]_0/[DPP]_0$ = 1050). DPP solution (0.12 M in DCM) was transferred to a scintillation vial containing a stir bar and solvent was removed under high vacuum. MDO was then added to the dry DPP in a glove box. All aliquots were quenched with 1 mL THF containing 1 μL NEt_3.

Table 3.9. Molar mass evolution with time for MDO CROP with DPP and no exogenous initiator

Entry	Time (min)	Conversion[a] (%)	M_n[b] (kg/mol)	M_w[b] (kg/mol)	D[b]	M_n[c] (kg/mol)	M_w[c] (kg/mol)	D[c]
1	2	22	41	56	1.4	28	54	1.9
2	4	30	39	55	1.4	27	53	1.9
3	6	36	41	55	1.4	24	50	2.1
4	8	39	41	54	1.3	20	49	2.5
5	10	42	37	51	1.4	25	48	1.9
6	12	44	37	48	1.3	24	44	1.9
7	30	52	29	38	1.3	19	36	1.9
8	60	57	25	34	1.4	15	29	2.0
9	90	60	31	38	1.3	18	32	1.8
10	120	58	26	34	1.3	14	31	2.2

[a]Determined from relative ^{1}H NMR integrations of MDO and PMDO resonances respectively of the quenched aliquots at the indicated times. [b]Determined from THF SEC-MALLS. Determined from THF SEC using conventional calibration analysis relative to polystyrene standards. The polymerization was conducted in neat MDO ($[MDO]_0$ = 10.19 M, $[MDO]_0/[DPP]_0$ = 981). DPP solution (0.12 M in DCM) was transferred to a scintillation vial containing a stir bar and solvent was removed under high vacuum. MDO was then added to the dry DPP in a glove box. All aliquots were quenched with 1 mL THF containing 1 μL NEt_3.

Figures 3.5 – 3.27

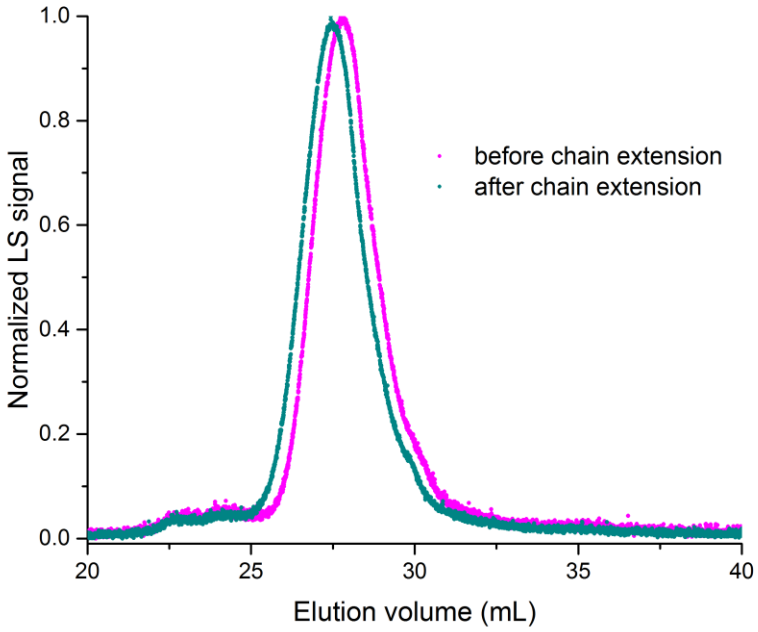

Figure 3.5. THF SEC-MALLS trace for PMDO prior to addition of fresh monomer (M_n =8.5 kg/mol, $Đ \approx 1.25$) and post MDO injection (M_n = 10.6 kg/mol, $Đ \approx 1.25$).

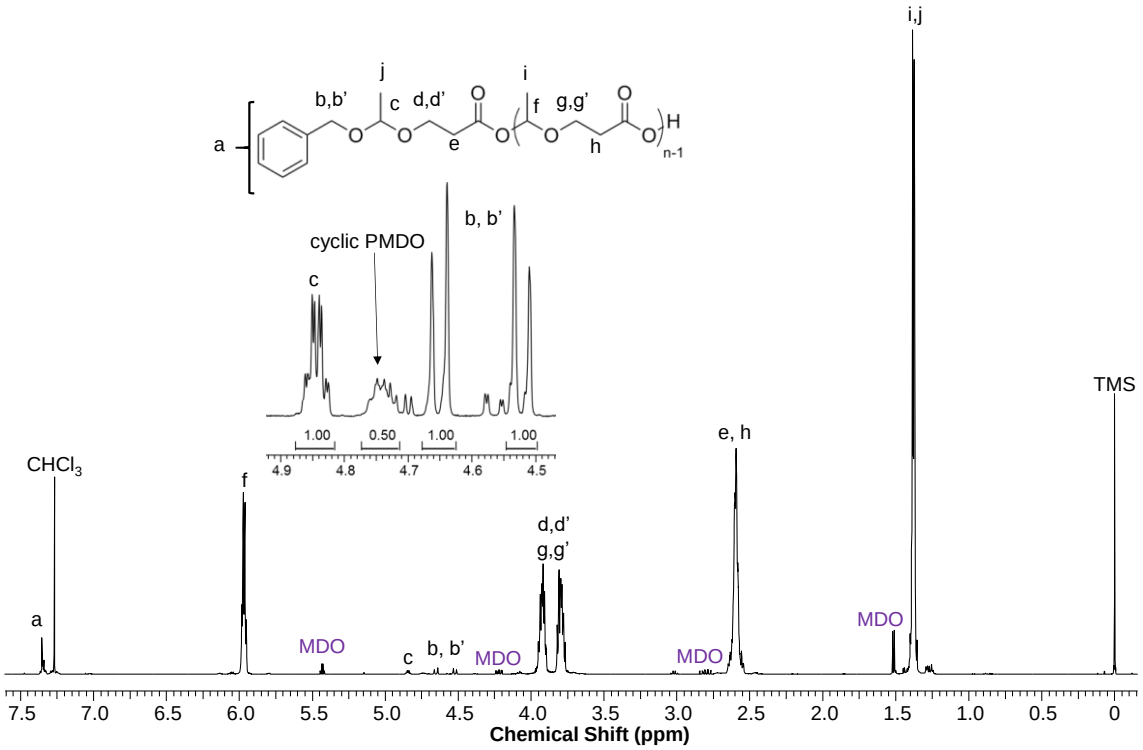

Figure 3.6. ^{1}H NMR spectrum of purified PMDO initiated with benzyl alcohol (Table 2, Entry 1).

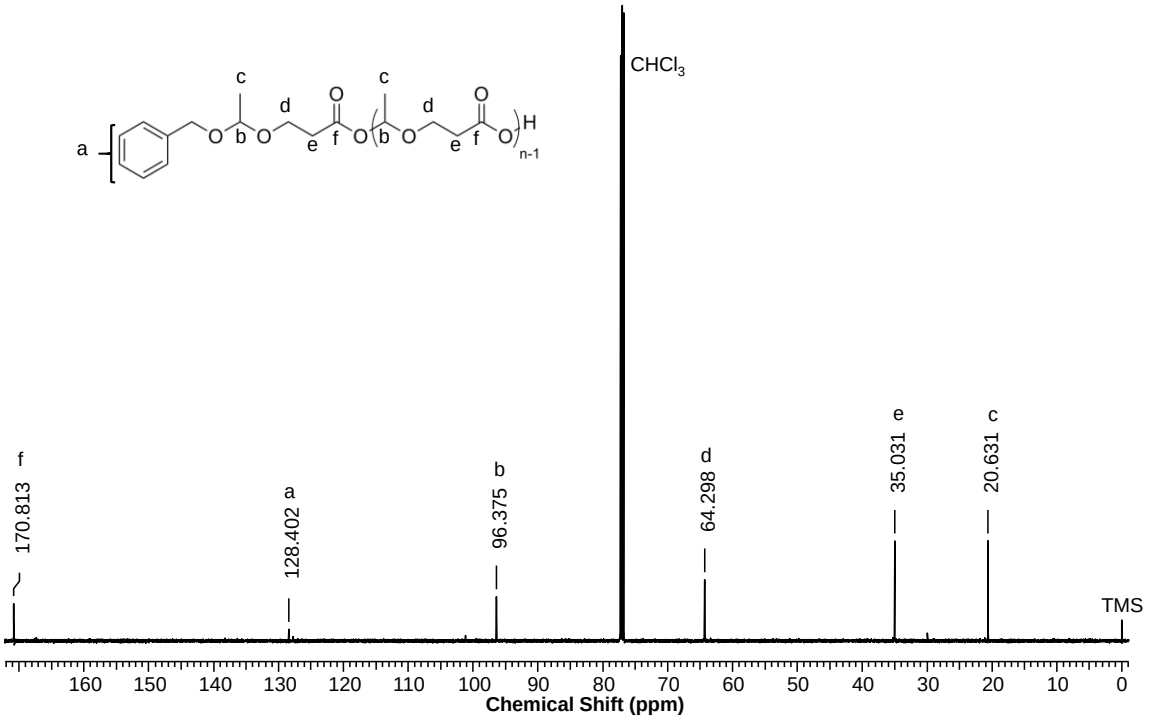

Figure 3.7. ^{13}C NMR spectrum of purified PMDO initiated with benzyl alcohol (Table 2, Entry 1).

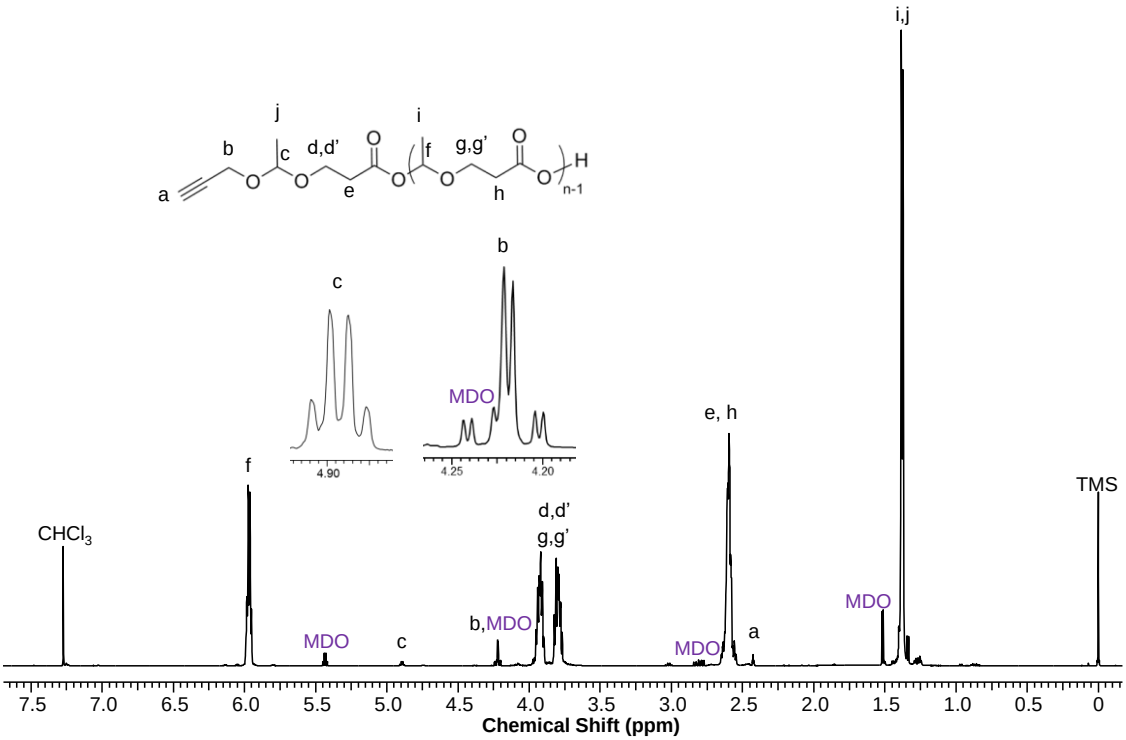

Figure 3.8. ^{1}H NMR spectrum of purified PMDO initiated with propargyl alcohol (Table 2, Entry 2).

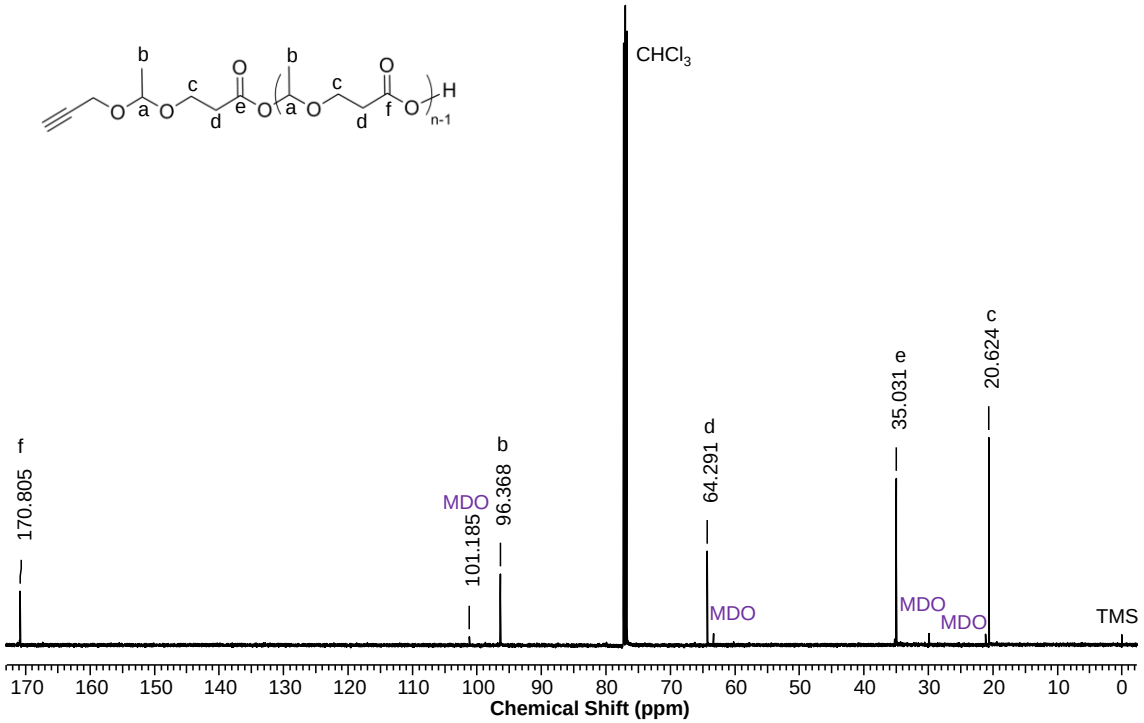

Figure 3.9. ^{13}C NMR spectrum of purified PMDO initiated with propargyl alcohol (Table 2, Entry 2).

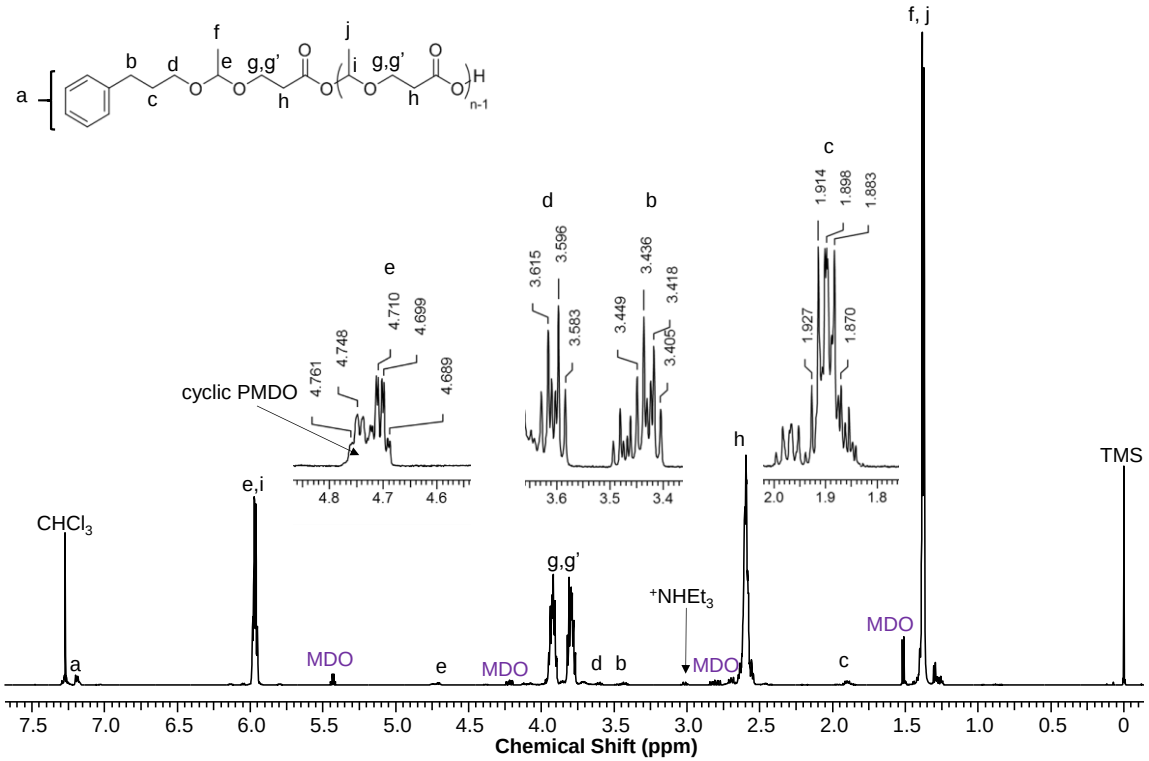

Figure 3.10. ^{1}H NMR spectrum of purified PMDO initiated with 3-phenyl-1-propanol (Table 2, Entry 3).

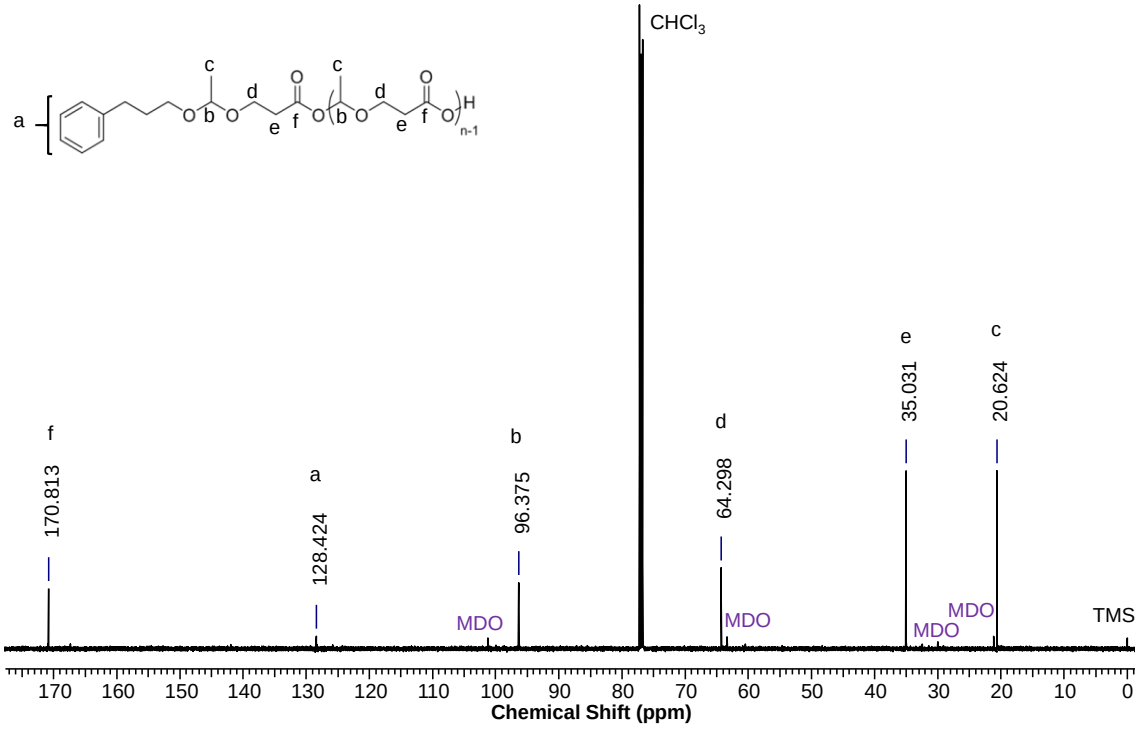

Figure 3.11. ^{13}C NMR spectrum of purified PMDO initiated with 3-phenyl-1-propanol (Table 2, Entry 3).

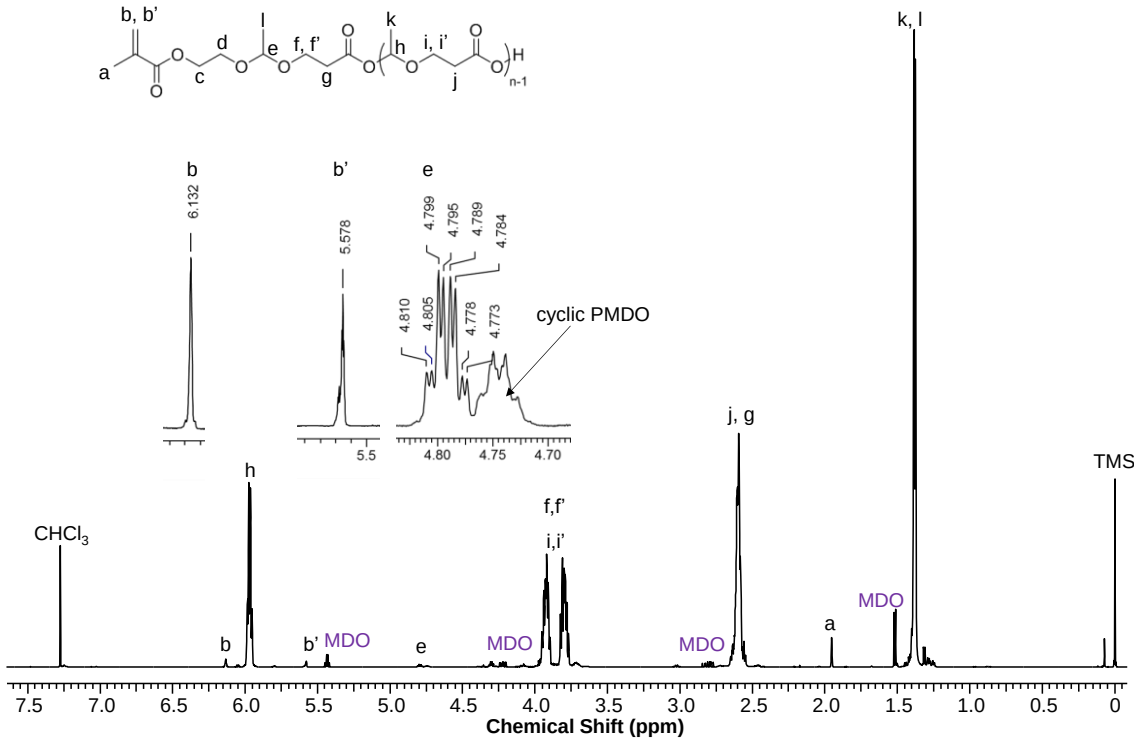

Figure 3.12. [1]H NMR spectrum of purified PMDO with 2-hydroxyethyl methacrylate (Table 2, Entry 4).

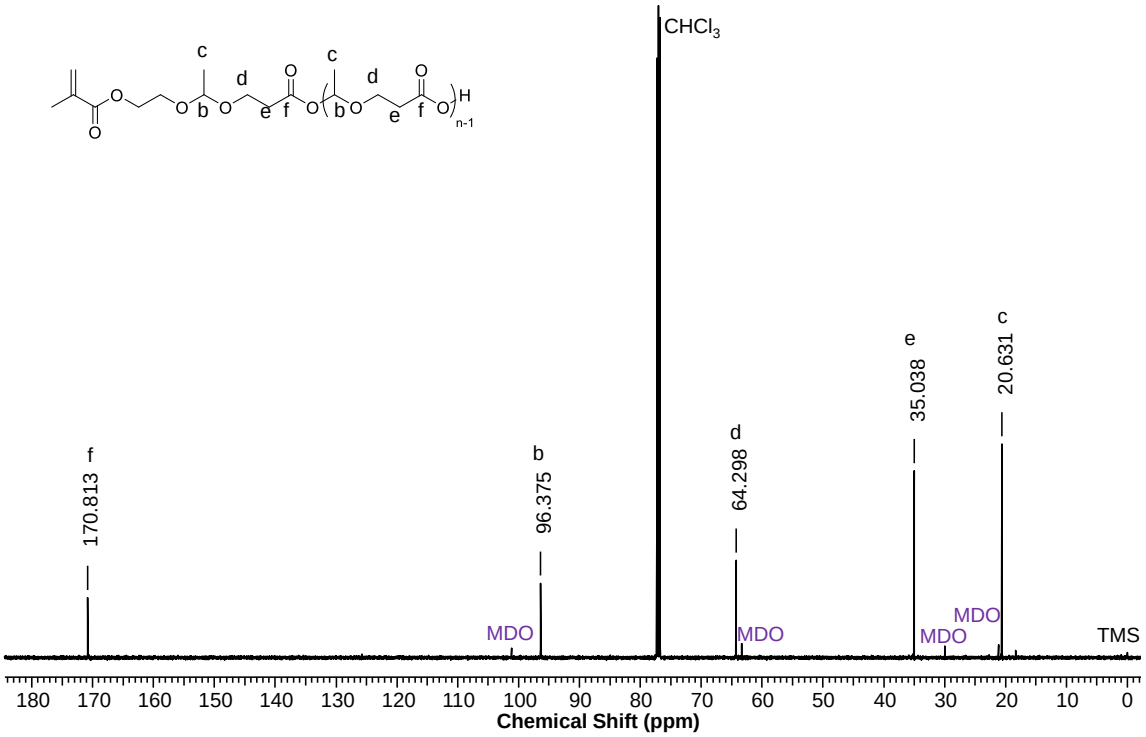

Figure 3.13. ^{13}C NMR spectrum of purified PMDO initiated with 2-hydroxyethyl methacrylate (Table 2, Entry 4).

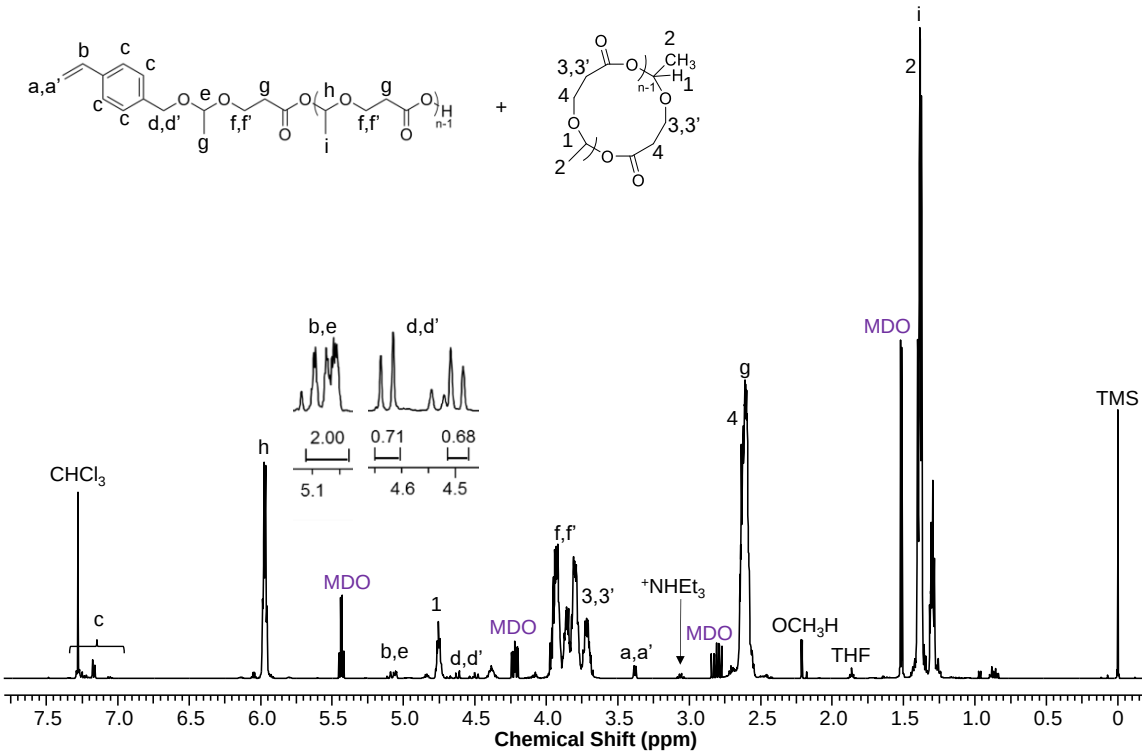

Figure 3.14. ^{1}H NMR spectrum of purified PMDO initiated with (4-vinylphenyl)methanol (Table 2, Entry 5).

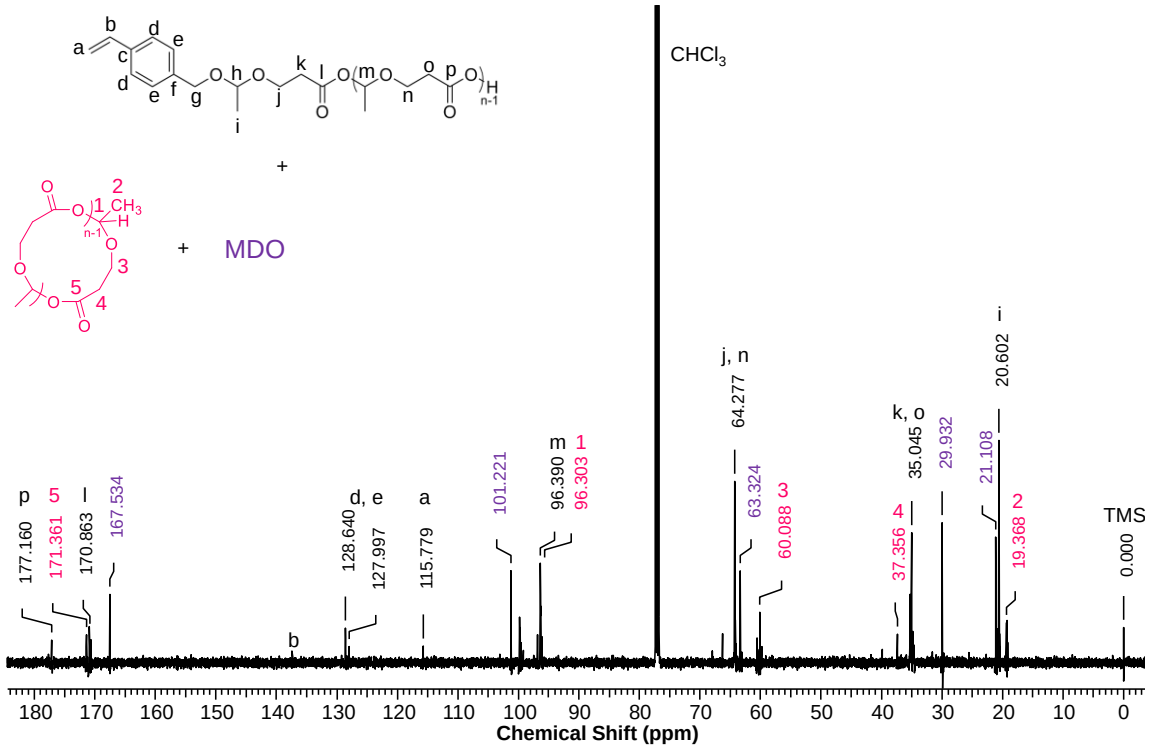

Figure 3.15. ^{13}C NMR spectrum of purified PMDO initiated with (4-vinylphenyl)methanol (Table 2, Entry 5).

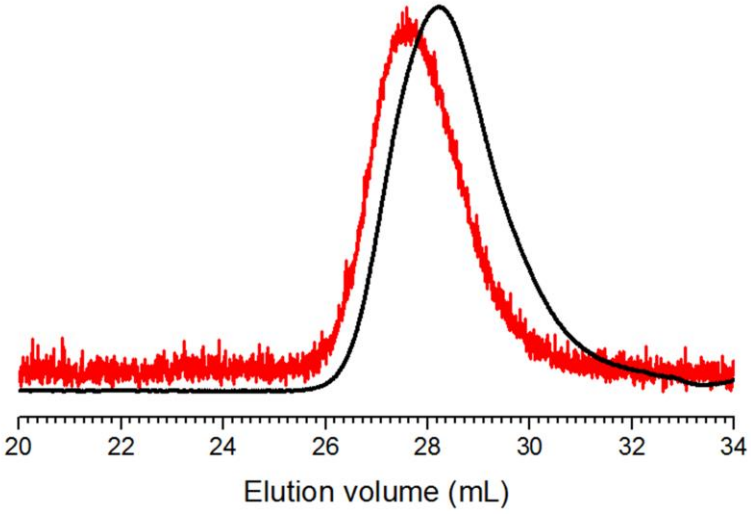

Figure 3.16. THF SEC trace (red = SEC-MALLS, black = dRI detector) for PMDO initiated with benzyl alcohol

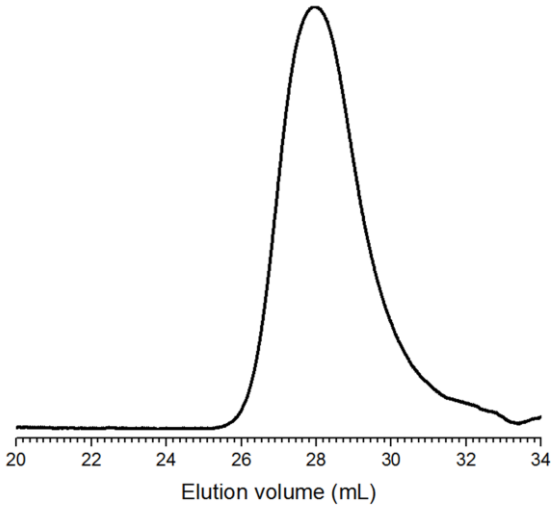

Figure 3.17. THF SEC trace (dRI detector) for PMDO initiated with propargyl alcohol.

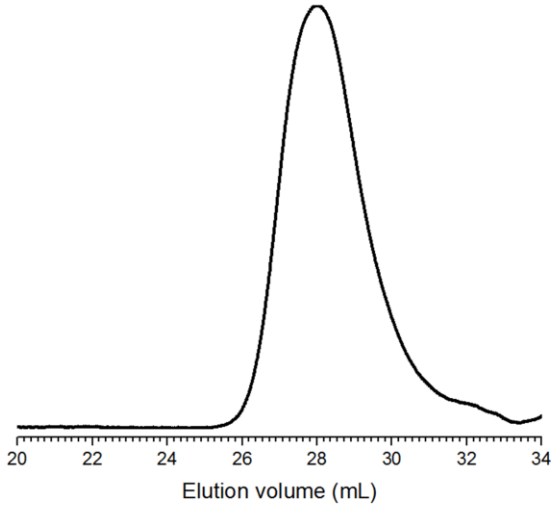

Figure 3.18. THF SEC trace (dRI detector) for PMDO initiated with 3-phenyl-1-propanol.

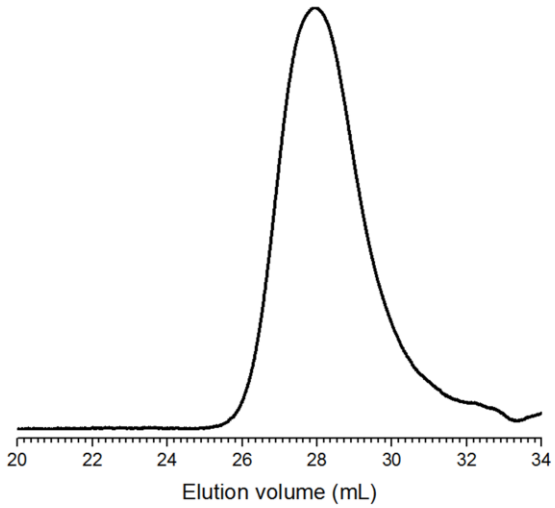

Figure 3.19. THF SEC trace (dRI detector) for PMDO initiated with 2-hydroxyethyl methacrylate.

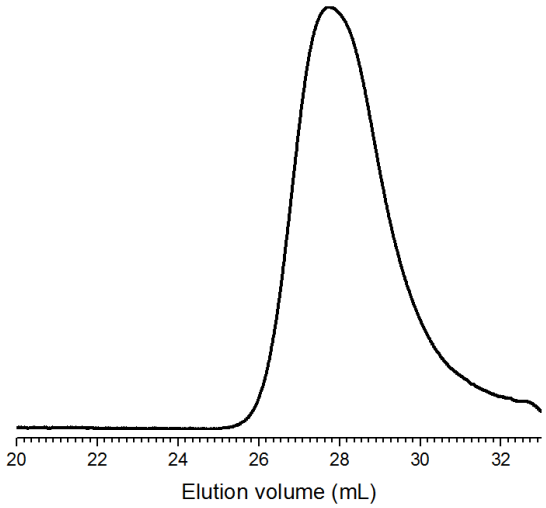

Figure 3.20. THF SEC trace (dRI detector) for PMDO initiated with (4-vinylphenyl)methanol.

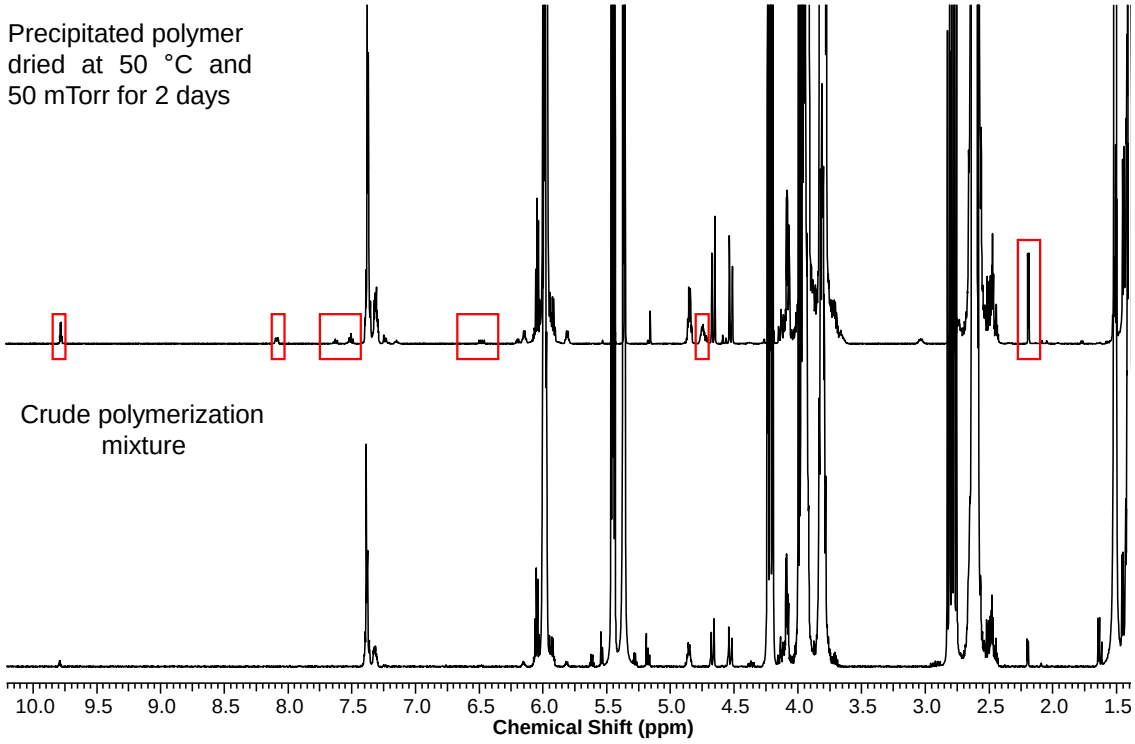

Figure 3.21. PMDO initiated with benzyl alcohol before and after precipitation and drying under high vacuum at 50 °C. Increased acetaldehyde evolution is observed after heating the polymer under vacuum and it appears that benzyl acetal end groups are diminished as the relative amounts of cyclic PMDO and vinyl ether terminated PMDO increase.

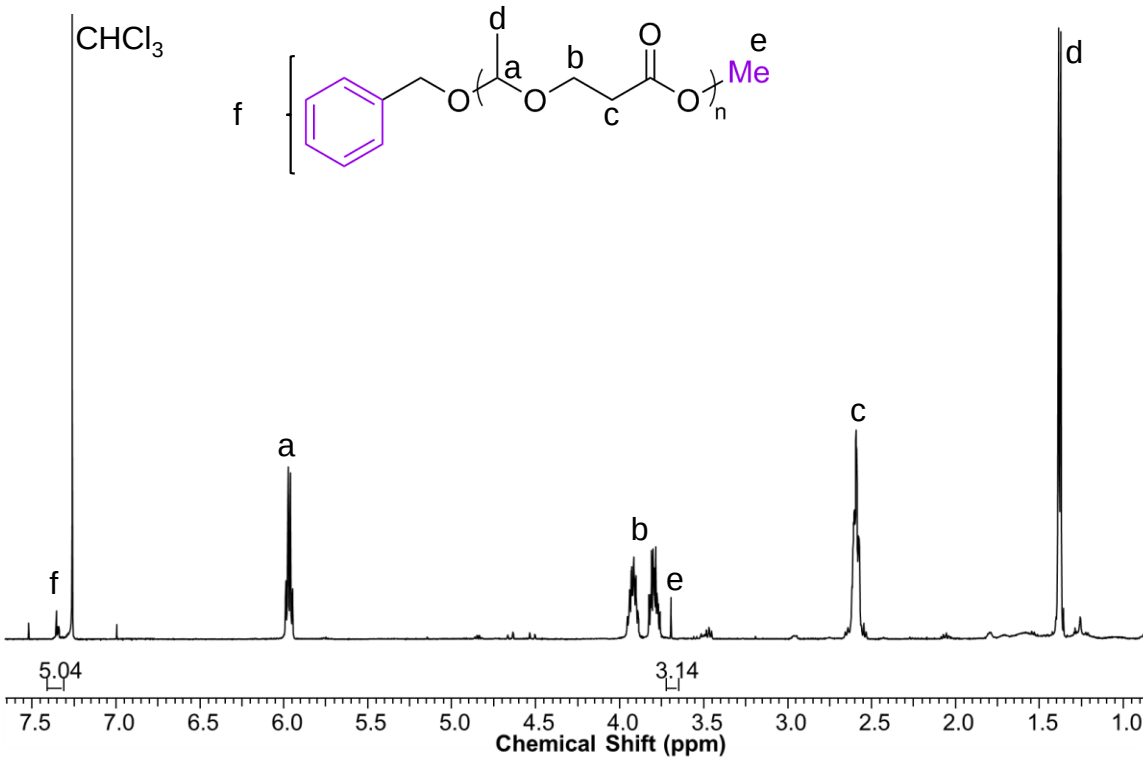

Figure 3.22. PMDO after esterification of the carboxylic acid terminus with MeI/DBU in DMF.

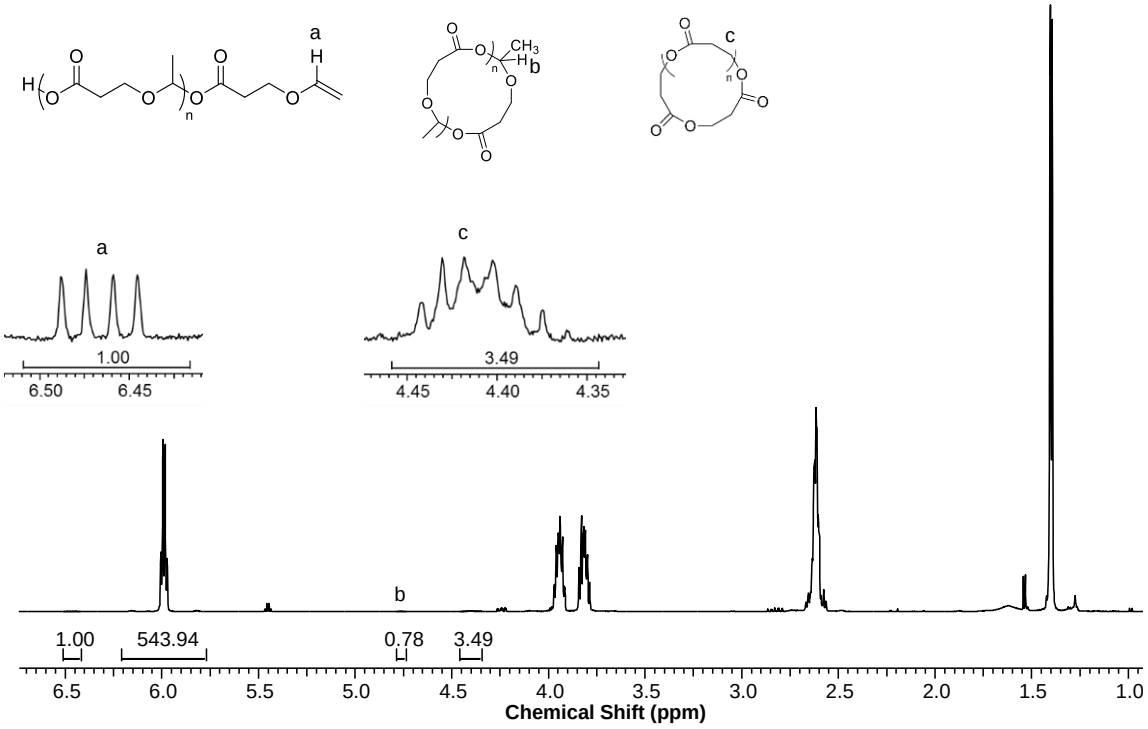

Figure 3.23. Precipitated PMDO prepared via ACE mechanism with $[MDO]_0/[DPP]_0$ = 4,000 (see Entry 4 Table 1). As molar masses were significantly higher in the polymerization of MDO via an ACE mechanism than in polymerization of MDO via an AM mechanism only a low concentration of low molar mass cyclic PMDO remained after precipitation.

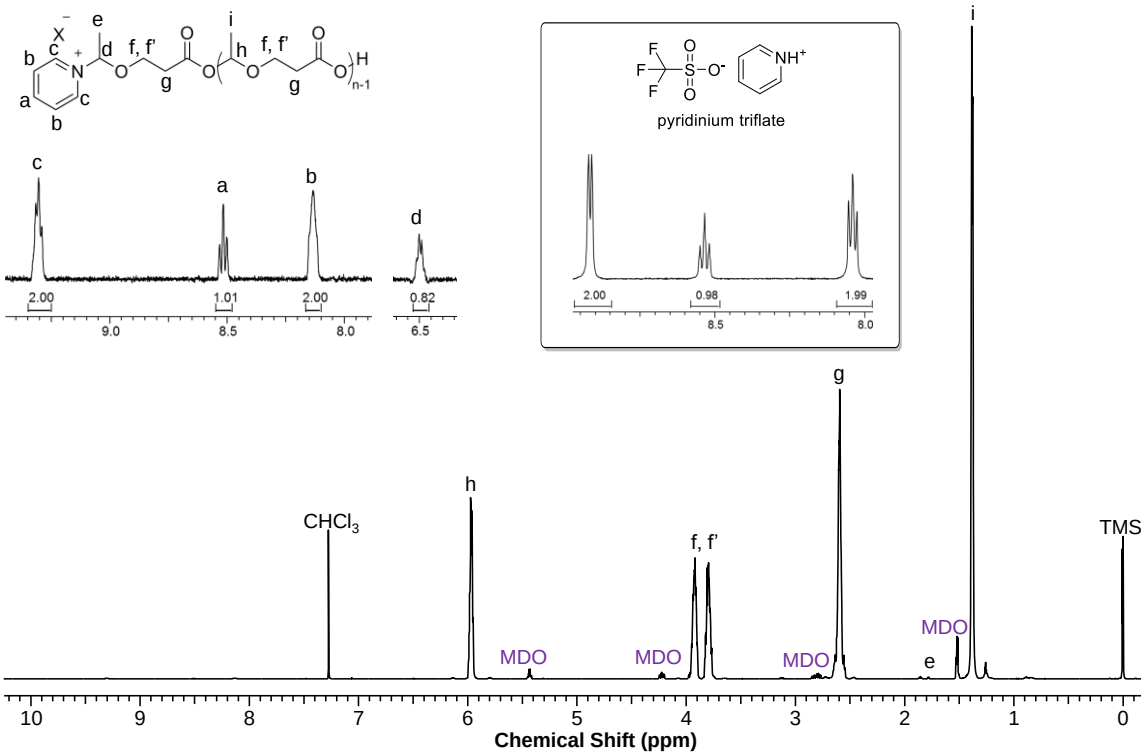

Figure 3.24. ^{1}H NMR spectrum obtained at 500 Mhz for purified PMDO synthesized with pyridinium triflate ($[MDO]_0/[PyHTfO]_0$ = 5,00). It appears that the pyridine has been incorporated into the chain end.

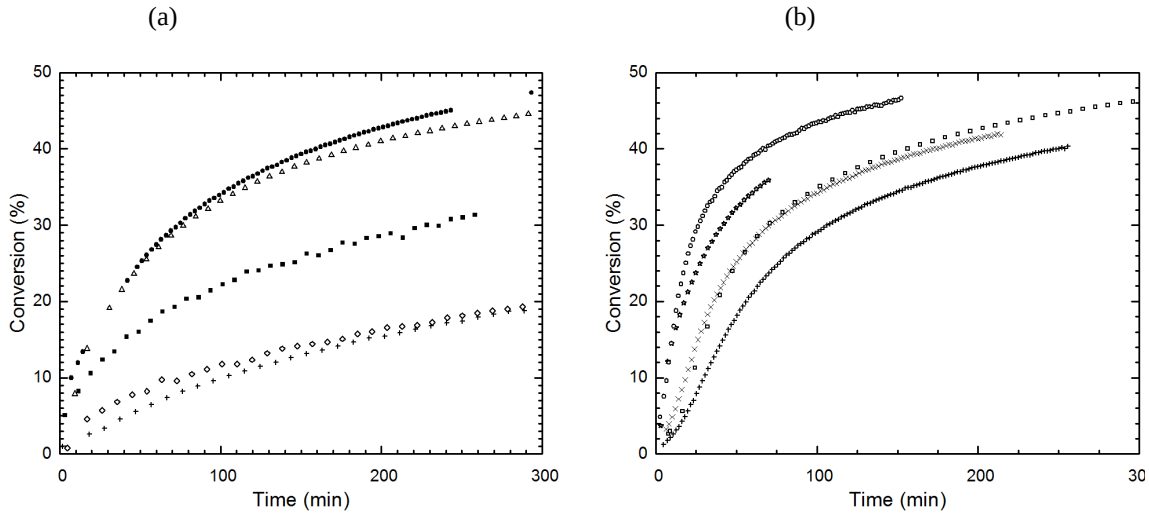

Figure 3.25. (a) MDO CROP with no exogenous initiator: $[MDO]_0$ = 10.1 M, $[MDO]_0/[DPP]_0$ = 1,000 (●), 2,000 (Δ), 3,000 (■), 4,000 (◊), and 5,000 (+). (b) MDO CROP with BnOH as initiator: $[MDO]_0$ = 10.1 M, $[BnOH]_0$ = 125 mM, and $[MDO]_0/[DPP]_0$ = 1,000 (○), 2,000 (*), 3,000 (×), 4,000 (□), and 5,000 (+).

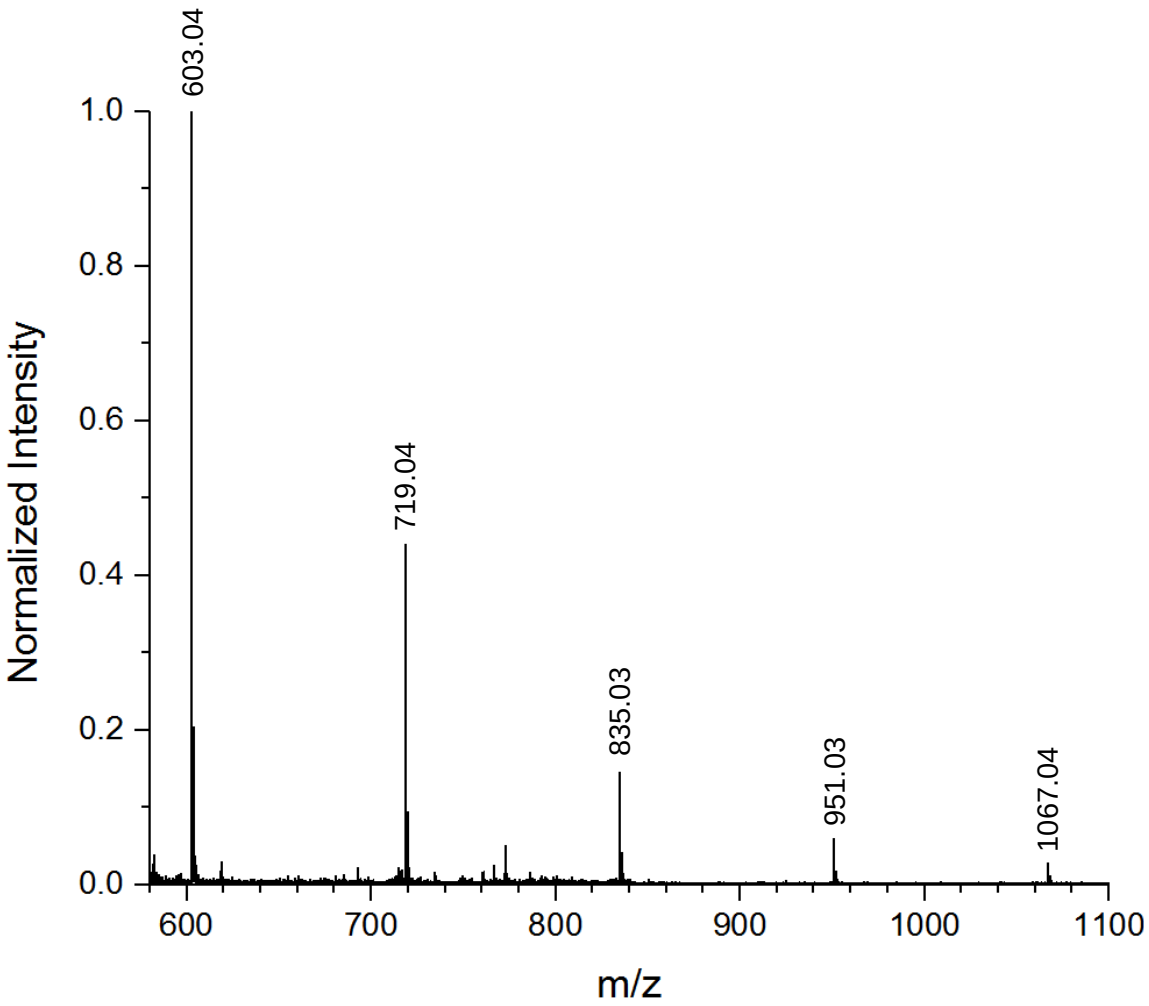

Figure 3.26. MALDI-TOF data for entry 10 of table 3. Molar mass analysis by THF SEC-MALLS for this aliquot gave M_n = 32 kg/mol and $Đ$ = 1.2. The displayed data was obtained using the reflector mode as the linear mode did not afford peaks of sufficient intensity for analysis. (a) Conditions: 10 mg unpurified PMDO sample was dissolved in 1 mL of anhydrous THF. Then 1 µL of polymer solution was mixed with 1 µL of 10 mg/mL NaI in THF, spotted onto a plate and allowed to dry. Last, 1 µL of 10 mg/mL dithranol in THF was spotted onto the polymer/salt mixture. The repeat unit molar mass is 116 g/mol and peaks can be analyzed to determine the end group via: N_n×116 g/mol + 22.9898 g/mol (M_{Na^+}). For example: 5×116 g/mol + 22.9898 g/mol = 602.99 g/mol, which is in good agreement with PMDO molecules that exhibit a cyclic architecture.

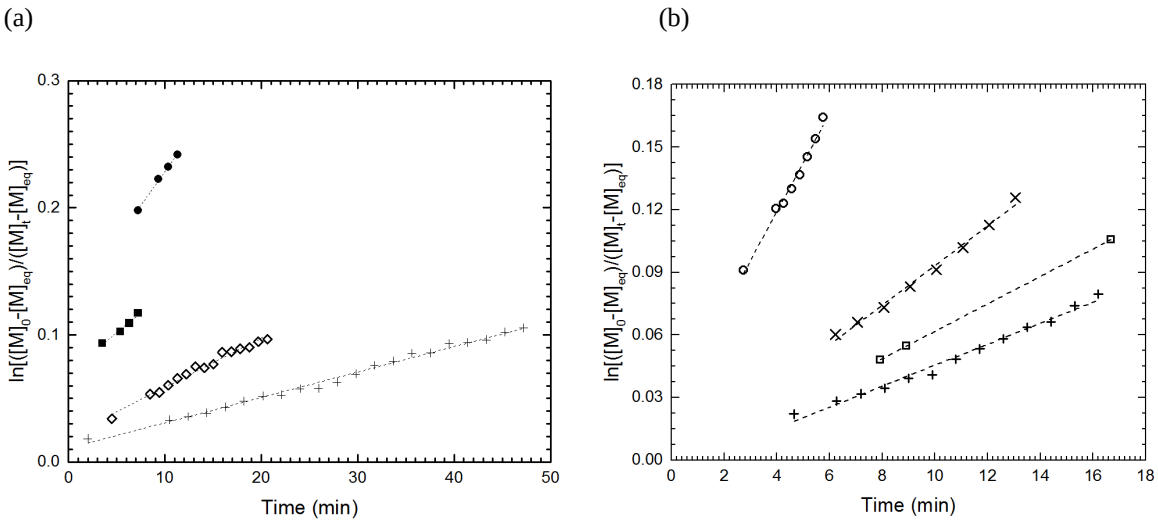

Figure 3.27. Semilogarithmic anamorphoses of the data shown in Figure 3.25 (a) and (b). (a) MDO CROP with no exogenous initiator: $[MDO]_0$ = 10.1 M, $[MDO]_0/[DPP]_0$ = 1,000 (●, k_{app} = 0.011 ± 5.7×10^{-19} min^{-1}, R^2 = 1.0), 3,000 (■, k_{app} = 0.0063 ± 6.2×10^{-4} min^{-1}, R^2 = 0.99), 4,000 (◊, k_{app} = 0.0039 ± 1.5×10^{-4} min^{-1}, R^2 = 0.99), and 5,000 (+, k_{app} = 0.002 ± 3.9×10^{-5} min^{-1}, R^2 = 0.99). (b) MDO CROP with BnOH as initiator: $[MDO]_0$ = 10.1 M, $[BnOH]_0$ = 125 mM, and $[MDO]_0/[DPP]_0$ = 1,000 (○, k_{app} = 0.023 ± 3.9×10^{-19} min^{-1}, R^2 = 0.99), 3,000 (×, k_{app} = 0.0095 ± 33.6×10^{-4} min^{-1}, R^2 = 0.99), 4,000 (□, k_{app} = 0.0066 ± 1.4×10^{-5} min^{-1}, R^2 = 0.99), and 5,000 (+, k_{app} = 0.0050 ± 1.75×10^{-4} min^{-1}, R^2 = 0.99).

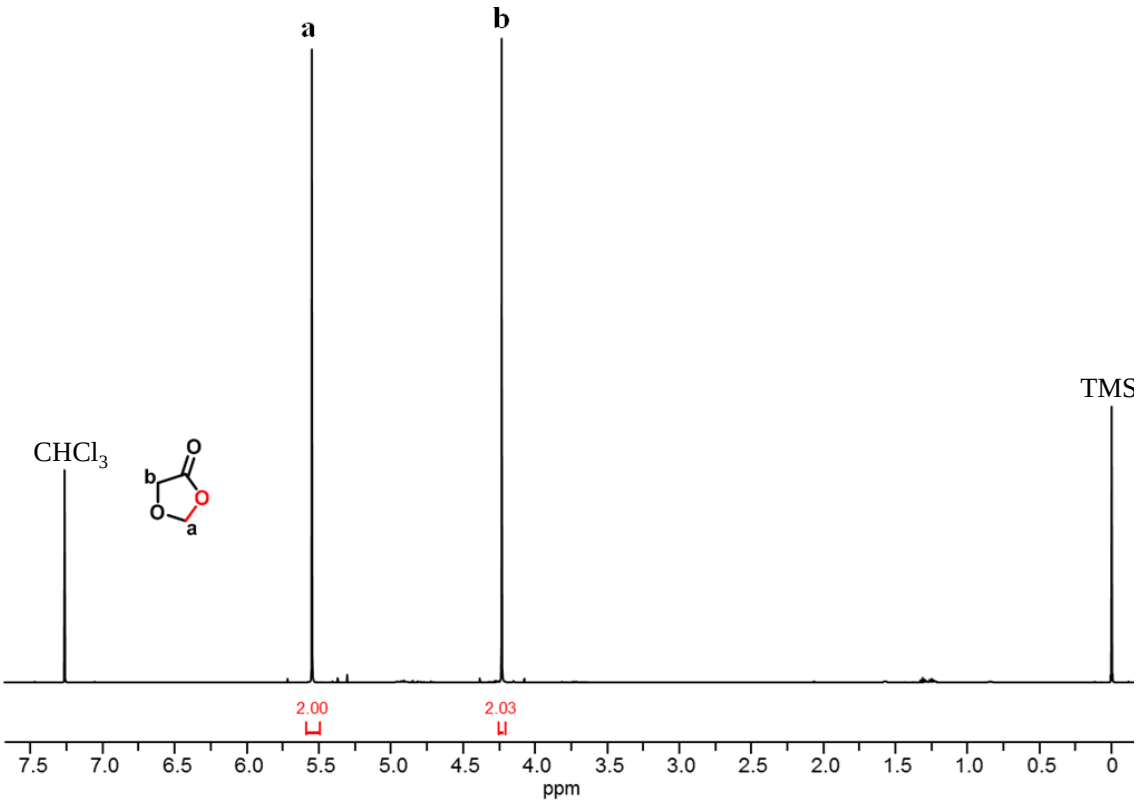

Figure 3.28. ^{1}H NMR spectrum of 1,3-dioxolan-4-one (DOX) prepared according to the reported procedure.[9]

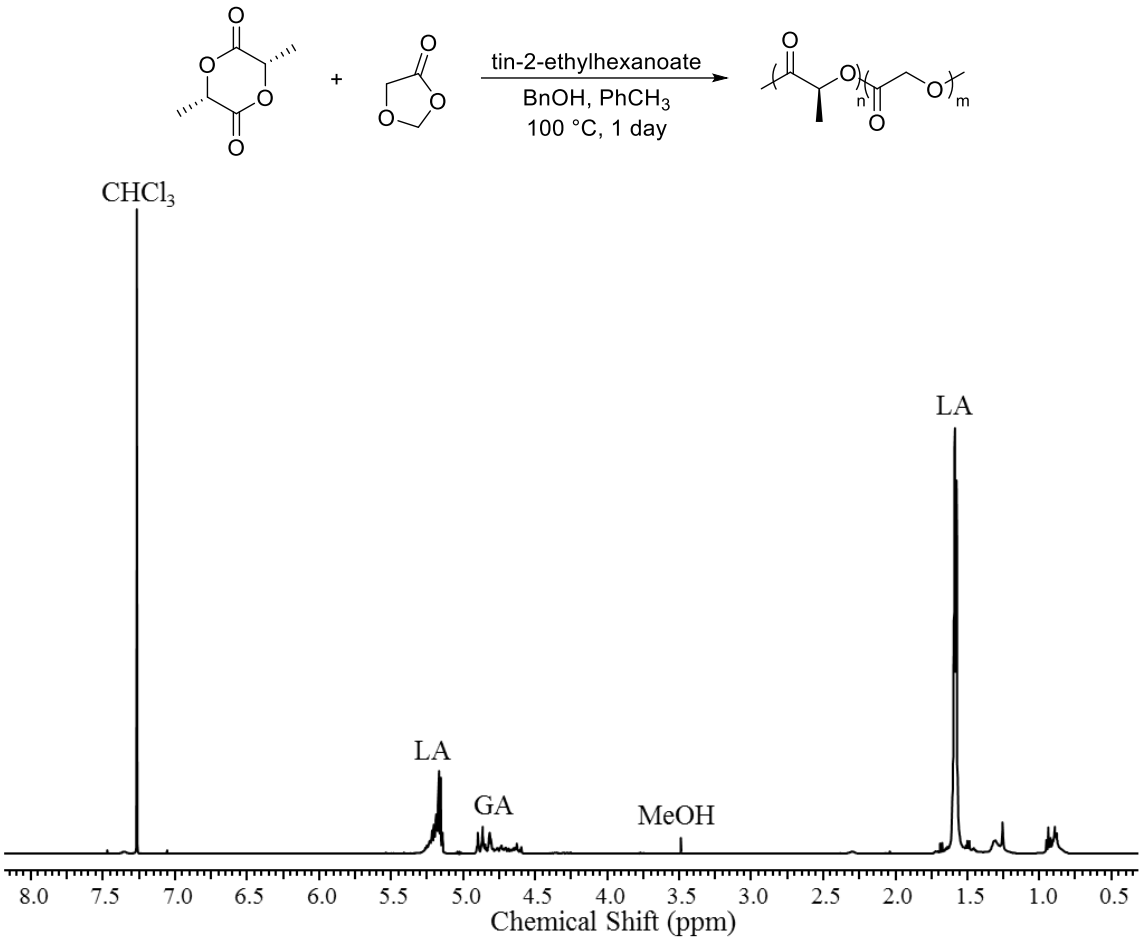

Figure 3.29. ^{1}H NMR spectrum of the product obtained from the copolymerization of DOX with L-lactide as described.[9] 100 mg DOX (1.1 mmol) and 140 mg L-lactide (1 mmol) were placed in a small pressure vessel in the glove box. A 0.006M stock solution of tin(II) 2-ethylhexanoate was prepared in anhydrous toluene of which 0.7 mL were added to dissolve the L-lactide/DOX mixture. To the solution were added 0.5 μL benzyl alcohol (0.0042 mmol) via microsyringe. The pressure vessel was sealed and removed from the glove box and heated in an oil bath at 100 °C for a day. The resultant polymer was precipitated into methanol and dried under vacuum. The observed shifts are in good agreement with those for poly(lactide-*co*-glycolic acid).[26] Units denoted GA present signals associated with carbon atoms of the glycolic acid units and units denoted LA present signals associated with lactide units in the copolymer.

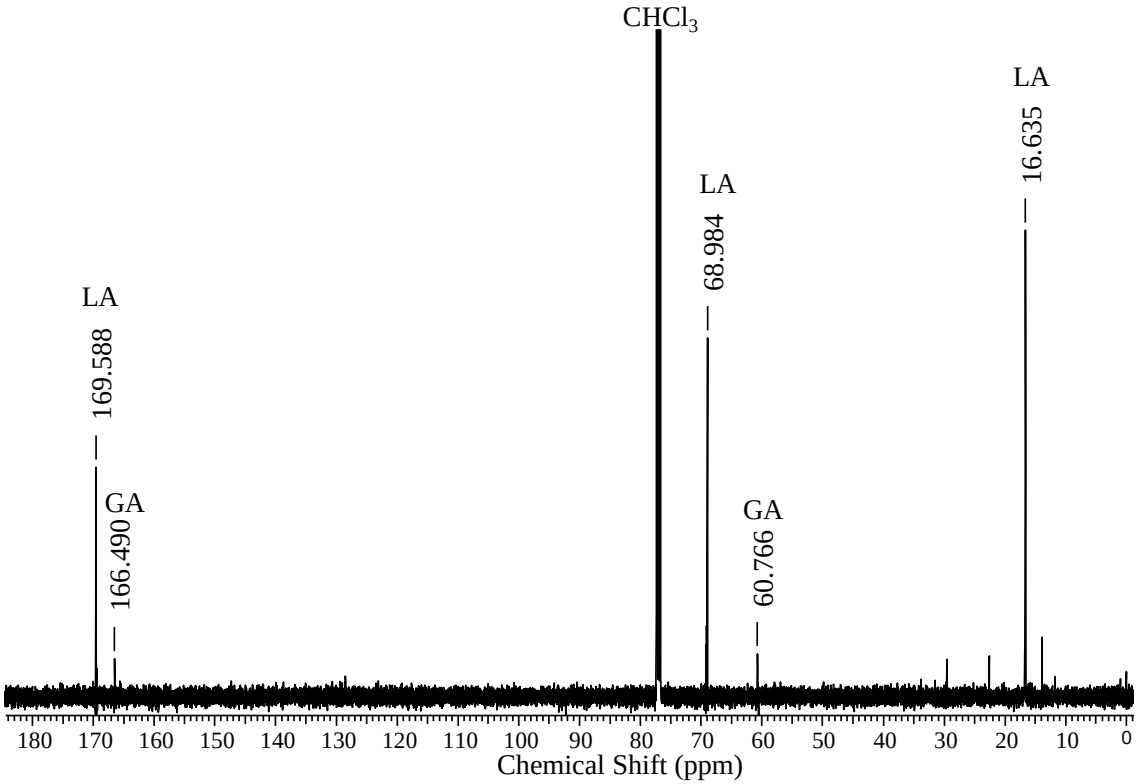

Figure 3.30. ^{13}C NMR spectrum of the product obtained from the copolymerization of DOX with L-lactide. The observed shifts are in good agreement with those for poly(lactide-*co*-glycolic acid).[26] Units denoted GA present signals associated with carbon atoms of the glycolic acid units and units denoted LA present signals associated with lactide units in the copolymer.

References

1) http://www.un.org/en/development/desa/news/population/2015-report.html, accessed 04/06/2016.

2) Andrady, A.; Neal, M. A. Applications and Societal Benefits of Plastics. *Phil. Trans. R. Soc. B*, **2009**, *364*, 1977−1984.

3) Bornscheuer, U. T. Feeding on plastic. *Science*, **2016**, *351*, 1154−1155.

4) ASTM Standard D6400, 2012, "Standard Specification for Labeling of Plastics Designed to be Aerobically Compostable in Municipal or Industrial Facilities," ASTM International, West Conshohocken, PA, 2012, DOI: 10.1520/D6400-12, www.astm.org.

5) Qian, H.; Wohl, A. R.; Crow, J. T.; Macosko, C. W.; Hoye, T. R. A Strategy for Control of "Random" Copolymerization of Lactide and Glycolide: Application to Synthesis of PEG-b-PLGA Block Polymers Having Narrow Dispersity. *Macromolecules*, **2011**, *44*, 7132−7140.

6) Galluci, R. R.; Going, R.C. Reaction of Hemiacetal Esters, Acetals, and Acylals with Alcohols or Acetic Acid. *J. Org. Chem.* **1982**, *47*, 3517−3521.

7) Otsuka, H.; Endo, T. Poly(hemiacetal ester)s: New Class of Polymers with Thermally Dissociative Units in the Main Chain. *Macromolecules* **1999**, *32*, 9059−9061.

8) Matsukawa, D.; Okamura, H.; Shirai, M. Preparation of Replicated Resin Mold for UV Nanoimprint Using Reworkable Dimethacrylate. *J. Photopolym. Sci. Technol.* **2010**, *23*, 781−787.

9) Martin, R. T.; Camargo, L. P.; Miller, S. A. Marine-degradable Polylactic Acid. *Green Chem.* **2014**, *16*, 1768−1773.

10) Athanasiou, K. A.; Niederauer, G. G.; Agrawal, C. M. Sterilization, Toxicity, Biocompatibility and Clinical Applications of Polylactic acid/ Polyglycolic Acid Copolymers. *Biomaterials* **1996**, *17*, 93−102.

11) Neitzel, A. E.; Petersen, M. A.; Kokkoli, E.; Hillmyer, M. A. Divergent Mechanistic Avenues to an Aliphatic Polyesteracetal or Polyester from a Single Cyclic Esteracetal. *ACS Macro Lett.* **2014**, *3*, 1156−1160.

12) Penczek, S.; Cypryk, M.; Duda, A.; Kubisa, P.; Słomkowski, S. Living Ring-opening Polymerization of Heterocyclic Monomers. *Prog. Polym. Sci*. **2007**, *32*, 247−282.

13) Nuyken, O.; Pask, S. D. Ring-Opening Polymerization—An Introductory Review. *Polymers* **2013**, *5*, 361−403.

14) Kammiyada, H.; Konishi, A.; Ouchi, M.; Sawamoto, M. Ring-Expansion Living Cationic Polymerization via Reversible Activation of a Hemiacetal Ester Bond. *ACS Macro Lett.***2013**, *2*, 531−534.

15) Rubush, D. M. **2014**. Diphenylphosphoric Acid. *e-EROS Encyclopedia of Reagents for Organic Synthesis*. 1–6.

16) Zhao, J.; Pahovnik, D.; Gnanou, Y.; Hadjichristidis, N. A "Catalyst Switch" Strategy for the Sequential Metal-Free Polymerization of Epoxides and Cyclic Esters/Carbonates. *Macromolecules* **2014**, *47*, 3814−3822.

17) Makiguchi, K.; Satoh, T.; Kakuchi, T. Diphenyl Phosphate as an Efficient Cationic Organocatalyst for Controlled/Living Ring-opening Polymerization of δ-Valerolactone and ε-Caprolactone. *Macromolecules* **2011**, *44*, 1999−2005.

18) Jacobson, H.; Stockmayer, W. H. Intramolecular Reaction in Polycondensations. I. The Theory of Linear Systems. *J. Chem. Phys.* **1950**, *18*, 1600−1606.

19) Chwiałkowska, W.; Kubisa, P.; Penczek, S. Preparation of Living Mono- and Dicationically Growing Polyacetals and Attempts to prepare Block Copolymers thereof. *Makromol. Chem.* **1982**, *183*, 753−769.

20) Hrkach, J. S.; Matyjaszewski, K. Reaction of 2-methyl-2-oxazoline with trimethylsilyl initiators: an unusual mode of ring opening. *Macromolecules* **1992**, *25*, 2070−2075.

21) University of Minnesota Chemistry Department NMR Facility Home Page, http://nmr.chem.umn.edu/manuals.html, accessed 07/20/2016.

22) Kubisa, P. Penczek, S. Cationic Activated Monomer Polymerization of Heterocyclic Monomers. *Prog. Polym. Sci.* **1999**, 24, 1409−1437.

23) Baśko, M.; Kubisa, P. Cationic Copolymerization of ε-Caprolactone and L,L-Lactide by an Activated Monomer Mechanism. *J. Polym. Sci. A Polym. Chem.* **2006**, *44*, 7071−7081.

24) Wojtania, M.; Kubisa, P.; Penczek, S. Polymerization of Propylene Oxide by Activated Monomer Mechanism. Suppression of Macrocyclics Formation. *Makromol. Chem., Makromol. Symp.* **1986**, *6*, 201−206.

25) Rolando, C.; Penhoat, M.; Gholamipour-Shirazi, A. Alkylation of carboxylic acids in a microfluidic device: kinetics parameters determination, Hammett reaction constant measurement and optimization of preparative experiment. *In Proceedings of the 13th Int. Electron. Conf. Synth. Org. Chem.*, 1–30 November 2009; Sciforum Electronic Conference Series, Vol. 13, 2009, a038.

26) Stayshich, R.M.; Meyer, T.Y. New Insights into Poly(lactic-*co*-glycolic acid) Microstructure: Using Repeating Sequence Copolymers To Decipher Complex NMR and Thermal Behavior. *J. Am. Chem. Soc.,* **2010**, *132,* 10920−10934.

Chapter 4 :

Cationic Ring-Opening Polymerization of 7-Methoxyoxepan-4-one

The work in this chapter was carried out in part in collaboration with Thomas Haversang and Dr. Leonel Barreda.

4.1 Introduction

The detailed understanding of mechanistic phenomena in cationic polymerization processes[1-6] has facilitated the development of living polymerization methods for a range of linear[7-17] and cyclic monomers,[18-21] and laid the foundation for the realization of powerful controlled radical polymerization[22,23] used widely by polymer scientists today. Recently, the reversible addition-fragmentation chain transfer (RAFT) polymerization, developed to exert control over radical polymerizations, has stimulated the expansion to analogous cationic RAFT polymerization methodology.[24-31] In our studies of cyclic hemiacetal esters, molecules only recently employed as monomers in polymer chemistry, we realized that a cationic process was operative in their transformation to polyhemiacetal esters. We have since worked to establish an understanding of the operative mechanisms in the polymerization of these molecules in an effort to achieve living polymerization kinetics that would eventually allow for the development of materials with tailored hydrolytic and thermal degradation profiles.

We previously disclosed the cationic ring-opening polymerization (CROP) of the cyclic hemiacetal ester 2-methyl(1,3-dioxan-4-one) (MDO) (Scheme 4.1. In our study of zinc alkoxides as initiating species we serendipitously discovered that cyclic hemiacetal esters could be used as masked lactones to generate polyesters; in the case of MDO swiftly producing poly(3-hydroxypropionic acid) at quantitative conversions due to the concurrent, entropically-driven extrusion of acetaldehyde. Similarly, Martin et. al published a paper around the same time disclosing the polymerization of the cyclic hemiacetal ester 1,3-dioxolane (DOX). As the homopolymer of DOX was challenging to characterize, the authors reasonably assumed they had produced the novel polyhemiacetal

ester poly(DOX), and did not capitalize on their discovery of the entropically-driven process due to loss of formaldehyde yielding polyglycolic acid. This methodology has been further developed by the Shaver group, who has beautifully demonstrated the synthesis of polyesters from both 5-membered cyclic hemiacetal and hemiketal esters, most notably producing polymandelic acid of any desired tacticity in the most efficient and economical way known to date.[32]

In the same initial study of MDO, we were able to show that at low initial concentrations of diethylzinc ($[Et_2Zn]_0$ < 14 mM) in neat MDO, acetaldehyde extrusion could be suppressed entirely and the novel poly(2-methyl-1,3-dioxan-4-one) (PMDO) was obtained exclusively with molar masses up to M_n ~ 30 kg/mol and dispersities of $Đ$ ~ 1.6. This result, albeit exciting, was impractical for the synthesis of polyhemiacetal esters as the low concentrations of catalyst required to avoid acetaldehyde expulsion resulted in lethargic rates of polymerization. The kinetic limitation of zinc-catalyzed ROP of MDO was successfully overcome by instead employing diphenylphosphoric acid as the catalyst. Cationic ring-opening polymerization of the cyclic hemiacetal ester MDO with DPP proceeds rapidly in the presence or absence of exogenous initiator to produce PMDO. Target molar masses were achieved at high concentrations of alcohol initiator *via* an activated monomer (AM) mechanism, yielding PMDO with molar masses not exceeding M_n ~ 10 kg/mol. High molar mass PMDO could be generated *via* an active chain-end (ACE) mechanism, operative in the absence of exogenous initiator. In the latter case we observed a non-linear correlation between $[MDO]_0/[DPP]_0$, manifesting in higher molar mass PMDO at lower initial concentrations of DPP and end groups arising primarily from chain transfer reactions.

Scheme 4.1. Summary of kinetic and thermodynamic considerations of MDO ROP to PMDO

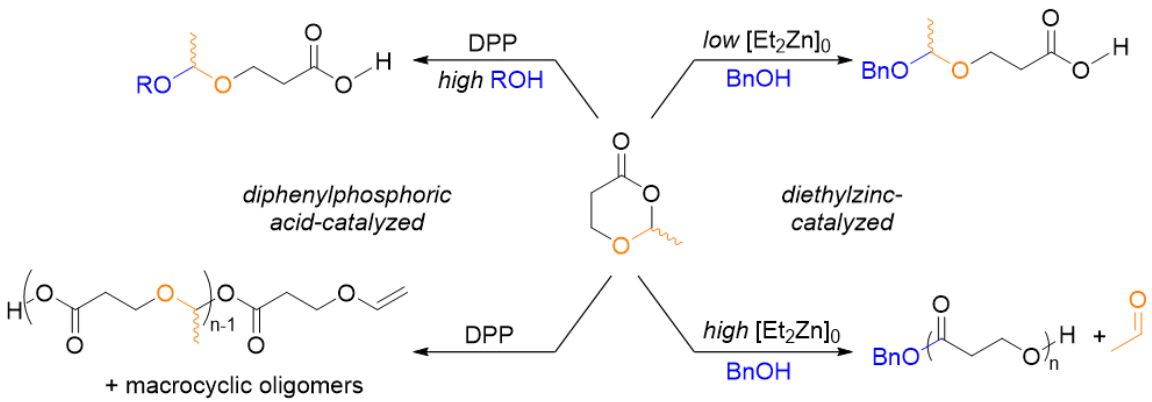

- fast rates of PMDO formation
- safe and inexpensive organocatalyst
- negligible aldehyde extrusion
- control up to $M_{n,PMDO}$~10 kg/mol

- slow rates of PMDO formation
- pyrophoric metal catalyst
- competitive aldehyde extrusion
- $M_{n,PMDO} \leq 30$ kg/mol

Limiting conversion of 60% at room temperature in neat MDO

It was shown previously that the ACE mechanism could be suppressed in the CROP of propylene oxide by keeping the instantaneous monomer concentration low, i.e. by slowly feeding monomer into the polymerization.[33] Due to the high equilibrium monomer concentration ($[MDO]_{eq}$ = 4.53 M) associated with ring-opening polymerization of MDO, lowering [MDO] to its equilibrium value would cease polymerization. We reasoned that monomers with higher ring-strain than MDO would be amenable to polymerization under monomer-starved conditions, thereby posing an avenue to well-defined polyhemiacetal esters. Furthermore, we were eager to improve on our current system to produce polyhemiacetal esters with near quantitative conversions to demonstrate their amenability to commercialization. As discussed in Appendix B, we initially investigated the synthesis and polymerization of the endocyclic hemiacetal esters 1,3-dioxepan-4-one (DPO) and 2-methyl-1,3-dioxepan-4-one (MDPO), the latter being the direct 7-membered analogue of

MDO by extension of the cyclic framework by a single methylene unit. As the synthesis of these molecules proved to be quite laborious and we struggled significantly with the purification of the final cyclic hemiacetal esters due to their high reactivity, we reasoned that investigation of a different 7-membered molecule that could be accessed more readily from commercial starting materials was in order.

The 7-membered cyclic hemiacetal ester 7-methoxyoxepan-4-one (MOPO) has been recently reported as an initiator in the cationic ring-expansion polymerization of vinyl ethers.[34] It is obtained by Baeyer-Villiger oxidation of 2-methoxycyclohexanone,[35,36] a molecule that is commercially available but can alternatively be produced by hydrogenation and subsequent dehydrogenation of lignin-derived guaiacol, making it of interest as a potentially renewable precursor.[37,38,39] MOPO lends an interesting comparison to MDO, DPO, and MDPO as it contains an exocyclic rather than an endocyclic hemiacetal ester as in MDO and its 7-membered analogues. In this Chapter we study MOPO as the monomer in cationic ring-opening polymerization (CROP) to hydrolytically degradable poly(7-methoxyoxepan-4-one) (PMOPO) and detail our ongoing efforts towards establishing living polymerization conditions for MOPO.

Scheme 4.2. Retrosynthetic disassembly of the MOPO framework to renewable guaiacol

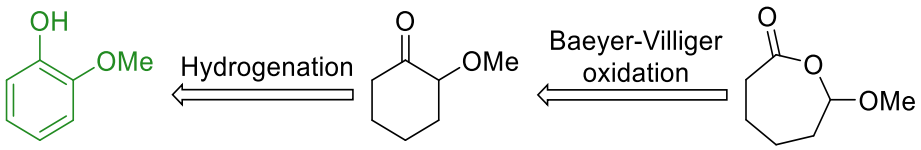

4.2 Results and Discussion

We first developed a reproducible procedure for the isolation, purification, and storage of the hydrolytically and thermally labile MOPO. MOPO is obtained by the

Baeyer-Villiger oxidation of 2-methoxycyclohexanone with *meta*-chloroperbenzoic acid (*m*-CPBA). High purity of the MOPO monomer was imperative for the conduction of careful polymerization studies and MOPO could be purified by flash column chromatography or Kugelrohr distillation (see Figure 4.6 and Figure 4.7 in section 4.4). We found that crude MOPO had to be stabilized during these processes towards hydrolysis and auto-polymerization induced by trace acids and water. Silica gel used in chromatography was treated with an eluent containing triethylamine and distillation glassware was base-treated and oven-dried. Similar to the reactivity of cyclic ketene acetals, MOPO was observed to polymerize when stored in glass containers that were not prior treated with base (see Figure 4.13 in section 4.4).[40] The purified monomer was stored in a Strauss flask over polymer-supported dimethylaminopyridine (polyDMAP) as a solution in deuterated chloroform at −20 °C under inert atmosphere to prevent auto-polymerization. This mode of storage proved to preserve MOPO successfully over time as even storing it as a neat, frozen solid over poly(DMAP) at −20 °C under inert atmosphere still led to slow autopolymerization with repeated melting of MOPO when measuring it out for the purpose of conducting experiments. MOPO could be obtained in good yields (up to 68%) when following the steps outlined for its synthesis in section 4.4. Using proton nuclear magnetic resonance (^{1}H NMR) spectroscopy and gas chromatography-mass spectrometry (GC-MS) high purity (>99%) of the MOPO monomer could be verified prior to polymerization (see Figure 4.9 in section 4.4).

Speculating that the ring-opening polymerization of MOPO catalyzed by Brønsted acids proceeds by AM and ACE mechanisms, we explored polymerization of MOPO with hydrochloric acid (2M in diethyl ether) at room temperature in neat MOPO with or without

benzyl alcohol initiator. As hypothesized, we observed formation of poly(MOPO) in both cases by ^{1}H and ^{13}C NMR spectroscopy (Figure 4.1, also see Figure 4.10 in section 4.4). In the presence of benzyl alcohol, formation of a benzyl acetal end group was confirmed by ^{1}H NMR spectroscopy, consistent with nucleophilic attack of benzyl alcohol onto the acetal moiety of an activated MOPO (MH^{+}) molecule (Scheme 4.3 and Figure 4.1).

Polymerizations conducted without exogenous initiator yielded PMOPO with a mixture of E- and Z-enol ether end groups (see Figure 4.11 in section 4.4),[41] presumably arising from elimination of a proton vicinal to the alkoxycarbenium ion on the propagating chain end (indicated in blue in Scheme 4.3). The ^{1}H NMR spectral signals attributed to end groups generated *via* the ACE mechanism were still observed in PMOPO generated *via* an AM mechanism, albeit in much lower concentration, which is consistent with some contribution of the ACE mechanism in the presence of alcohol initiator (c.f. Figure 4.1 and Figure 4.11). Thermal properties of purified PMOPO obtained by polymerization with HCl were studied by thermogravimetric analysis (TGA) and differential scanning calorimetry (DSC), characterizing PMOPO as an amorphous polymer with a low glass transition temperature of $T_g = -58$ °C and of relatively low thermal stability (99 wt% at 160 °C by TGA, see Figure 4.12 in section 4.4).

Scheme 4.3. Cationic ring-opening polymerization of MOPO by activated monomer and active chain-end mechanisms

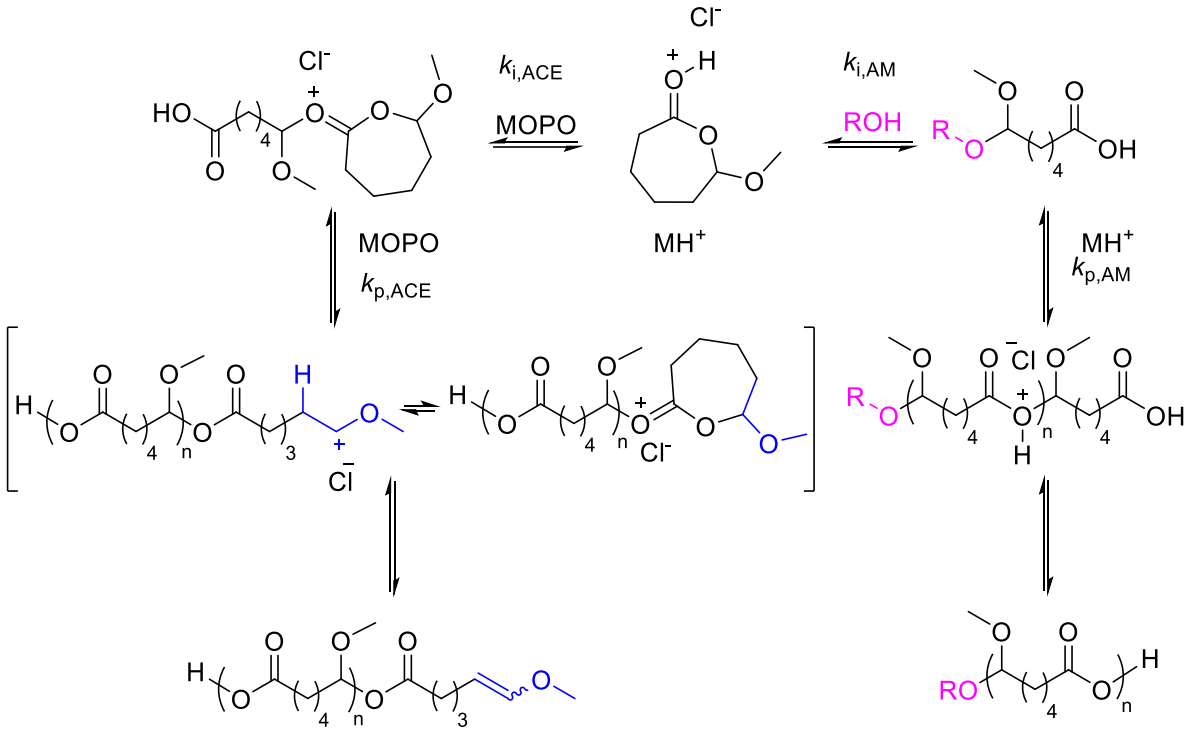

In addition to signals attributed to PMOPO we observed formation of a small amount of 6-oxohexanoic acid[42] and its (hemi)acetal derivatives obtained from addition of water or methanol to the aldehyde in the cationic ring-opening polymerization of MOPO. We previously identified these compounds during the intentional hydrolysis of MOPO in a mixture of acetonitrile and water (see Figure 4.13, Figure 4.14, and Figure 4.15 in section 4.4). Formation of aldehyde when treating MOPO with hydrochloric acid (HCl) was not surprising, as hemiacetal esters have been implicated as intermediates in the acidolysis of acetals to aldehydes under anhydrous conditions.[43] To ensure that the observed aldehyde was not derived from cleavage of polymer chains and present as a PMOPO end group, we examined a sample containing PMOPO and ca. 1% of the aldehyde contaminant in the presence of 4-nitrobenzaldehyde as the internal standard by diffusion-ordered (DOSY)

NMR spectroscopy (see Figure 4.16 in section 4.4). The observed diffusion coefficient for the aldehyde contaminant was much closer in magnitude to the 4-nitrobenzaldehyde standard than the broad diffusion coefficient range associated with PMOPO signals, convincing us that the aldehyde formed was present as a small molecule contaminant rather than a polymer chain end.

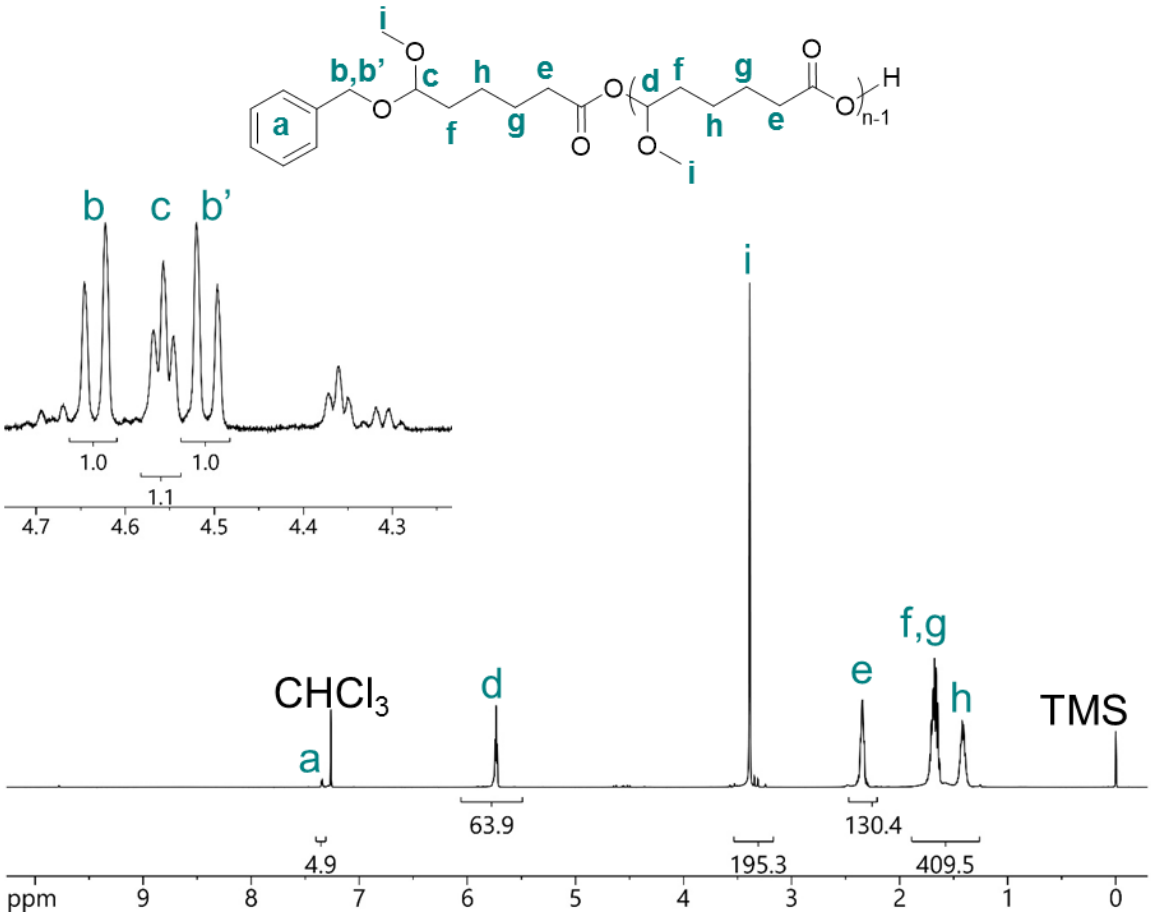

Figure 4.1. ^{1}H NMR spectrum ($CDCl_3$) of precipitated and dried PMOPO obtained by CROP of neat MOPO with HCl and benzyl alcohol initiator($[MOPO]_0/[BnOH]_0$ = 50, $[MOPO]_0/[HCl]_0$ = 500).

Polymerization of neat MOPO by an AM mechanism ($[MOPO]_0/[BnOH]_0$ = 50, $M_{n,theo}$ ~ 9 kg/mol) with $[MOPO]_0/[HCl]_0$ = 500 reached only 64% conversion over the course of 20 hours. When no benzyl alcohol initiator was added, a polymerization under otherwise identical conditions did not exceed 40% conversion in over 27 hours. Low

conversions could be attributed to quenching of the active chain end *via* chloride anion collapse onto the propagating alkoxycarbenium ion formed in the ACE mechanism.[44] We probed this hypothesis by adding more HCl catalyst to a polymerization initiated with benzyl alcohol that had ceased at 64% conversion. The addition of more catalyst drove conversion to 76% over another 22 h at room temperature but was accompanied by significant peak broadening of PMOPO signals by ^{1}H NMR spectroscopy (see Figure 4.17 in section 4.4).

To further examine our conjecture that chloride anion terminated polymerization by irreversibly collapsing onto the chain end we also monitored MOPO polymerization with HCl in deuterated chloroform ($CDCl_3$) solution ($[MOPO]_0$ = 1M) by ^{1}H NMR spectroscopy. Increasing the initial concentration of HCl to $[MOPO]_0/[HCl]_0$ = 100 in this solution experiment afforded 99% conversion to PMOPO in only 10 minutes. At high conversion a small triplet at 5.45 ppm was observed by ^{1}H NMR spectroscopy, which was in good agreement with previously reported shifts for protons geminal to methoxy and chloro substituents (see Figure 4.18 in section 4.4).[45] This signal was no longer present in ^{1}H NMR spectra of PMOPO that had been precipitated into 9/1 hexanes/tetrahydrofuran containing a small amount of triethylamine, presumably due to transformation of the chloromethyl ether to the observed enol ether end groups in the presence of base (c.f. Figure 4.11 in section 4.4).

In addition to the methine proton of the chloromethyl ether end group, a broad peak at 9.58 ppm was observed by ^{1}H NMR spectroscopy, which we attributed to the proton of the carboxylic acid end group arising from initiation by the protonic acid. We were able to trap the putative propagating alkoxycarbenium ion on the opposite chain end *via* addition

of a small amount of triphenylphosphine (PPh_3) to the polymerization at 99% conversion. Upon addition of PPh_3, phosphorous (^{31}P) NMR spectroscopy exhibited an additional peak to the parent PPh_3 peak with the characteristic shift of a phosphonium salt, consistent with an alkoxycarbenium propagating chain end in the polymerization of MOPO by an ACE mechanism.[46]

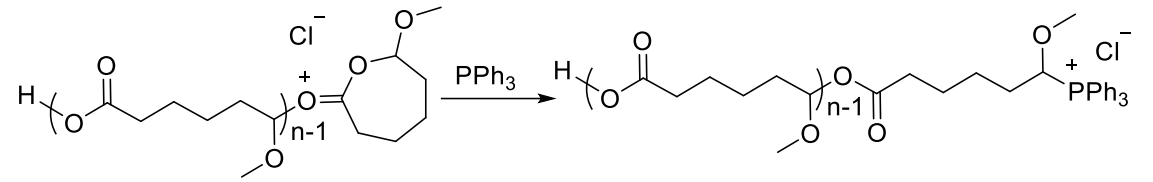

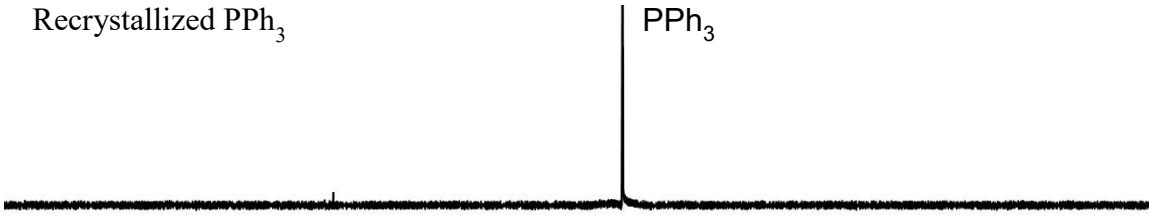

After addition of PPh_3 to PMOPO in solution

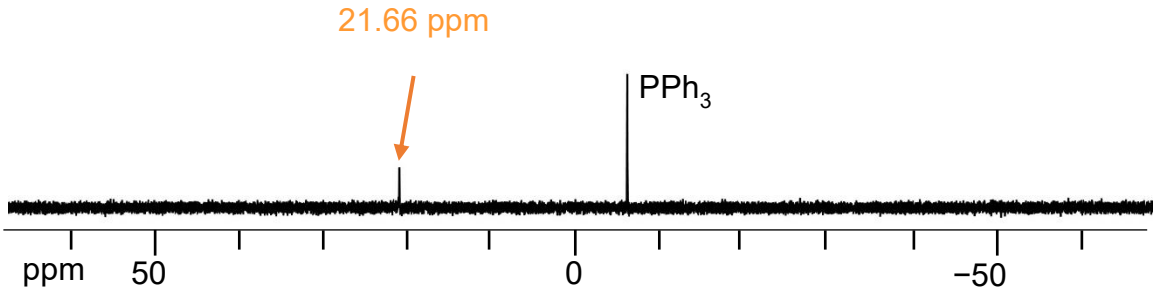

Figure 4.2. ^{31}P NMR ($CDCl_3$) spectra of triphenylphosphine and the triphenylphosphonium salt formed in MOPO CROP *via* an ACE mechanism upon addition of PPh_3 to an NMR experiment ($[MOPO]_0$ = 1M in $CDCl_3$, $[MOPO]_0/[HCl]_0$ = 100).

Having confirmed polymerization of MOPO by an ACE mechanism when treated with HCl, we next investigated whether the ACE mechanism could be suppressed in the presence of exogenous initiator to favor polymerization by a controlled AM mechanism. When neat MOPO was treated with HCl and benzyl alcohol ($[MOPO]_0/[HCl]_0$ ~ 1,000 and

$[MOPO]_0/[BnOH]_0 \sim 100$) and molar mass followed by size exclusion chromatography (SEC) relative to polystyrene standards, we observed constant molar mass with increasing monomer conversion, suggesting the presence of short-lived reactive species that are predominantly terminated *via* intermolecular chain transfer to MOPO (Figure 4.3). This indicated that the ACE mechanism was dominant even at high exogenous initiator concentrations and raised the question whether benzyl alcohol initiated polymerization *via* an AM mechanism, yielding a propagating carboxylic acid, or reversibly added to the alkoxycarbenium ion generated *via* an ACE mechanism throughout the polymerization. Comparison of PMOPO molar masses achieved in solution polymerization with those obtained in bulk polymerizations indicated that higher molar mass PMOPO was attained in bulk, further indicative of polymerization by an ACE mechanism where unimolecular back- and/or end-to-end biting reactions become prevalent over bimolecular propagation events at high dilutions (c.f. Figure 4.3 and Figure 4.18 in section 4.4).[44]

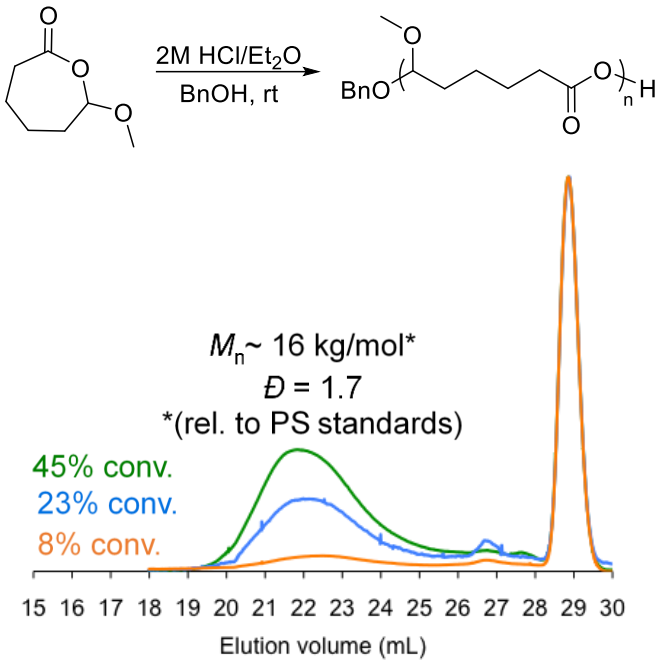

Figure 4.3. Evolution of molar mass in the CROP of neat MOPO with HCl and BnOH ($[MOPO]_0/[HCl]_0$ ~ 1,000 and $[MOPO]_0/[BnOH]_0$ ~ 100).

In an effort to suppress irreversible termination events, we exchanged HCl for methyl trifluoromethanesulfonate (methyl triflate, MeOTf). Triflate anion is a weaker nucleophile than chloride due to the resonance- and electronic stabilization of its negative charge by oxygen and fluorine respectively and therefore is less likely to irreversibly collapse onto the propagating alkoxycarbenium ion.[47] In our previous work with the monomer MDO we observed rapid decomposition of MDO when treating it with trifluoromethanesulfonic acid (triflic acid) or alkylating agents such as methyl triflate and triethyloxonium hexafluorophosphate even at low temperatures. MOPO proved to be more robust than MDO, which was exemplified by its clean conversion to PMOPO in a solution polymerization of MOPO ($[MOPO]_0$ = 2.25M) with MeOTf ($[MOPO]_0/[MeOTf]_0$ ~550) at −20 °C. Under the aforementioned conditions, near quantitative conversion to PMOPO (> 95%) was achieved in 65 minutes without observable discoloration of the

polymerization medium. We expected methyl triflate to initiate polymerization by alkylation of the most basic oxygen in MOPO, thereby activating it for nucleophilic attack by another MOPO molecule (Scheme 4.4). Interestingly, when monitoring solution polymerizations of MOPO with MeOTf by ^{1}H NMR spectroscopy we did not observe consumption of methyl triflate even at near quantitative conversions to PMOPO. This suggested that methyl triflate did not take on the role of cationic initiator but rather appeared to act as a catalyst, promoting ring-opening of MOPO without observable methylation.

Scheme 4.4. Predicted mechanism for cationic ring-opening polymerization of MOPO with the alkylating agent methyl triflate

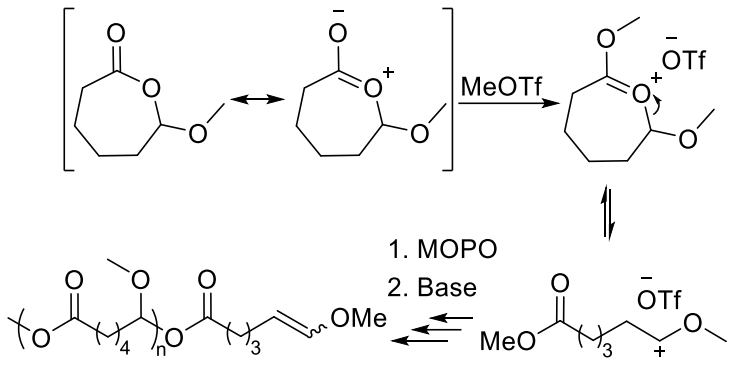

The apparent absence of methyl ester end groups in the ^{1}H NMR spectra of precipitated PMOPO produced with methyl triflate may be explained by either a very low concentration of end groups or by a cyclic rather than linear PMOPO topology. To gain a better understanding of species formed we monitored MOPO polymerization with MeOTf by ^{19}F NMR spectroscopy. Any new species formed due to incorporation of methyl triflate into the polymer would yield additional signals by ^{19}F NMR spectroscopy upon addition of MOPO to MeOTf. The ^{19}F NMR spectrum of commercial methyl triflate in $CDCl_3$ was found to in fact exhibit 2 peaks, the major one was assigned to methyl triflate, meanwhile

we speculated that the smaller secondary peak at −78.8 ppm was indicative of trifluoromethanesulfonic acid, arising from hydrolysis of methyl triflate. Consistent with our observations by ^{1}H NMR spectroscopy, we did not detect any change in the ^{19}F NMR spectral shift of methyl triflate upon addition of MOPO; however, the putative triflic acid ^{19}F NMR signal shifted downfield by approximately 1 ppm with monomer addition (Figure 4.4). This suggested that the initiator in the polymerization of MOPO with methyl triflate was actually a low concentration of triflic acid.

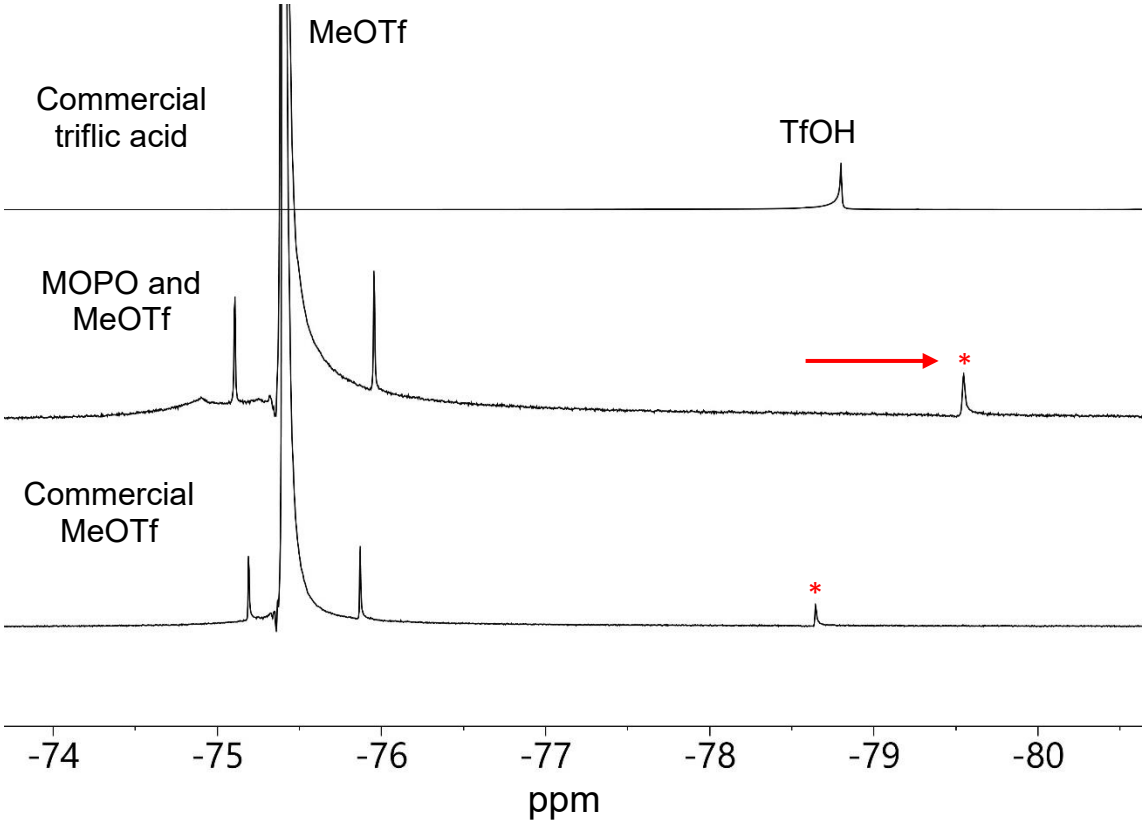

Figure 4.4. ^{19}F NMR spectra ($CDCl_3$) of: methyl triflate (bottom), a 1/1 mixture of methyl triflate and MOPO (middle), and triflic acid (top).

As the fluorine NMR spectral shift of triflic acid is highly sensitive to concentration we probed our hypothesis that the secondary peak corresponded to triflic acid *via* incremental addition of pure triflic acid to the methyl triflate solution and analyzed the resultant ^{19}F NMR spectra (Figure 4.5). Addition of a low amount of TfOH to the methyl

triflate solution produced no significant change in the ^{19}F NMR spectrum and sequential addition of larger amounts resulted in upfield shifting of the putative triflic acid peak, as a consequence of its increased concentration in the chloroform solvent. This result was in good agreement with our hypothesis that the additional signal in the ^{19}F NMR spectrum of methyl triflate originated from triflic acid contaminant. Relative integration of the ^{19}F NMR signals for methyl triflate and triflic acid and high relaxation delays allowed us to estimate a concentration of triflic acid in methyl triflate of [TfOH] < 0.3%, indicating that a loading of $[MOPO]_0/[MeOTf]_0 \sim 550$ corresponded to a ratio of $[MOPO]_0/[TfOH]_0 > 1800$.

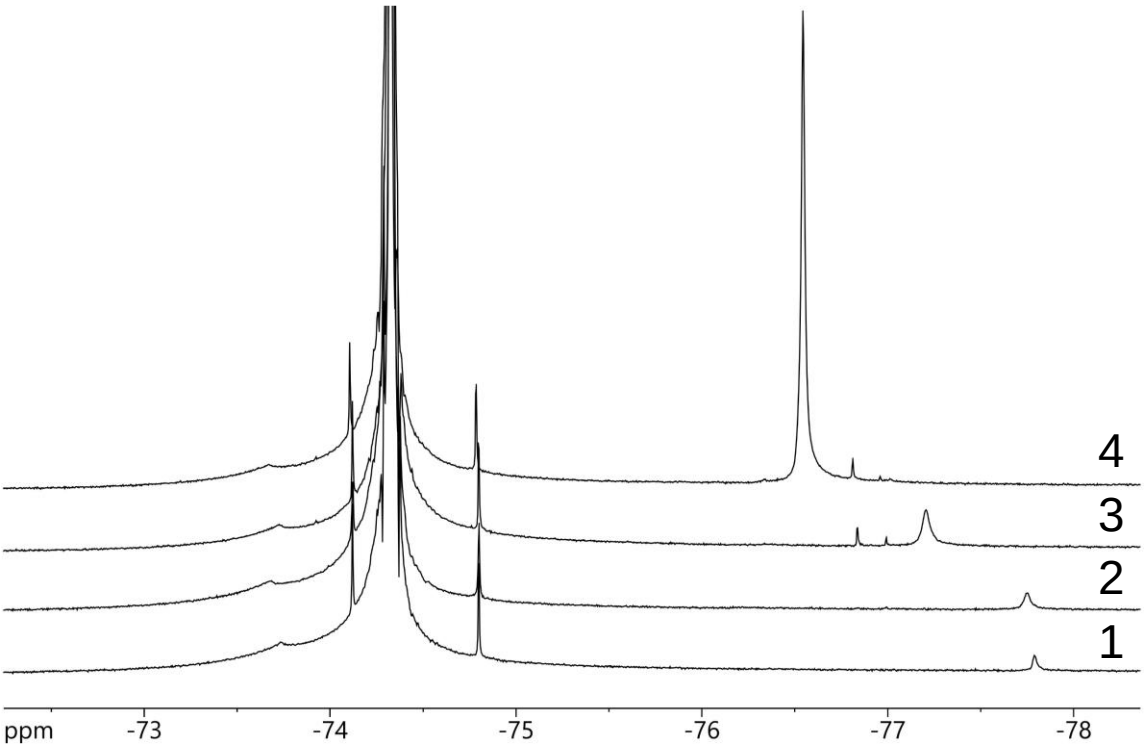

Figure 4.5. Dependence of triflic acid ^{19}F NMR shift on concentration. **1:** 10 μL commercial MeOTf in 0.4 mL $CDCl_3$. **2:** After addition of 1 μL 0.94 M TfOH to **1**. **3:** After addition of another 8 μL of 0.94M TfOH to **2**. **4:** after addition of 1 μL concentrated TfOH to **3**.

Size exclusion chromatography with a multi-angle laser light-scattering detector using dimethylformamide as the solvent (DMF SEC-MALLS) indicated that high molar mass PMOPO had been formed in solution polymerization of MOPO with MeOTf

([MOPO]$_0$/[MeOTf]$_0$ ~ 550, M_n ~ 54 kg/mol, $Đ$ = 1.4, see Figure 4.19 in section 4.4). This was most likely explained by the fact that only a very low concentration of active initiator, i.e. triflic acid, was present in the polymerization. Encouraged by this result we probed if there was a correlation between [MOPO]$_0$/[MeOTf]$_0$ and $M_{n,PMOPO}$. We studied the polymerization of MOPO with MeOTf at −20 °C employing 3 different monomer to catalyst ratios: [MOPO]$_0$/[MeOTf]$_0$ = 250, 500, 1000. The polymerizations were conducted to conversions greater than 98% and $CHCl_3$ SEC analysis of the crude polymerization mixtures indicated that PMOPO of M_n ~ 19 kg/mol (relative to polystyrene standards) was formed in all cases, irrespective of [MeOTf]$_0$ (see Figure 4.20 in section 4.4). From this we concluded that the use of an initiator with a non-nucleophilic counterion suppressed irreversible termination events but failed to prevent transfer reactions, a common roadblock to living conditions in cationic polymerizations.[48]

We showed that the propagating species in MOPO polymerization is an alkoxycarbenium or dioxacarbenium ion, the latter being indistinguishable from the former upon trapping with a nucleophile such as triphenylphosphine. In the cationic polymerization of vinyl ethers the establishment of an active-dormant equilibrium between the propagating alkoxycarbenium ion and its dormant form has successfully lowered the concentration of active species, thereby mediating both transfer and irreversible termination processes (Scheme 4.5). Inspired by this elegant approach we set out to apply the methods developed to achieve living polymerization of vinyl ethers to our system.

Scheme 4.5. Living cationic polymerization of vinyl ethers by reversible deactivation mechanisms: 1) dissociation-combination, 2) atom transfer, and 3) degenerative chain transfer

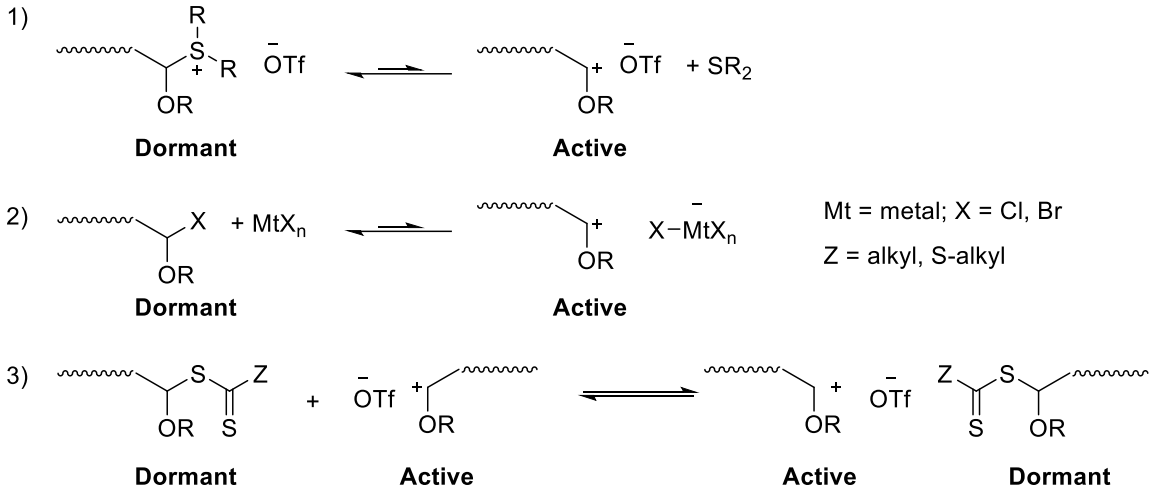

Adapted from Uchiyama, M.; Satoh, K.; Kamigaito, M. *Macromolecules* **2015**, *48*, 5533.

There are three types of reversible activation-deactivation of vinyl ethers: 1) dissociation-combination, 2) atom-transfer, and 3) degenerative chain transfer. Sulfide-mediated cationic polymerization is one form of the dissociation-combination type polymerization and was the first we investigated in MOPO polymerization as it did not require the synthesis of initiators or chain-transfer agents. Probing MOPO polymerization using our methyl triflate stock solution as a source of triflic acid in the presence of a high concentration of dimethyl sulfide (DMS) at −20 °C, we observed significant retardation of the reaction rate, indicating interaction of the propagating alkoxycarbenium ion with DMS. However, analysis of the molar mass of PMOPO at different conversion points revealed no living polymerization kinetics (see Figure 4.21 in section 4.4).

In order to investigate the potential for the controlled polymerization of MOPO *via* atom transfer and/or degenerative chain transfer, we synthesized chloromethylether **I** by treating MOPO with a stoichiometric amount of HCl (see Figure 4.22 and Figure 4.23 in section 4.4 for ^{1}H and ^{13}C NMR spectral data for both **I** and **II**). The chloromethylether

could then be further transformed to dithiocarbamate **II** (Scheme 4.6). We first probed polymerization of MOPO by an atom-transfer type mechanism using zinc chloride ($ZnCl_2$) as the Lewis acid. The success of this method relies on selective activation of the carbon-chloride bond of **I** by the Lewis acid, any reaction between the monomer and Lewis acid is undesirable. As a control we treated a solution of MOPO in $CDCl_3$ with a stock solution of dry $ZnCl_2$ in diethyl ether (Et_2O) and observed the immediate formation of a highly viscous liquid. Analysis by ^1H NMR spectroscopy elucidated full conversion of MOPO to PMOPO in the presence of $ZnCl_2$, presumably due to initiation with low level amounts of water, and we therefore abandoned this route (see Figure 4.24 in section 4.4). Our current efforts are focused on establishing whether polymerization of MOPO in the presence of chain transfer agent **II** or structurally related molecules could induce living polymerization kinetics in the cationic polymerization of MOPO.

Scheme 4.6. Synthesis of novel chloromethylether and dithiocarbamate from MOPO

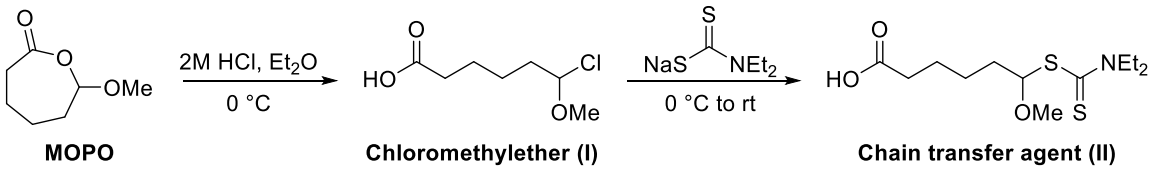

4.3 Conclusion

We have demonstrated the synthesis of the unprecedented poly(7-methoxyoxepan-4-one) *via* cationic ring-opening polymerization with low amounts of triflic acid present as an impurity in a solution of methyl triflate. A large component of this work focused on understanding the reactivity of MOPO toward different stimuli in an effort to provide this molecule, and others like it, in high purity, and to guarantee its long-term storage without

auto-polymerization or hydrolysis. Our initial studies of MOPO polymerization with hydrochloric acid as the cationic initiator allowed us to deduce that the polymerization proceeds primarily *via* an active chain-end mechanism, even in the presence of high concentrations of exogenous benzyl alcohol initiator. The two main challenges in achieving living polymerization conditions in the cationic ring-opening polymerization of MOPO were found to be irreversible termination and chain transfer reactions. To this end, we were able to suppress irreversible termination by employing triflic acid as the cationic initiator, yielding PMOPO of high molar mass and dispersities < 2. Studies examining the achievable range of PMOPO molar masses *via* uncontrolled polymerization with triflic acid and the effects of introducing a chain transfer agent to the polymerization are ongoing in our laboratories. We are confident that by choosing the additive in MOPO polymerization appropriately this process will eventually prove to be controllable.

4.4 Experimental Procedures and Characterization Data

Materials and Analysis.

All chemicals were obtained from Sigma-Aldrich and used as received unless otherwise indicated. 2-methoxycyclohexanone was obtained from TCI America (97%) and used as received. Benzyl alcohol was distilled under vacuum and stored over activated 3 Ångstrom molecular sieves in the glovebox. When indicated as dry, solvents were either obtained from a JC Meyer solvent drying system or were distilled prior to use according to standard purification methods.[49] ^{1}H and ^{13}C NMR spectra were obtained on a 400 or 500 MHz Bruker Avance III HD. Gas chromatography-mass spectrometry (GC-MS) was carried out on an Agilent 6890 GC and Agilent 5973 MS system. The GC-MS column used was a HP-5ms with dimensions 30m x 0.25mm. The standard method for all runs, unless

otherwise indicated, consisted of holding the sample at 50 °C for 1.5 min, then ramping to 250 °C at a ramp rate of 20 °C min^{-1}, and holding it at 250 °C for 3.5 min (50to250SPLIT15).

Scheme 4.7. Synthesis of 7-methoxyoxepan-4-one (MOPO)

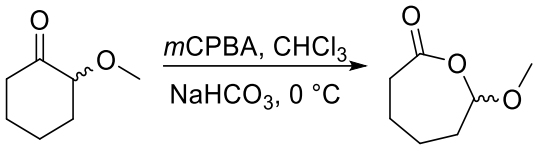

7-Methoxyoxepan-2-one. 14.8 g *m*CPBA at room temperature (≥77% active oxygen content, 66 mmol, 1.7 eq.) were placed into an Erlenmeyer flask equipped with a stir bar. To the oxidant were added 130 mL of chloroform and the solution stirred over magnesium sulfate ($MgSO_4$) until no further caking was observed. While the *m*CPBA solution was drying over $MgSO_4$, a 250 mL 3-neck round bottom flask equipped with a stir bar, vacuum adapter, internal thermometer, and septum was flame-dried and backfilled with argon. Under positive pressure of argon the septum sealing one of the necks was removed and 4.25 g of sodium bicarbonate (51 mmol, 1.3 eq.) were added into the flask. Then the *m*CPBA solution was carefully decanted through a funnel into the flask and the neck resealed with the septum. The heterogeneous solution was placed in an ice/water bath and cooled under stirring until the internal temperature reached 0 °C. Using a syringe pump, a 6 mL disposable syringe with a Luer lock and an 18-gauge, long metal needle, 4.9 mL of 2-methoxycyclohexanone (5 g, 39 mmol, 1 eq.) were added to the solution over ca. 30 minutes, ensuring that the solution temperature did not exceed 10 °C at any point during the addition. The progress of the reaction was monitored by GC-MS (50to250SPLIT15), looking for disappearance of 2-methoxycyclohexanone at 6.4 min and appearance of

MOPO at 8.0 min. Once the starting material was consumed the heterogenous mixture was filtered through a fritt funnel into a sidearm flask. The filtrate was transferred to a separatory funnel containing 100 mL of 10% w/v sodium sulfite to quench residual peracid. The organic layer was separated, washed with 100 mL of a saturated sodium bicarbonate solution, and 50 mL of brine. The combined aqueous layers were extracted with chloroform (2X 250 mL) and the combined organic fractions were dried over $MgSO_4$. At this point the integrity of MOPO was again verified by GC-MS analysis. Solvent was removed *in vacuo* and the residue transferred to a 25 mL 14/20, base-treated round bottom flask equipped with a stir bar. A spatula tip of calcium hydride was added to the round bottom flask and the crude material stirred over the drying agent for 1h. The crude was fractionally distilled in a Kugelrohr with two receiving bulbs (70 °C pot temperature, 500 – 200 mTorr), collecting the first droplets into the bulb furthest from the still pot and MOPO into the second bulb charged with 30 mg of polymer-supported dimethylaminopyridine (poly(DMAP)). MOPO was collected onto poly(DMAP) as a clear, colorless liquid (3.8 g, 68% yield), was transferred into a 5 mL PTFE vial under inert atmosphere, and pumped into the glovebox immediately. The PTFE container was kept in the −20 °C freezer in the glovebox and purity of MOPO assessed before each experiment by GCMS.

Scheme 4.8. Synthesis of chloromethylether and dithiocarbamate.

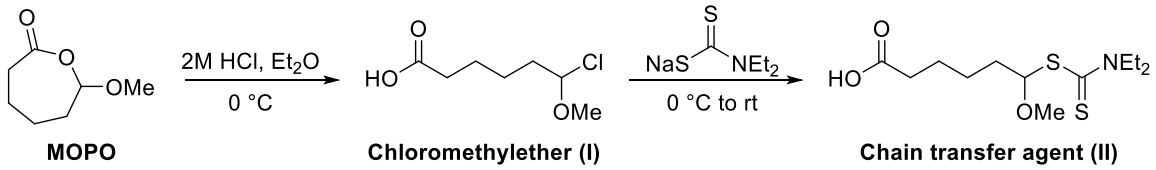

*6-Chloro-6-methoxyhexanoic acid **(I)***. In a glovebox 200 mg MOPO on poly(DMAP) were weighed into a vial and dissolved in 1.25 mL Et_2O. The solution was filtered into a clean vial through a 0.2 μm filter to remove poly(DMAP) beads from the solution. The vial was capped with a septum, removed from the glovebox and placed under argon in an ice/water bath. To the MOPO solution were added 0.85 mL 2 M HCl in Et_2O solution dropwise at 0 °C. The solution was warmed to room temperature and full conversion to the chloromethylether verified by ^{1}H NMR spectroscopy.

*6-((Diethylcarbamothioyl)thio)-6-methoxyhexanoic acid **(II)***. Sodium N,N-diethyl dithiocarbamate trihydrate was dried by azeotropic distillation with toluene and stored in a vacuum desiccator. For the preparation of the chain transfer agent (CTA) 642 mg of the dried salt were placed in a dry vial and diluted with 10.3 mL Et_2O. The resultant suspension was stirred and cooled to 0 °C, then the previously prepared solution of chloromethylether in Et_2O was added dropwise to the salt suspension. The ice bath was removed and the suspension stirred at room temperature for 1.5h. Full conversion to the chain transfer agent **II** was verified by ^{1}H NMR spectroscopy. Ether was evaporated under vacuum and the residual solid dissolved in a minimum amount methylene chloride. The crude was purified by flash column chromatography on silica (2X, 100/1 mass silica/sample, first with 8/2

hexanes/EtOAC containing 5% AcOH, then 6.5/3.5 hexanes/EtOAC containing 5% AcOH to eliminate streaking of the acid on silica) yielding 60 mg of pure CTA **II** (15% yield).

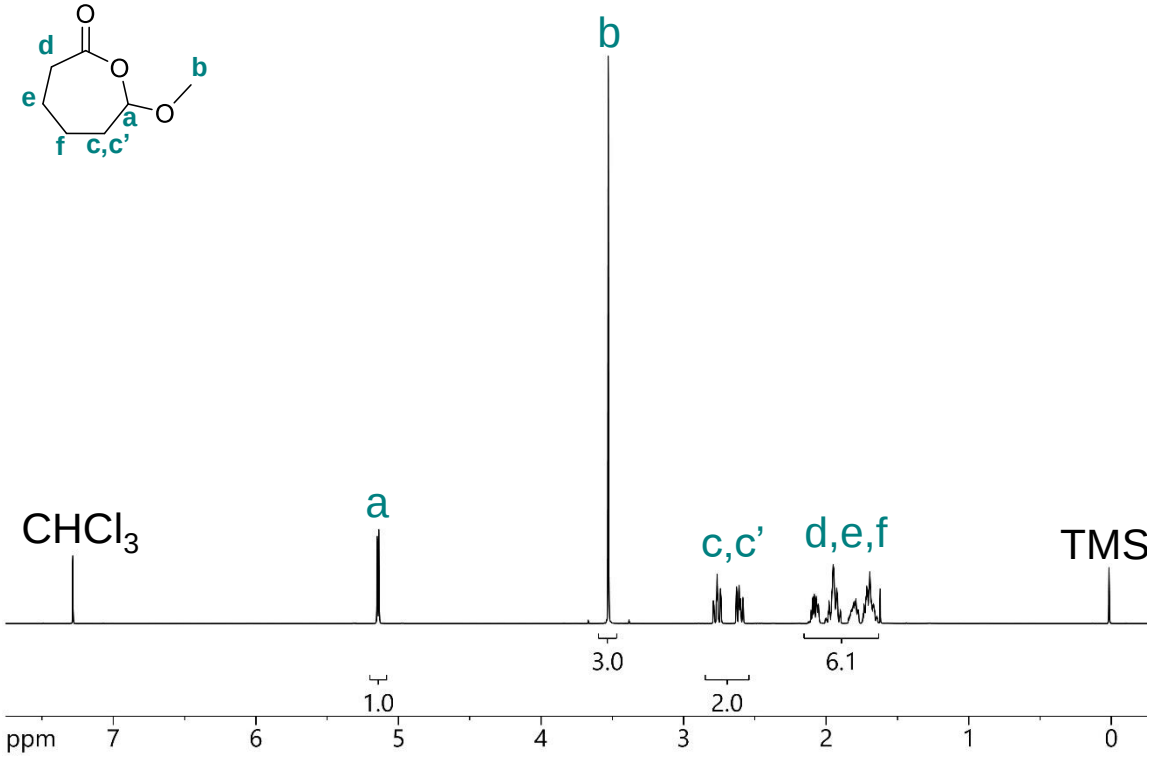

Figure 4.6. ^{1}H NMR spectrum ($CDCl_3$) of MOPO purified by Kugelrohr distillation.

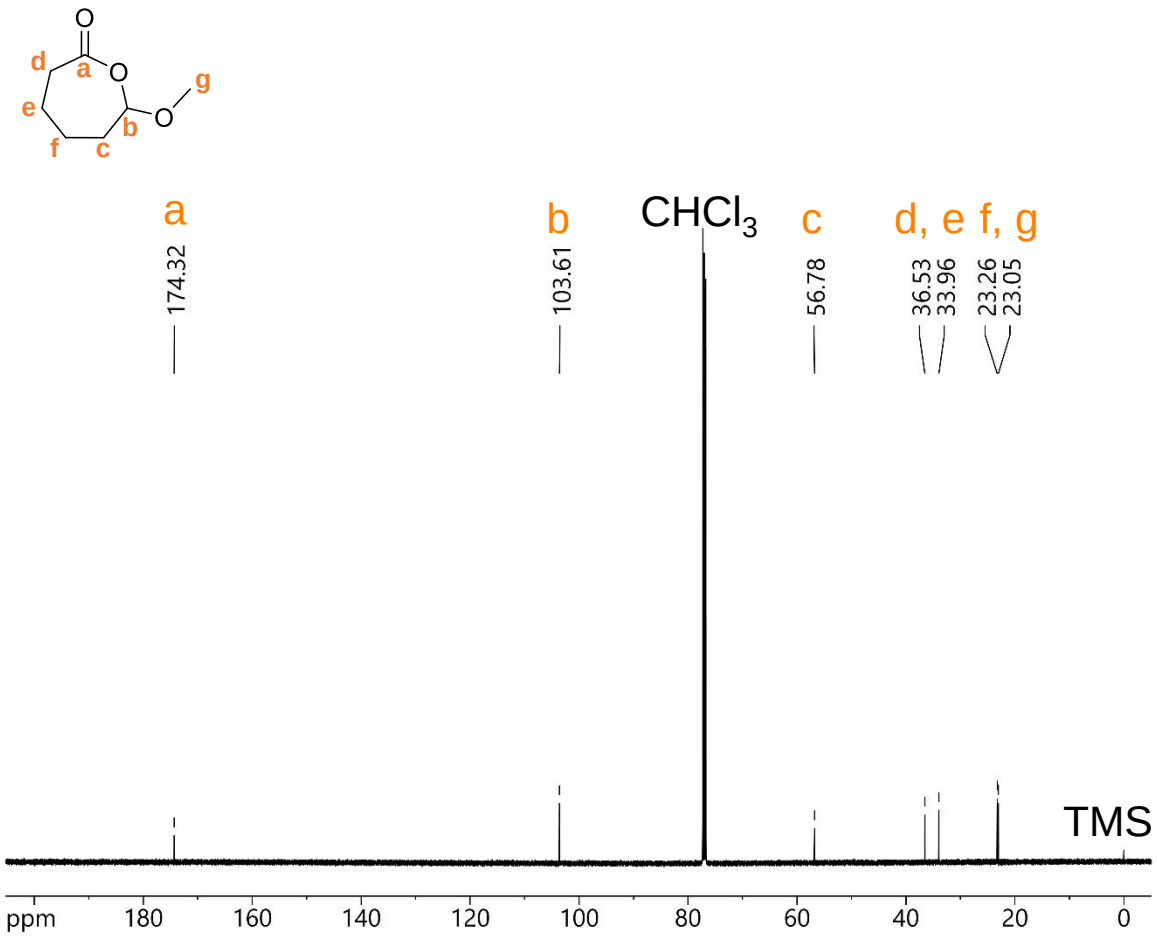

Figure 4.7. ^{13}CNMR spectrum ($CDCl_3$) of MOPO purified by Kugelrohr distillation.

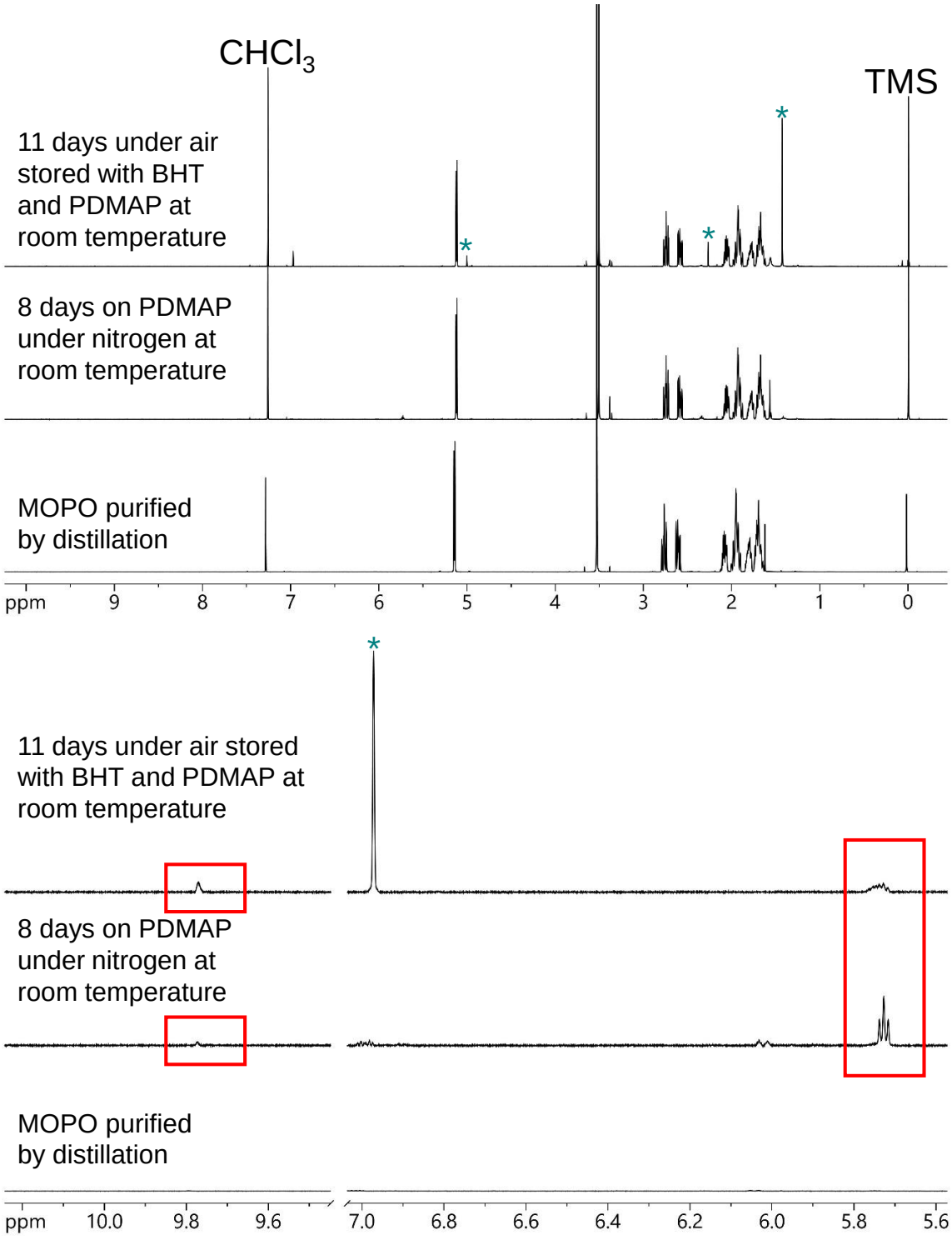

Figure 4.8. Stability studies carried out with MOPO purified *via* Kugelrohr distillation. Neat MOPO was stored on polymer-supported dimethylaminopyridine (PDMAP) in a glovebox at room temperature or over PDMAP and butylated hydroxytoluene (BHT = *) under air at room temperature. In the magnified regions of the bottom spectral overlay it can be seen that even when stred over PDMAP and BHT the monomer still undergoes slow hydrolysis and/or auto-polymerization.

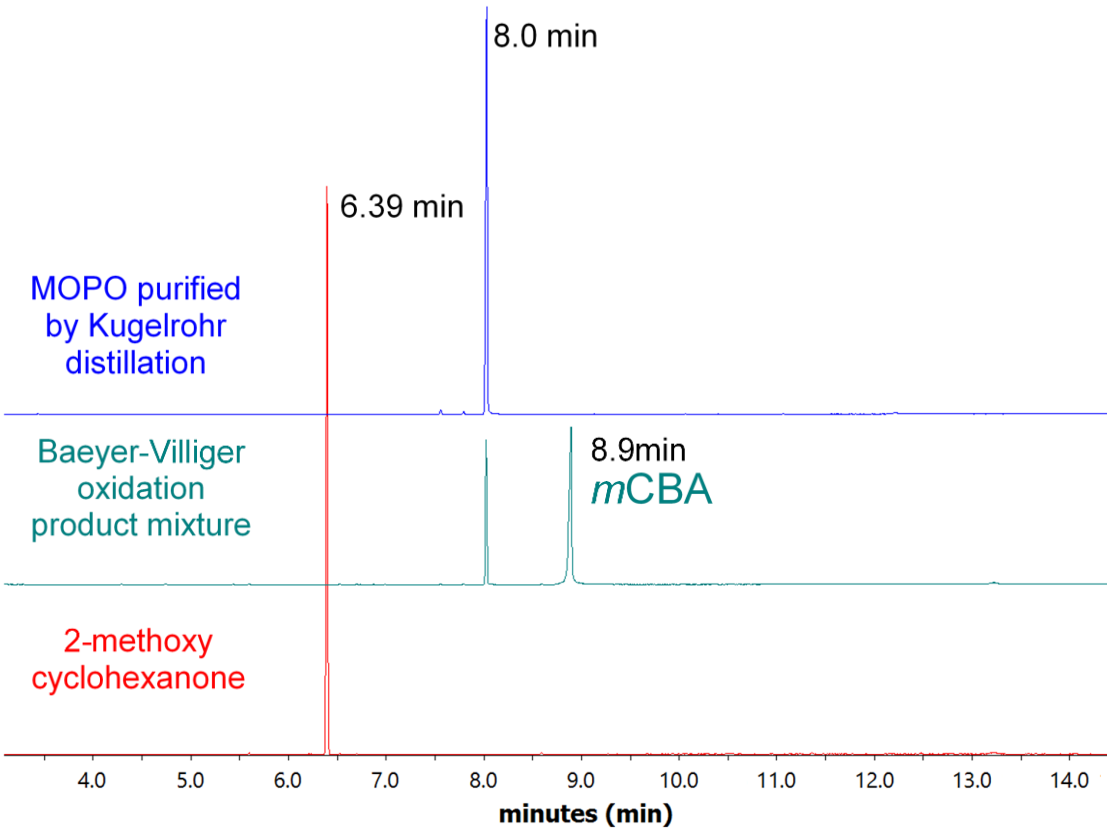

Figure 4.9. Gas chromatography traces of commercial 2-methoxycyclohexanone, product mixture after Baeyer-Villiger oxidation of 2-methoxycyclohexanone, and 7-methoxyoxepan-4-one (MOPO) after purification by Kugelrohr distillation. All samples were analyzed with the method 50to250SPLIT15.

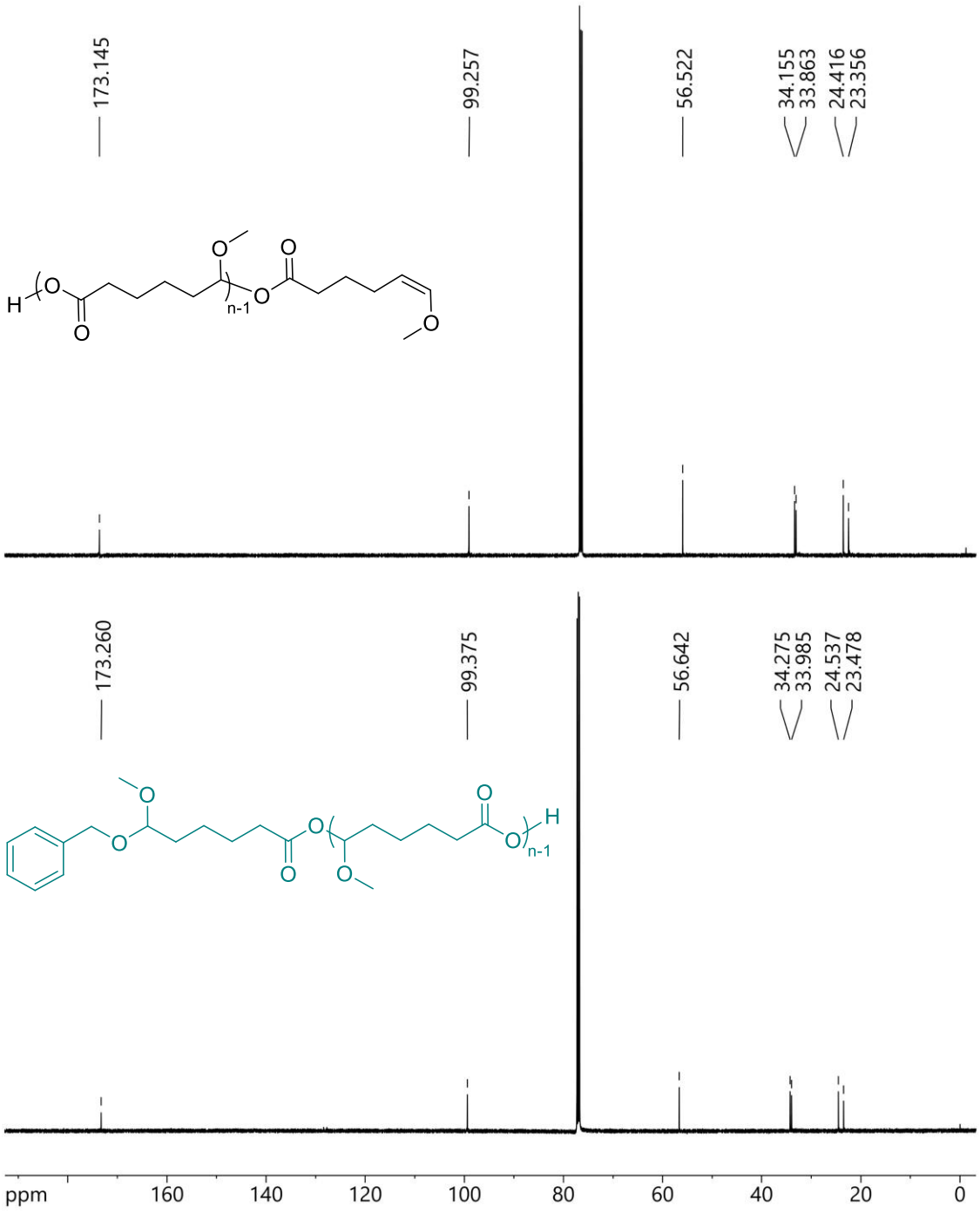

Figure 4.10. ^{13}C NMR spectra ($CDCl_3$) of PMOPO obtained *via* an ACE mechanism (in black) and *via* an AM mchanism (in turquoise) using HCl as the catalyst ($[MOPO]_0/[HCl]_0 = 500$, $[MOPO]_0/[BnOH]_0 = 50$).

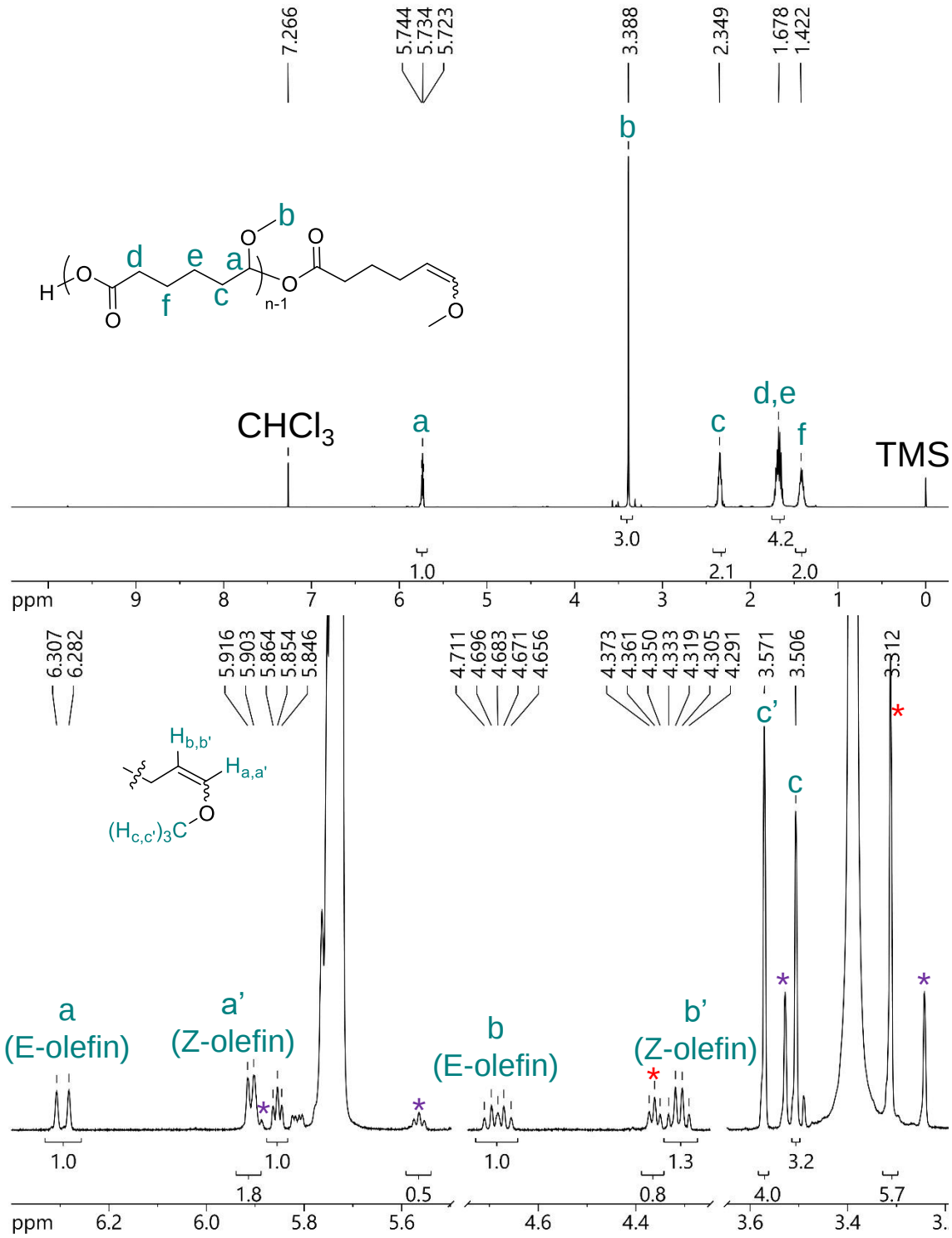

Figure 4.11. ^{1}H NMR spectrum ($CDCl_3$) of precipitated PMOPO obtained by an ACE mechanism (in neat MOPO, $[MOPO]_0/[HCl]_0$ = 500). A mixture of E- and Z-enol ethers were observed as end groups, in good agreement with spectral data reported previously.[41] *Indicates satellite peaks of PMOPO backbone resonaces. *These signals are attributed to 6,6-dimethoxyhexanoic acid, a MOPO degradation product.

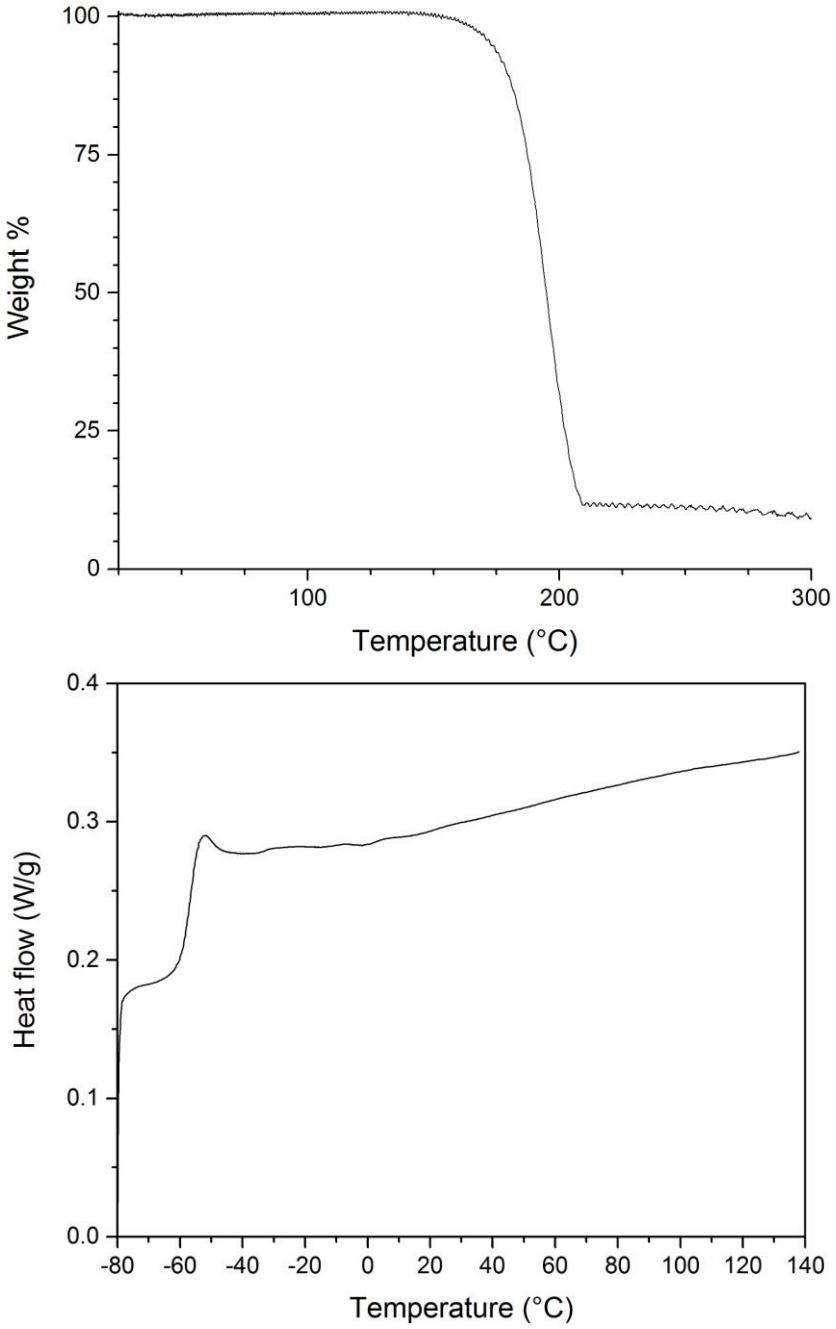

Figure 4.12. Top: Mass loss profile of PMOPO (M_n ~ 14.5 kg/mol relative to PS standards) observed by thermogravimetric analysis (TGA) under nitrogen with a heating rate of 10 °C/min. A mass loss of 1% was obtained at 160 °C. Bottom: Differential scanning calorimetry (DSC) curve obtained for PMOPO (M_n ~ 4.6 kg/mol relative to PS standards with a heating rate of 10 °C/min. A second-order phase transition was observed at T_g ~ −58 °C.

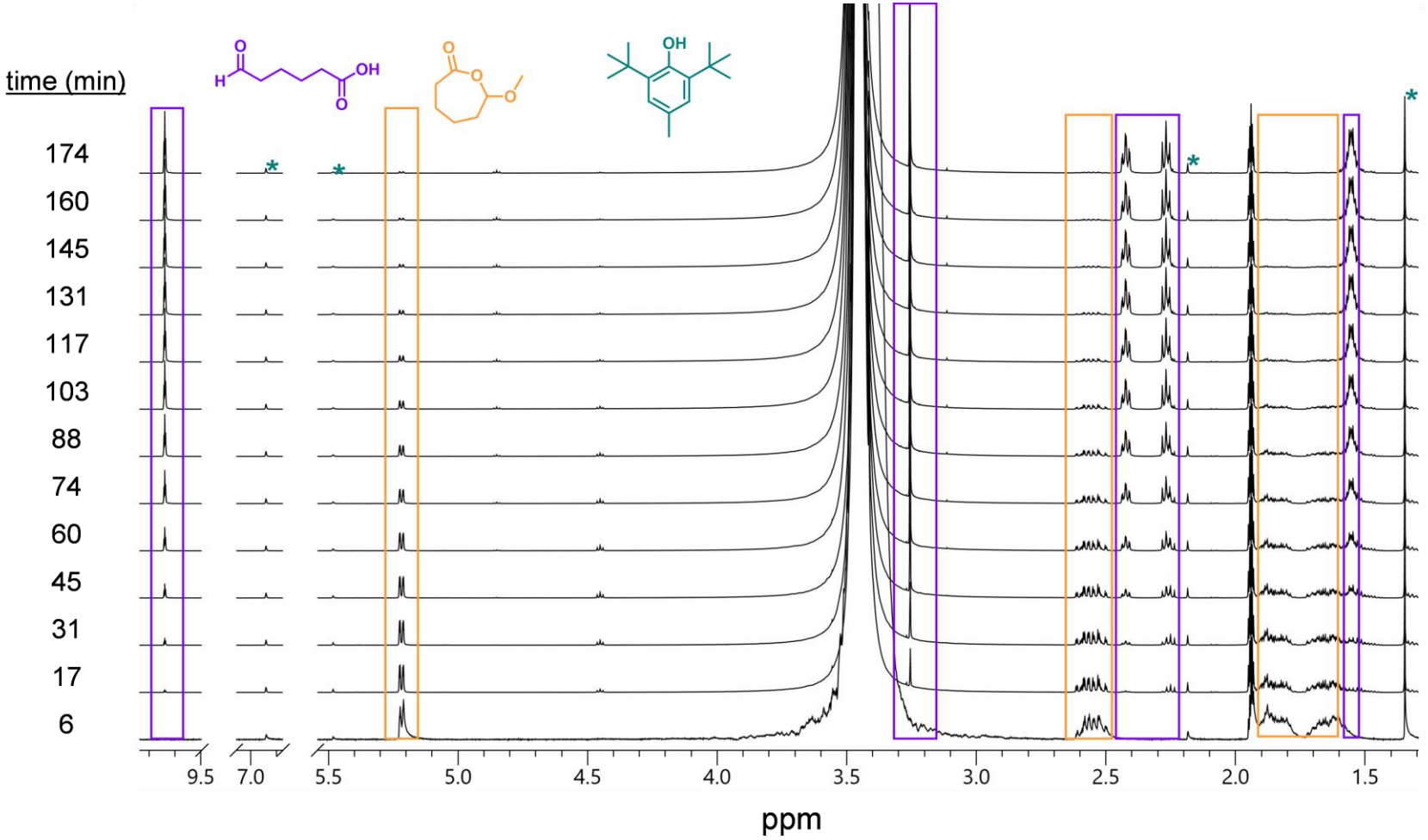

Figure 4.13. Hydrolysis of MOPO containing ca. 1% butylated hydroxytoluene (3.6 mg in 0.45 mL CD_3CN) treated with 0.1 mL H_2O and monitored by ^1H NMR spectroscopy over time.

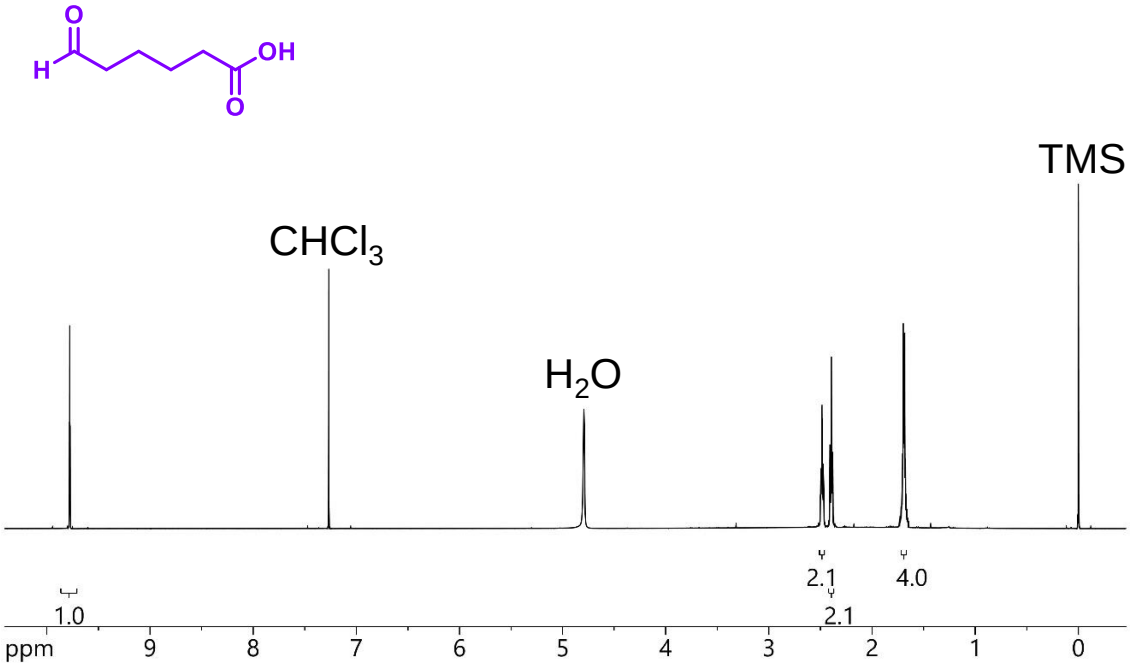

Figure 4.14. ^{1}H NMR spectrum ($CDCl_3$) of the MOPO hydrolysis product obtained in acetonitrile/water, extracted into $CDCl_3$. The observed signals are in good agreement with those previously reported for 6-oxohexanoic acid.[42]

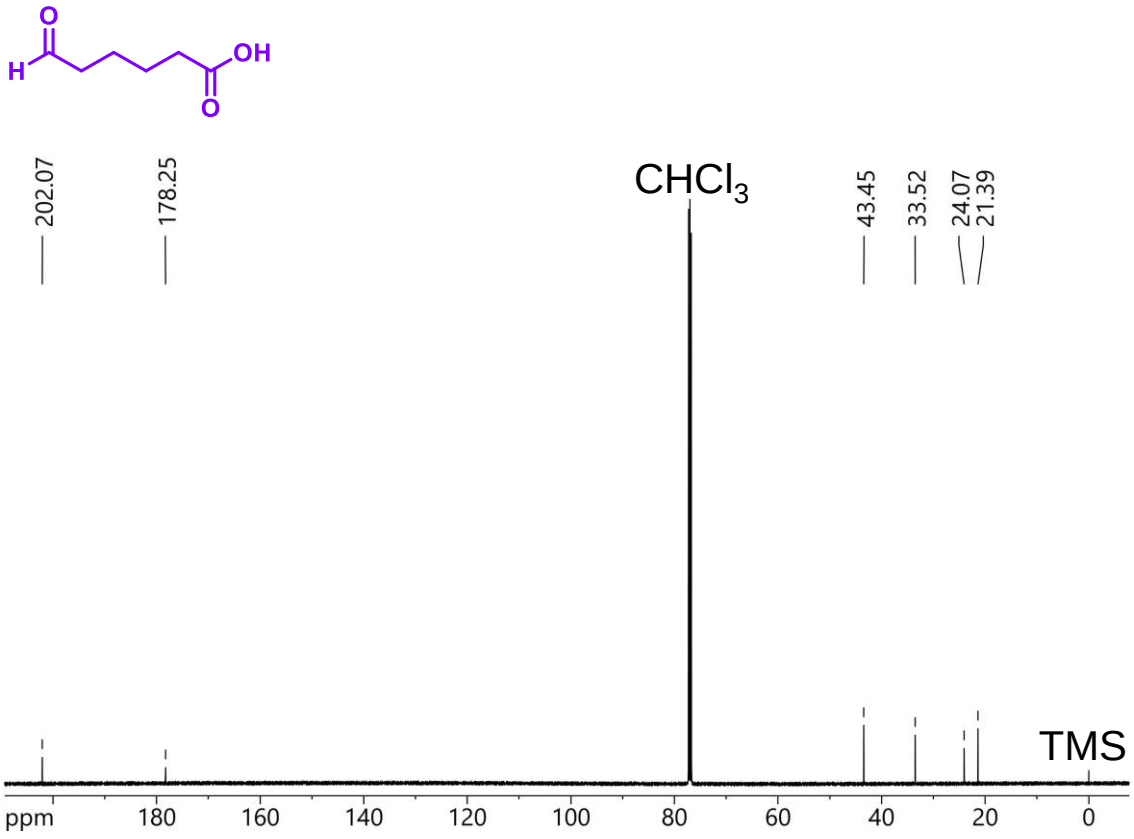

Figure 4.15. ^{13}C NMR spectrum ($CDCl_3$) of the MOPO hydrolysis product obtained in acetonitrile/water, extracted into $CDCl_3$. The observed signals are in good agreement with those previously reported for 6-oxohexanoic acid.[42]

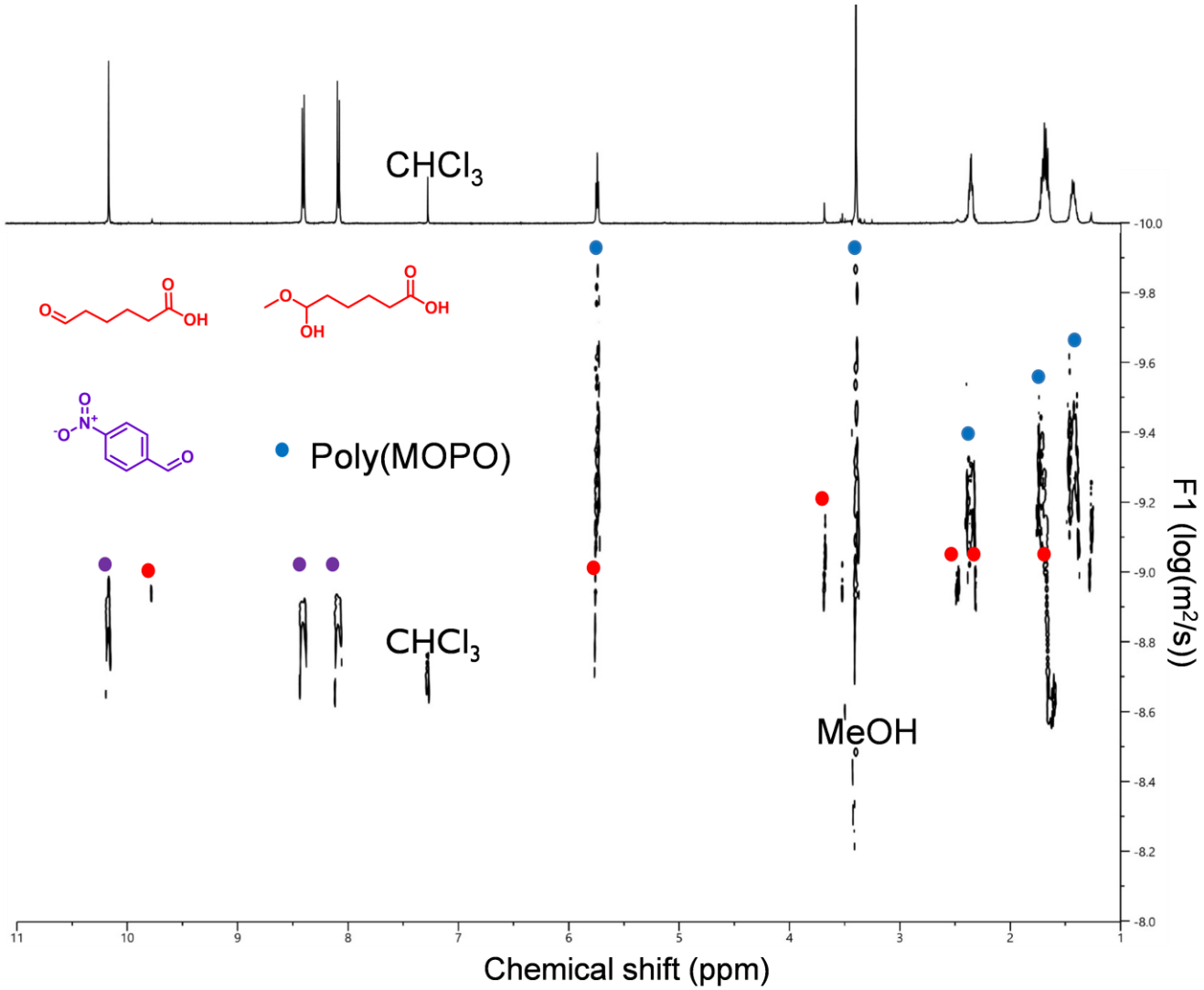

Figure 4.16. DOSY NMR spectrum of PMOPO containing 1% 6-oxohexanoic acid contaminant. It should be noted that PMOPO in this instance was synthesized using diethylzinc as the catalyst rather than HCl. However, the NMR shifts observed for 6-oxohexaoic acid in this instance are in good agreement with those observed in HCl-catalyzed MOPO CROP.

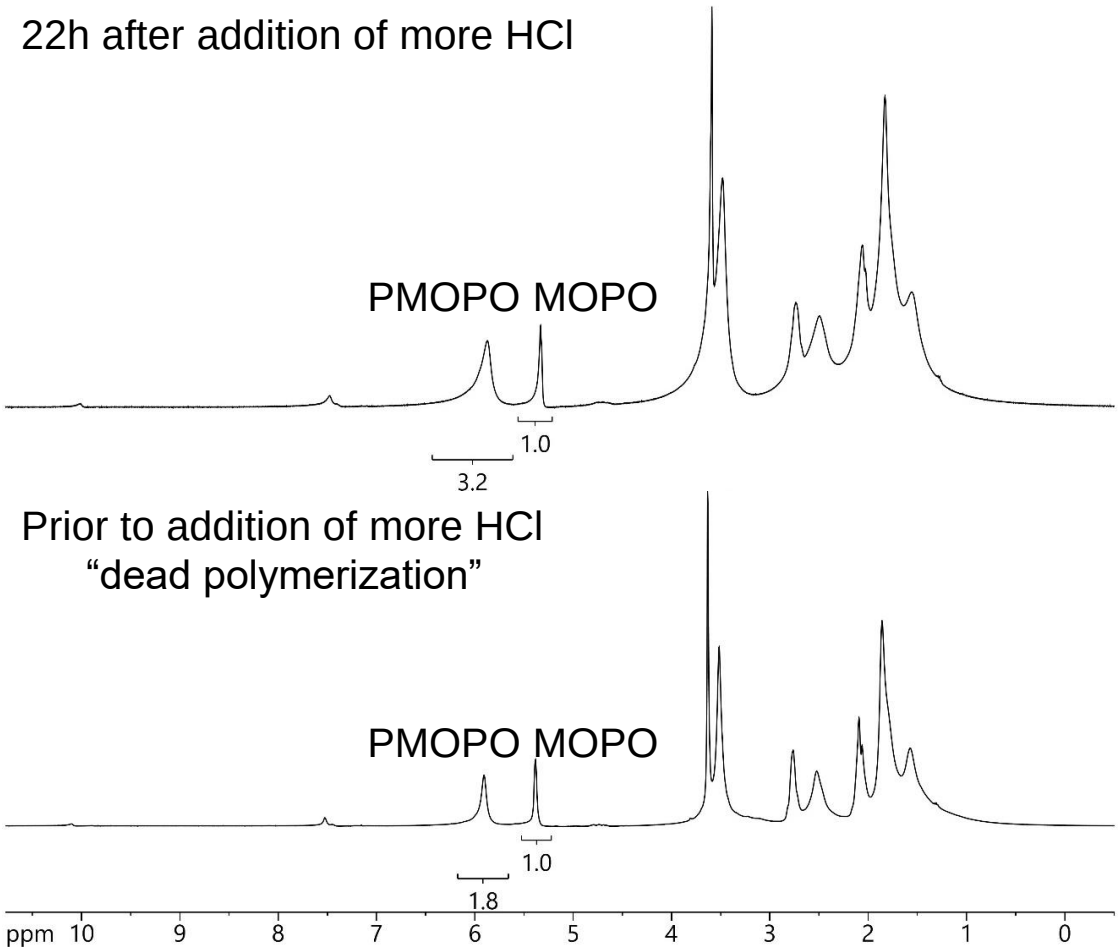

Figure 4.17. No deuterium ^{1}H NMR spectra ($CDCl_3$) of PMOPO obtained *via* an AM mechanism. The bottom spectrum depicts a neat MOPO polymerization where polymerization has ceased at 64% conversion. After addition of more HCl catalyst to the NMR experiment and waiting 22h conversion has increased to 76%, suggesting that the active species in the polymerization with HCl is quenched prior to reaching equilibrium conversion.

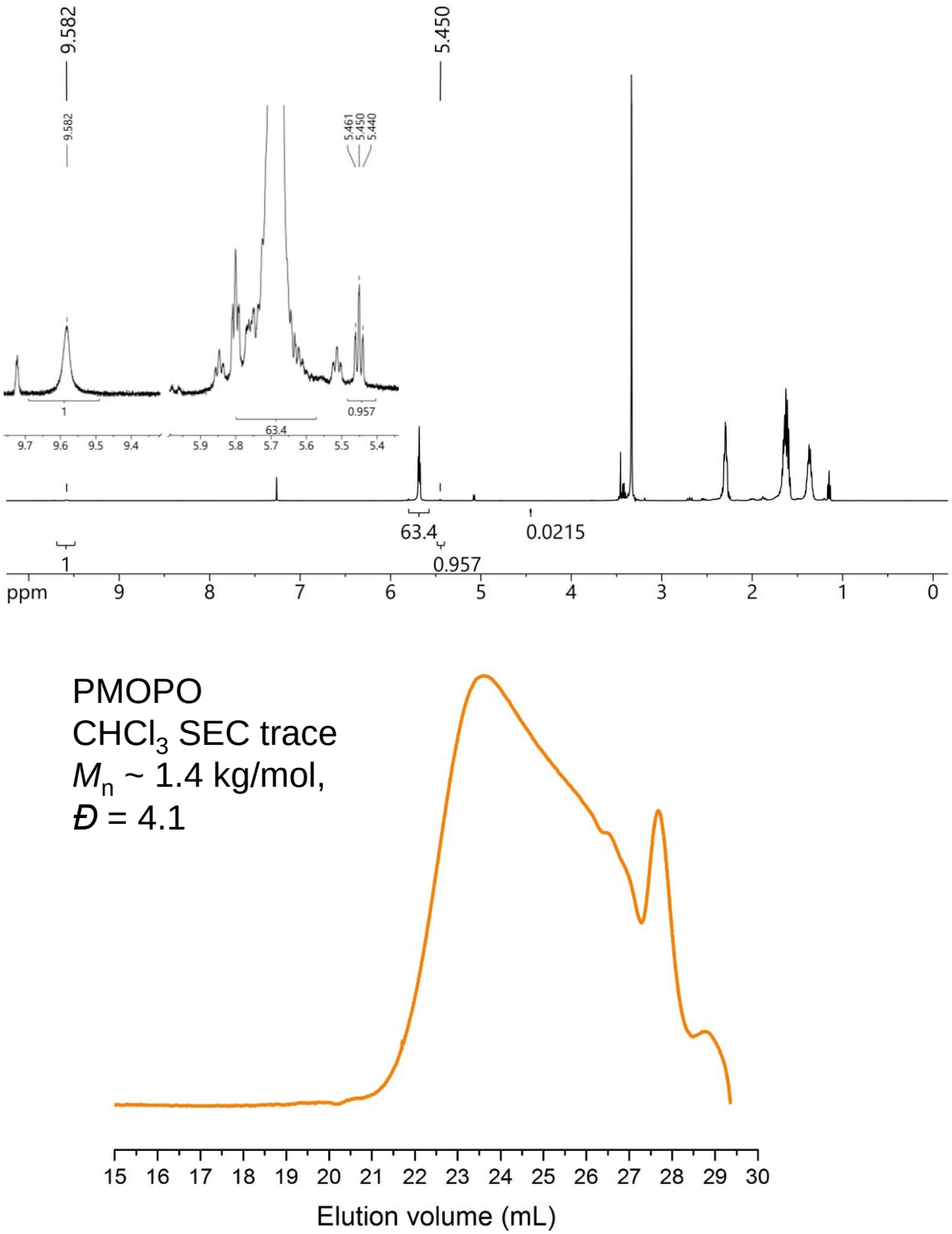

Figure 4.18. Top: ^{1}H NMR spectra showing 99% conversion of MOPO to PMOPO when polymerized in solution ($[MOPO]_0$ = 1M, $[MOPO]_0/[HCl]_0$ = 100). A chloromethylether end group is observed as a triplet at 5.48 ppm as well as the proton geminal to the alkoxycarbenium propagating species. Bottom: $CHCl_3$ SEC trace of the PMOPO obtained *via* solution polymerization indicating that low molar mass oligomers of MOPO are formed under these conditions.

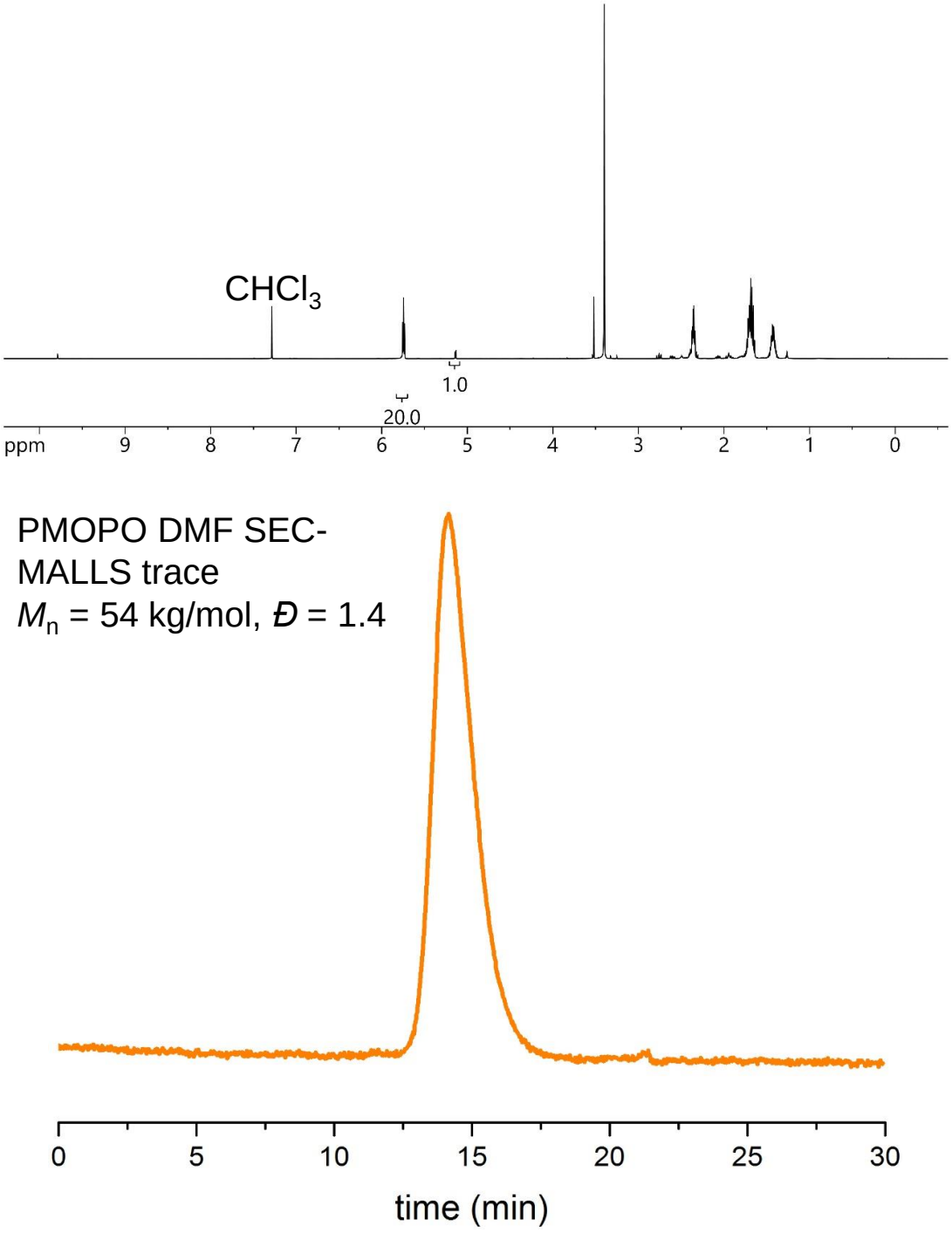

Figure 4.19. Top: ^{1}H NMR spectrum showing > 95% conversion of MOPO to PMOPO when polymerized in $CDCl_3$ solution with MeOTf ($[MOPO]_0$ = 2.25M, $[MOPO]_0/[MeOTf]_0$ = 550). Bottom: DMF SEC-MALLS trace of purified PMOPO obtained *via* solution polymerization with MeOTf.

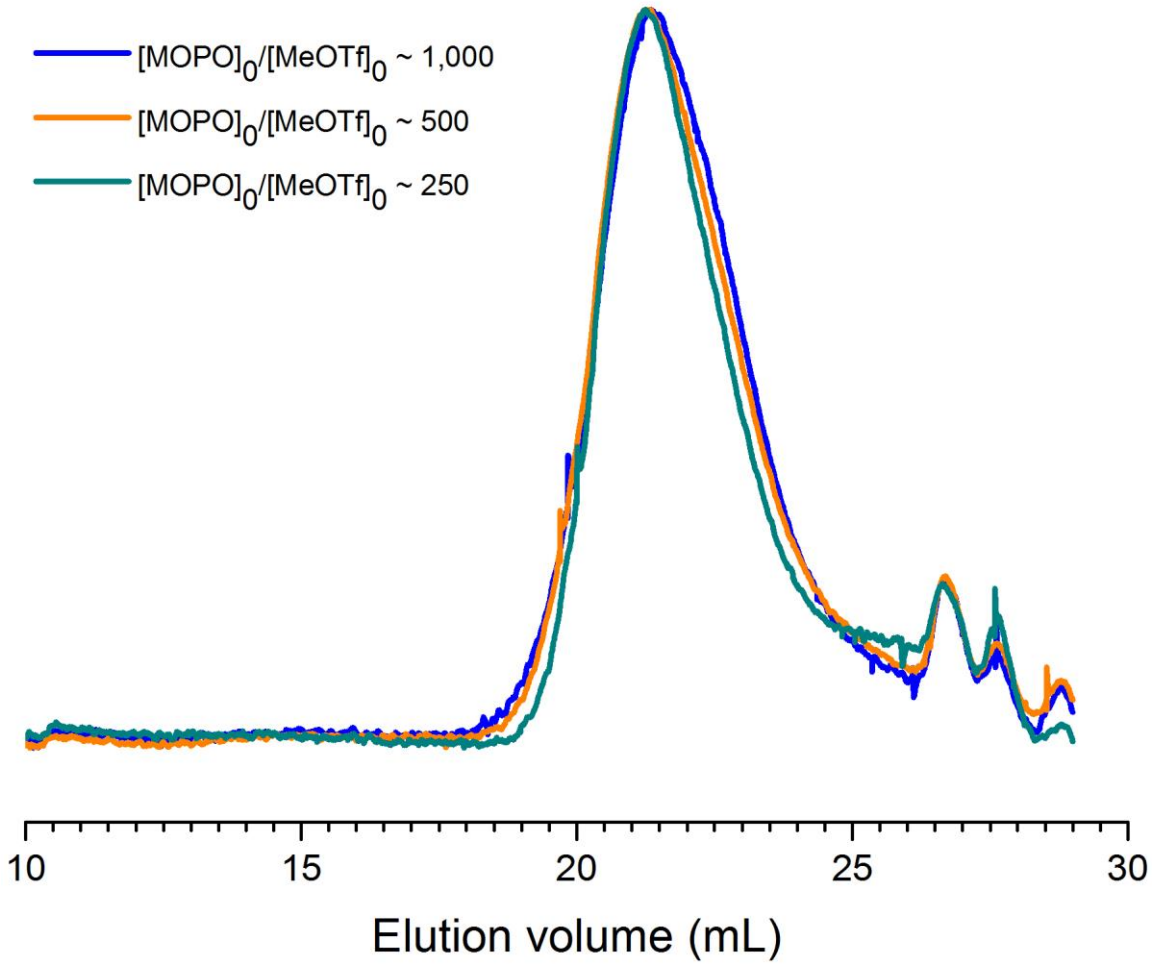

Figure 4.20. $CHCl_3$ SEC data for PMOPO synthesized with different ratios of $[MOPO]_0/[MeOTf]_0$. In all cases molar masses of M_n ~ 19 kg/mol were attained, with dispersities between $Đ$ = 1.8-2.1.

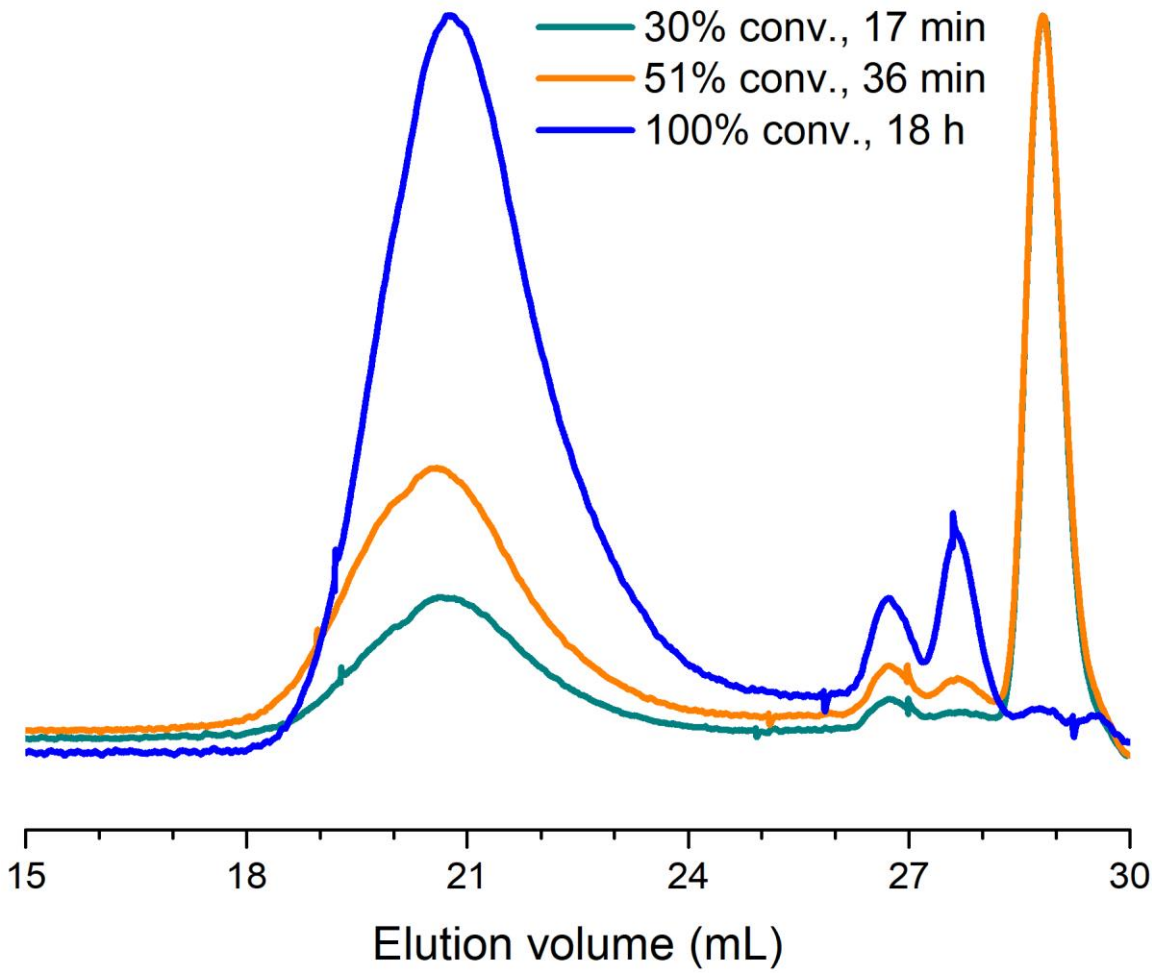

Figure 4.21. Polymerization of 2.5 M MOPO in $CDCl_3$ at −20 °C with $[MOPO]_0/[MeOTf]_0 = 500$ and $[DMS]_0/[MeOTf]_0 = 100$. No linear increase in molar mass was observed with conversion albeit the rate was significantly slowed.

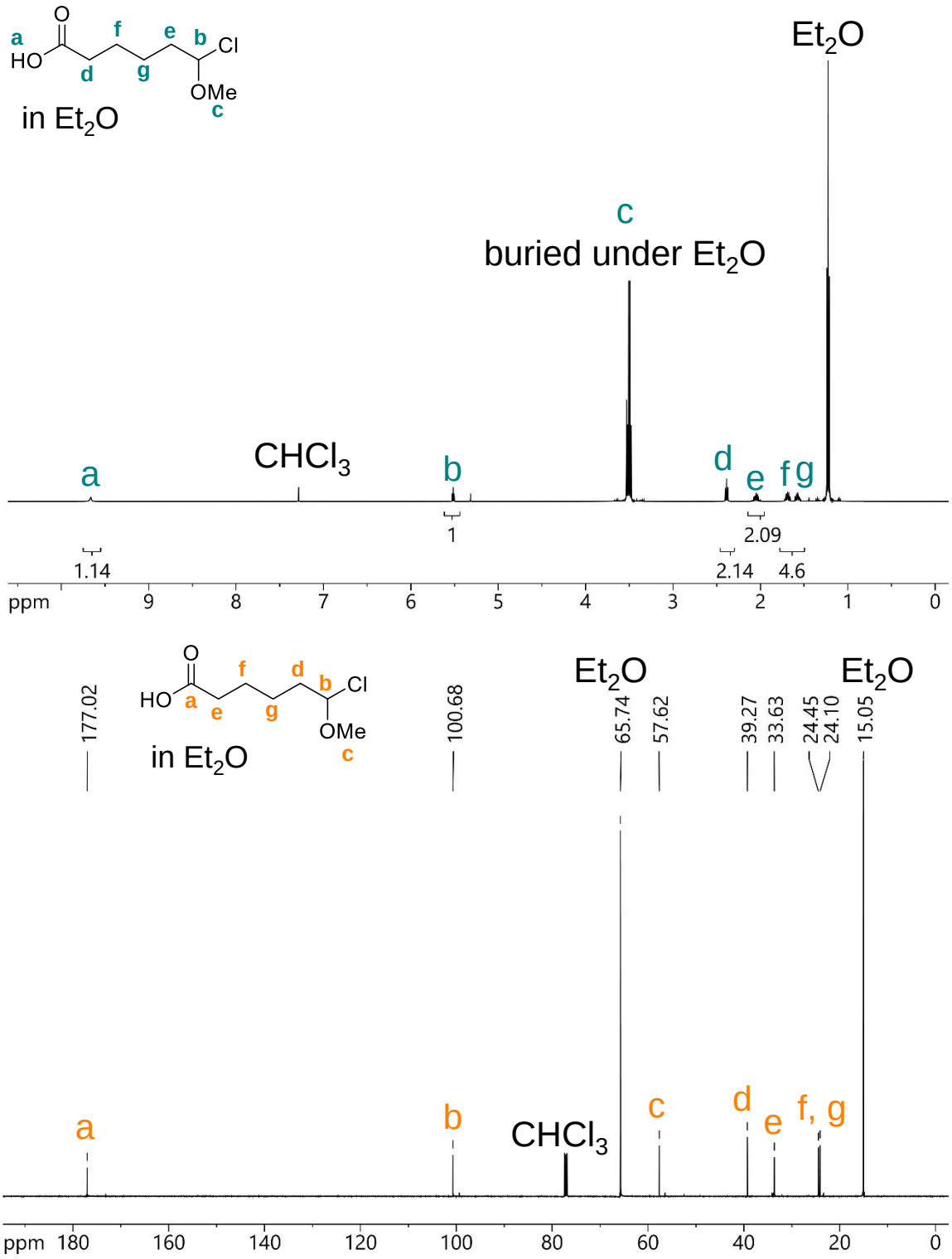

Figure 4.22. Top: ^{1}H NMR spectrum of chloromethylether in $CDCl_3$ and Et_2O. Bottom: ^{13}C NMR spectrum of chloromethylether in $CDCl_3$ and Et_2O.

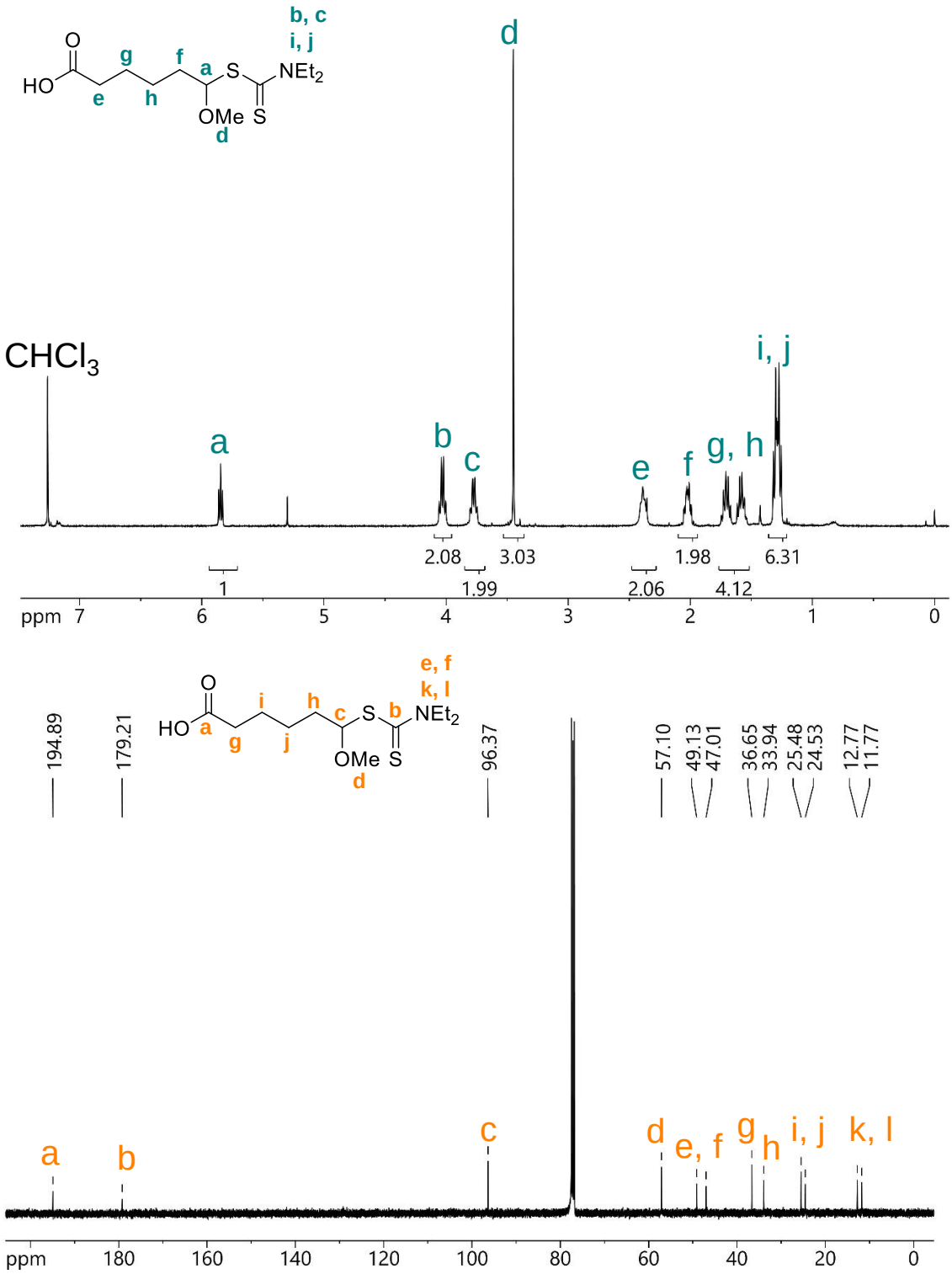

Figure 4.23. Top: ^{1}H NMR spectrum of dithiocarbamate in $CDCl_3$. Bottom: ^{13}C NMR spectrum of dithiocarbamate in $CDCl_3$.

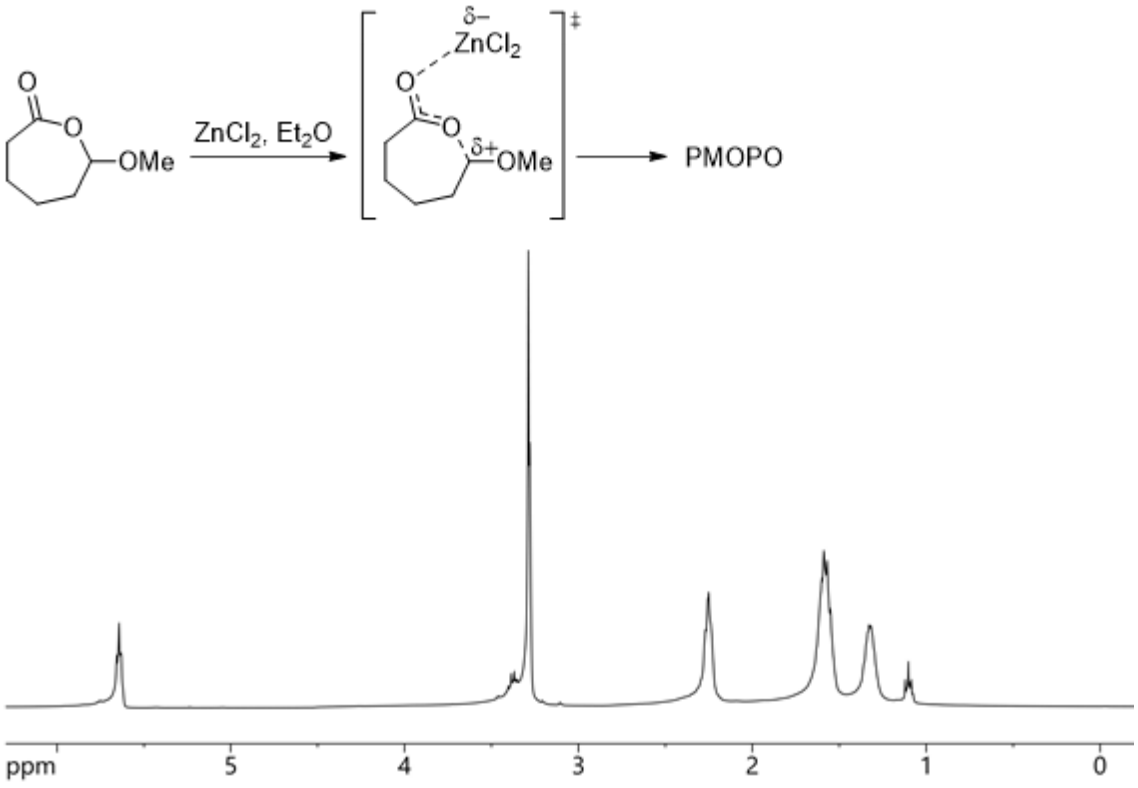

Figure 4.24. ^{1}H NMR spectrum of 2.24 M MOPO in $CDCl_3$ treated with 3 μL of 0.215 M $ZnCl_2$ in Et_2O at room temperature, resulting in the immediate and quantitative formation of PMOPO as seen here.

References

1) Penczek, S. *Makromol. Chem.* **1974**, *175*, 1217-1252.

2) Szymański, R.; Kubisa, P.; Penczek, S. *Macromolecules* **1983**, *16*, 1000-1008.

3) Kubisa, P.; Penczek, S. *Prog. Poly. Sci.* **1999**, *24*, 1409-1437.

4) Penczek, S. *J. Polym. Sci. Part A: Polym. Chem.* **2000**, *38*, 1919-1933.

5) Szwarc, M.; van Beylen, M. *Ionic Polymerization and Living Polymers*, Chapman and Hall, New York, 1993.

6) Matyjaszewski, K.; Szymański, R.; Kubisa, P.; Penczek, S. *Acta Polym.* **1984**, *35*, 14–22.

7) Aoshima, S.; Higashimura, T. *Poly. J.* **1984**, *16*, 249-258.

8) Higashimura, T.; Law, Y.-M.; Sawamoto, M. *Polym. J.* **1984**, *16*, 401-406.

9) Sawamoto, M.; Okamoto, C.; Higashimura, T. *Macromolecules* **1987**, *20*, 2693-2697.

10) Higashimura, T.; Kishimoto, Y.; Aoshima, S. *Polym. Bull.* **1987**, *18*, 111-115.

11) Kojima, K.; Sawamoto, M.; Higashimura, T. *Macromolecules* **1989**, *22*, 1552-1557.

12) Cho, G. C.; Feit, B. A.; Webster, O. W. *Macromolecules* **1990**, *23*, 1918-1923.

13) Cho, G. C.; Feit, B. A.; Webster, O. W. *Macromolecules* **1992**, *25*, 2081-2085.

14) Kamigaito, M.; Yamaoka, K.; Sawamoto, M.; Higashimura, T. *Macromolecules* **1992**, *25*, 6400-6406.

15) Kamigaito, M.; Maeda, Y.; Sawamoto, M.; Higashimura, T. *Macromolecules* **1993**, *26*, 1643-1649.

16) Aoshima, S.; Kanaoka, S. *Chem. Rev.* **2009**, *109*, 5245-5287.

17) Sawamoto M., Kamigaito M. (1995) Precision polymer synthesis by living cationic polymerization. In: Ebdon J.R., Eastmond G.C. (eds) *New Methods of Polymer Synthesis*. Springer, Dordrecht.

18) Penczek, S., Cypryk, M., Duda, A., Kubisa, P. and Słomkowski, S. (2009) Living Ring-Opening Polymerization of Heterocyclic Monomers, in *Controlled and Living Polymerizations: From Mechanisms to Applications* (eds A. H. E. Müller and K. Matyjaszewski), Wiley-VCH Verlag GmbH & Co. KGaA, Weinheim, Germany.

19) Chwiałkowska, W.; Kubisa, P.; Penczek, S. *Makromol. Chem.* **1982**, *183*, 753-769.

20) Smith, S.; Schultz, W. J.; Newmark, R. A. In *Ring-Opening Polymerization*; ACS Symposium Series; American Chemical Society, 1977; Vol. 59, pp. 2–13.

21) Penczek, S.; Kubisa, P.; Matyjaszewski, K. *Cationic ring-opening polymerization of heterocyclic monomers*; Springer-Verlag: Berlin, 1985.

22) Matyjaszewski, K. *Polimery* **2014**, *1*, 24-37.

23) Matyjaszewski, K. *Ionic Polymerizations and Related Processes* **1999**, 259–268.

24) Kumagai, S.; Nagai, K.; Satoh, K.; Kamigaito, M. *Macromolecules* **2010**, *43*, 7523-7531.

25) Aoshima, H.; Uchiyama, M.; Satoh, K.; Kamigaito, M. *Angew. Chem. Int. Ed.* **2014**, *53*, 10932-10936.

26) Uchiyama, M.; Satoh, K.; Kamigaito, M. *Macromolecules* **2015**, *48*, 5533-5542.

27) Uchiyama, M.; Satoh, K.; Kamigaito, M. *Polym. Chem.* **2016**, *7*, 1387-1396.

28) Uchiyama, M.; Satoh, K.; Kamigaito, M. *Angew. Chem. Int. Ed.* **2015**, *54*, 1924-1928.

29) Uchiyama, M.; Satoh, K.; Kamigaito, M. *ACS Macro Lett.* **2016**, *5*, 1157-1161.

30) Kottisch, V.; Michaudel, Q.; Fors, B. P. *J. Am. Chem. Soc.* **2016**, *138*, 15535-15538.

31) Kottisch, V.; Michaudel, Q.; Fors, B. P. *J. Am. Chem. Soc.* **2017**, *139*, 10665-10668.

32) Cairns, S. A.; Schultheiss, A.; Shaver, M. P. *Polym. Chem.* **2017**, 8, 2990-2996.

33) Bednarek, M.; Kubisa, P.; Penczek, S. *Makromol. Chem., Suppl.* **1989**, *15*, 49-60.

34) Kammiyada, H.; Konishi, A.; Ouchi, M.; Sawamoto, M. *ACS Macro Lett.* **2013**, *2*, 531-534.

35) Mazzini, C.; Lebreton, J.; Furstoss, R. *J. Org. Chem.* **1996**, *61*, 8-9.

36) Hata, E.; Takai, T.; Yamada, T.; Mukaiyama, T. *Chem. Lett.* **1994**, *23*, 535-538.

37) Schutyser et al. *ChemSusChem* **2015**, *8*, 1805-1818.

38) Cho et al. *Green Chem*. **2012**, *14*, 428-439.

39) Sergeev, A. G. and Hartwig, J. F. *Science* **2011**, *332*, 439-443.

40) Crivello, J. V.; Malik, R.; Lai, Y.-L. *J. Polym. Sci. A* **1996**, *34*, 3091-3102.

41) Xu, H.-C., Campbell, J. M., Moeller, K. D. *J. Org. Chem.* **2014**, *79*, 379-391.

42) Rajabi, M.; Lanfranchi, M.; Campo, F.; Panza, L. *Synth. Commun.* **2014**, *44*, 1149-1154.

43) Li, W.; Li, J.; Wu, Y.; Fuller, N.; Markus, M. A. *J. Org. Chem.* **2010**, *75*, 1077-1086.

44) Penczek, S.; Goethals, E. J. in Comprehensive polymer science: the synthesis, characterization, reactions & applications of polymers; Pergamon Press: Oxford, 1989, pp 711-717.

45) Benneche, T.; Srtrande, P.; Oftebro, R.; Undheim, K. *Eur. J. Med. Chem.* **1993**, *28*, 463-472.

46) Albright, T. A.; Freeman, W. J.; Schweizer, E. E. *J. Am. Chem. Soc.* **1975**, *97*, 2946-2950.

47) Chwiałkowska, W.; Kubisa, P.; Penczek, S. *Makromol. Chem.* **1982**, *183*, 753-769.

48) Uchiyama, M.; Satoh, K.; Kamigaito, M. *ACS Macro Lett.* **2016**, *5*, 1157-1161.

49) Armarego, W. L. F.; Chai, L. L. *Purification of Laboratory Chemicals*, 6th ed.; Elsevier, 2009.

Bibliography

Albright, T. A.; Freeman, W. J.; Schweizer, E. E. *J. Am. Chem. Soc.* **1975**, *97*, 2946-2950.

Ali Shah, A.; Hasan, F.; Hameed, A.; Ahmed, S. *Biotechnol. Adv.* **2008**, *26*, 246−265.

Andrady, A. L. *Marine Poll. Bull.* **2011**, *62*, 1596−1605.

Andrady, A. L. *J. Macromol. Sci. Polym. Rev.* **1994**, 34, 25–76.

Andrady, A.; Neal, M. A. *Phil. Trans. R. Soc. B,* **2009**, *364*, 1977−1984.

Andreeβen, B.; Steinbüchel, A. *Appl. Environ. Microbiol.* **2010**, *76*, 4919−4925.

Aoshima, S.; Higashimura, T. *Poly. J.* **1984**, *16*, 249-258.

Aoshima, S.; Kanaoka, S. *Chem. Rev.* **2009**, *109*, 5245-5287.

Aoshima, H.; Uchiyama, M.; Satoh, K.; Kamigaito, M. *Angew. Chem. Int. Ed.* **2014**, *53*, 10932-10936.

Aoshima, S.; Higashimura, T. *Macromolecules* **1989**, *22*, 1009−1013.

Armarego, W. L. F.; Chai, L. L. *Purification of Laboratory Chemicals*, 6th ed.; Elsevier, 2009.

ASTM Standard D6400, 2012, "Standard Specification for Labeling of Plastics Designed to be Aerobically Compostable in Municipal or Industrial Facilities," ASTM International, West Conshohocken, PA, 2012, DOI: 10.1520/D6400-12, www.astm.org.

Athanasiou, K. A.; Niederauer, G. G.; Agrawal, C. M. *Biomaterials* **1996**, *17*, 93−102.

Baker, G. L. Cyclic alkyl substituted glycolides and polylactides therefrom. US Patent, 20070142461 A1, Jun 21, 2007.

Bartlett, P. A.; Green, F. R. III, *J. Am. Chem. Soc.,* **1978**, *100*, 4858−4865.

Baśko, M.; Kubisa, P. *J. Polym. Sci. A Polym. Chem.* **2006**, *44*, 7071−7081.

Bastos, C. M.; Munoz, B.; Tait, B. Compounds, compositions, and methods for increasing CFTR activity. WO 2015/138934 A1, Sep 17, 2015.

Bednarek, M.; Kubisa, P.; Penczek, S. *Makromol. Chem., Suppl.* **1989**, *15*, 49-60.

Benneche, T.; Srtrande, P.; Oftebro, R.; Undheim, K. *Eur. J. Med. Chem.* **1993**, *28*, 463-472.

Bihovsky, R.; Kumar, M. U.; Ding, S. Goyal, A. *J. Org. Chem*. **1989**, *54*, 4291−4293.

Binauld, S.; Stenzel, M. H. *Chem. Commun.* **2013**, *49*, 2082−2102.

Bornscheuer, U. T. *Science*, **2016**, *351*, 1154−1155.

Brown, H. C.; Prasad, J. V. N. V.; Zee, S.-H. *J. Org. Chem.,* **1985**, *50*, 1582-1589.

Cairns, S. A.; Schultheiss, A.; Shaver, M. P. *Polym. Chem.* **2017**, *8*, 2990−2996.

Cao, A.; Kasuya, K.; Abe, H.; Doi, Y.; Inoue, Y. *Polymer***1998**, *39*, 4801–4816.

Chamberlain, B. M.; Cheng, M.; Moore, D. R.; Ovitt, T. M.; Lobkovsky, E. B.; Coates, G. W. *J. Am. Chem. Soc.* **2001**, *123*, 3229−3238.

Chisholm, M. H.; Gallucci, J.; Phomphrai, K. *Inorg. Chem.* **2002**, *41*, 2785−2794.

Cho, G. C.; Feit, B. A.; Webster, O. W. *Macromolecules* **1990**, *23*, 1918-1923.

Cho, G. C.; Feit, B. A.; Webster, O. W. *Macromolecules* **1992**, *25*, 2081-2085.

Cho et al. *Green Chem*. **2012**, *14*, 428-439.

Chwiałkowska, W.; Kubisa, P.; Penczek, S. *Makromol. Chem.* **1982**, *183*, 753-769.

Claisen, L. *Ber. Dtsch. Chem. Ges*. **1898**, *31*: 1010–1019.

Clark, F. E.; Cox, S. F.; Mack, E. *J. Am. Chem. Soc.* **1917,** *39*, 712–716.

Corey, E. J.; Ulrich, P.; Fitzpatrick, J. M. *J. Am. Chem. Soc.*, **1976**, *98*, 222−224.

Crivello, J. V.; Malik, R.; Lai, Y.-L. *J. Polym. Sci. A* **1996**, *34*, 3091-3102.

Das, S. S.; Andrews, A. P.; Greer, S. C. *J. Chem. Phys.* **1995**, *102*, 2951−2959.

Deming, T. J. *J. Polym. Sci., Part A Polym. Chem.* **2000**, *38*, 3011−3018.

Doane, T. L.; Clemens, B. *Chem. Soc. Rev.* **2012**, *41*, 2885−2911.

Doi, Y. *Macromol. Symp.* **1995**, *98*, 585−599.

Erickson, J.; Woskow, M. *J. Org. Chem.* **1958**, *23*, 670-672.

Esser-Kahn, A. P.; Odom, S. A.; Sottos, N. R.; White, S. R.; Moore, J. S. *Macromolecules* **2011**, *44*, 5539−5553.

Faraji, A. H.; Wipf, P. *Biorg. Med. Chem.* **2009**, *17*, 2950−2962.

Fernandes, R. A.; Chavan, V. P. *Eur. J. Org. Chem.*, **2010**, 4306-4311.

Fréchet, J. M. J. *Bioconjug. Chem.* **2008**, *19*, 911−919.

Gallucci, R. R.; Going, R. C. *J. Org. Chem.* **1982**, *47*, 3521−3524.

Geisow, M. J.; Evans, W. H. *Exp. Cell Res.* **1984**, *150*, 36−46.

Gillies, E. R.; Fréchet, J. M. J. *Chem. Commun.* **2003**, 1640−1641.

Goodman, M.; Brandup, J. *J. Polym. Sci., Part A Gen. Pap.* **1965**, *3*, 327−340.

Greer, S. C. *Annu. Rev. Phys. Chem.* **2002**, *53*, 173−200.

Gresham, T. L.; Jansen, J. E.; Shaver, F. W. *J. Am. Chem. Soc.* **1948**, *70*, 998−999.

Hashimoto, T.; Iwata, T.; Minami, A.; Kodaira, T. *J. Polym. Sci., Part A: Polym. Chem.* **1998**, *36*, 3173−3185.

Hata, E.; Takai, T.; Yamada, T.; Mukaiyama, T. *Chem. Lett.* **1994**, *23*, 535-538.

Heffernan, M. J.; Murthy, N. *Bioconjug. Chem.* **2005**, *16*, 1340−1342.

Heller, J.; Penhale, D. W. H.; Helwing, R. F. *J. Polym. Sci. Polym. Lett. Ed.* **1980**, *18*, 293−297.

Higashimura, T.; Law, Y.-M.; Sawamoto, M. *Polym. J.* **1984**, *16*, 401-406.

Higashimura, T.; Kishimoto, Y.; Aoshima, S. *Polym. Bull.* **1987**, *18*, 111-115.

Hiki, S.; Taniguchi, I.; Miyamoto, M.; Kimura, Y. *Macromolecules* **2002**, *35*, 2423-2425.

Hoffman, A. S. *Adv. Drug Delivery Rev.* **2013**, *65*, 10−16.

Hrkach, J. S.; Matyjaszewski, K. *Macromolecules* **1992**, *25*, 2070−2075.

Hu, J.; Liu, S. *Macromolecules* **2010**, *43*, 8315−8330.

Huck, W. T. S. *Mater. Today* **2008**, *11*, 24−32.

Ishii, Y.; Osakada, K.; Ikariya, T.; Saburi, M.; Yoshikawa, S. *J. Org. Chem.*, **1986**, *51*, 2034–2039.

Jacobson, H.; Stockmayer, W. H. *J. Chem. Phys.* **1950**, *18*, 1600−1606.

Jain, R.; Standley, S. M.; Fréchet, J. M. J. *Macromolecules* **2007**, *40*, 452−457.

John, A.; Hogan, L. T.; Hillmyer M. A; Tolman W. B. *Chem. Commun.* **2015**, *51*, 2731−2733.

Juge, S.; Genet, J.-P.; Mallart, S. Preparation of 1,3-dioxan-4-one Derivatives as Intermediates for Beta-Hydroxy-Alpha-Amino Acids. FR 2 632 642-A1, June 14, 1988.

Kamigaito, M.; Sawamoto, M.; Higashimura, T. *Macromolecules* **1991**, *24*, 3988−3992.

Kamigaito, M.; Yamaoka, K.; Sawamoto, M.; Higashimura, T. *Macromolecules* **1992**, *25*, 6400-6406.

Kamigaito, M.; Maeda, Y.; Sawamoto, M.; Higashimura, T. *Macromolecules* **1993**, *26*, 1643-1649.

Kammiyada, H.; Konishi, A.; Ouchi, M.; Sawamoto, M. *ACS Macro Lett*. **2013**, *2*, 531−534.

Kammiyada, H.; Ouchi, M.; Sawamoto, M. *Polym. Chem.* **2016**, *7*, 6911−6917.

Keith, D. D.; Tortora, J. A.; Yang, R. *J. Org. Chem*. **1978**, *43*, 3711−3713.

Khaja, S. D.; Lee, S.; Murthy, N. *Biomacromolecules* **2007**, *8*, 1391−1395.

Komatsu, H.; Hino, T.; Endo, T. *J. Polym. Sci. A Polym. Chem.* **2006**, *44*, 3966−3977.

Kojima, K.; Sawamoto, M.; Higashimura, T. *Macromolecules* **1989**, *22*, 1552-1557.

Kottisch, V.; Michaudel, Q.; Fors, B. P. *J. Am. Chem. Soc.* **2016**, *138*, 15535-15538.

Kottisch, V.; Michaudel, Q.; Fors, B. P. *J. Am. Chem. Soc.* **2017**, *139*, 10665-10668.

Komatsu, H.; Ochiai, B.; Endo, T. *J. Polym. Sci. A Polym. Chem.* **2008**, *46*, 1427−1439.

Kricheldorf, H. R. *Angew. Chem. Int. Ed.* **2006**, *45*, 5752−5784.

Kubisa, P.; Penczek, S. *Prog. Poly. Sci.* **1999**, *24*, 1409-1437.

Kumagai, S.; Nagai, K.; Satoh, K.; Kamigaito, M. *Macromolecules* **2010**, *43*, 7523-7531.

Le Hellaye, M.; Fortin, N.; Guilloteau, J.; Soum, A.; Lecommandoux, S.; Guillaume, S. M. *Biomacromolecules* **2008**, *9*, 1924−1933.

Lee, S. J.; Min, K. H.; Lee, H. J.; Koo, A. N.; Rim, H. P.; Jeon, B. J.; Jeong, S. Y.; Heo, J. S.; Lee, S. C. *Biomacromolecules* **2011**, *12*, 1224−1233.

Levine, R. M.; Scott, C. M.; Kokkoli, E. *Soft Matter* **2013**, *9*, 985−1004.

Li, S.; Garreau, H.; Vert, M. *J. Mater. Sci. Mater. Med.* **1990**, *1*, 123−130.

Li, W.; Li, J.; Wu, Y.; Fuller, N.; Markus, M. A. *J. Org. Chem.* **2010**, *75*, 1077-1086.

Li, S.; Vert, M. In *Degradable Polymers*; Springer Netherlands, 2002; pp 71–131.

Li, W.; Li, J.; Wu, Y.; Fuller, N.; Markus, M. A. *J. Org. Chem.* **2010**, *75*, 1077−1086.

Li, J.; Rothstein, S. N.; Little, S. R.; Edenborn, H. M.; Meyer, T. Y. *J. Am. Chem. Soc.*, **2012**, *134*, 16352−16359.

Liu, F.; Urban, M. W. *Prog. Polym. Sci.* **2010**, *35*, 3−23.

Löfgren, A.; Albertsson, A.-C.; Dubois, P.; Jérôme, C. *J Macromol. Sci. Polymer Rev.* **1995**, *35*, 379−418.

Lowe, J. R.; Martello, M. T.; Tolman, W. B.; Hillmyer, M. A. *Polym. Chem.* **2011**, *2*, 702−708.

Lowe, J. R.; Tolman, W. B.; Hillmyer, M. A. *Biomacromolecules* **2009**, *10*, 2003–2008.

Löpfe, M.; Linden, A.; Heimgartner, H. *Heterocycles* **2011**, *82*, 1267-1282.

Makiguchi, K.; Satoh, T.; Kakuchi, T. *Macromolecules* **2011**, *44*, 1999−2005.

Martello, M. T.; Burns, A.; Hillmyer, M. A. *ACS Macro Lett.* **2012**, *1*, 131−135.

Martin, R. T.; Camargo, L. P.; Miller, S. A. *Green Chem.* **2014**, *16*, 1768−1773.

Matsukawa, D.; Okamura, H.; Shirai, M. *J. Photopolym. Sci. Technol.* **2010**, *23*, 781−787.

Matyjaszewski, K.; Szymański, R.; Kubisa, P.; Penczek, S. *Acta Polym.* **1984**, *35*, 14–22.

Matyjaszewski, K. *Polimery* **2014**, *1*, 24-37.

Matyjaszewski, K. *Ionic Polymerizations and Related Processes* **1999**, 259–268.

Mazzini, C.; Lebreton, J.; Furstoss, R. *J. Org. Chem.* **1996**, *61*, 8-9.

McKenna, R.; Nielsen, D. R. *Metab. Eng.* **2011**, *13*, 544−554

Meng, H.; Jinlian, H. *J. Intell. Mater. Syst. Struct.* **2010**, *21*, 859−885.

Miranda, M. O.; Pieterangelo, A.; Hillmyer, M. A.; Tolman, W. B. *Green Chem.* **2012**, *14*, 490−494

Miller, S. A. Polyesteracetals. U.S. Patent 2009/066417, December 2, **2009**.

Miller, S. A. *ACS Macro Lett*. **2013**, *2*, 550−554.

Moriguchi, T.; Endo, T. *J. Org. Chem*. **1995**, *60*, 3523−3528.

Moriguchi, T.; Endo, T.; Takata, T.; Nakane, Y. *Macromolecules* **1995**, *28*, 4334–4339.

Murthy, N.; Thng, Y. X.; Schuck, S.; Xu, M. C.; Fréchet, J. M. J. *J. Am. Chem. Soc.* **2002**, *124*, 12398−12399.

Nanba, T.; Ito, H.; Kobayashi, H.; Hayashi, T. Preparation of poly(hydroxyalkanoates) with low cost and good safety. JP 06329774 A 19941129, November 29, 1994.

Nava, H. Methods of Preparing Polyesters from Cyclic Organic Carbonates in the Presence of Alkali Metal-Containing Catalysts. U.S. Patent 5,714,568, February 3, 1998.

Neises, B.; Steglich, W. *Angew. Chem. Int. Ed. Engl.;* **1978**, *17*, 522−524.

Neitzel, A. E.; Petersen, M. A.; Kokkoli, E.; Hillmyer, M. A. *ACS Macro Lett.* **2014**, *3*, 1156−1160.

Nuyken, O.; Pask, S. D. *Polymers* **2013**, *5*, 361−403.

Otsuka, H.; Endo, T. *Macromolecules* **1999**, *32*, 9059−9061.

Ouchi, M.; Kammiyada, H.; Sawamoto, M. *Polym. Chem.* **2017**, *8*, 4970−4977.

Ouhadi, T.; Heuschen, J. M. *J. Macromol. Sci. Part A - Chem.* **1975**, *9*, 1183−1193.

Pangburn, T. O.; Petersen, M. A.; Waybrant, B.; Adil, M. M.; Kokkoli, E. *J. Biomech. Eng.* **2009**, *131*, 074005−074005-20.

Panyam, J.; Labhasetwar, V. *Adv. Drug Delivery Rev.* **2012**, *64, Supple*, 61−71.

Paramonov, S. E.; Bachelder, E. M.; Beaudette, T. T.; Standley, S. M.; Lee, C. C.; Dashe, J.; Heller, J.; Barr, J.; Ng, S. Y.; Abdellauoi, K. S.; Gurny, R. *Adv. Drug Delivery Rev.* **2002**, *54*, 1015−1039.

Penczek, S. *J. Polym. Sci., Part A Polym. Chem.* **2000**, *38*, 1919−1933.

Penczek, S.; Cypryk, M.; Duda, A.; Kubisa, P.; Słomkowski, S. Living Ring-opening Polymerization of Heterocyclic Monomers. *Prog. Polym. Sci*. **2007**, *32*, 247−282.

Penczek, S. *Makromol. Chem.* **1974**, *175*, 1217-1252.

Penczek, S. *J. Polym. Sci. Part A: Polym. Chem.* **2000**, *38*, 1919-1933.

Penczek, S., Cypryk, M., Duda, A., Kubisa, P. and Słomkowski, S. (2009) Living Ring-Opening Polymerization of Heterocyclic Monomers, in *Controlled and Living Polymerizations: From Mechanisms to Applications* (eds A. H. E. Müller and K. Matyjaszewski), Wiley-VCH Verlag GmbH & Co. KGaA, Weinheim, Germany.

Penczek, S.; Kubisa, P.; Matyjaszewski, K. *Cationic ring-opening polymerization of heterocyclic monomers*; Springer-Verlag: Berlin, 1985.

Penczek, S.; Goethals, E. J. in *Comprehensive polymer science: the synthesis, characterization, reactions & applications of polymers*; Pergamon Press: Oxford, 1989, pp 711-717.

Petersen, M. A.; Hillmyer, M. A.; Kokkoli, E. *Bioconjug. Chem.* **2013**, *24*, 533−543.

Petersen, M. A.; Yin, L.; Kokkoli, E.; Hillmyer, M. A. *Polym. Chem.* **2010**, *1*, 1281−1290.

Poland, D. *J. Chem. Phys.* **1999**, *111*, 8214−8224.

Qian, H.; Wohl, A. R.; Crow, J. T.; Macosko, C. W.; Hoye, T. R. *Macromolecules* **2011**, *44*, 7132−7140.

Rajabi, M.; Lanfranchi, M.; Campo, F.; Panza, L. *Synth. Commun.* **2014**, *44*, 1149-1154.

Ramis, X.; Salla, J. M.; Manteco, A.; Gonza, L. *J. Appl. Polym. Sci.* **2009**, *111*, 1805−1811.

Reddy, C. S. K.; Ghai, R.; Kalia, R. V. C. *Bioresour Technol.* **2003**, *87*, 137–146.

Rolando, C.; Penhoat, M.; Gholamipour-Shirazi, A. Alkylation of carboxylic acids in a microfluidic device: kinetics parameters determination, Hammett reaction constant measurement and optimization of preparative experiment. *In Proceedings of the 13th Int. Electron. Conf. Synth. Org. Chem.*, 1–30 November 2009; Sciforum Electronic Conference Series, Vol. 13, 2009, a038.

Roy, D.; Cambre, J. N.; Sumerlin, B. S. *Prog. Polym. Sci.* **2010**, *35*, 278−301.

Rubush, D. M. **2014**. Diphenylphosphoric Acid. *e-EROS Encyclopedia of Reagents for Organic Synthesis*. 1–6.

Save, M.; Schappacher, M.; Soum, A. *Macromol. Chem. Phys.* **2002**, *203*, 889−899.

Sawamoto, M.; Okamoto, C.; Higashimura, T. *Macromolecules* **1987**, *20*, 2693-2697.

Sawamoto M., Kamigaito M. (1995) Precision polymer synthesis by living cationic polymerization. In: Ebdon J.R., Eastmond G.C. (eds) *New Methods of Polymer Synthesis*. Springer, Dordrecht.

Schacht, E.; Toncheva, V.; Vandertaelen, K.; Heller, J. *J. Control. Release* **2006**, *116*, 219−225.

Schutyser et al. *ChemSusChem* **2015**, *8*, 1805-1818.

Sergeev, A. G. and Hartwig, J. F. *Science* **2011**, *332*, 439-443.

Shohi, H.; Sawamoto, M.; Higashimura, T. *Macromolecules* **1992**, *25*, 58−63.

Smith, S.; Schultz, W. J.; Newmark, R. A. In *Ring-Opening Polymerization*; ACS Symposium Series; American Chemical Society, 1977; Vol. 59, pp. 2–13.

Stayshich, R.M.; Meyer, T.Y. *J. Am. Chem. Soc.*, **2010**, *132*, 10920−10934.

Stridsberg, K.; Albertsson, A. C. *Polymer* **2000**, *41*, 7321−7330.

Szwarc, M.; van Beylen, M. *Ionic Polymerization and Living Polymers*, Chapman and Hall, New York, 1993.

Szymański, R.; Kubisa, P.; Penczek, S. *Macromolecules* **1983**, *16*, 1000-1008.

Tannock, I. F.; Rotin, D. *Cancer Res.* **1989**, *49*, 4373.

Tokiwa, Y.; Calabia, B. P.; Ugwu, C. U.; Aiba, S. *Int. J. Mol. Sci.* **2009**, *10*, 3722–3742.

Tomlinson, R.; Klee, M.; Garett, S.; Heller, J.; Duncan, R.; Brocchini, S. *Macromolecules* **2002**, *35*, 473−480.

Tsuruta, T.; Matsuura, K.; Inoue, S. *Die Makromol. Chemie* **1964**, *75*, 211−214.

Tsutsui, H.; Mitsunobu, O. *Tet. Lett.*, **1984**, *17*, 2455−2166.

Turova, N.; Turevskaya, E.; Kessler, V. G.; Yanovskaya, M. I. *The Chemistry of Metal Alkoxides*; Kluwer Academic Publishers, 2002.

Uchiyama, M.; Satoh, K.; Kamigaito, M. *Macromolecules* **2015**, *48*, 5533-5542.

Uchiyama, M.; Satoh, K.; Kamigaito, M. *Polym. Chem.* **2016**, *7*, 1387-1396.

Uchiyama, M.; Satoh, K.; Kamigaito, M. *Angew. Chem. Int. Ed.* **2015**, *54*, 1924-1928.

Uchiyama, M.; Satoh, K.; Kamigaito, M. *ACS Macro Lett.* **2016**, *5*, 1157-1161.

University of Minnesota Chemistry Department NMR Facility Home Page, http://nmr.chem.umn.edu/manuals.html, accessed 07/20/2016.

U.S. Field Production of Crude Oil (Thousand Barrels per Day) https://www.eia.gov/dnav/pet/hist/LeafHandler.ashx?n=PET&s=MCRFPUS2&f=A (accessed Aug 31, 2017).

Uyanik, M.; Akakura, M.; Ishihara, K. *J. Am. Chem. Soc.*, **2009**, *131*, 251-262.

Vangeyte, P.; Jérôme, R. *J. Poly. Sci. Part A: Polym. Chem.* **2004**, *42*, 1132–1142.

Vidil, T.; Tournilhac, F.; Musso, S.; Robisson, A.; Leibler, L. *Prog. Polym. Sci.* **2016**, *62*, 126–179

Wade, L. G. *Organic chemistry*, 6th ed.; Pearson Prentice Hall: Upper Saddle River, NJ, 2006.

Wanamaker, C. L.; Tolman, W. B.; Hillmyer, M. A. *Biomacromolecules* **2009**, *10*, 443−448.

Washington, M. A.; Swiner, D. J.; Bell, K. R.; Fedorchak, M. V.; Little, S. R.; Meyer, T. Y. *Biomaterials* **2017**, *117*, 66–76.

Werpy, T.; Petersen, G.; Aden, A.; Bozell, J.; Holladay, J.; White, J.; Manheim, A.; Elliot, D.; Lasure, L.; Jones, S.; Gerber, M.; Ibsen, K.; Lumberg, L.; Kelley, S. *Top Value Added Chemicals from Biomass Volume I—Results of Screening for Potential Candidates from Sugars and Synthesis Gas*, Pacific Northwest National Laboratory and the National Renewable Energy Laboratory, 2004.

Williams, C. K.; Breyfogle, L. E.; Choi, S. K.; Nam, W.; Hillmyer, M. A.; Tolman, W. B. *J. Am. Chem. Soc.* **2003**, *125*, 11350−11359.

Wojtania, M.; Kubisa, P.; Penczek, S. *Makromol. Chem., Makromol. Symp.* **1986**, *6*, 201−206.

Wolfe, P. S.; Wagener, K. B. *Macromol. Rapid Commun.* **1998**, *19*, 305−308.

World Economic Forum, Ellen Mac Arthur Foundation and McKinsey and Company, The New Plastics Economy Rethinking the Future of Plastics; 2016; [report] http://www.ellenmacarthurfoundation.org/publications.

Wynkoop, M. (2017). *COMMERCIAL COMPOSTING, "GREEN-WASHING" AND ECO LABELS*. [ebook] World Centric. Available at: http://worldcentric.org/images/newsletter/Compostable%20vs%20%20Biodegradable.pdf [Accessed 28 Aug. 2017].

Xie, X.; Stahl, S. S. *J. Am. Chem. Soc.*, **2015**, *137*, 3767−3770.

Xu, H.-C., Campbell, J. M., Moeller, K. D. *J. Org. Chem.* **2014**, *79*, 379-391.

Yamashita, M.; Nishida, H. Process for Preparation of 1,3-Dioxane-4-one Compounds by Cyclization. JP 09194450 A 19970729, March 31, 1997.

Yamashita, M.; Takemoto, Y.; Ihara, E.; Yasuda, H. *Macromolecules* **1996**, *29*, 1798−1806.

Zhang, L.; Bernard, J.; Davis, T. P.; Barner-Kowollik, C.; Stenzel, M. H. *Macromol. Rapid Commun.* **2008**, *29*, 123−129.

Zhang, D.; Hillmyer, M. A.; Tolman, W. B. *Macromolecules* **2004**, *37*, 8198−8200.

Zhang, Z.; Ortiz, O.; Goyal, R.; Kohn, J. In *Principles of Tissue Engineering*; Academic Press: Boston, MA, 2014; pp 441–473.

Zhao, J.; Pahovnik, D.; Gnanou, Y.; Hadjichristidis, N. *Macromolecules* **2014**, *47*, 3814−3822.

Zhdanko, A.; Maier, M. E. *Chem. Eur. J.*, **2013**, *19*, 3932–3942.

Zhuang, J.; Das, S. S.; Nowakowski, M. D.; Greer, S. C. *Physica A* **1997**, *244*, 522−535.

Zupancich, J. A.; Bates, F. S.; Hillmyer, M. A. *Macromolecules* **2006**, *39*, 4286–4288.

Appendix A

Towards the Synthesis of a Perfectly Alternating Copolymer of Lactic and 3-Hydroxypropionic Acid

The work in this chapter was carried out in part in collaboration with Quentoria Walton, a center for sustainable polymers undergraduate student, summer 2017.

A1. Introduction

The synthesis of well-defined copolymers is a necessary first step in understanding how sequence affects bulk polymer properties. Copolymers of lactic acid hold the potential of tailoring polylactide properties whilst conserving amenability to biodegradation. For example, random lactide/glycolide copolymers are widely used in medical applications due to their optimal hydrolysis kinetics under physiological conditions when compared to the hydrolysis of either homopolymer under identical conditions.[1] In a recent study it was shown that sequenced glycolic and lactic acid copolymers exhibited a slower yet more constant rate of hydrolysis when compared to samples of random glycolide/lactide copolymers.[2] A more gradual and consistent degradation profile is especially desirable in drug delivery, where a small molecule is ideally released at a constant rate. In a different approach, researchers synthesized [*R*]-4-methyl-1,5-dioxepane-2,6-dione (MDP), which is a condensation product of 3-hydroxybutyric acid with glycolic acid. [3] The ring-opening polymerization of MDP to perfectly alternating poly([*R*]-3-hydroxybutyrate-*co*-glycolate) under cationic, anionic or metal-catalyzed conditions was however unsuccessful. But when copolymerizing MDP with [*R*]-*β*-butyrolactone, up to 15 mol% of MDP could be incorporated into a MDP/[*R*]-*β*-butyrolactone copolymer.

Inspired by this report we set out to prepare a perfectly alternating copolymer of lactic and 3-hydroxypropionic acid. We targeted the cyclic diester monomer 3-methyl-1,4-dioxepane-2,5-dione (DXD), which is comprised of lactic acid condensed onto 3-hydroxypropionic acid. Controlled ring-opening polymerization of DXD is hypothesized to yield perfectly alternating lactic/3-hydroxypropionic acid copolymers *via* a

coordination-insertion mechanism, where the relative reactivities of the two distinct ester moieties will need to be determined.

A2. Results and Discussion

Following the method of Hiki et al. we prepared a linear α-bromo-ω-acid precursor to DXD and probed various ring-closing methods. Unfortunately all attempts to ring-close this linear precursor were thwarted by the competitive elimination of bromide to form the corresponding acrylate (Scheme A2.1) .

Scheme A2.1. Attempted ring-closure of 2-((3-bromopropanoyl)oxy)propanoic acid

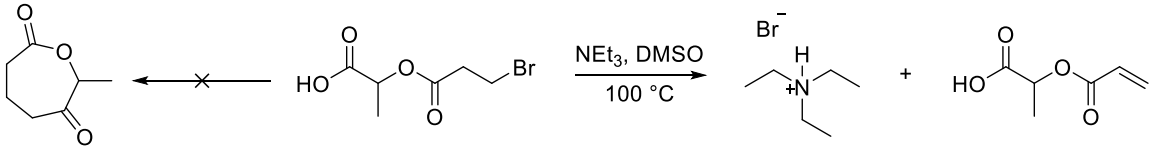

Hence, we redesigned the acid-bromide precursor such that ring-closing would have to proceed *via* attack of the carboxylic acid onto a secondary rather than a primary alkyl bromide, a procedure adapted from Baker's synthesis of substituted glycolides.[4] Esterification of 3-hydroxypropionic acid with 2-bromopropionylbromide yielded 3-((2-bromopropanoyl)oxy)propanoic acid and the purified product was subjected to intramolecular cyclization in dilute acetone solution with excess sodium bicarbonate. Using this approach, formation of the α,β-unsaturated system was effectively suppressed and a mixture of two structurally similar compounds was obtained (Scheme A2.2)The two compounds could be separated by column chromatography and recrystallization. The ^{1}H NMR signals of the individual compounds were in good agreement with cyclic structures (monomeric or oligomeric) of the parent hydroxyacid. However, the 3-hydroxypropionic

acid precursor used in this synthetic route became unavailable, forcing us to re-strategize once again.

Scheme A2.2. Ring-closing to the ester via intramolecular attack of a carboxylic acid onto a secondary bromide.

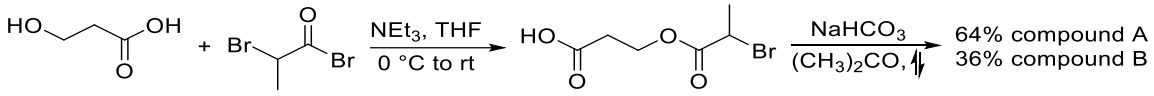

Oxidative lactonization of the diol precursor 3-hydroxypropyl 2-hydroxypropanoate using a ruthenium catalyst[5] or the (2,2,6,6-tetramethylpiperidin-1-yl)oxyl (TEMPO)-based Stahl aerobic oxidation[6] system was unsuccessful, the former yielding no reaction under the published conditions and the latter producing a complex mixture of products. In another approach we attempted Baeyer-Villiger oxidation of the β-ketoester 3-methyldihydro-*2H*-pyran-2,4(*3H*)-dione to DXD but this led exclusively to epoxidation of the enol form of the β-ketoester (Scheme A2.3).

Scheme A2.3. Attempted oxidative lactonization of a linear diol (a) and Baeyer-Villiger oxidation of a 6-membered β-ketoester (b)

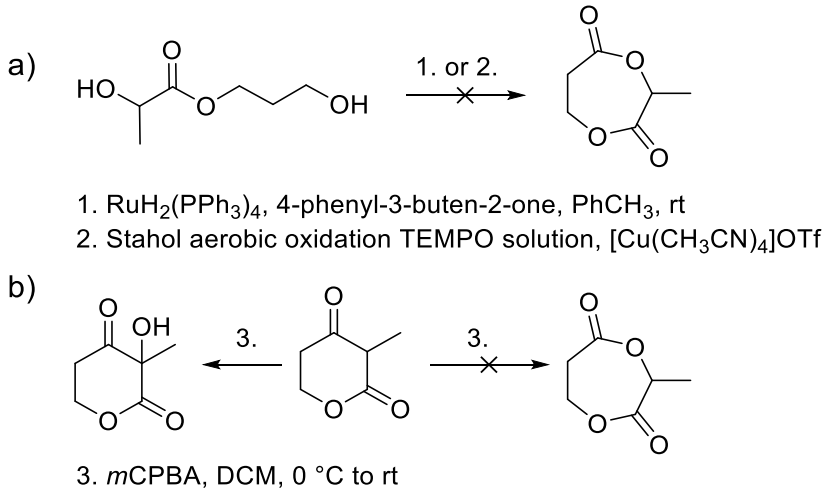

Upon receiving a donation of ethyl 3-hydroxypropionate we proposed another synthetic pathway to DXD using protected lactic and 3-hydroxypropionic acid starting materials. Starting with (−)-methyl L-lactate we first transformed the secondary hydroxyl group to a benzyl ether. The methyl ester was then saponified to yield, upon acidification, the free acid. Coupling of the benzyl-protected lactic acid with ethyl 3-hydroxypropionate was successful with dicyclohexylcarbodiimide (DCC) or 1-ethyl-3-(3-dimethylaminopropyl)carbodiimide (EDC) hydrochloride in the presence of catalytic dimethylaminopyridine (DMAP). Coupling with EDC hydrochloride was preferential as it afforded clean material upon work up and did not necessitate further purification by distillation or chromatography. The benzyl ether was hydrogenated with palladium on carbon (Pd/C) at room temperature under a hydrogen atmosphere to afford the alcohol.

Scheme A2.4. Synthesis of linear precursor to DXD from methyl L-lactate and ethyl 3-hydroxypropionate

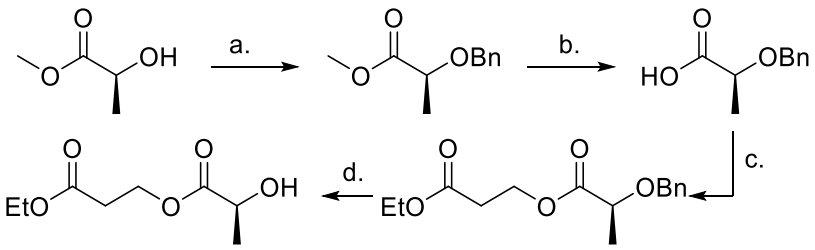

a. 1) NaH, THF, 0 °C; 2) BnBr, 0 °C to rt. b. 1) KOH, 9/1 MeOH/H_2O, rt; 2) HCl. c. Ethyl 3-hydroxypropionate, EDC, DMAP, DCM. d. Pd/C, H_2, EtOH/AcOH (3/2 v/v), rt.

We then probed the acid-catalyzed intramolecular cyclization of the secondary alcohol onto the ethyl ester in dilute methylene chloride (DCM) solution in the presence of activated 5 Ångstrom molecular sieves (5 Å MS) to drive the reaction by sequestration of ethanol. No reaction was observed under these conditions at room temperature or under reflux. Probing the cyclization in dilute toluene solution at 120 °C and removing the

toluene/ethanol azeotrope while trapping ethanol with 5 Å MS in a Dean-Stark trap was also unsuccessful. The hydroxyester proved to be quite robust and did not display appreciable degradation under these conditions. We thus concluded that the ethyl ester required activation to facilitate nucleophilic attack of the secondary alcohol onto the carbonyl.

There are a number of excellent reports on activation of hydroxyacids toward intramolecular attack by secondary alcohols.[78910] Inspired by this literature we attempted saponification of the hydroxyester to the hydroxyacetate but were not able to find conditions under which the ethyl ester was saponified selectively. Preliminary studies suggest that the ethyl ester may be transesterified to the benzyl ester, which could then be selectively cleaved *via* catalytic hydrogenolysis to afford the hydroxyacid. When following reaction of the hydroxyester with benzyl alcohol and *p*-toluenesulfonic acid in toluene at 120 °C by gas chromatography-mass spectrometry (GC-MS) we indeed observed enrichment in benzyl ester over time.

Our preliminary data suggests that DXD is accessed most efficiently from ring-closing of 3-((2-bromopropanoyl)oxy)propanoic acid. However, further characterization data will be needed to definitively establish the identity of the two major products obtained in this route. Alternatively, cyclization of a secondary alcohol onto an activated carboxylic acid may present a viable route to this monomer.

A3. Experimental Procedures and Characterization Data

Materials and Analysis.

α-Bromopropionyl bromide, 3-bromopropionyl chloride, sodium bicarbonate, (−)-methyl L-lactate, 1,3-propanediol, Amberlyst® 15 hydrogen form,

dihydrotetrakis(triphenylphosphine)ruthenium(II), 4-phenyl-3-buten-2-one, Stahl aerobic oxidation TEMPO solution, tetrakisacetonitrile copper(I) triflate, sodium hydride, 10% palladium on activated carbon, 1-ethyl-3-(3-dimethylaminopropyl)carbodiimide, dimethylaminopyridine, *para*-toluenesulfonic acid, and benzyl alcohol were obtained from Sigma Aldrich and used as received. Molecular sieves were received from Sigma Aldrich and activated under high vacuum (100 mTorr) at 200 °C for 2-3 days. A 4L bottle of aqueous 3-hydroxypropionic acid (20 %w/v) was donated by Cargill and 20 g of ethyl-3-hydroxypropionate were donated by Karp. Racemic lactic acid was obtained from J. T. Baker Chemical Co. and triethylamine was purchased from Macron Chemicals. Benzyl bromide was obtained from Alfa Aesar. When indicated as dry, solvents were either obtained from a JC Meyer solvent drying system or were distilled prior to use according to standard purification methods.[11] ^{1}H and ^{13}C NMR spectra were obtained on one of the following instruments: Varian 300 MHz, Varian 500 MHz, and a 400 or 500 MHz Bruker Avance III HD. Gas chromatography-mass spectrometry (GC-MS) was carried out on an Agilent 6890 GC and Agilent 5973 MS system. The GC-MS column used was a HP-5ms with dimensions 30m x 0.25mm. The standard method for all runs, unless otherwise indicated, consisted of holding the sample at 50 °C for 1.5 min, then ramping to 250 °C at a ramp rate of 20 °C min^{-1}, and holding it at 250 °C for 3.5 min.

Experimental Procedures.

Methyl (*R*)-2-(benzyloxy)propanoate and (*R*)-2-(benzyloxy)propanoic acid were synthesized according to previously published procedures.[12,13]

Scheme A3.1. Synthesis of 2-((3-bromopropanoyl)oxy)propanoic acid

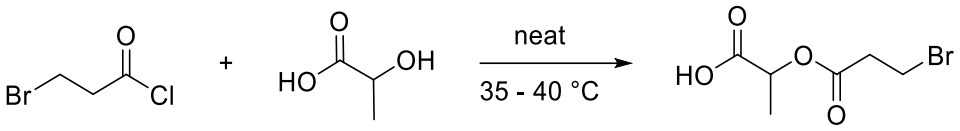

A 25 mL flame-dried two-neck round-bottom flask was charged with 2.2 mL 3-bromopropionyl bromide (22 mmol, ρ = 1.2 g/mL, 1 eq.) and 2.0 mL lactic acid (22 mmol, ρ = 1.7 g/mL, 1 eq.). The mixture was heated to 40 °C upon which vigorous bubbling was observed. Once bubbling ceased (ca. 30 min on this scale), the reaction mixture was cooled to room temperature, diluted with diethyl ether (Et_2O) and filtered through a plug of silica to afford a yellow oil after removal of solvent under high vacuum. The crude material was purified twice by Kugelrohr distillation (35-50 mTorr, 70-90 °C pot temperature) to afford clean 2-((3-bromopropanoyl)oxy)propanoic acid (1.9 g, 42% yield).

Scheme A3.2 Synthesis of 3-((2-bromopropanoyl)oxy)propanoic acid

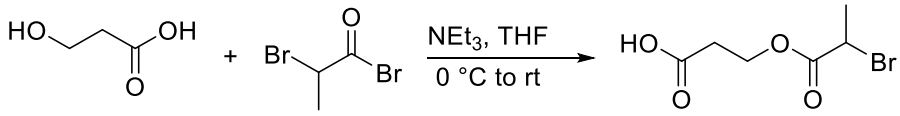

3-Hydroxypropionic acid was extracted with ethyl acetate from a 20 wt% aqueous solution and the yellow oil obtained further purified by Kugelrohr distillation (100 mTorr, 120 °C). A flame-dried, 2-neck flask was charged with 400 mg of 3-hydroxypropionic acid (4.4 mmol, 1 eq.) and 11 mL tetrahydrofuran (THF). Then 0.56 mL of 2-bromopropionyl bromide (5.3 mmol, 1.2 eq.) were added *via* syringe and the solution cooled in a salt-ice bath. Once cooled, a solution of triethylamine (0.8 mL, 5.8 mmol, 1.3 eq.) in 2.9 mL THF was added. The reaction was allowed to come to room temperature and stirred for a total of 12 hours. The white precipitate that had formed during this time was filtered off and the filtrate concentrated *in vacuo*, yielding a clear yellow oil. The oil was re-suspended in ethyl

acetate and washed with 2M hydrochloric acid (3 x) and brine, and the organic fraction dried over magnesium sulfate, filtered, and concentrated to yield a clear yellow oil (1g crude yield). The crude was purified by flash column chromatography (50/1 mass of silica/sample, 6/4 hexanes/ethyl acetate with 1% acetic acid to suppress streaking on the column, column height = 6"), affording 200 mg of pure 3-((2-bromopropanoyl)oxy)propanoic acid (20% yield).

Scheme A3.3. Cyclization of 3-((2-bromopropanoyl)oxy)propanoic acid

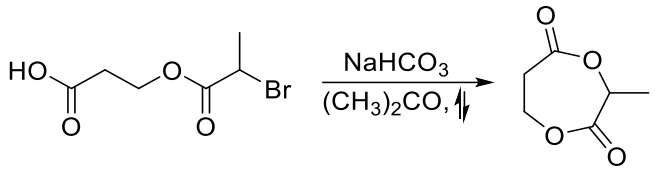

A 25 mL 2-neck flask was charged with sodium bicarbonate (300 mg, 3.56 mmol, 4 eq.) and the flask was flame-dried and backfilled with argon. A solution of 3-((2-bromopropanoyl)oxy)propanoic acid (200 mg, 0.9 mmol, 1 eq.) in dry acetone (17.8 mL) was added to the sodium bicarbonate. The mixture was refluxed for 2 days and then brought to room temperature, filtered through a pad of celite and acetone removed *in vacuo* to afford an off-white solid. ^{1}H NMR spectrometry showed a mixture of two structurally similar compounds in a 64/36 ratio. Recrystallization of the off-white solid in hexanes yielded transparent, colorless, rectangular crystals and analysis by ^{1}H NMR spectrometry identified the crystals as the minor compound present in the mixture with ca. 10% contamination by the major compound. The motherliquor was concentrated to yield 150 mg of a red/brown heterogeneous mixture, which was purified by column chromatography (50/1 mass of silica/sample, 6/4 hexanes/ethyl acetate, column height = 6"), yielding some separation of the two observed compounds.

Scheme A3.4. Coupling of ethyl 3-hydroxypropionate with benzyl ether-protected (−)-lactic acid

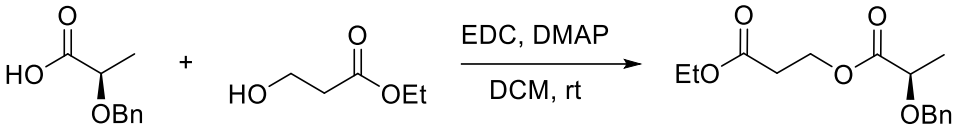

An oven-dried 500 mL 2-neck round bottom flask and condenser were assembled under a stream of argon. (*R*)-2-(benzyloxy)propanoic acid (5g, 27.8 mmol, 1.1 eq.) and ethyl 3-hydroxypropionate (3 g, 25.3 mmol, 1 eq.) were quantitatively transferred to the flask using anhydrous methylene chloride (211 mL). 1-ethyl-3-(3-dimethylaminopropyl)carbodiimide (8.73 g, 45.5 mmol, 1.8 eq.) and dimethylaminopyridine (3.7 g, 30.4 mmol, 1.2 eq.) were weighed out and added to the flask. Reaction progress was monitored by thin-layer chromatography (TLC) and full conversion of starting material was achieved after 35 min. The solution was transferred to a separatory funnel, washed with 220 mL of 1M hydrochloric acid, and brine. The organic layer was dried over magnesium sulfate, filtered, and solvent removed *in vacuo* to afford 6.54 g of clean 3-ethoxy-3-oxopropyl (*R*)-2-(benzyloxy)propanoate, which did not require further purification (92% yield).

Scheme A3.5. Hydrogenolysis of benzyl ether to afford secondary alcohol

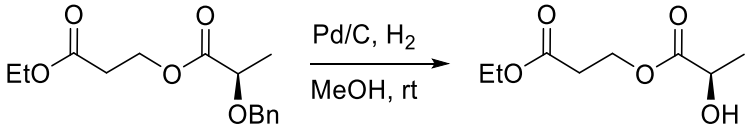

A dry 2L 3-neck round bottom flask was assembled with septa under a stream of nitrogen. The flask was charged with 10% palladium on carbon (1.7 g, 25 mass% of benzyl ether) and 790 mL methanol (0.03M). The benzyl ether (6.65 g, 23.8 mmol) was quantitatively transferred to the flask using 2 mL of methanol and a balloon filled with hydrogen gas was attached to the flask. The reaction mixture was sparged with hydrogen and left to react

under an atmosphere of hydrogen until TLC indicated full conversion of starting material (ca. 3.75 h on this scale). The reaction mixture was filtered through a pad of celite and the solvent evaporated from the filtrate *in vacuo* to afford 3.77 g of clean material, which could be carried forward without further purification (84% yield).

Characterization Data.

Characterization data is displayed for compounds that have not been previously reported in the literature.

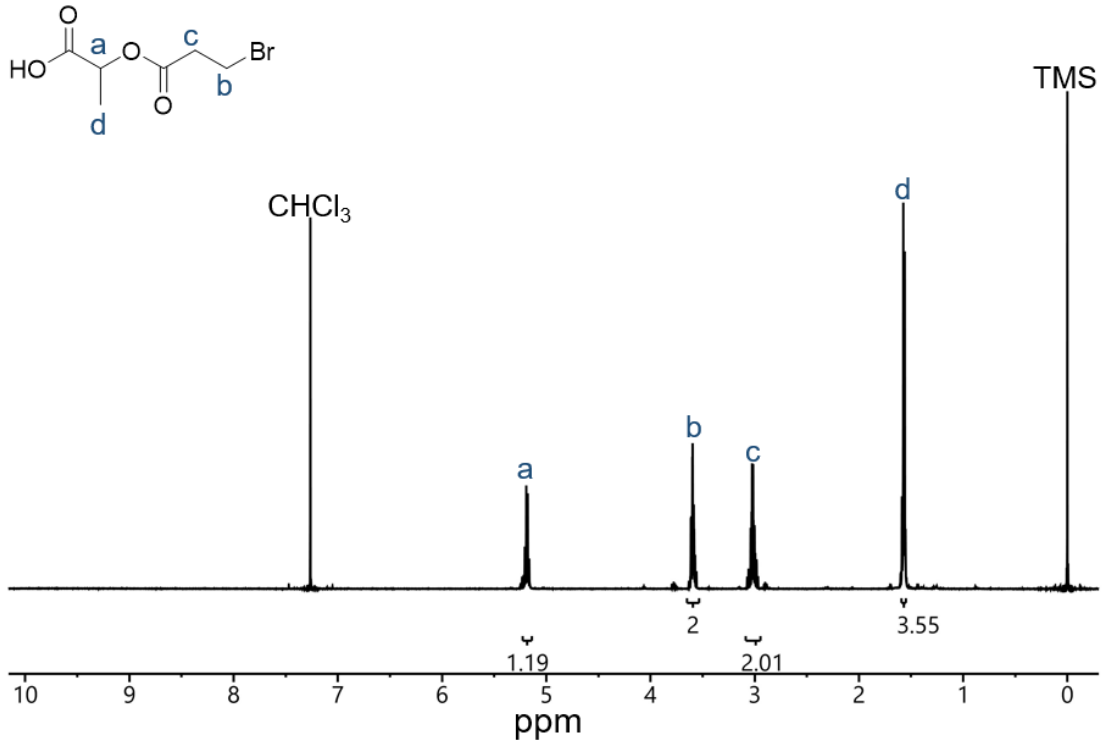

Figure A.1. ^{1}H NMR spectrum of 2-((3-bromopropanoyl)oxy)propanoic acid.

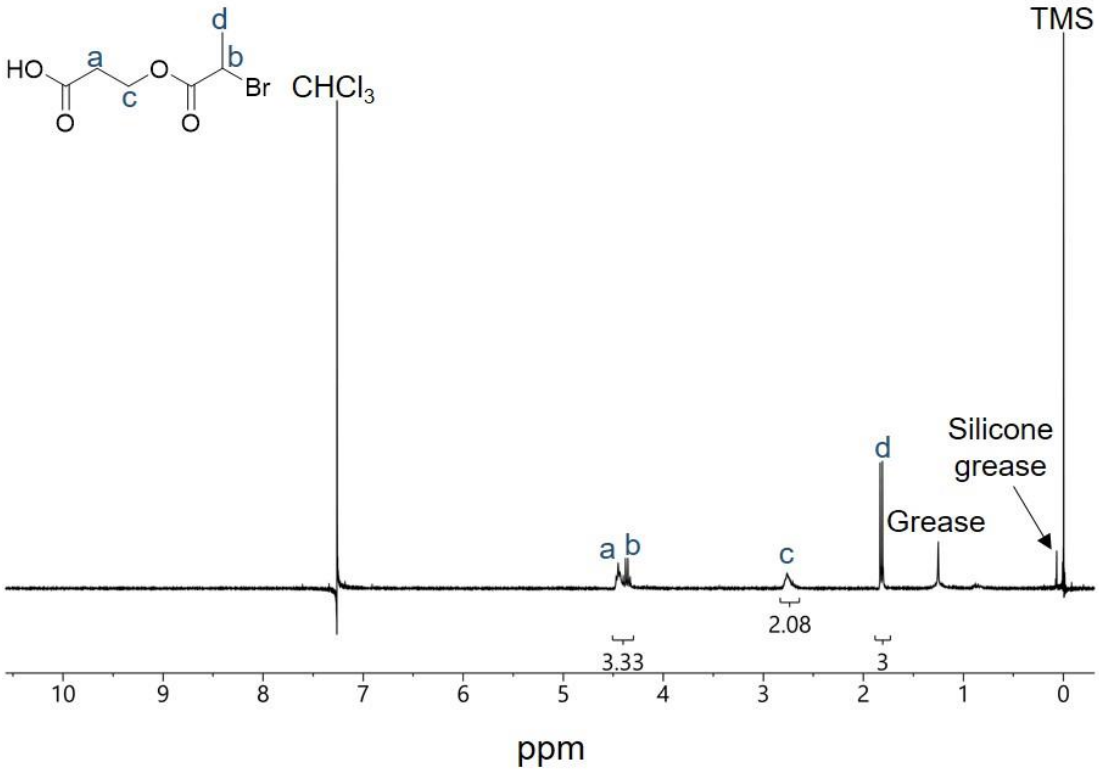

Figure A.2. ^{1}H NMR spectrum of 3-((2-bromopropanoyl)oxy)propanoic acid.

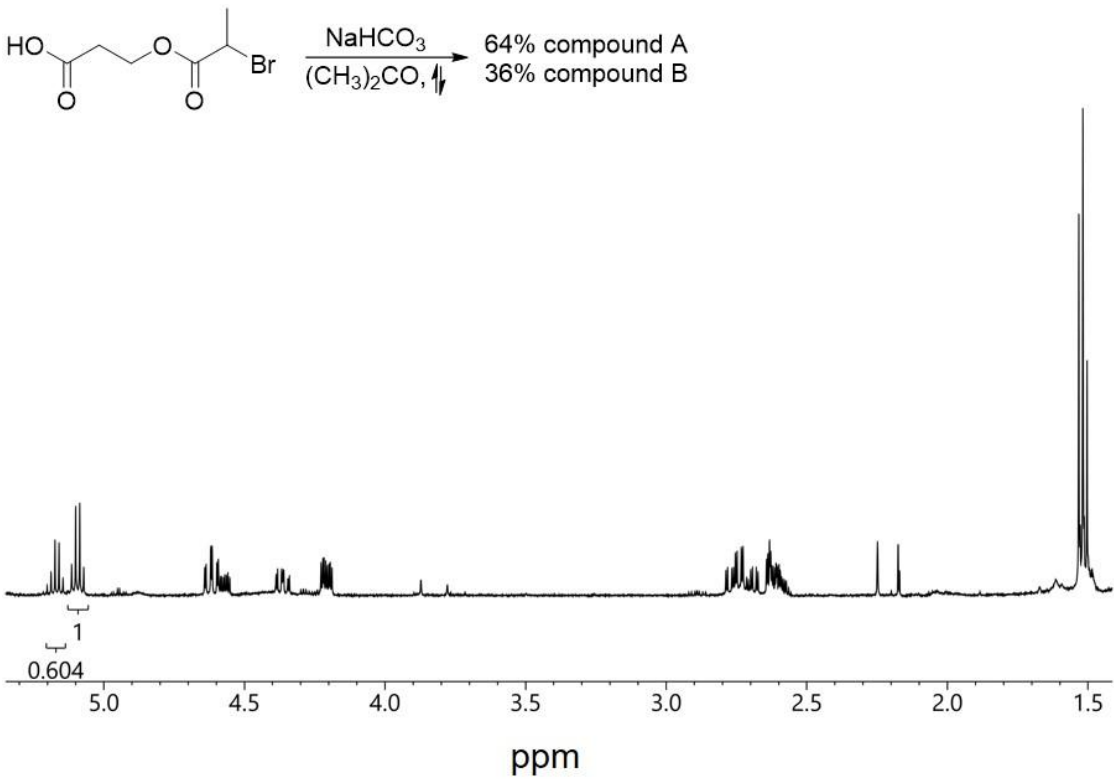

Figure A.3. ^{1}H NMR spectrum of the mixture obtained after refluxing 3-((2-bromopropanoyl)oxy)propanoic acid for 2 days in acetone in the presence of $NaHCO_3$.

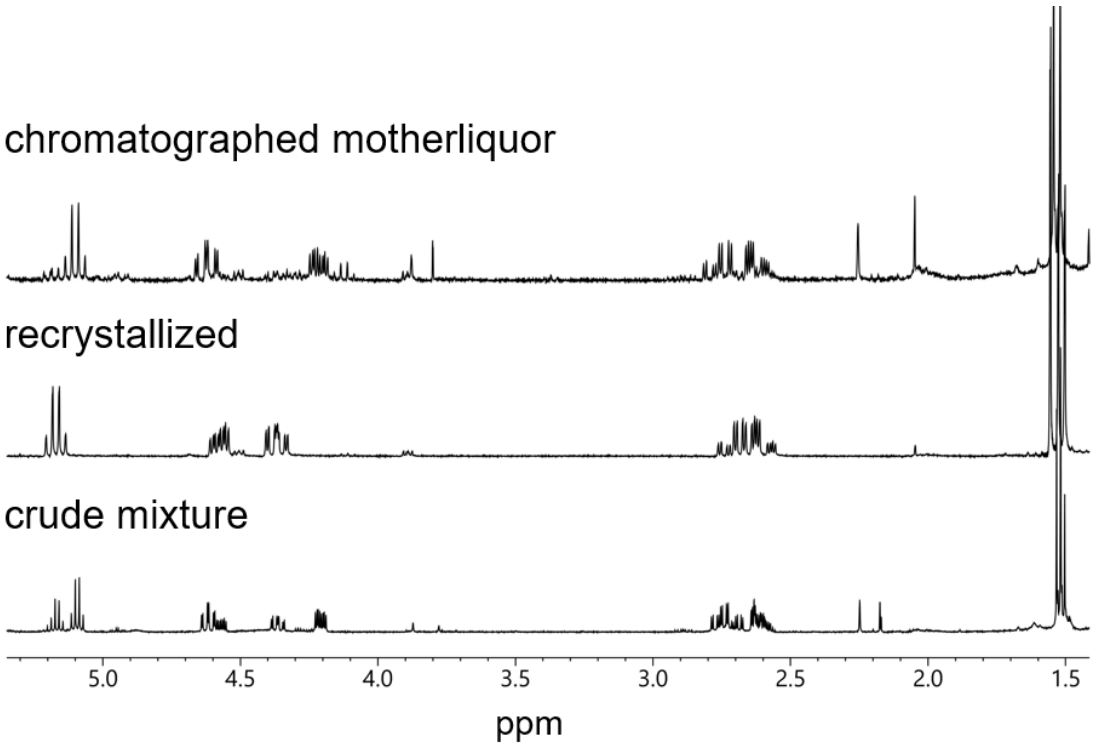

Figure A.4. ^{1}H NMR spectrum of the compounds separated *via* recrystallization and column chromatography of the motherliquor.

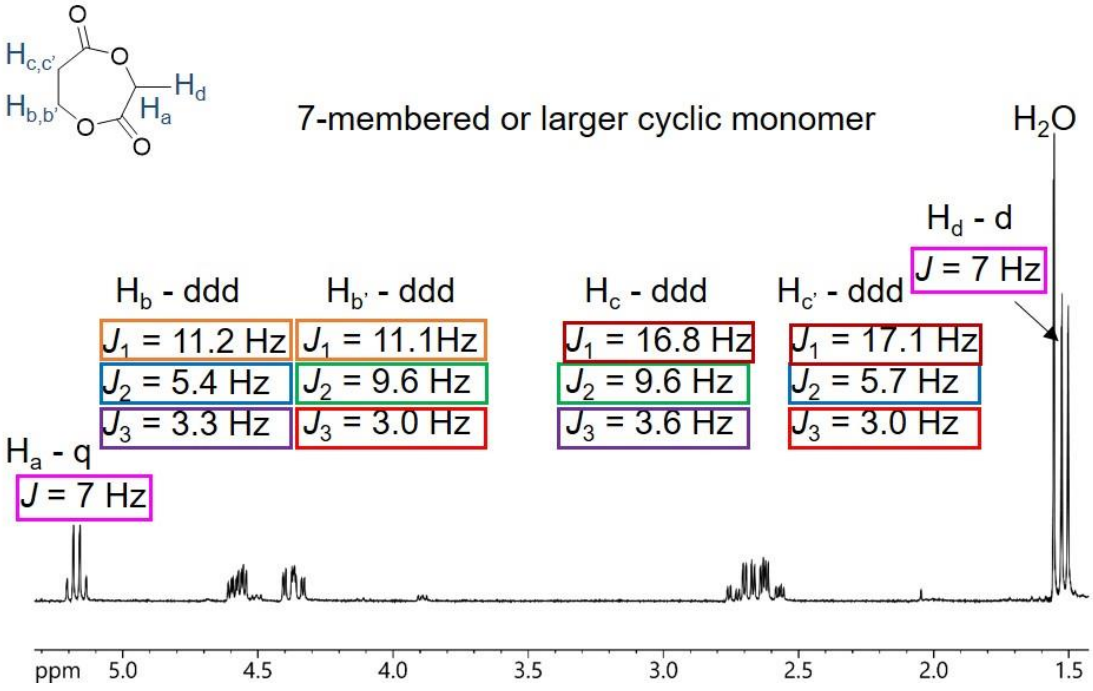

Figure A.5. ^{1}H NMR spectrum of the compound obtained from recrystallization of the crude mixture and assignment of coupling constants.

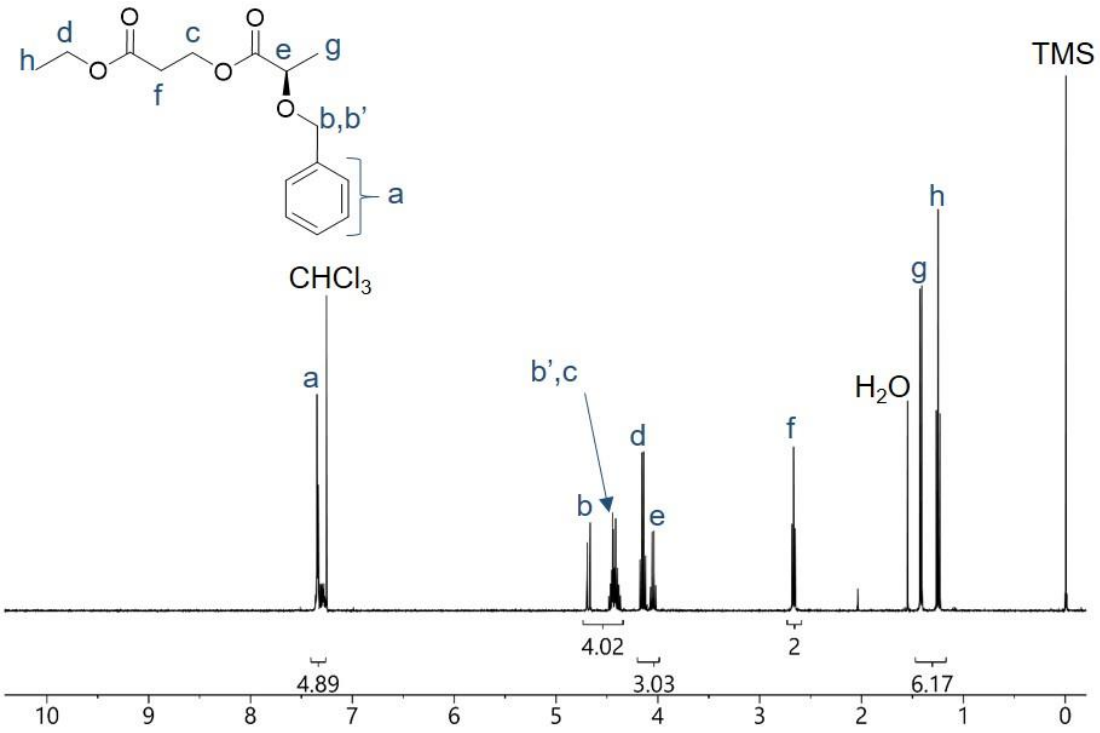

Figure A.6. ^{1}H NMR spectrum of 3-ethoxy-3-oxopropyl (*R*)-2-(benzyloxy)propanoate.

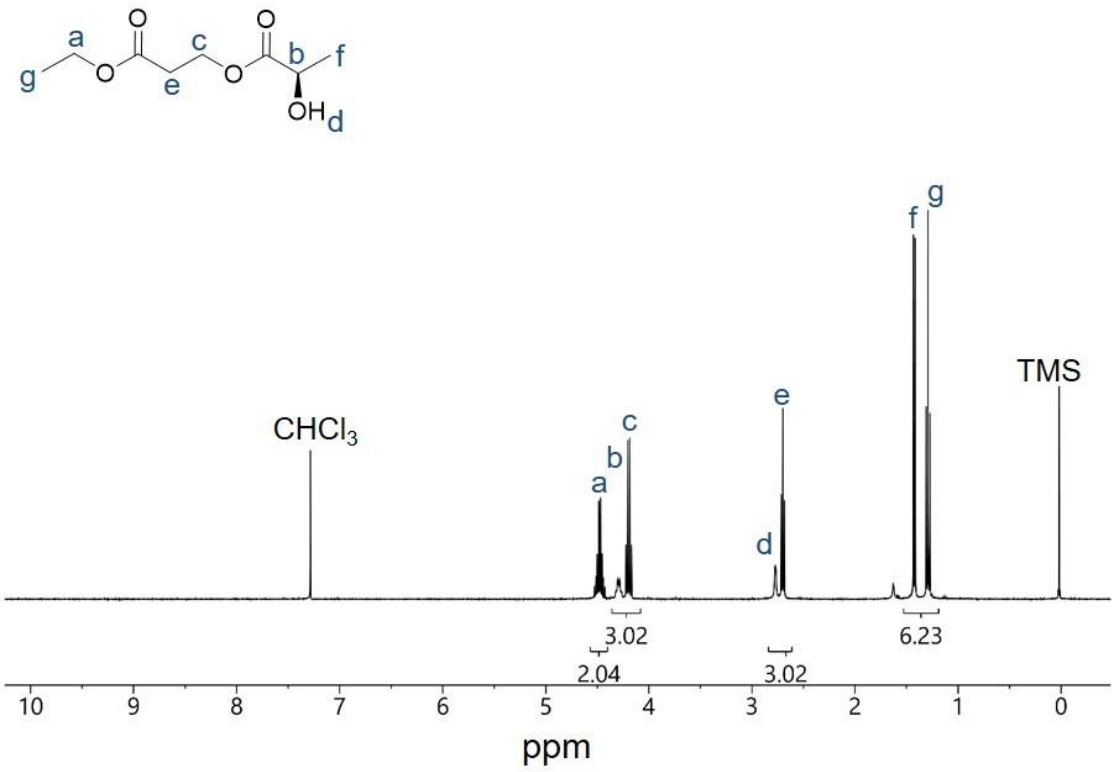

Figure A.7. ^{1}H NMR spectrum of 3-ethoxy-3-oxopropyl (R)-2-hydroxypropanoate.

References

1) Zhang, Z.; Ortiz, O.; Goyal, R.; Kohn, J. In *Principles of Tissue Engineering*; Academic Press: Boston, MA, 2014; pp 441–473.

2) Li, J.; Rothstein, S. N.; Little, S. R.; Edenborn, H. M.; Meyer, T. Y. *J. Am. Chem. Soc.*, **2012**, *134*, 16352−16359.

3) Hiki, S.; Taniguchi, I.; Miyamoto, M.; Kimura, Y. *Macromolecules* **2002**, *35*, 2423-2425.

4) Baker, G. L. Cyclic alkyl substituted glycolides and polylactides therefrom. US Patent, 20070142461 A1, Jun 21, 2007.

5) Ishii, Y.; Osakada, K.; Ikariya, T.; Saburi, M.; Yoshikawa, S. *J. Org. Chem.*, **1986**, *51*, 2034–2039.

6) Xie, X.; Stahl, S. S. *J. Am. Chem. Soc.*, **2015**, *137*, 3767−3770.

7) Corey, E. J.; Ulrich, P.; Fitzpatrick, J. M. *J. Am. Chem. Soc.*, **1976**, *98*, 222−224.

8) Bartlett, P. A.; Green, F. R. III, *J. Am. Chem. Soc.*, **1978**, *100*, 4858−4865.

9) Tsutsui, H.; Mitsunobu, O. *Tet. Lett.*, **1984**, *17*, 2455−2166.

10) Neises, B.; Steglich, W. *Angew. Chem. Int. Ed. Engl.;* **1978**, *17*, 522−524.

11) Armarego, W. L. F.; Chai, L. L. *Purification of Laboratory Chemicals*, 6th ed.; Elsevier, 2009.

12) Fernandes, R. A.; Chavan, V. P. *Eur. J. Org. Chem.*, **2010**, 4306-4311.

13) Bastos, C. M.; Munoz, B.; Tait, B. Compounds, compositions, and methods for increasing CFTR activity. WO 2015/138934 A1, Sep 17, 2015.

Appendix B.

Preliminary Results on Synthesis and Polymerization of Unprecedented 7-Membered Cyclic Hemiacetal Esters

The work in this chapter was carried out in part in collaboration with Thomas Haversang.

B1. Syntheses of 1,3-Dioxepan-4-one and 2-Methyl 1,3-dioxepan-4-one

In Chapter 4 we discuss the synthesis and polymerization of the 7-membered cyclic hemiacetal ester 7-methoxyoxepan-4-one (MOPO). MOPO is an example of a cyclic hemiacetal ester where the acetal group is exocyclic, rather than endocyclic as in 2-methyl-1,3-dioxan-4-one (MDO). In a first attempt to produce more strained cyclic hemiacetal esters we investigated the synthesis and polymerization of the endocyclic hemiacetal esters 1,3-dioxepan-4-one (DPO) and 2-methyl 1,3-dioxepan-4-one (MDPO), the latter being the 7-membered analogue of MDO. We reasoned that, much like MDO, these molecules could be obtained from the Baeyer-Villiger oxidation of their corresponding pyranone precursors **IV** (Scheme B1.1). The pyranones are obtained by oxidation of the pyranols **III**, which in turn are derived from 3,4-dihydro-2H-pyran **I** by hydroboration. The vinyl ether **I** can be alkylated prior to hydroboration, yielding alkyl-substituted cyclic hemiacetal esters, where the choice of R-group depends on the availability and reactivity of the corresponding alkyl halide.

Scheme B1.1. Retrosynthetic disassembly of dioxepan-4-one frameworks

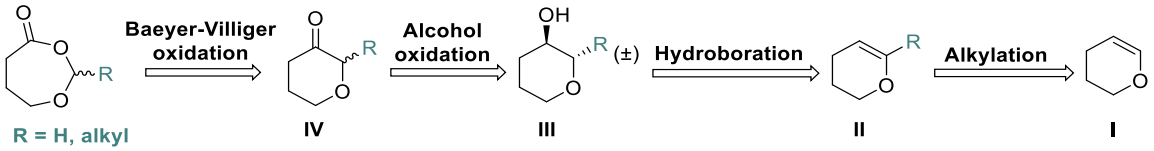

As previously reported, 3,4-dihydro-2H-pyran **1a** could be oxidized to tetrahydro-2H-pyran-3-ol (**2a**) *via* hydroboration. We found it necessary to employ a hindered alkyl borane, such as 9-borabicyclo[3.3.1]nonane (9-BBN), to reduce competitive Lewis acid-catalyzed ring-opening of the vinyl ether *via* coordination of borane to the ether oxygen as reported by Brown.[1] Hydroboration of **1a** with borane tetrahydrofuran complex

(BH_3•THF) produced primarily butanol under conditions reported elsewhere.[2] Use of 9-BBN and purification of the crude product mixture by flash column chromatography afforded tetrahydro-2H-pyran-3-ol (**2a**) in up to 68% yield. We were not able to entirely suppress ring-opening of the starting material to afford 4-penten-1-ol as the most prominent side product of this reaction. Oxidation of tetrahydro-2H-pyran-3-ol with pyridinium chlorochromate (PCC) generated the ketone **3a** in fair yields (≤ 50% purified yield). More environmentally friendly reagents, such as oxone/2-iodobenzenesulfonic acid (IBS)[3] or the reagents employed in Swern oxidations, gave poor yields of ketone **3a**.

Scheme B1.2. DPO and MDPO synthesis

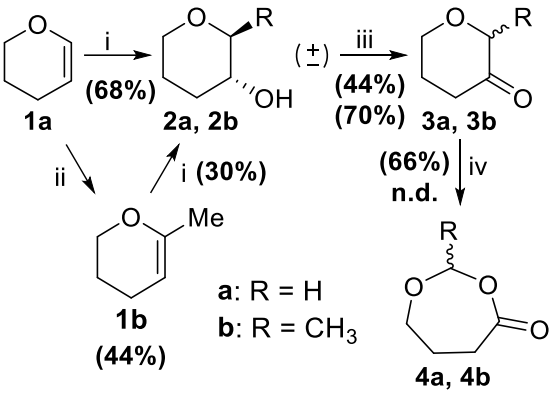

i. 1) 9-BBN, THF, rt, 2) NaOH, H_2O_2
ii. 1) *t*-BuLi, THF, 2) MeI; iii. PCC, 3 Å MS, DCM, rt; iv. *m*CPBA, DCM, 0 °C-10 °C.

Baeyer-Villiger oxidation of pure **3a** following our procedure for synthesis of MDO delivered DPO (**4a**) with quantitative conversion by ^{1}H NMR spectroscopy of the crude reaction mixture. However, purification of DPO proved difficult due to its high reactivity. DPO could be obtained in good crude yields upon aqueous work-up (77%) but we also observed trace amounts (~1%) of signals attributable to *meta*-chlorobenzoic acid (*m*CBA) generated from reduction of *meta*-chloroperbenzoic acid (*m*CPBA) after basic work-up. Comparison of crude DPO to commercial *meta*-chlorobenzoic acid (*m*CBA) by GC-MS

indicated that the impurity observed was not free *m*CBA but rather a product of reaction between DPO and *m*CBA. When trying to remove the impurity by column chromatography on alumina or base-treated silica, cold-recrystallization, distillation or sublimation, DPO frequently decomposed or auto-polymerized. Stabilization of DPO by the radical inhibitor butylated hydroxytoluene (BHT) proved non-reproducible as even stabilized DPO would exhibit degradation in some cases.

The methyl-substituted DPO monomer (**4b**) could be obtained in a similar manner by first alkylating the vinylic position alpha to the ether oxygen of 3,4-dihydro-2H-pyran (**1a**) in the presence of *tert*-butyllithium, and methyl iodide. Alkylation with the milder *n*-butyllithium in the presence of tetramethylethylenediamine (TMEDA), proceeded to comparatively much lower conversions. Purification by fractional distillation afforded **1b** in up to 44% yield. Following the sequence of steps outlined for the synthesis of DPO we were able to oxidize and ring-expand in three steps to MDPO. However, purification of this molecule was extremely challenging and crude material stored at – 10 °C auto-polymerized over a period of 3 weeks. When attempting purification by chromatography the molecule decomposed to the thermodynamically favored γ-butyrolactone with concurrent expulsion of acetaldehyde.

B2. Ring-Opening Polymerization of Dioxepan-4-one

With DPO containing less than 0.5% *m*CBA-derived impurity in hand, we probed its ROP to poly(DPO) using diphenylphosphoric acid (DPP) as the organocatalyst and benzyl alcohol as the initiator. DPO is an off-white solid and was therefore polymerized in a methylene chloride solution ($[DPO]_0$ = 0.9 M) at room temperature. Employing $[DPO]_0/[DPP]_0$ ~ 250 and $[DPO]_0/[BnOH]_0$ = 130 we observed 91% conversion to

poly(DPO) by ^{1}H NMR spectroscopy. Precipitation into 9/1 hexanes/tetrahydrofuran, followed by drying of the precipitate under high vacuum afforded semicrystalline polymer in 60% yield. Interestingly, treatment of DPO with diethylzinc and benzyl alcohol, did not result in the formation of poly(γ-hydroxybutyric acid) *via* extrusion of formaldehyde but instead generated γ-butyrolactone and formaldehyde. This is in good agreement with established thermodynamics of γ-butyrolactone ring-opening polymerization, which drive the cyclization to the lactone over formation of the aliphatic polyester.

Characterization of the precipitated polymer by ^{1}H and ^{13}C NMR spectroscopy suggested the presence of both benzyl acetal and hemiacetal *meta*-chlorobenzylester end groups, the latter most likely derived from reaction of the impurity with DPO. Poly(DPO) of M_n ~ 6 kg/mol and $Đ$ = 1.3 by SEC analysis (referenced to polystyrene standards) exhibited a low glass transition temperature (T_g) of – 67 °C and a melting endotherm (T_m) of 46 °C.

Scheme B2.1. Divergent ring-opening of DPO with diethylzinc or diphenylphosphoric acid catalysts

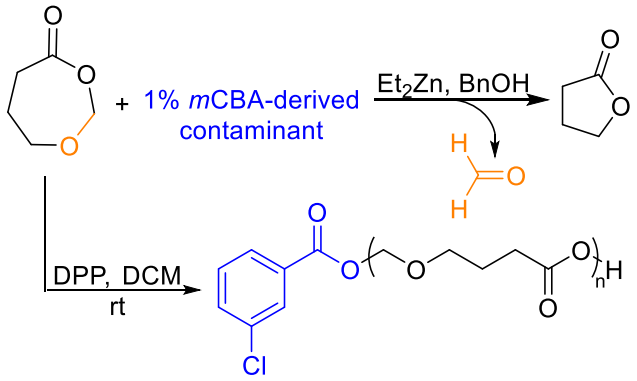

B3. Experimental Procedures and Characterization Data

Materials and Analysis.

All chemicals were obtained from Sigma-Aldrich and used as received unless otherwise indicated. Benzyl alcohol was distilled under vacuum and stored over activated 3 Ångstrom molecular sieves in the glovebox. Diphenylphosphoric acid was ground into a fine powder and dried under high vacuum. When indicated as dry, solvents were either obtained from a JC Meyer solvent drying system or were distilled prior to use according to standard purification methods.[4] ^{1}H and ^{13}C NMR spectra were obtained on a 400 or 500 MHz Bruker Avance III HD. Chemical shifts were referenced to tetramethylsilane (TMS) at 0.00 ppm for ^{1}H and ^{13}C NMR spectra taken in $CDCl_3$ containing 10 % w/v TMS. Thermal gravimetric analysis was performed on a TA Instruments Q500 TGA under the conditions specified. Differential scanning calorimetry (DSC) was carried out using a TA Instruments Q2000 at a scanning rate of 5 °C/min. DSC data analysis was performed using TA Instruments TRIOS software using the second heating curve. Polymer samples were injected into an Agilent 1260 S3 series chromatograph (THF, 25 °C, 1 mL/min) with three Styragel columns. . Molar mass analysis was carried out using size exclusion chromatography with multi-angle laser light-scattering (SEC-MALLS) to determine absolute weight average molar mass (M_w) with a dn/dc = 0.0578 mL/g and conventional calibration analysis relative to polystyrene standards using THF SEC equipped with an Optilab T-rEX RI detector.

Scheme B3.1. Alkylation of 3,4-dihydro-2H-pyran

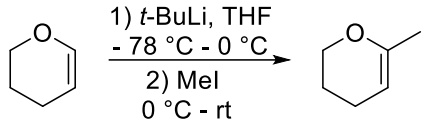

6-Methyl-3,4-dihydro-2H-pyran. A 3-neck 500 mL round bottom flask equipped with a stir bar was flame-dried and back-filled with argon. 3,4-dihydro-2H-pyran (28.2 g, 335 mmol, 1.0 eq.) was weighed into a flame-dried round bottom flask, dissolved in 70 mL THF ([3,4-dihydro-2H-pyran] = 4.8 M in THF), and added to the flask *via* cannula. The clear, colorless solution was cooled to −78 °C in a dry ice/isopropanol bath. Two freshly obtained bottles of *tert*-butyllithium in pentane ([*t*-BuLi] = 1.7 M, 2 x 100 mL bottles, 340 mmol, 1.01 eq.) were transferred to the cold solution *via* cannula. The solution turned yellow and a yellow precipitate formed. The reaction mixture was warmed and stirred at 0 °C for 30 min. During this time the precipitate disappeared and the solution became lighter in color. Methyl iodide was passed through a pipette packed with activated basic alumina and 25.4 mL (408 mmol, 1.2 eq.) added to the solution at 0 °C *via* syringe pump. Upon complete addition the mixture was stirred for an additional 30 min at 0 °C, then warmed to rt. Saturated ammonium chloride solution was then added (50 mL), leading to precipitation of white salts, followed by addition of water (160 mL), which re-dissolved the salts. The solution was transferred to a separatory funnel and the organic layer was separated. The aqueous phase was extracted with 1/1 diethyl ether/pentane (3x 300 mL). The combined organic extracts were dried over magnesium sulfate, the mixture filtered, and solvent volume reduced *in vacuo* to 300 mL of a yellow solution. ^{1}H NMR spectral analysis of the crude product indicated 80% conversion of the starting material to 6-methyl-3,4-dihydro-2H-pyran. The yellow solution was stirred over neutral alumina to remove residual iodine,

filtered, and further purified by fractional distillation at ambient pressure. The desired compound collected in the 3rd fraction, distilling over at 75 °C as a clear, colorless oil (14.6 g. 44% yield). ^{1}H NMR ($CDCl_3$): δ 4.46 (m, 1 H, -O-C(CH_3)-C*H*-CH_2), 3.99 (m, 2 H, -O-C*H*$_2$-CH_2-), 1.98 (m, 2 H, -O-CH_2-C*H*$_2$-CH_2), 1.78 (m, 2 H, -CH_2-C*H*$_2$-CH-C(CH_3)-O-), 1.71 (m, 3 H, -CH_2-CH_2-CH-C(C*H*$_3$)-O-). The ^{1}H NMR data matches that of a previous report.[5]

Scheme B3.2. Hydroboration of vinyl ethers

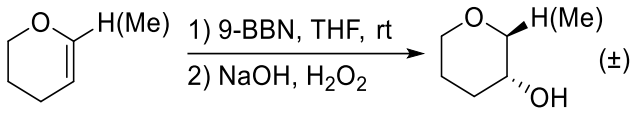

Tetrahydro-2H-pyran-3-ol. A 2L round bottom flask containing a stir bar was flame-dried and backfilled with argon. 9-BBN in THF (800 mL, 0.5 M, 400 mmol, 1.0 eq.) was transferred to the flask *via* cannula. 3,4-Tetrahydro-2H-pyran was weighed into a flame-dried conical flask (33.6 g, 399 mmol, 1.0 eq.) and then added dropwise to the 9-BBN solution *via* cannula. As emphasized by Brown, it is important that the pyran is added to the hydroborating agent, rather than the other way around. We also found that slower additions correlated with higher yields of pyranol. The clear, colorless solution was stirred for 2h at rt, then it was cooled to 0 °C, the flask fitted with an addition funnel, and 3M NaOH solution was added dropwise (400 mL), followed by hydrogenperoxide solution (170 mL of 30% v/v in H_2O), carefully monitoring the temperature of the solution especially with addition of H_2O_2, which is highly exothermic. The biphasic solution was vigorously stirred at 55 °C in a heating mantle for 1h to ensure the oxidation was complete. Upon cooling back to rt, 600 g of potassium carbonate were added, slowly in the beginning to avoid boiling over of the solution. The mixture was stirred for another 30 minutes, then

it was transferred to a 2L separatory funnel, the organic layer was separated, and dried over magnesium sulfate. The aqueous phase was extracted with diethyl ether (2 x with equal volumes to aqueous layer), the combined organic extracts were dried over $MgSO_4$, the mixture filtered, and solvents removed *in vacuo* to afford a viscous oil. The crude was first purified *via* short path distillation (pot temperature = 120 °C, collecting product at 40 °C/250 mTorr) to separate liquid products from 1,5-cyclooctanediol derived from 9-BBN. The oil was then further purified by flash column chromatography (50/1 mass of silica to mass of sample, typically purifying 16g at a time on 280 g silica, 5/1 Et_2O/pentane, packed to a height of 6', collecting 12 fractions of 125-150 mL each with product eluding typically between fractions 5-10) to afford a clear colorless oil in up to 68% yield.). ^{1}H NMR ($CDCl_3$): δ 3.76 (m, 2 H, -O-C*H*$_2$-CH(OH)), 3.65 (m, 2 H, -O-C*H*$_2$-CH_2-), 3.45 (m, 1 H, -CH_2-C*H*(OH)-CH_2-), 1.91 (m, 2 H, -CH(OH)-C*H*$_2$-CH_2-CH_2-O-), 1.84 (d, *J* = 6.5 Hz, 1 H, -CH_2-CH(O*H*)-CH_2-), 1.59 (m, 2H, -O-CH_2-C*H*$_2$-CH_2-). The ^{1}H NMR data matches that of a previous report.[6]

2-Methyltetrahydro-2H-pyran-3-ol. 6-Methyl-3,4-dihydro-2H-pyran (3g, 30.6 mmol, 1.0 eq.) was added to a flame-dried 300 mL round bottom flask using 2-3 mL of dry THF for quantitative transfer. 9-BBN was added to the flask containing the pyran *via* syringe (61 mL , 0.5 M in THF, 30.6 mmol) and the solution stirred at rt for 3h. The solution was cooled to 0 °C and sodium hydroxide solution (3M, 31 mL) was slowly added *via* addition funnel, followed by H_2O_2 (13 mL, 30% v/v in H_2O). The flask was transferred to an oil bath, equipped with a reflux condenser, and heated under stirring to 55 °C for 2h. The mixture was cooled back to rt and 42.3 g potassium carbonate were added. The mixture was stirred for an additional 15 minutes, then it was transferred to a separatory funnel, the

organic layer separated, and the aqueous fraction extracted with diethyl ether (3 x with equal volumes to aqueous layer). The combined organic layers were dried over $MgSO_4$, the mixture filtered, and solvent removed from the filtrate *in vacuo* to afford a viscous oil. The crude material was stored in the freezer, during which time white crystals formed at the bottom of the flask. The oil was filtered away from the crystals and ^{1}H NMR spectral analysis confirmed reduction of 1,5-cyclooctanediol in the crude. The 3.77 g of crude material were purified by flash column chromatography (170 g silica, 2/1 ethyl acetate/hexanes, 7' column height, collecting 39 fractions of 20 mL each, product eluded between fractions 15-29) to afford 1g of pure product as a yellow oil (30% yield). ^{1}H NMR ($CDCl_3$): δ 3.84 (d, *J* = 12.5 Hz, 1 H, -O-C*H*(CH_3)-CH(OH)-), 3.37-3.31 (m, 3 H, -O-C*H*$_2$-CH_2-CH_2-C*H*(OH)-), 2.76 (br s, 1 H, -CH_2-CH(O*H*)-CH(CH_3)-), 2.09-1.37 (m, 4 H, -CH(OH)-C*H*$_2$-C*H*$_2$-CH_2-O-), 1.28 (d, *J* = 6 Hz, 3 H, -CH_2-CH(OH)-CH(C*H*$_3$)-). ^{13}C NMR ($CDCl_3$): δ 78.51, 72.29, 67.52, 32.80, 25.77, 18.23.

Scheme B3.3. Oxidation of pyranols to pyranones

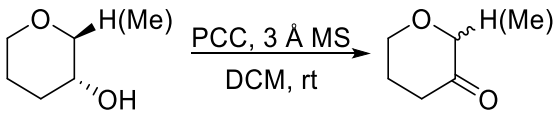

Dihydro-2H-pyran-3(4H)-one. A 2L round bottom flask was charged with 167 g pyridinium chlorochromate (775 mmol, 2.9 eq.), 135 g of activated, ground 3 Å molecular sieves, and 500 mL of methylene chloride ([pyranol] = 0.5 M). Pyranol (27g, 264 mmol, 1.0 eq.) was added dropwise to the mixture *via* addition funnel. The initially bright orange solution turned black with addition of the substrate. The solution was stirred at rt until full conversion of starting material was confirmed by thin layer chromatography (TLC) or ^{1}H NMR spectral analysis. 1 L of diethyl ether was added to the reaction mixture and the

resultant slurry filtered through a pad of silica. The solvent was evaporated from the filtrate yielding a black oil. The crude was purified by flash column chromatography (40/1 mass of silica/mass of sample, 4/1 Et_2O/pentane, packed to 6' column height) to afford a faintly yellow oil (11.53 g, 44% yield). ^{1}H NMR ($CDCl_3$): δ 4.05 (s, 2 H, -O-C*H*$_2$-CO-), 3.86 (t, *J* = 5.5 Hz, 2 H, -O-C*H*$_2$-CH_2-CH_2-), 2.56 (t, *J* = 6.5 Hz, 2 H, -CH_2-CO-C*H*$_2$-CH_2-), 2.12 (dt, *J* = 6.5, 5.5 Hz, 2 H, -CO-C*H*$_2$-C*H*$_2$-CH_2-O-). The ^{1}H NMR data matches that of a previous report.[6]

2-Methyldihydro-2H-pyran-3(4H)-one. Pyridinium chlorochromate (4.6 g, 21.5 mmol, 2.5 eq.) and 4g of ground 3 Å molecular sieves were suspended in 10 mL of methylene chloride in a round bottom flask ([pyranol] = 0.6 M). The pyranol was added dropwise as a solution in methylene chloride (1.0 g, 8.6 mmol, 1.0 eq. of pyranol in 4.3 mL CH_2Cl_2). After 1.25h disappearance of the starting material was observed by thin layer chromatography. Diethyl ether (25 mL) was added and the black, heterogeneous solution filtered through a pad of silica. Solvent was removed *in vacuo* to afford 1.18 g of a crude black oil. The crude was purified by flash column chromatography (35/1 mass of silica/mass of sample, 4/1 hexanes/EtOAc, packed to 6" column height, 10 mL fractions, product eluded between fractions 6-12) to afford 700 mg of a yellow oil (70% yield). ^{1}H NMR ($CDCl_3$): δ 4.06 (m, 1 H, -O-C(H)*H*-CH_2-CH_2-CO-), 3.94 (q, *J* = 7 Hz, 1 H, -O-C*H*(CH_3)-CO-CH_2-), 3.76 (ddd, *J* = 3, 10.5, 12 Hz, 1 H, -O-C(*H*)H-CH_2-CH_2-CO-), 2.62-2.41(m, 2 H, -CO-C*H*$_2$-CH_2-CH_2-O-), 2.21-2.06 (m, 2H, -CO-CH_2-C*H*$_2$-CH_2-O), 1.3 (d, *J* = 6.5 Hz, 3 H, -O-CH(C*H*$_3$)-CO-CH_2-). ^{13}C NMR ($CDCl_3$): δ 208.86, 79.64, 65.90, 37.58, 26.60, 15.20.

Scheme B3.4. Baeyer-Villiger oxidation of pyran-4-ones to DPO and MDPO

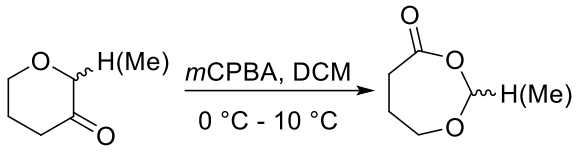

1,3-Dioxepan-4-one. A 500 mL Erlenmeyer flask equipped with a stir bar was charged with 28.5 g *meta*-chloroperbenzoic acid (≤ 77% active oxygen content, 127 mmol, 1.1 eq.), 270 mL methylene chloride, and the solution was dried over copious amounts of $MgSO_4$. The mixture was filtered into a dry round bottom flask and the solution cooled to 0°C. Pyranone (11.6 g, 115 mmol, 1 eq.) was added dropwise to the solution. The ice bath was replaced with a room temperature water bath, and after 10 min formation of thick white precipitate was observed. Full conversion to 1,3-dioxepan-4-one was confirmed by ^{1}H NMR spectral analysis and the reaction mixture filtered through a Büchner funnel to remove the precipitates. The filtrate was cooled to −78 °C to force precipitation of more *meta*-chlorobenzoic acid and the mixture was filtered again. Solvent was reduced *in vacuo* to ¼ of its initial volume and the solution once more cooled to −78 °C, and filtered. The filtrate was transferred to a separatory funnel and washed with saturated $NaHCO_3$. The organic layer was separated and the aqueous layer extracted with DCM (3x). The combined organic fractions were washed with brine, and dried over $MgSO_4$. After filtration, the solution was passed through basic alumina and solvent removed *in vacuo* to afford a yellow oil (8.84 g, 66% yield). By ^{1}H NMR spectral analysis, the product was 99% pure, containing 1% of a *m*CBA-derived impurity. Upon storage of the product over activated 3 Å MS in a glovebox freezer at −20 °C, the compound solidified to yield an off-white solid, which did not liquefy again at rt. ^{1}H NMR ($CDCl_3$): δ 5.25 (s, 2 H, -O-C*H*$_2$-O-CO-), 3.98

(t, *J* = 5 Hz, 2 H, -O-C*H*$_2$-CH$_2$-), 2.83 (m, 2 H, -CO-C*H*$_2$-CH$_2$-), 1.91 (m, 2 H, -CO-CH$_2$-C*H*$_2$-CH$_2$-O). ^{13}C NMR ($CDCl_3$): δ 174.0, 93.25, 73.59, 34.22, 24.77. T_m = 30 °C by DSC.

2-Methyl-1,3-dioxepan-4-one. This monomer was obtained in the manner described above. However, upon removal of solvent the cyclic hemiacetal ester auto-polymerized in part. Analysis of fractions obtained from purification of the crude by flash column chromatography by ^{1}H NMR spectroscopy indicated the presence of polymerized MDPO, which rapidly degraded to γ-butyrolactone and acetaldehyde over the course of 2h. ^{1}H NMR ($CDCl_3$): δ 5.40 (q, *J* = 5 Hz, 1H, -O-C(CH$_3$)*H*-O-CO-), 4.25 (dddd, *J* = 1.6, 2, 4.4, 12.4 Hz, 1 H, -CH$_2$-CH$_2$-C(H)*H*-O-), 3.74 (ddd, *J* = 2.4, 12.4, 12.4 Hz, 1 H, -CH$_2$-CH$_2$-C(*H*)H-O-), 2.85 (dddd, *J* = 1.6, 2.4, 6, 14.8, H, -CO-C(H)*H*-CH$_2$-), 2.79 (ddd, 1 H, -CO-C(*H*)H-CH$_2$-), 2.00 (ddddd, *J* = 2.4, 4.4, 12.4, 12.4, 15.2, 1 H, -CO-CH$_2$-C(H)*H*-CH$_2$-), 1.8 (ddddd, 1 H, -CO-CH$_2$-C(*H*)H-CH$_2$-). ^{13}C NMR ($CDCl_3$): δ 173.71, 100.67, 72.48, 34.65, 24.67, 21.61.

Spectral characterization data

Spectral data is shown for unprecedented compounds and those for which spectra have not been previously displayed in the literature.

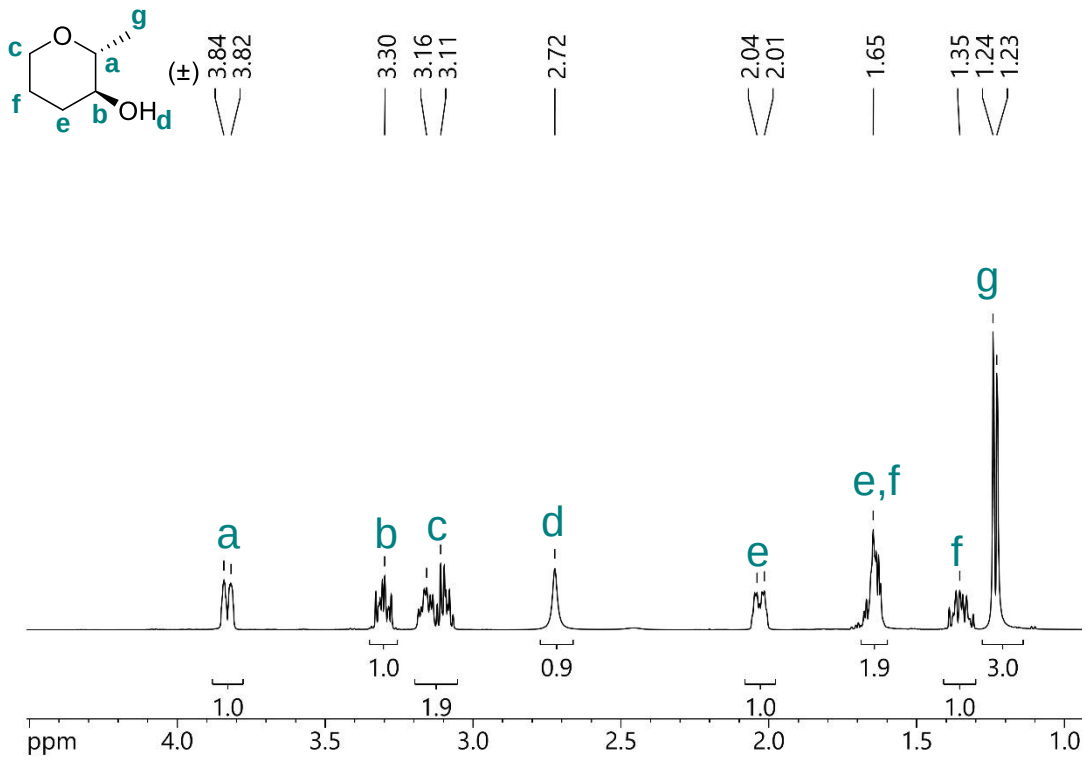

Figure B.1. ^{1}H NMR spectrum ($CDCl_3$) of 2-Methyltetrahydro-2H-pyran-3-ol.

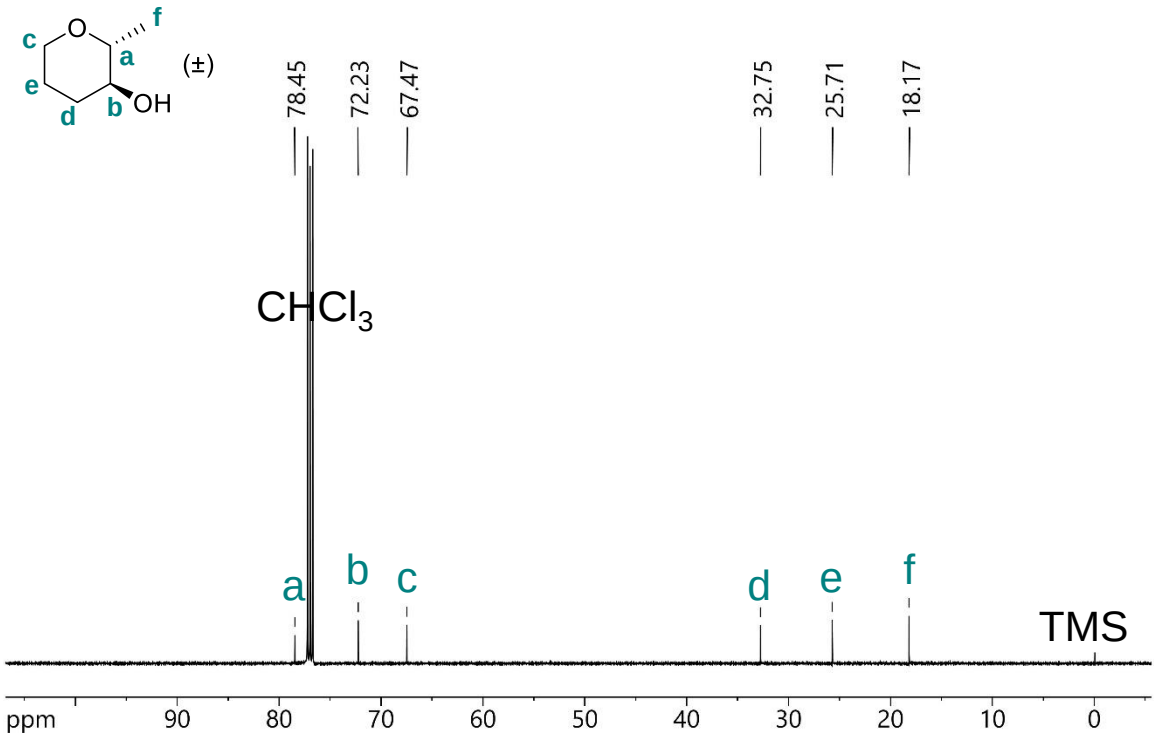

Figure B.2. ^{13}C NMR spectrum ($CDCl_3$) of 2-Methyltetrahydro-2H-pyran-3-ol.

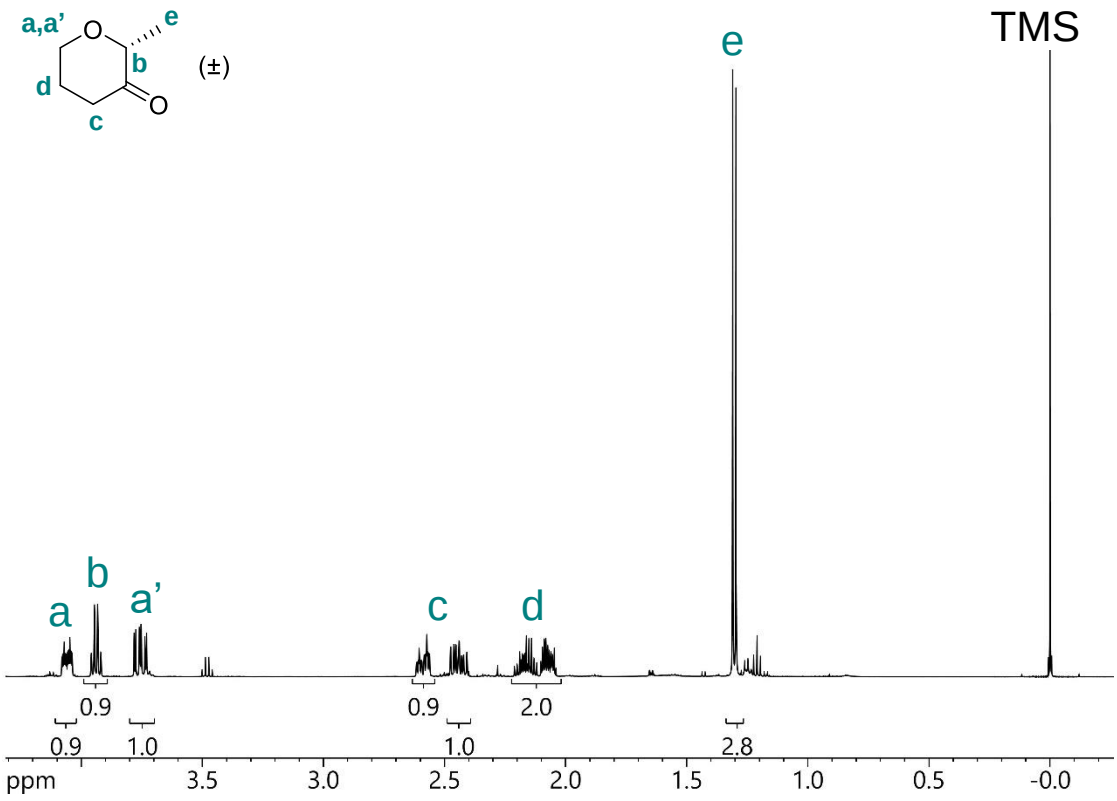

Figure B.3. ^{1}H NMR spectrum ($CDCl_3$) of 2-Methyldihydro-2H-pyran-3(4H)-one.

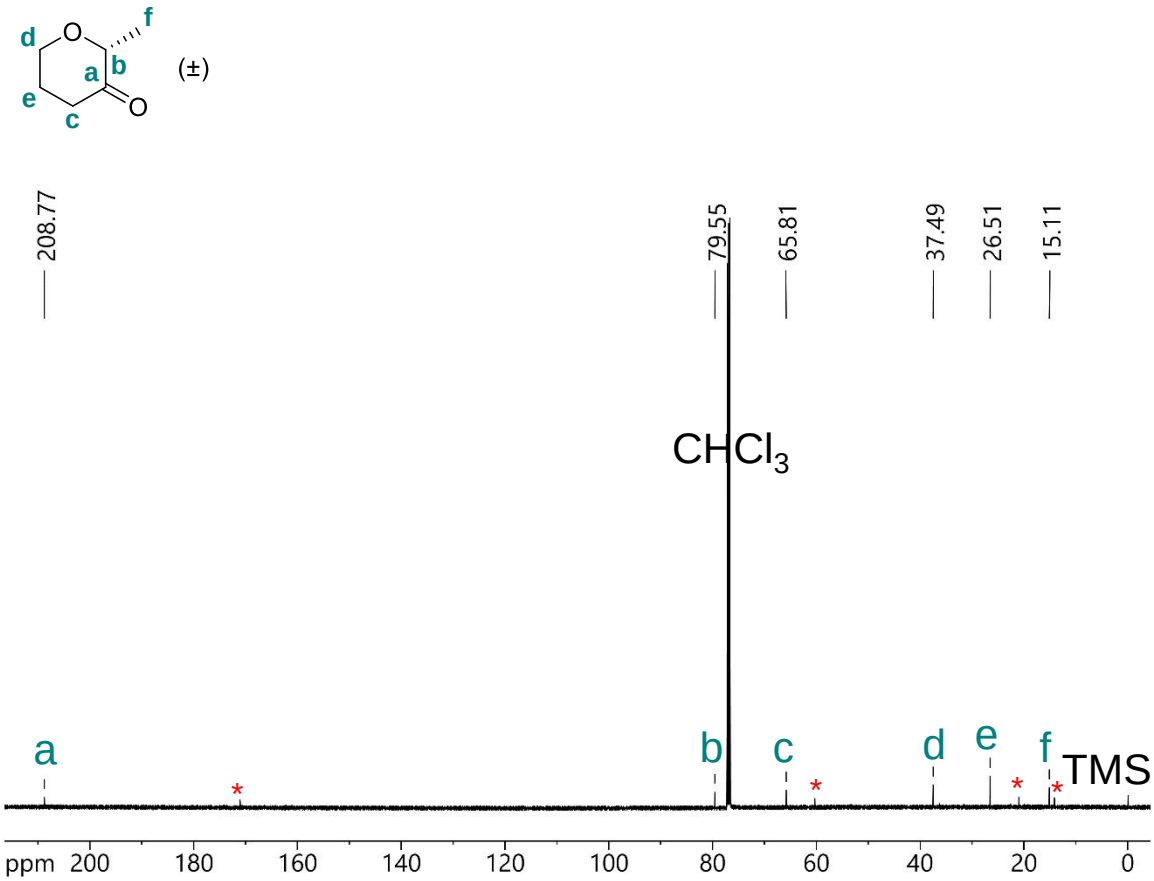

Figure B.4. ^{13}C NMR spectrum ($CDCl_3$) of 2-Methyldihydro-2H-pyran-3(4H)-one. *Indicates residual ethyl acetate.

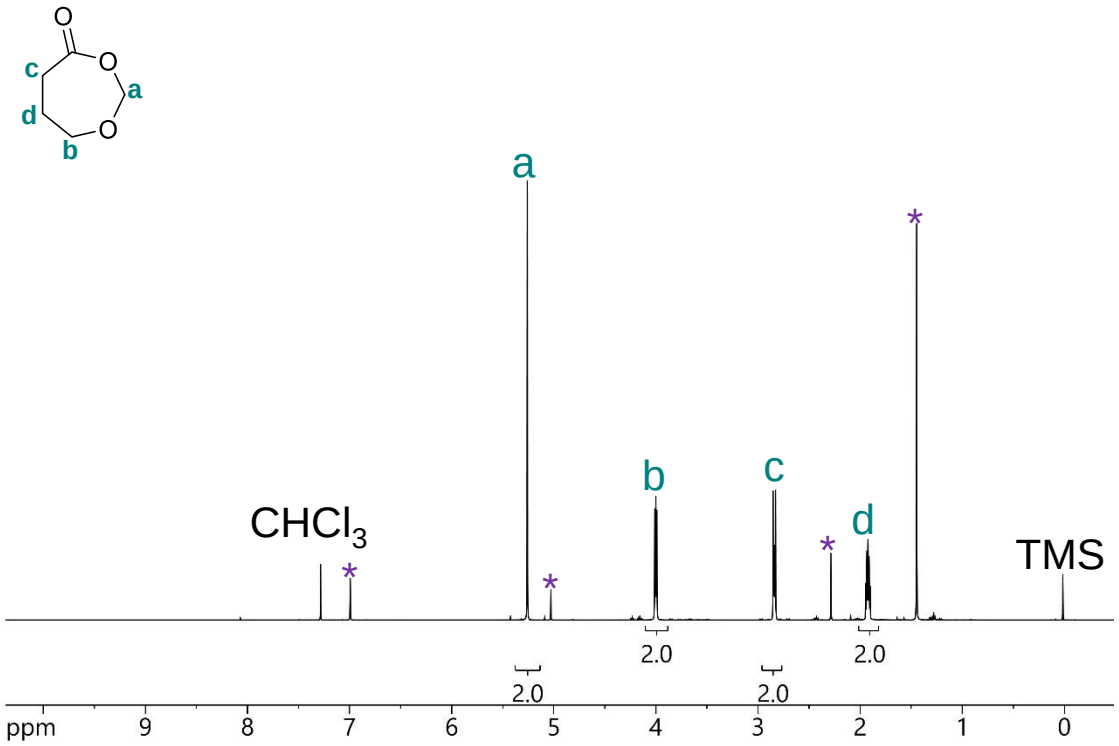

Figure B.5. ^{1}H NMR spectrum ($CDCl_3$) of 1,3-dioxepan-4-one (DPO). *Indicates butylated hydroxytoluene added as a stabilizer.

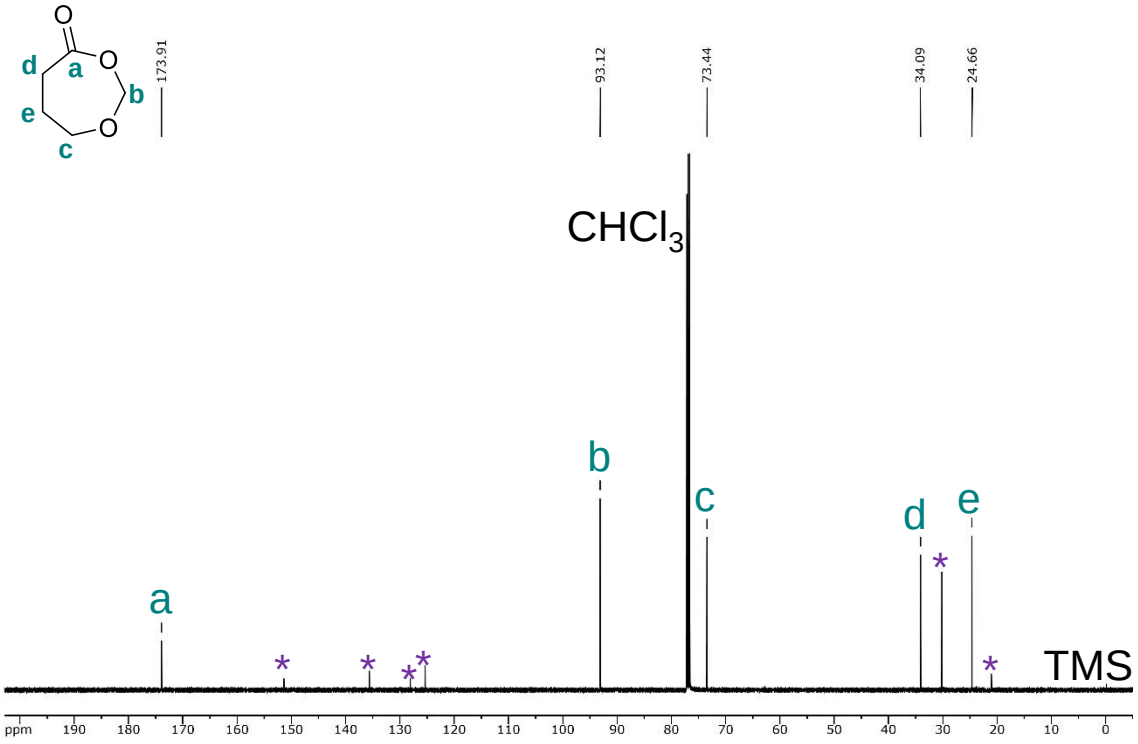

Figure B.6. ^{13}C NMR spectrum ($CDCl_3$) of 1,3-dioxepan-4-one (DPO). *Indicates butylated hydroxytoluene added as stabilizer.

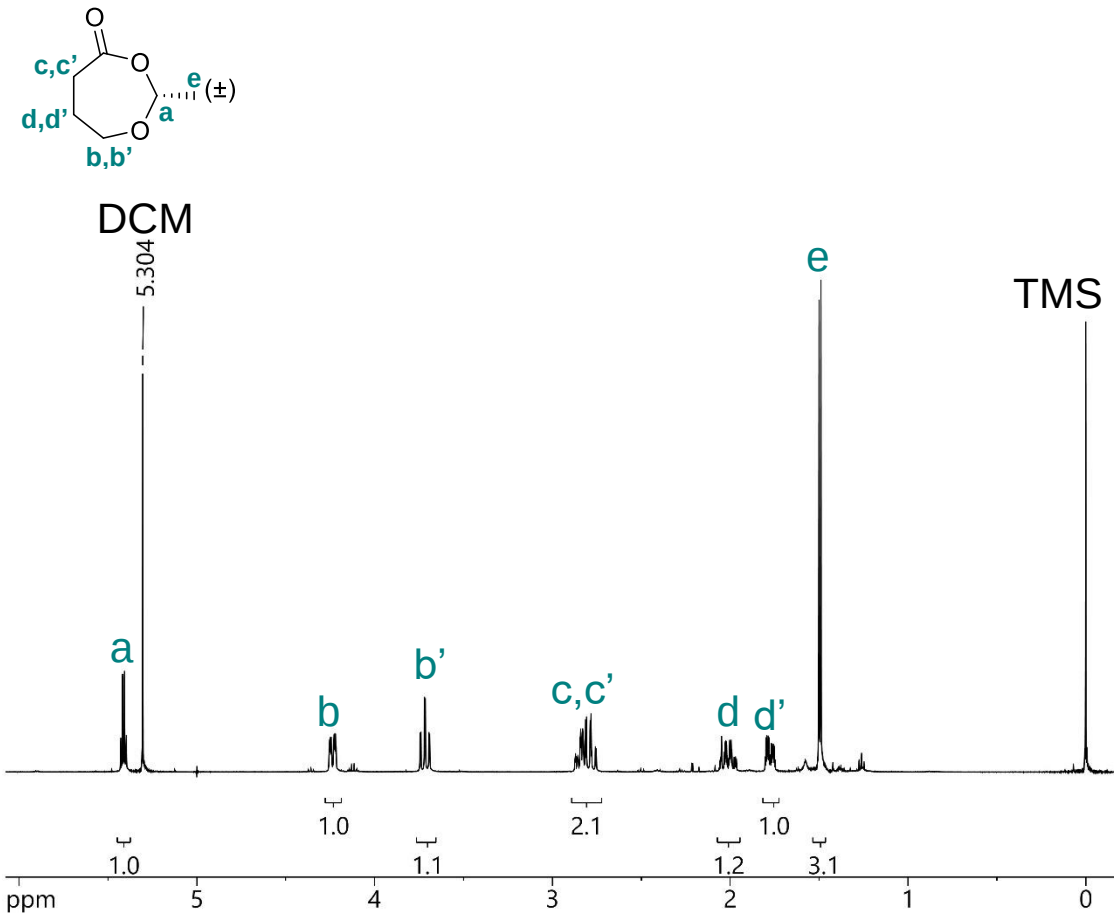

Figure B.7. ^{1}H NMR spectrum ($CDCl_3$) of 2-methyl-1,3-dioxepan-4-one (MDPO).Due to the low stability of this molecule a spectrum of a further purified product could not be obtained.

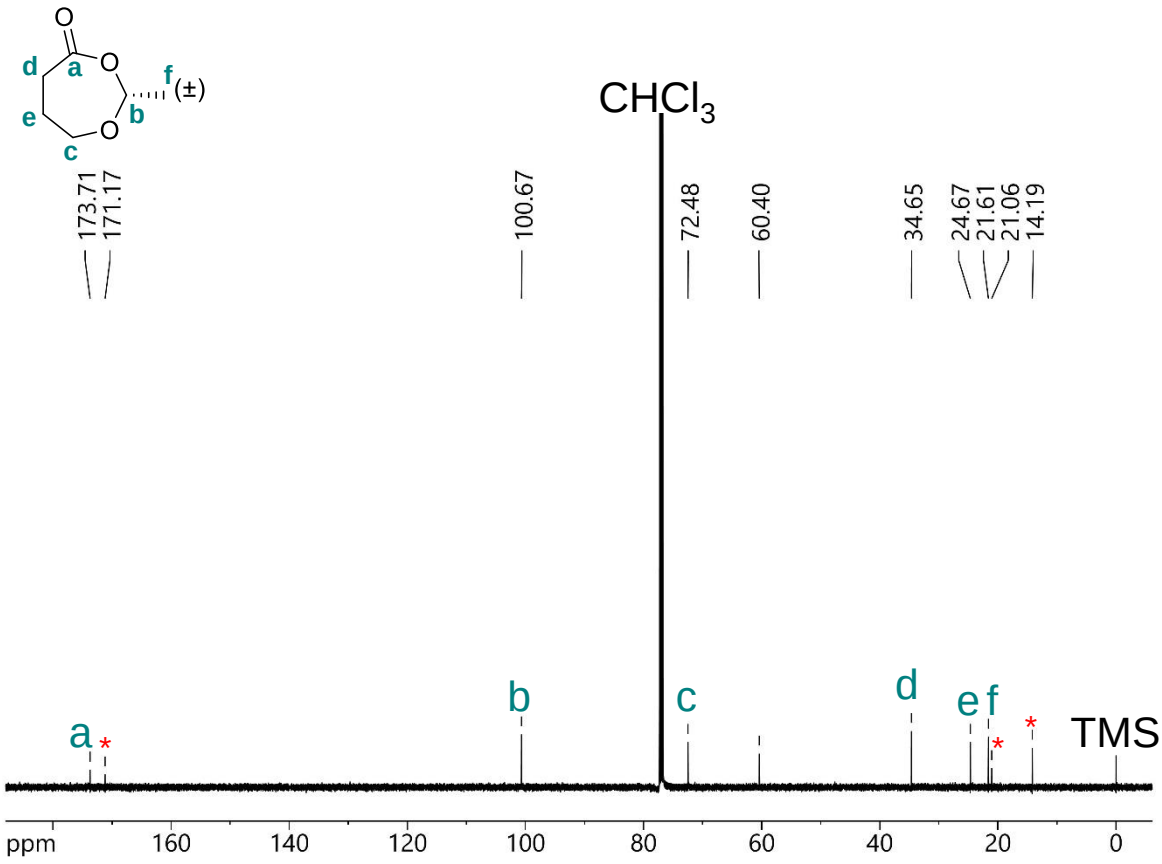

Figure B.8. ^{13}C NMR spectrum ($CDCl_3$) of 2-methyl-1,3-dioxepan-4-one (MDPO). *Indicates residual ethyl acetate.

Poly(DPO) characterization data.

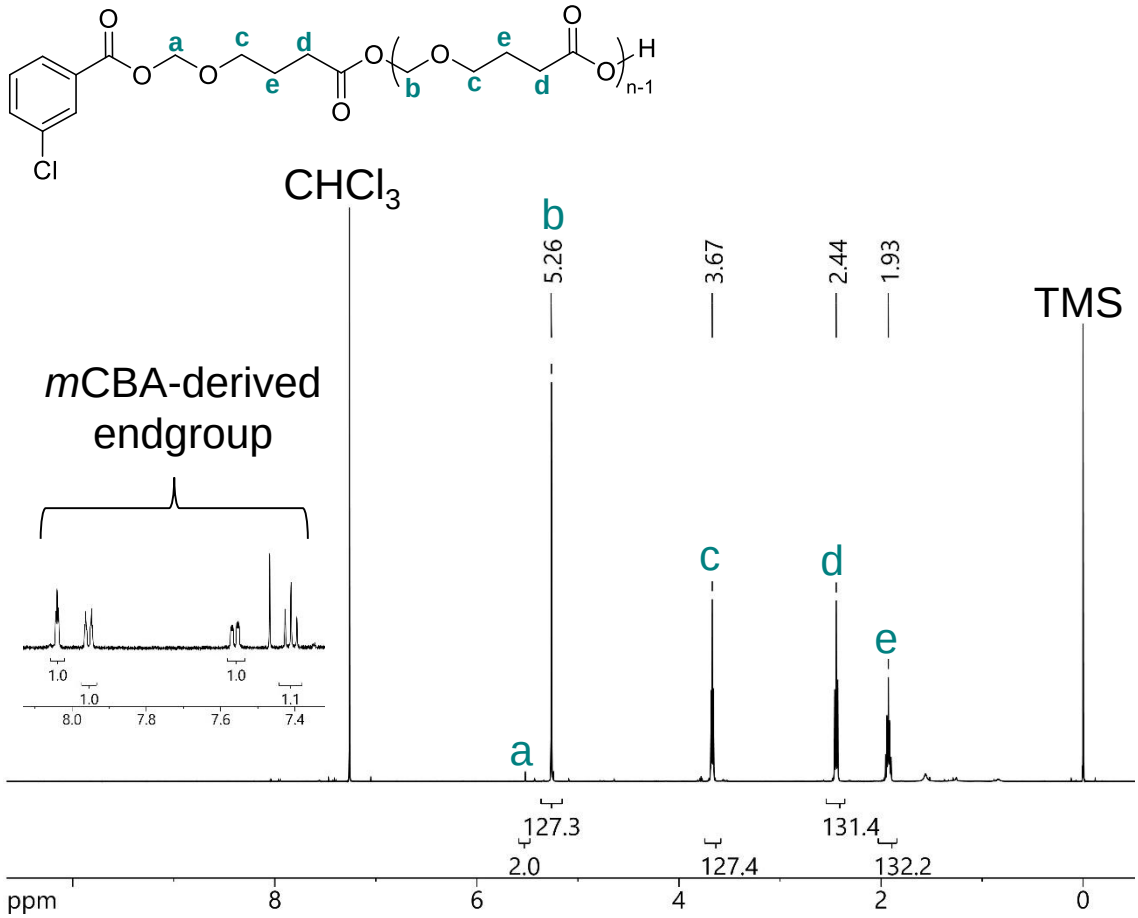

Figure B.9. ^{1}H NMR spectrum ($CDCl_3$) of poly(1,3-dioxepan-4-one) (PDPO). DPO containing ca. 1% of an *m*CBA-derived impurity was polymerized with DPP to yield a PDPO with an *m*CBA end group.

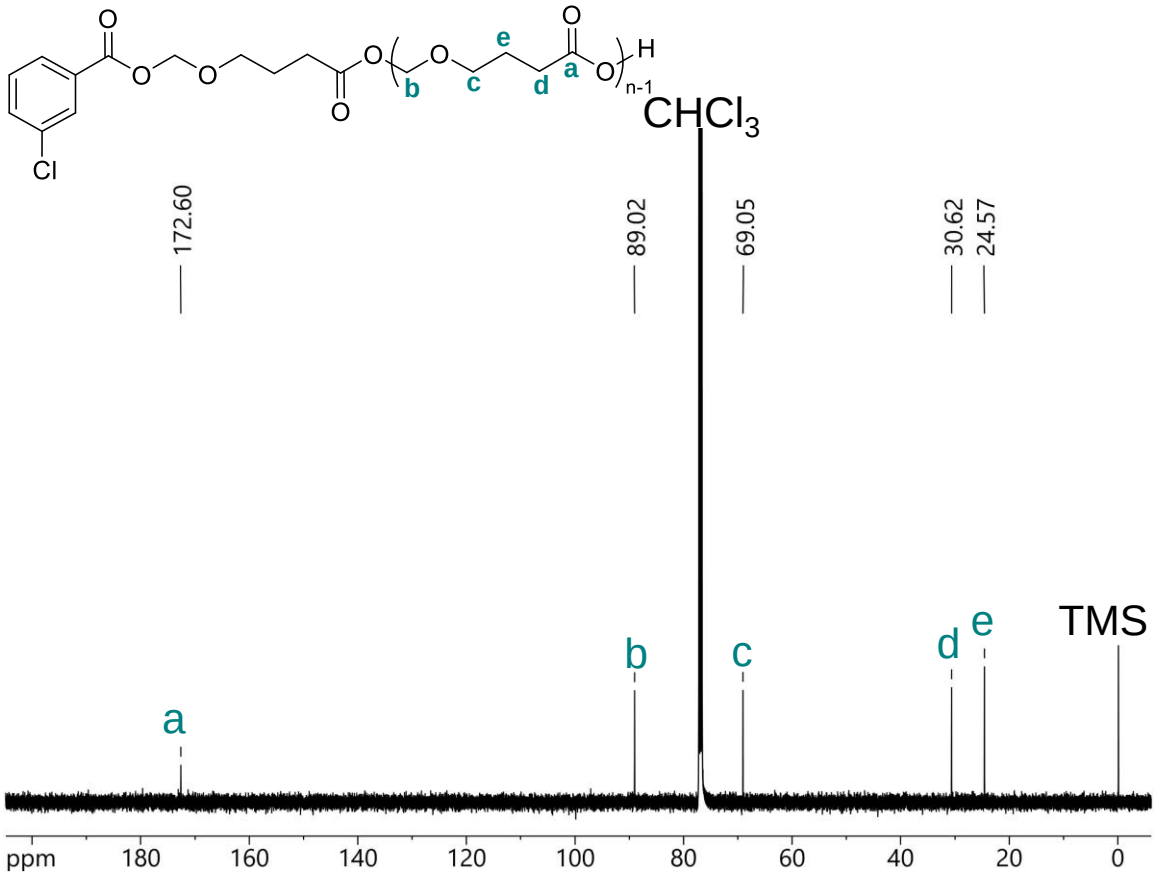

Figure B.10. ^{13}C NMR spectrum ($CDCl_3$) of poly(1,3-dioxepan-4-one) (PDPO). DPO containing ca. 1% of an *m*CBA-derived impurity was polymerized with DPP to yield a PDPO with an *m*CBA end group.

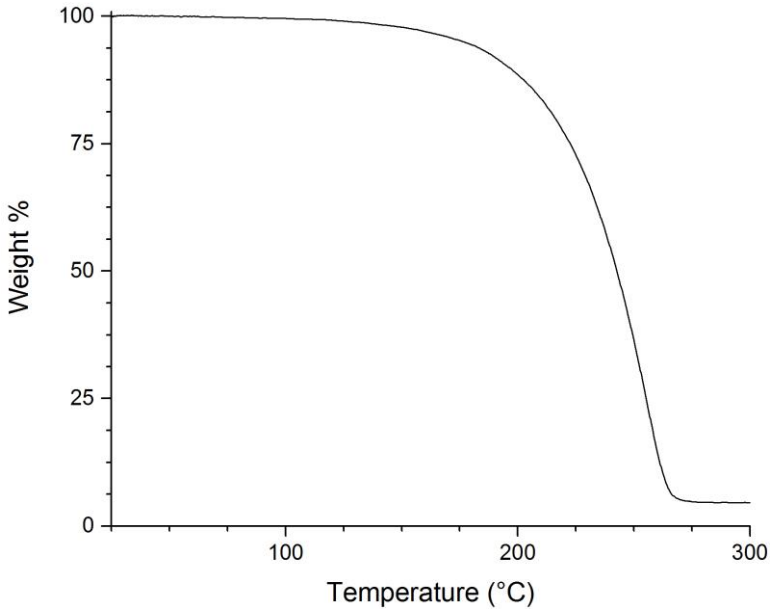

Figure B.11. Thermal gravimetric analysis of poly(1,3-dioxepan-4-one) (PDPO (M_n ~ 6 kg/mol as determined by THF SEC (relative to PS standards)) under air with a heating ramp rate of 10 °C/min.

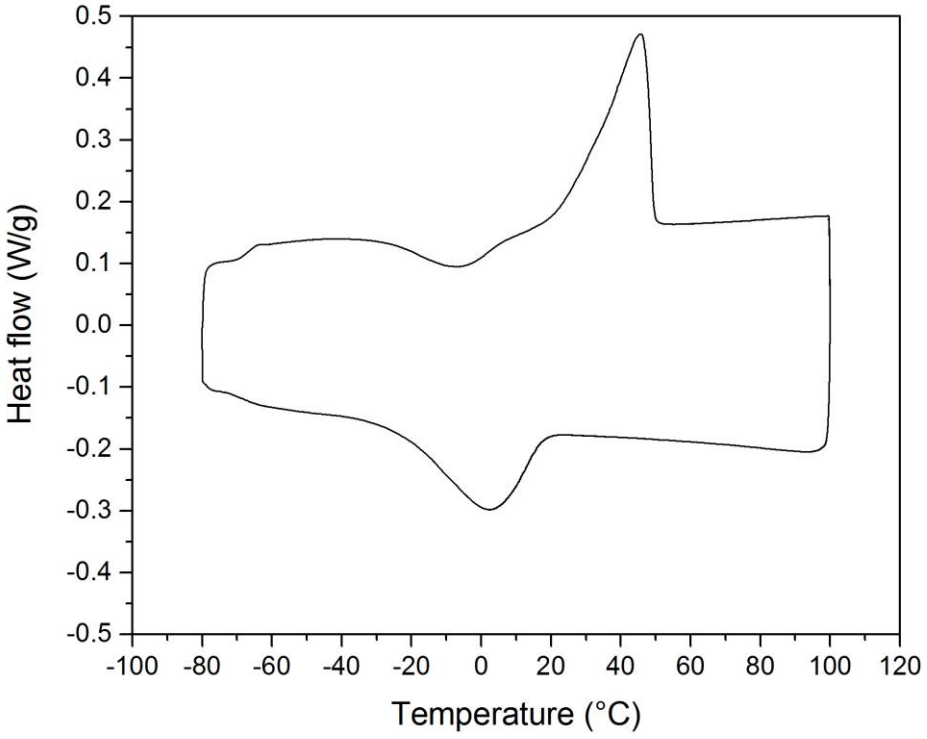

Figure B.1. Differential scanning analysis of poly(1,3-dioxepan-4-one) (PDPO (M_n ~ 6 kg/mol as determined by THF SEC (relative to PS standards)).

References

1) Brown, H. C.; Prasad, J. V. N. V.; Zee, S.-H. *J. Org. Chem.*, **1985**, *50*, 1582-1589.

2) Löpfe, M.; Linden, A.; Heimgartner, H. *Heterocycles* **2011**, *82*, 1267-1282.

3) Uyanik, M.; Akakura, M.; Ishihara, K. *J. Am. Chem. Soc.*, **2009**, *131*, 251-262.

4) Armarego, W. L. F.; Chai, L. L. *Purification of Laboratory Chemicals*, 6th ed.; Elsevier, 2009.

5) Zhdanko, A.; Maier, M. E. *Chem. Eur. J.*, **2013**, *19*, 3932–3942.

6) Löpfe, M.; Linden, A.; Heimgartner, H. *Heterocycles* **2011**, *82*, 1267-1282.